frontiers | Research Topics

Protein-RNA interplay-regulated signaling in stem cells and cancer

Edited by
Liang Zhou, William K. K. Wu, Xiaoxing Li, Yanquan Zhang and Xichen Bao

Published in
Frontiers in Cell and Developmental Biology

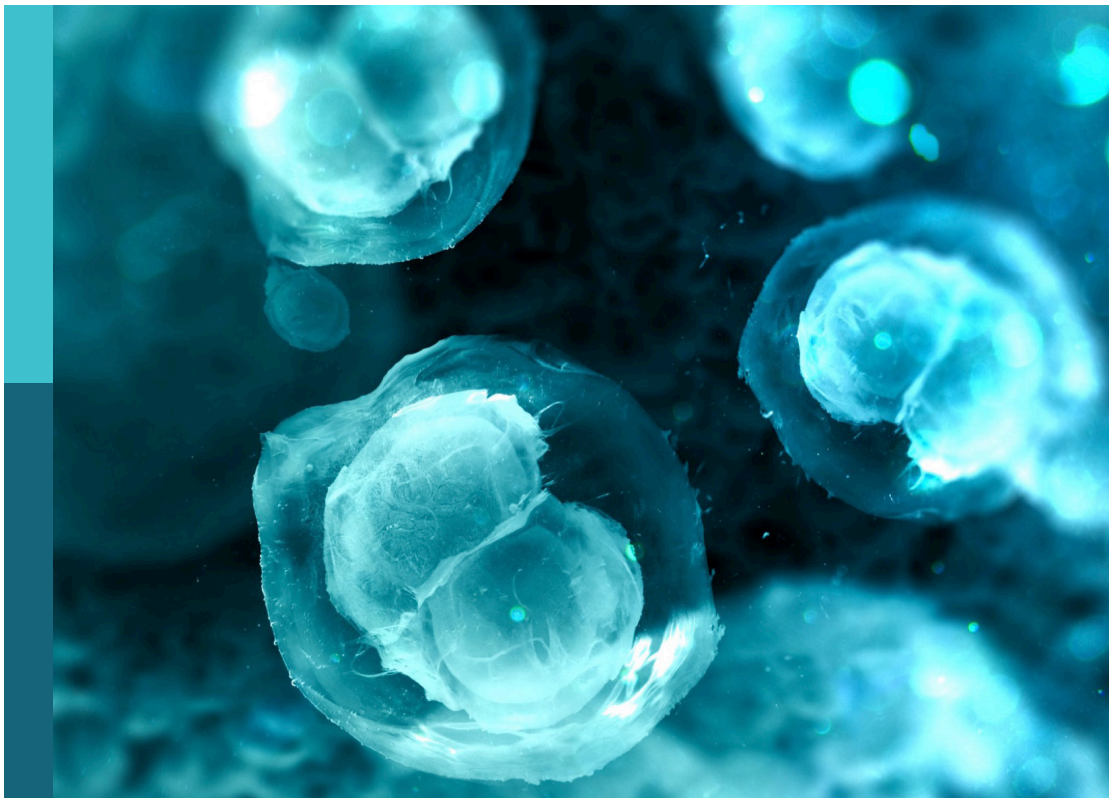

ISSN 1664-8714
ISBN 978-2-8325-3820-3
DOI 10.3389/978-2-8325-3820-3

About Frontiers

Frontiers is more than just an open access publisher of scholarly articles: it is a pioneering approach to the world of academia, radically improving the way scholarly research is managed. The grand vision of Frontiers is a world where all people have an equal opportunity to seek, share and generate knowledge. Frontiers provides immediate and permanent online open access to all its publications, but this alone is not enough to realize our grand goals.

Frontiers journal series

The Frontiers journal series is a multi-tier and interdisciplinary set of open-access, online journals, promising a paradigm shift from the current review, selection and dissemination processes in academic publishing. All Frontiers journals are driven by researchers for researchers; therefore, they constitute a service to the scholarly community. At the same time, the *Frontiers journal series* operates on a revolutionary invention, the tiered publishing system, initially addressing specific communities of scholars, and gradually climbing up to broader public understanding, thus serving the interests of the lay society, too.

Dedication to quality

Each Frontiers article is a landmark of the highest quality, thanks to genuinely collaborative interactions between authors and review editors, who include some of the world's best academicians. Research must be certified by peers before entering a stream of knowledge that may eventually reach the public - and shape society; therefore, Frontiers only applies the most rigorous and unbiased reviews. Frontiers revolutionizes research publishing by freely delivering the most outstanding research, evaluated with no bias from both the academic and social point of view. By applying the most advanced information technologies, Frontiers is catapulting scholarly publishing into a new generation.

What are Frontiers Research Topics?

Frontiers Research Topics are very popular trademarks of the *Frontiers journals series*: they are collections of at least ten articles, all centered on a particular subject. With their unique mix of varied contributions from Original Research to Review Articles, Frontiers Research Topics unify the most influential researchers, the latest key findings and historical advances in a hot research area.

Find out more on how to host your own Frontiers Research Topic or contribute to one as an author by contacting the Frontiers editorial office: frontiersin.org/about/contact

Protein-RNA interplay-regulated signaling in stem cells and cancer

Topic editors

Liang Zhou — Southern Medical University, China
William K. K. Wu — The Chinese University of Hong Kong, China
Xiaoxing Li — The First Affiliated Hospital of Sun Yat-sen University, China
Yanquan Zhang — University of Kentucky, United States
Xichen Bao — Guangzhou Institutes of Biomedicine and Health, Chinese Academy of Sciences (CAS), China

Citation

Zhou, L., Wu, W. K. K., Li, X., Zhang, Y., Bao, X., eds. (2023). *Protein-RNA interplay-regulated signaling in stem cells and cancer*. Lausanne: Frontiers Media SA. doi: 10.3389/978-2-8325-3820-3

Table of contents

frontiers | Frontiers in Cell and Developmental Biology

TYPE Editorial
PUBLISHED 16 October 2023
DOI 10.3389/fcell.2023.1304817

OPEN ACCESS

EDITED AND REVIEWED BY
Ana Cuenda,
Spanish National Research Council (CSIC), Spain

*CORRESPONDENCE
Xichen Bao,
bao_xichen@gibh.ac.cn
Xiaoxing Li,
lixiaox23@mail.sysu.edu.cn
William K. K. Wu,
wukakei@cuhk.edu.hk
Yanquan Zhang,
yanquan.zhang@uky.edu
Liang Zhou,
zhzliang@smu.edu.cn

RECEIVED 30 September 2023
ACCEPTED 06 October 2023
PUBLISHED 16 October 2023

CITATION
Bao X, Li X, Wu WKK, Zhang Y and Zhou L (2023), Editorial: Protein-RNA interplay-regulated signaling in stem cells and cancer.
Front. Cell Dev. Biol. 11:1304817.
doi: 10.3389/fcell.2023.1304817

Editorial: Protein-RNA interplay-regulated signaling in stem cells and cancer

Xichen Bao[1]*, Xiaoxing Li[2]*, William K. K. Wu[3]*, Yanquan Zhang[4]* and Liang Zhou[5]*

[1]Laboratory of RNA Molecular Biology, Guangdong Provincial Key Laboratory of Stem Cell and Regenerative Medicine, CAS Key Laboratory of Regenerative Biology, GIBH-CUHK Joint Research Laboratory on Stem Cell and Regenerative Medicine, Guangzhou Institutes of Biomedicine and Health, Chinese Academy of Sciences, Guangzhou, China, [2]Institute of Precision Medicine, The First Affiliated Hospital of Sun Yat-sen University, Guangzhou, China, [3]Department of Anaesthesia and Intensive Care, State Key Laboratory of Digestive Diseases, Li Ka Shing Institute of Health Sciences, The Chinese University of Hong Kong, Hong Kong, China, [4]Department of Toxicology and Cancer Biology, College of Medicine, University of Kentucky, Lexington, KY, United States, [5]Department of Toxicology, Guangdong Provincial Key Laboratory of Tropical Disease Research, School of Public Health, Southern Medical University, Guangzhou, China

KEYWORDS

epitranscriptome, RNA modifications, stem cells, cancer, transcriptional regulatinon

Editorial on the Research Topic
Protein-RNA interplay-regulated signaling in stem cells and cancer

The RNA-protein interplay has been proven to be essential for precise regulation of both RNA and protein, which has many implications in various biological processes including stem cell maintenance, differentiation, carcinogenesis and so on (Ye and Blelloch, 2014; Pereira et al., 2017). More specifically, RNA binding proteins (RBPs) have been shown to regulate RNA metabolism ranging from transcription, modification, processing, nuclear export, translation to RNA decay (Hentze et al., 2018; He et al., 2023). On the other hand, RNA molecules have also been shown to regulate RBP functions such as protein stability, enzymatic activity, translocations (Ni et al., 2019; Deng et al., 2020; Huppertz et al., 2022). In this Research Topic, we focused mainly on the RNA-protein interplay in specific physiological (e.g., stem cell and neurogenesis) and pathological (e.g., cancer or heart diseases) contexts, with emphasis on the RNA modifications in cancer.

Mammalian development begins with a fertilized egg. This process is associated with proper organ or tissue formation with precise cell fate determination. Deng et al. reviewed how RNA degradation machinery selectively clears specific transcripts during early cell fate determinations including maternal-to-zygotic transition, pluripotency maintenance, as well as somatic cell reprogramming Deng et al. Moreover, Chan et al. reviewed the function of many RBPs (e.g., CPEB3, FXR2) in later-stage adult neurogenesis. The authors also discussed that RBPs are involved in many aspects of neurogenesis including cell proliferation, migration, and differentiation (Chan et al., 2022).

The dysregulation of RNA-protein interplay leads to diseases including neuronal diseases, learning defects as discussed by Chan and colleagues (Chan et al., 2022). Moreover, its dysfunction can also cause many other diseases including various cancers and heart diseases. In this Research Topic, Xu et al. demonstrated that 13 out of 14 5-methylcytosine (m^5C)-associated RBPs are generally amplified in ovarian cancer, suggesting

a direct role of m^5C and its associated RBPs in cancer development or therapy. Moreover, the authors established a prognostic prediction model based on several of the m^5C regulators including ALYRER, NOP2, and TET2 for overall survival prediction Xu et al.. Besides m^5C modification and its associated RBPs, other types of RNA modifications are also involved in cancer development or cancer therapy through various mechanisms (Deng X. et al., 2023). Liu W. et al. conducted a comprehensive analysis on one of the N6-methyladenosine (m^6A) readers, YTHDF2, across various cancers. They showed that YTHDF2 might be a biomarker for tumor detection or prognostic analysis Liu W. et al. Chen et al. summarized m^6A and its associated protein partners in regulating cancer stemness properties Chen et al. Cancer stem cells are a small subpopulation of cancer cells with the capacity of self-renewal or contributing to the spread of cancer cells, the understanding of m^6A and its associated RBPs in cancer stemness provides potential therapeutic strategies for future cancer treatment.

ADAR-mediated A-to-I editing is a more traditional RNA modification to modulate RNA structure, coding sequences on RNAs, which plays critical roles in regulating tumorigenesis and has many implications in therapeutics or prognosis (Jiang et al., 2017; Liu J. et al.) discussed both the editing-dependent and editing-independent roles of ADAR1 in mature mRNA and non-coding RNA (e.g., microRNA, long non-coding RNA and circular RNA) during cancer development. They also discussed the A-to-I editing events in intron or untranslated region, and their effect on translation or mRNA stability in cancer Liu J. et al.

Besides the roles of RNA-protein interplay in cancer, Liu et al. explored the m^6A pattern in heart failure with preserved ejection fraction (HFpEF), compared with the HFpEF plus exercise mouse model. They showed that HFpEF plus exercise mouse model displays higher total m^6A level and reduced FTO level. Further investigation demonstrated that FTO can promote myocyte apoptosis, myocardial fibrosis, and hypertrophy, which could be a therapeutic target for HFpEF Liu K. et al.

In this Research Topic, we also included two papers focusing on the specific cellular processes regulated by RNA-protein interplay. Chen et al. summarized the enhancer RNA and its partners in regulating gene transcription. The authors also discussed the involvement of RNA modifications and liquid phase condensates in gene transcription Chen et al. Cheung et al. reviewed the roles of RNA modifications and their associated proteins in the regulation of ferroptosis, a new type of programmed cell death. Moreover, they also discussed their potential applications for therapeutic manipulation in cancer Cheung et al.

Altogether, our Research Topic included relevant work or reviews on RNA-protein interplay in both development and diseases. We hope that our topic will be helpful for improving the understanding of RNA-protein interplay at both cellular and molecular level.

Author contributions

XB: Conceptualization, Investigation, Supervision, Validation, Writing–original draft, Writing–review and editing. XL: Investigation, Validation, Writing–review and editing. WW: Investigation, Validation, Writing–review and editing. YZ: Investigation, Validation, Writing–review and editing. LZ: Conceptualization, Investigation, Supervision, Validation, Writing–original draft, Writing–review and editing.

Funding

The author(s) declare that no financial support was received for the research, authorship, and/or publication of this article.

Conflict of interest

The authors declare that the research was conducted in the absence of any commercial or financial relationships that could be construed as a potential conflict of interest.

Publisher's note

References

Chan, J. N., Sánchez-Vidaña, D. I., Anoopkumar-Dukie, S., Li, Y., and Benson Wui-Man, L. (2022). RNA-binding protein signaling in adult neurogenesis. *Front. Cell Dev. Biol.* 10, 982549. doi:10.3389/fcell.2022.982549

Deng, X., Li, S., Kong, F., Ruan, H., Xu, X., Zhang, X., et al. (2020). Long noncoding RNA PiHL regulates p53 protein stability through GRWD1/RPL11/MDM2 axis in colorectal cancer. *Theranostics* 10 (1), 265–280. doi:10.7150/thno.36045

Deng, X., Qing, Y., Horne, D., Huang, H., and Chen, J. (2023b). The roles and implications of RNA m(6)A modification in cancer. *Nat. Rev. Clin. Oncol.* 20 (8), 507–526. doi:10.1038/s41571-023-00774-x

He, S., Valkov, E., Cheloufi, S., and Murn, J. (2023). The nexus between RNA-binding proteins and their effectors. *Nat. Rev. Genet.* 24 (5), 276–294. doi:10.1038/s41576-022-00550-0

Hentze, M. W., Castello, A., Schwarzl, T., and Preiss, T. (2018). A brave new world of RNA-binding proteins. *Nat. Rev. Mol. Cell Biol.* 19 (5), 327–341. doi:10.1038/nrm.2017.130

Huppertz, I., Perez-Perri, J. I., Mantas, P., Sekaran, T., Schwarzl, T., Russo, F., et al. (2022). Riboregulation of Enolase 1 activity controls glycolysis and embryonic stem cell differentiation. *Mol. Cell* 82 (14), 2666–2680.e11. doi:10.1016/j.molcel.2022.05.019

Jiang, Q., Crews, L. A., Holm, F., and Jamieson, C. H. M. (2017). RNA editing-dependent epitranscriptome diversity in cancer stem cells. *Nat. Rev. Cancer* 17 (6), 381–392. doi:10.1038/nrc.2017.23

Ni, W., Yao, S., Zhou, Y., Liu, Y., Huang, P., Zhou, A., et al. (2019). Long noncoding RNA GAS5 inhibits progression of colorectal cancer by interacting with and triggering YAP phosphorylation and degradation and is negatively regulated by the m(6)A reader YTHDF3. *Mol. Cancer* 18 (1), 143. doi:10.1186/s12943-019-1079-y

Pereira, B., Billaud, M., and Almeida, R. (2017). RNA-binding proteins in cancer: old players and new actors. *Trends Cancer* 3 (7), 506–528. doi:10.1016/j.trecan.2017.05.003

Ye, J., and Blelloch, R. (2014). Regulation of pluripotency by RNA binding proteins. *Cell Stem Cell* 15 (3), 271–280. doi:10.1016/j.stem.2014.08.010

frontiers in Cell and Developmental Biology

ORIGINAL RESEARCH
published: 18 March 2022
doi: 10.3389/fcell.2022.807786

RNA 5-Methylcytosine Regulators Contribute to Metabolism Heterogeneity and Predict Prognosis in Ovarian Cancer

*Jie Xu†, Xiaoyi Liu†, Yanjie Chen, Yuya Wang, Tao Liu and Ping Yi**

Department of Obstetrics and Gynecology, The Third Affiliated Hospital of Chongqing Medical University, Chongqing, China

5-Methylcytosine (m^5C) is an abundant and highly conserved modification in RNAs. The dysregulation of RNA m^5C methylation has been reported in cancers, but the regulatory network in ovarian cancer of RNA m^5C methylation-related genes and its implication in metabolic regulation remain largely unexplored. In this study, RNA-sequencing data and clinical information of 374 ovarian cancer patients were downloaded from The Cancer Genome Atlas database, and a total of 14 RNA m^5C regulators were included. Through unsupervised consensus clustering, two clusters with different m^5C modification patterns were identified with distinct survivals. According to enrichment analyses, glycosaminoglycan and collagen metabolism–related pathways were specifically activated in cluster 1, whereas fatty acid metabolism–related pathways were enriched in cluster 2, which had better overall survival (OS). Besides the metabolism heterogeneity, the higher sensitivity to platinum and paclitaxel in cluster 2 can further explain the improved OS. Ultimately, a least absolute shrinkage and selection operator prediction model formed by ALYREF, NOP2, and TET2 toward OS was constructed. In conclusion, distinct m^5C modification pattern exhibited metabolism heterogeneity, different chemotherapy sensitivity, and consequently survival difference, providing evidence for risk stratification.

Keywords: ovarian cancer, 5-methylcytosine, RNA modification, metabolism heterogeneity, LASSO cox regression

OPEN ACCESS

Edited by:
Xiaoxing Li,
The First Affiliated Hospital of Sun Yat-sen University, China

Reviewed by:
Yubin Xie,
Sun Yat-sen University, China
Qian Yang,
Cedars Sinai Medical Center, United States

****Correspondence:***
Ping Yi
yiping@cqmu.edu.cn

†These authors have contributed equally to this work

Specialty section:
This article was submitted to Signaling, a section of the journal Frontiers in Cell and Developmental Biology

Received: *02 November 2021*
Accepted: *08 February 2022*
Published: *18 March 2022*

Citation:
Xu J, Liu X, Chen Y, Wang Y, Liu T and Yi P (2022) RNA 5-Methylcytosine Regulators Contribute to Metabolism Heterogeneity and Predict Prognosis in Ovarian Cancer. Front. Cell Dev. Biol. 10:807786. doi: 10.3389/fcell.2022.807786

INTRODUCTION

Ovarian cancer (OVC) is the most lethal gynecological cancer (Siegel et al., 2021). Because of asymptomatic onset and lack of efficient screening tests, more than 75% of patients are diagnosed at an advanced stage with a 5-year survival rate of 29%, in contrast to 92% for early stage (Singer et al., 2003). The standard frontline care is the debulking surgery to no tumor residual and platinum-based adjuvant chemotherapy, with antiangiogenic therapy applied in patients who have suboptimal tumor reduction and stage IV disease (Lheureux et al., 2019). The poly-ADP-ribose polymerase (PARP) inhibitors have been applied in frontline care for maintenance therapy and in patients with recurrence (Kristeleit et al., 2017; Pujade-Lauraine et al., 2017; Moore et al., 2018). However, the moderate activity of PARP inhibitors was found in patients with homologous recombination dysfunction, and a worse therapeutic effect was observed in homologous recombination–proficient patients (Kaufman et al., 2015). Despite initial response to the first-line treatment, 25% of patients have a relapse within 6 months (Jemal et al., 2003), and more than 80% of patients eventually have a recurrence (Kim et al., 2020). Immunotherapy has demonstrated

modest response rates of 10% to 15%, despite a large proportion of OVCs with high expression of programmed death ligand 1 (Pujade-Lauraine, 2017). Facing those challenges in diagnosis and treatment, seeking predictive biomarkers could enable early diagnosis, survival prediction, and identification of patient subgroups who would maximally benefit from those treatments (Lheureux et al., 2019). Consequently, investigations are devoted to molecular and function profiling of OVC for optimal biomarkers.

Dysregulation of RNA expression profile is an important hallmark of tumors (Chai et al., 2019a). RNA 5-methylcytosine (m^5C) modification, the methylation of the fifth carbon in cytosine base in RNA sequences, has emerged as one of the critical posttranscriptional regulators of gene expression and has been identified in tRNA, rRNA, and mRNA (Nombela et al., 2021). The distribution of m^5C site in mRNA has been reported to be mainly deposited in the coding sequences and enriched around the translation initiation codon (Amort et al., 2017; Yang et al., 2017; Yang et al., 2019; Tang et al., 2020). RNA m^5C modification is a reversible and dynamic process mediated by a group of proteins named "writers," "erasers," and "readers," which work as methyltransferases (NSUN, DNMT, and TRDMT families), demethylases (TET family), and binding proteins (ALYREF and YBX1), respectively. RNA m^5C modification has been involved in the regulation of gene expression (Roundtree et al., 2017; Chai et al., 2019b) and thus has participated in a series of physiological and pathological processes including cancers (Chen et al., 2021).

Cancer is considered as a disease characterized by the accumulation of genetic or epigenetic alterations of different oncogenes and tumor suppressors (Nombela et al., 2021). Metabolism reprogramming is another indispensable hallmark of cancer. Mutation of oncogene and tumor suppressors drives the reprogramming of metabolism and rewiring of epigenetic modification. Cancer cell fate can also be modified by epigenetic modification and alteration of metabolites. m^5C regulator dysregulation has been reported in multiple cancers such as breast cancer, leukemia, bladder cancer, and skin squamous cell carcinoma (Freeman et al., 1991; Blanco et al., 2016; Cheng et al., 2018; Chen et al., 2019). It has also been demonstrated that RNA m^5C modification could promote glucose metabolism through enhancing PKM2 mRNA stability in bladder cancer (Wang et al., 2021). However, the role of RNA m^5C regulators-mediated m^5C methylation modification, as well as its effect on metabolism reprogramming in OVC, remains unclear.

In this study, we revealed the landscape of genetic variation and gene expression of m^5C regulators in OVC and established a prognostic prediction model formed by ALYRER, NOP2, and TET2 for overall survival (OS). We also dissected the potential roles of m^5C modification in metabolism heterogeneity and altered chemotherapeutic drug sensitivity, which could result in survival differences of OVC patients.

MATERIALS AND METHODS

Data Resources

The workflow of our study is shown in **Supplementary Figure S1A** . The fragments per kilobase of exon model per million mapped fragments (FPKM) files of RNA-seq transcriptome data, as well as clinical information of 374 cases of OVC, were downloaded from The Cancer Genome Atlas (TCGA) database. The SOFT formatted matrix files of three Gene Expression Omnibus (GEO) datasets (GSE27651, GSE52037, GSE54388, and GSE19829) (Clough and Barrett, 2016) were downloaded using R package getGEO. The Masked Copy Number Segment data of DNA copy number variation (CNV) data of OVC were downloaded from the Genomic Data Commons (https://portal.gdc.cancer.gov).

RNA m^5C Regulators

Fourteen m^5C regulators including eight writers (NOP2, NSUN2, NSUN3, NSUN4, NSUN5, NSUN6, NSUN7, TRDMT1); four erasers (TET1, TET2, TET3, ALKBH1); and two readers (YBX1, ALYREF) were enrolled in this study (Chen et al., 2021). DMNT3A and DMNT3B were excluded because they have only been reported in *Arabidopsis thaliana* for now.

m^5C Regulators Mutation and CNV Analysis

The somatic mutation investigation of m^5C regulators in pan-cancer and the CNV analysis in OVC were performed using cBioPortal website (www.cbioportal.org) (Gao et al., 2013). The Pan-Cancer Project of TCGA was enrolled for somatic mutation evaluation in pan-cancer. The Pan-Cancer Project of TCGA-OV with both somatic mutation and mRNA data was enrolled for CNV analysis in OVC.

Differentially Expressed Gene Analysis

Principal component analysis (PCA) using R package FactoMineR and differential gene expression analysis using R package limma (Ritchie et al., 2015) were conducted, in order to display the different profiles of m^5C regulators between human ovarian surface epithelium (HOSE) and OVC. Differential analysis was also utilized in seeking DEGs that were specifically up-regulated in each cluster. DEGs were defined as genes with $p < 0.05$ and $|\text{fold change}| > 1.2$.

Interaction Between 14 m^5C Regulators

The protein–protein interaction (PPI) network plot was constructed using the STRING 11.0 b website (https://string-db.org/). The correlation analysis of the m^5C regulators among mRNA expression and CNV level and between them was conducted by R package corrplot.

Clustering Analysis of 14 m^5C Regulators

The ConsensusClusterPlus package (Wilkerson and Hayes, 2010) was performed to identify distinct m^5C phenotype based on the expression of 14 m^5C regulators, and 1,000 times repetitions were conducted to ensure the stability of the classification.

Cluster Function Annotation and Exploration of Cluster Metabolism Heterogeneity

The cluster function annotation was conducted using R package Gene Set Variation Analysis (GSVA) to explore the Gene Ontology (GO) and Kyoto Encyclopedia of Genes and Genomes (KEGG)

enrichment among different m^5C clusters. GO hallmark and KEGG hallmark gene sets were downloaded from MsigDB dataset (http://www.gsea-msigdb.org/gsea/msigdb). Further functional annotation of each m^5C cluster was performed by R package ClusterProfiler (Yu et al., 2012) using the top 500 expressed genes and DEGs in each cluster for GO and KEGG pathways. Then, Gene Set Enrichment Analysis (GSEA) was performed using cluster DEGs by ClusterProfiler package to further identify up-regulated pathways in the individual cluster. The up-regulated pathways identified in multiple methods were finally visualized in circos plot using R package circlize. Then, metabolic pathways were downloaded from KEGG database including 1,653 human genes assigned to 91 pathways. The GSVA scores of metabolic pathways were calculated using the GSVA package for further correlation with mRNA level of m^5C regulators.

Prediction of Drug Sensitivity

The drug sensitivity was predicted using calcPhenotype function in R package oncoPredict (Maeser et al., 2021) based on Genomics of Drug Sensitivity in Cancer cell line dataset (https://www.cancerrxgene.org/). The prediction ability by drug sensitivity score calculation was validated in OVC clinical trial (GSE51373) with area under the curve (AUC) of 0.786. Imputed lower sensitivity score represents higher sensitivity of the drug.

Cell Culture and Cell Growth

OVCAR3 cells were cultured in Dulbecco modified eagle medium (GIBCO, United States) supplemented with 10% fetal bovine serum (GIBCO, United States), penicillin (GIBCO, United States), and streptomycin (GIBCO, United States) and maintained at 37°C in 5% CO_2 cell culture incubator. The cells transfected with siRNA targeting TET2 or control (TsingkeBiotechnology, China) were seeded in 96-well plates for the cell viability test. CCK-8 reagent (DOJINDO, Japan) was added into the plate and incubated for 2 h. The cell absorbance at 450-nm wavelengths was measured by using the microplate reader (BioTek, United States) at 0, 1, 2, 3, and 4 days. All experiments were performed in triplicate.

Western Blot

Cells were collected and lysed with cell lysis buffer (Beyotime, China) on ice for 30 min, and the lysate was obtained by centrifugation at 12,000*g* for 10 min. Proteins were fractionated by sodium dodecyl sulfate–polyacrylamide gel electrophoresis and then transferred onto 0.22-μm NC membranes. The membranes were blocked with 5% nonfat milk in TBS/Tween-20 and blotted with the antibody (anti-TET2; ProteinTech) at 4°C overnight. Corresponding secondary antibodies (ZSGB-BIO, China) were added on the membrane at room temperature for 1.5 h. Immunoreactive bands were visualized using enhanced chemiluminescence detection reagent (Millipore, United States).

Statistical Analysis

Correlations among different m^5C regulators were evaluated by Spearman correlation analyses using R package corrplot. Correlations between m^5C regulators and clinicopathological parameters were evaluated by Spearman correlation analyses using SPSS 25.0. A χ^2 test was conducted to compare the clinicopathological parameters of clusters. Kruskal–Wallis test was used to compare gene expression among different samples. R packages survival and survminer (Scrucca et al., 2007) were used to perform the univariate Cox proportional hazards analysis and Kaplan–Meier analysis for OS. R package forestplot and survminer were used for visualized the Cox analysis results and survival curves, respectively. Genes with $p < 0.05$ in univariate analysis were selected to the least absolute shrinkage and selection operator (LASSO) method regression analysis using R package glmnet. Patients with survival information were randomly divided into two groups (75% in the training group and 25% in the test group) by createDataPartition function from R package caret. Three gene signature and their corresponding coefficients were determined in the training group by glmnet package, and the risk score was calculated for each patient using the prediction function. The AUC of receiver operating characteristic (ROC) curve was calculated by R package survivalROC (Heagerty and Zheng, 2005). True positive (TP) and false positive (FP) of every patient in the training group were calculated through survivalROC function, and the minimum value of the formula (TP-1)*2 + FP*2 was determined as the best cutoff value. This cutoff value was used in the internal training set, internal testing set, and external testing set to divide the samples into the high-score group and the low-score group. R 4.0.3 was used for all the statistical analyses in this study. $p < 0.05$ is the significance threshold for all the data.

RESULTS

Profiles of Genetic Variation and Gene Expression of RNA m^5C Regulators in Ovarian Cancer

First, we comprehensively studied the profile of the genetic variation frequency of m^5C regulators in the pan-cancer cohort. The amplification is the prevalent variation pattern of m^5C regulator genes in OVC, and 13 of 14 (92.9%) regulators were amplified (**Figures 1A,B**). Among those regulators, YBX1, NOP2, and NSUN4 genes exhibited the highest amplification frequencies of 7%, 6%, and 5%, respectively (**Figure 1B**). The significant positive correlation of CNV among regulators was demonstrated especially between ALYREF and writers, as well as TET2 and writers (**Figure 1C**). Then, we explored the correlation between CNV and mRNA levels of each regulator and found a significant positive correlation in all 14 regulators (**Figure 1D**). Differential analysis was further performed to profile the expressions of 14 m^5C regulators between HOSE and OVC. Consistent with the CNV pattern, most regulators were significantly up-regulated in OVC compared with HOSE tissues, whereas TET2 expression was decreased in two GEO cohorts (**Figures 1F,G**). Besides, a significant distinction of m^5C

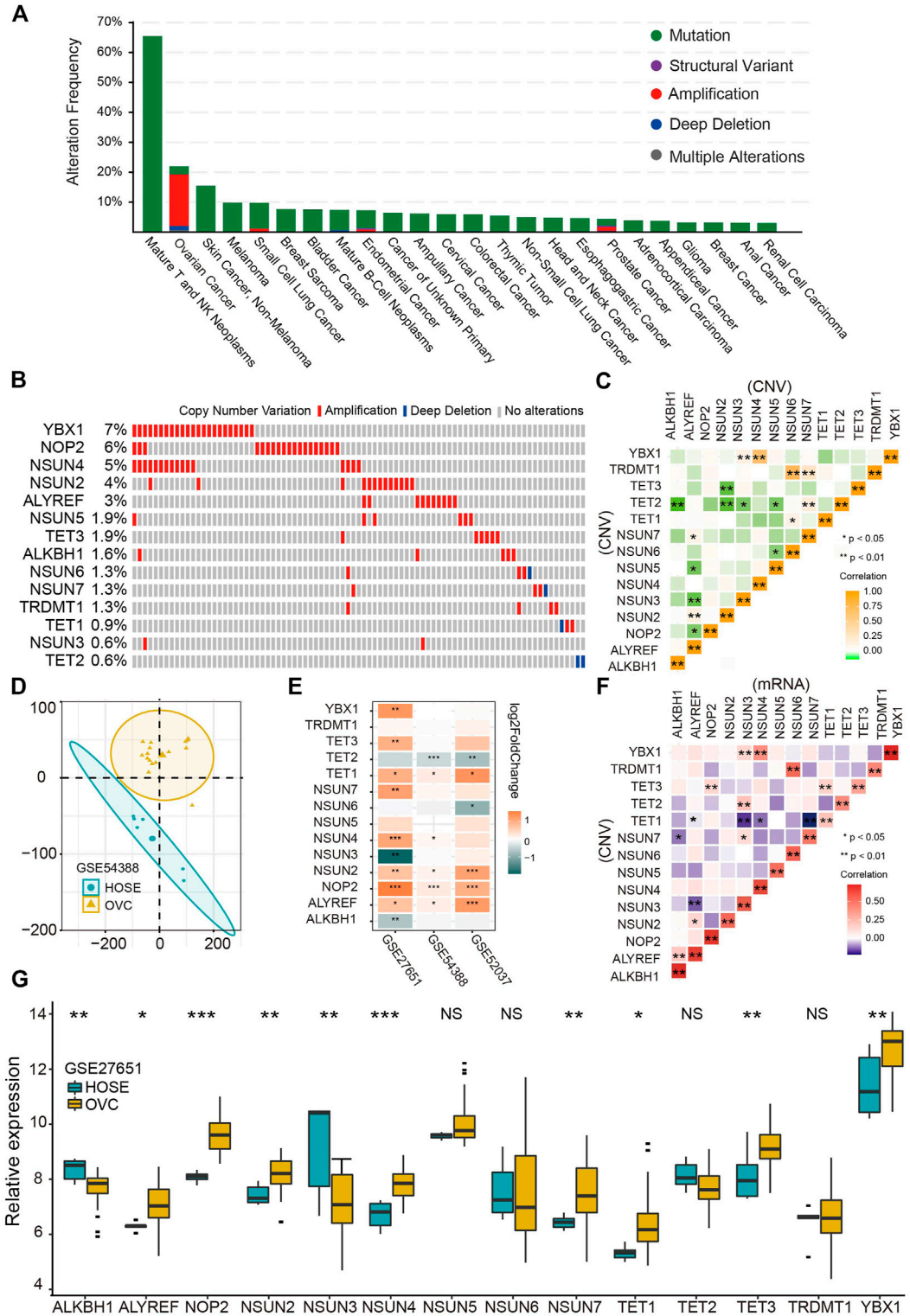

FIGURE 1 | Genetic variation and gene expression of RNA m^5C regulators in ovarian cancer. **(A)** Genetic alteration frequencies of m^5C regulators in pan-cancer. **(B)** Copy number variation of m^5C regulators in ovarian cancer. **(C)** Correlation of copy number variations among m^5C regulators. **(D)** Principal component analysis for the expression profile of m^5C regulators to distinguish OVC from HOSE samples in GSE54388 cohort. OVC, ovarian cancer, HOSE, human ovarian surface epithelium. **(E)** The differential expression analysis of 14 m^5C regulators between OVC and HOSE samples in three independent GEO cohorts. Up-regulated in OVC: orange; up-regulated in HOSE samples: blue. **(F)** Correlation between copy number variation and mRNA level of m^5C regulators. **(G)** The boxplot of expression of 14 m^5C regulators in OVC and HOSE samples in GSE27651 cohort.*$p < 0.05$, **$p < 0.01$, ***$p < 0.001$.

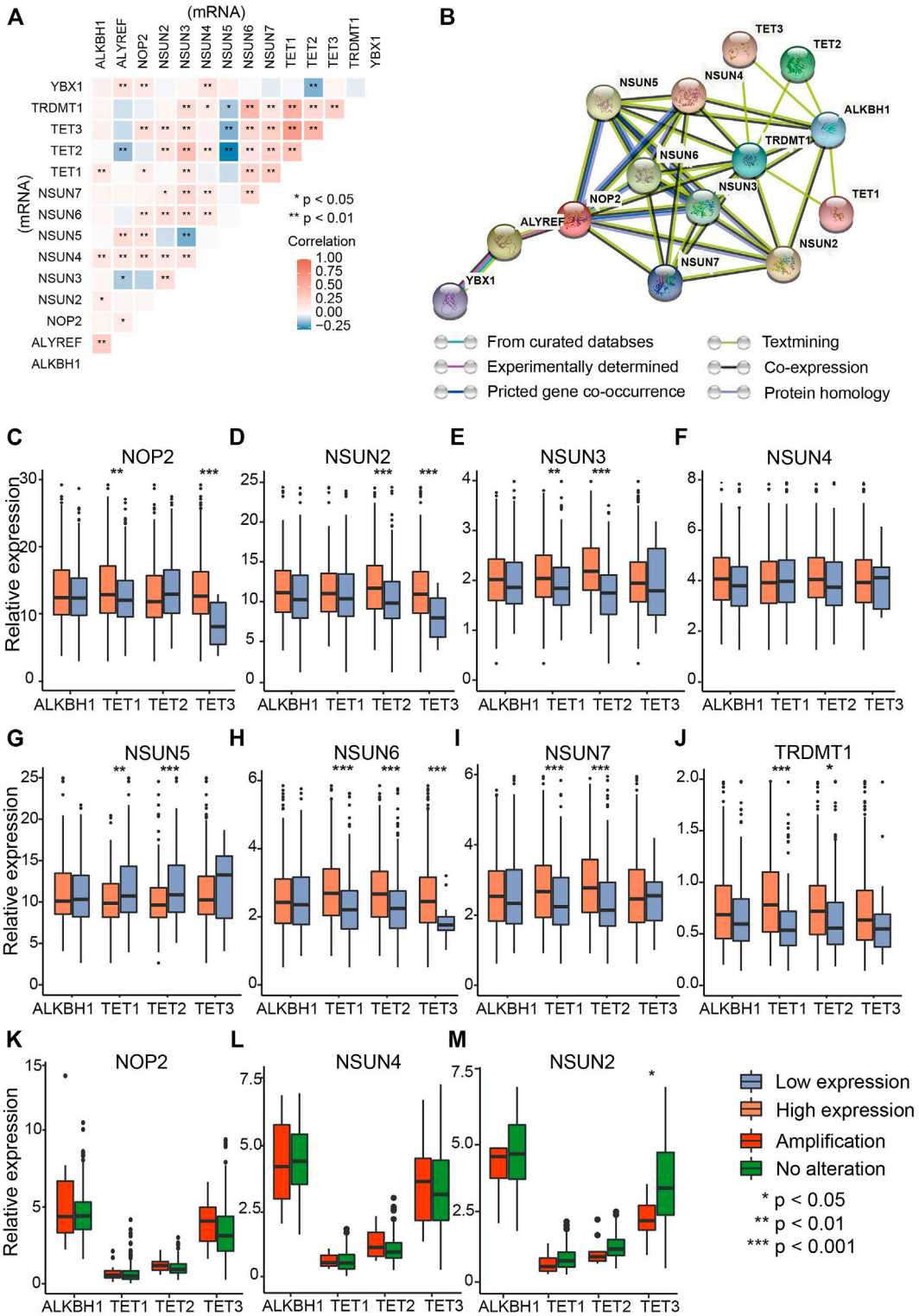

FIGURE 2 | The interaction and correlation analysis between RNA m^{5}C regulators in ovarian cancer. **(A)** Correlation of mRNA levels among m^{5}C regulators. **(B)** Protein–protein interaction plot among the 14 m^{5}C regulators. **(C–J)** Correlations between "writers" (NUSN1, NSUN2, NSUN3, NSUN4, NSUN5, NSUN6, NSUN7, TRDMT1) and "erasers" (TET1, TET2, TET3, ALHBK1) at mRNA level (RPKM). **(K–M)** Differential mRNA levels of "erasers" between amplified type and wild type of "writers" with the highest CNV frequencies (NOP2, NSUN4, and NSUN2).

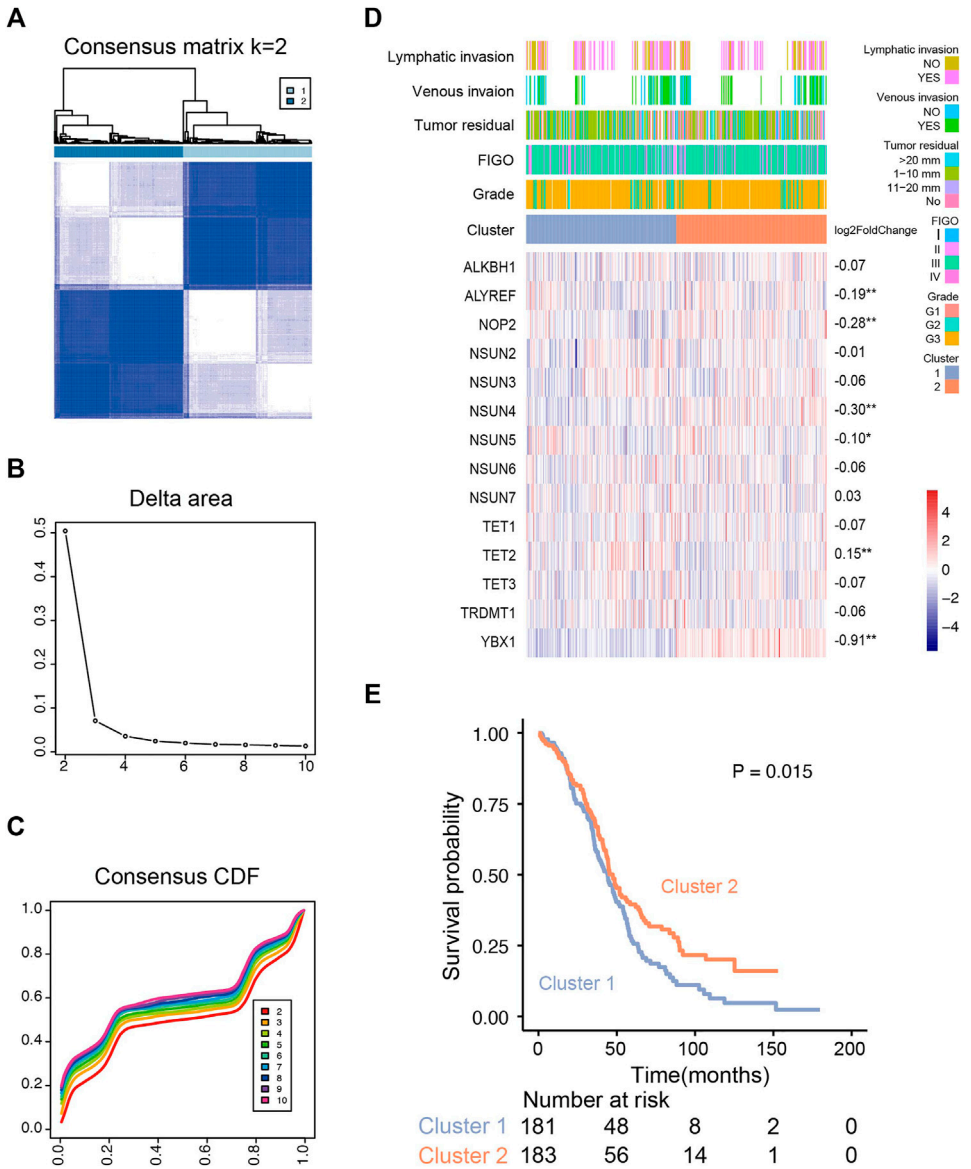

FIGURE 3 | Unsupervised consensus clustering analysis of RNA m^{5}C regulators. **(A)** Consensus clustering matrix for the most suitable *k* (k = 2). **(B)** Relative changes in the area under the clustering cumulative function (CDF) curve at k = 2–10. **(C)** Consensus clustering CDF for k = 2–10. **(D)** The m^{5}C regulator expression profiles and clinicopathological characteristics in two clusters. **(E)** Kaplan–Meier overall survival curves for ovarian cancer patients of two clusters in the TCGA cohort.

regulators' expression profiles among HOSE and OVC was illustrated by PCA (**Figure 1E**).

The Interaction and Correlation Analysis of RNA m^{5}C Regulators in Ovarian Cancer

To testify whether m^{5}C regulators have correlations among each other, Spearman correlation analysis of mRNA levels of 14 regulators indicated significant positive correlation among most regulators (**Figure 2A**). The comprehensive landscape of m^{5}C regulators was depicted with the PPI network according to the STRING 11.0 b website (**Figure 2B**). The writers and erasers had remarkable interactions within each other except the readers (YBX1 and ALYREF). To further investigate the correlations of writers and erasers who work as methyltransferases and demethyltransferases and affect the amount and distribution of m^{5}C modification, comparisons of writer gene expression were performed in patients with high and low eraser gene expression (**Figures 2C–J**) (Zhang et al., 2020). The results showed that writer genes exhibited different correlations with eraser genes. NSUN6 expression was positively correlated with TET1/2/3, whereas NSUN7 expression was negatively correlated with eraser genes TET1/2 (**Figures 2H,I**). As writer genes NOP2, NSUN4, and NSUN2 have relatively higher amplification (**Figure 1B**), we analyzed whether the CNV of those writer genes is correlated with eraser genes. Of these, only TET3 was

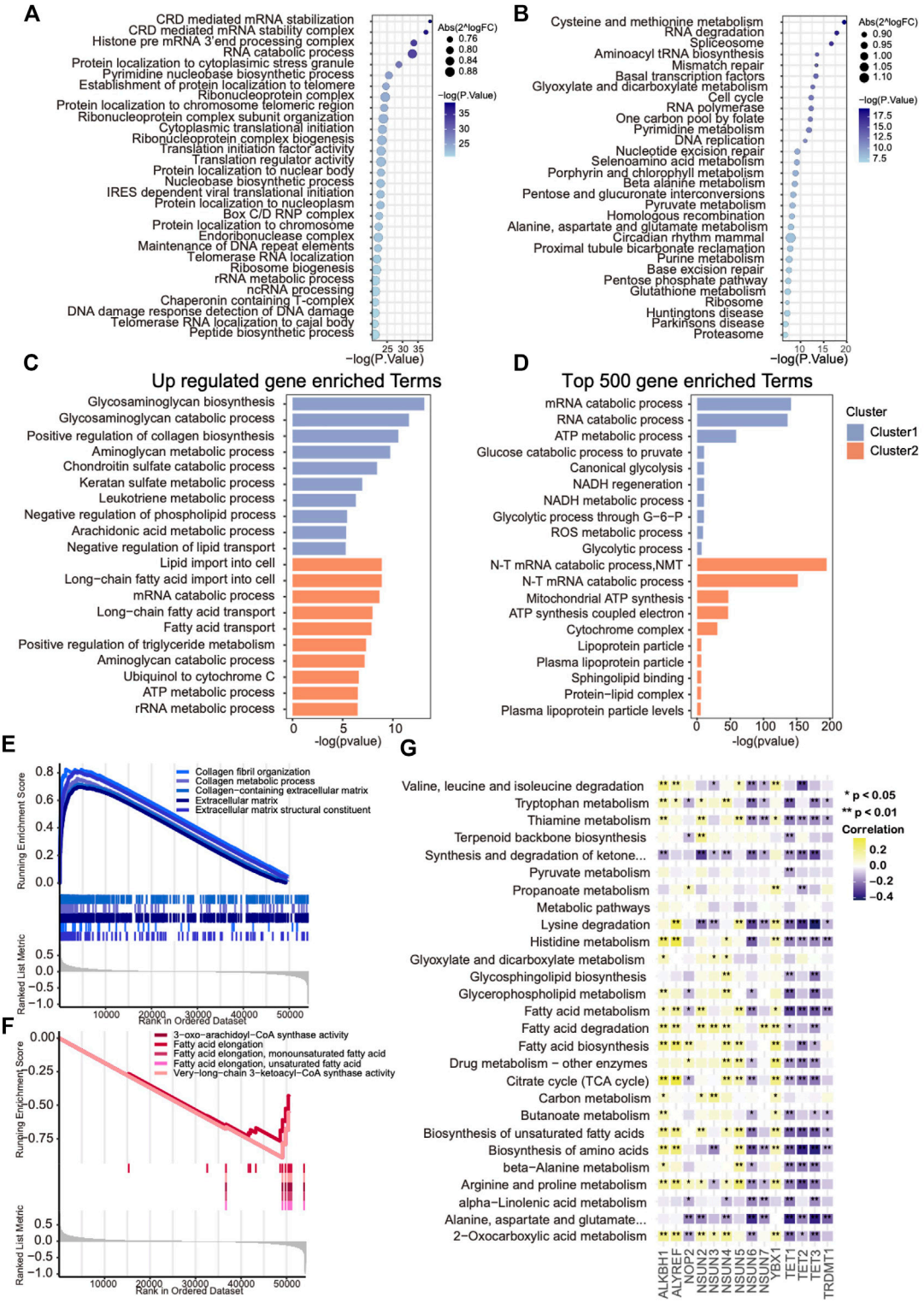

FIGURE 4 | Metabolic heterogeneity in ovarian cancers with distinct m^{5}C modification patterns. **(A,B)** Bubble plot showing GSVA enrichment analysis of the top 30 changed GO and KEGG hallmark pathways between two m^{5}C clusters. **(C)** The most enriched metabolism-related GO pathways using differentially expressed genes in each m^{5}C cluster. **(D)** The most enriched metabolism-related GO pathways using the top 500 up-regulated genes in each m^{5}C cluster. **(E,F)** GSEA analysis showing the significant metabolism-related pathways up-regulated in each m^{5}C cluster. **(G)** Correlation analysis between GSVA enrichment scores of the changed metabolism-related pathways in each m^{5}C cluster and mRNA levels of m^{5}C regulators.

significantly down-regulated in patients with NSUN2 amplification compared with wild type (**Figures 2K-M**). These data indicate the complex cross-talk among m^5C regulators in OVC.

Consensus Clustering of m^5C RNA Methylation Regulators Identifying Two Clusters With the Distinct OS

Based on the expression profile of m^5C regulators in 374 OVC patients (TCGA), we used unsupervised consensus clustering analysis to distinguish different m^5C modification patterns, and two clusters were identified (**Figures 3A–C**). k = 2 is the optimal stable clustering when compared with k = 3–8 (**Supplementary Figure S1B**). Distinct expression profiles of m^5C RNA methylation regulators, clinicopathological parameters, and log2 (fold change) of regulators are illustrated in **Figure 3D**. According to χ^2 test results, no statistical differences were found in lymphatic invasion (p = 1), venous invasion (p = 0.60), tumor residual (p = 0.28), International Federation of Gynecology and Obstetrics stage (p = 0.59), and grade (p = 0.13) between two clusters. TET2 was significantly up-regulated in cluster 1; ALYREF, NOP2, NSUN4, NSUN5, and YBX1 were substantially up-regulated in cluster 2. Despite similar clinicopathological parameters, the OS of patients in cluster 2 was better than cluster 1 (p = 0.015) (**Figure 3E**). We also examined the correlations of m^5C regulators and clinicopathological parameters, and the results showed weak correlation between them (**Supplementary Figure S2A**).

Functional Annotation Revealing the Metabolism Heterogeneity of the Two Subtypes

To further investigate the activated biological processes that may result in distinct survival in each cluster, functional annotations were conducted through three different methods. First, GSVA scores of GO and KEGG hallmark gene sets were calculated, and the differential analysis was performed to explore the discrepancies in pathways among two clusters, of which metabolism-related pathways occupied more than half of the top 30 enriched pathways (**Figures 4A,B**). Then, the top 500 expressed genes of each cluster and phenotype-related DEGs were selected for GO enrichment analysis. The results revealed that glycosaminoglycan and collagen metabolism–related pathways were up-regulated in cluster 1, whereas fatty acid metabolism–related pathways were up-regulated in cluster 2, which were further supported by the GSEA results (**Figures 4C–F**). To further explore the metabolism heterogeneity between the two clusters, the enrichment scores of 91 metabolic pathways downloaded from the KEGG database were calculated, and the varied metabolic pathways between the two clusters were analyzed. Differences were found in 27 of 91 (29.7%) metabolic pathways between two clusters. In addition, a correlation analysis was performed between those metabolic pathway enrichment scores and mRNA levels of m^5C regulators. A significant negative correlation with these metabolism processes was found in eraser genes and positive correlation in writer genes except for NSUN6 and NOP2 (**Figure 4G**). Taken together, these results indicate that m^5C modification might contribute to OVC survival difference through regulating metabolism heterogeneity.

Representative Metabolism-Related Genes With the Prognostic Value in Different m^5C Modification Patterns

An overlapping analysis was made to explore the leading metabolic genes that contributed to survival difference of two clusters (**Figure 5A**). 13 m^5C cluster-specific metabolism genes with prognostic values were identified, as is illustrated in the Venn plot. According to the results of GO enrichment analysis using phenotype-related DEGs, GSEA, and GSVA, the collagen, glycosaminoglycan, and aminoglycan metabolism were up-regulated in cluster 1, whereas fatty acid metabolism was up-regulated in cluster 2. We visualized those genes in activated pathways of two m^5C modification phenotype clusters (**Figures 5B,C**), and those important genes with prognostic value were marked in the circos plot. The fold change and p of 13 representative genes are shown in the volcano plot (**Figure 5D**). Kaplan–Meier analysis curves for OS in eight representative genes are presented (**Figures 5E–L**).

Different Sensitivity to Chemotherapies Between Two Clusters

In order to detect whether the two clusters with m^5C modification patterns had different drug sensitivity, we made the sensitivity prediction of 199 drugs for 374 OVC patients from TCGA dataset. Two clusters exhibited different sensitivities in a total of 44 drugs *via* t test for imputed sensitivity score, including Paclitaxel_1,080, Docetaxel_1,007, and Cisplatin_1,005, which were included in the standard chemotherapy of OVC. Higher sensitivities of these three chemotherapeutic drugs were observed in cluster 2 (**Figure 6**).

Establishment and Evaluation of a Risk Score Signature With RNA m^5C Methylation Regulators

As clusters with different m^5C modification patterns exhibited altered metabolism pathways and chemotherapeutic drug sensitivity that were associated with the differences in prognosis, we further explored the predictive value of RNA m^5C methylation regulators for OS. The univariate survival analyses using Cox proportional hazards models were performed, and three genes with $p < 0.1$ were selected for the LASSO Cox algorithm (**Supplementary Figure S2B**). Then, the LASSO algorithm with 10 folds of cross-validation was applied to establish a risk score prediction model for OS. Two hundred eighty of 374 OVC patients in TCGA cohorts formed the internal training set, and the rest of 94 patients formed the internal testing set. The GSE19829 formed the external testing set. ALYREF, NOP2, and TET2 finally entered in the model (**Figures 7A,B**),

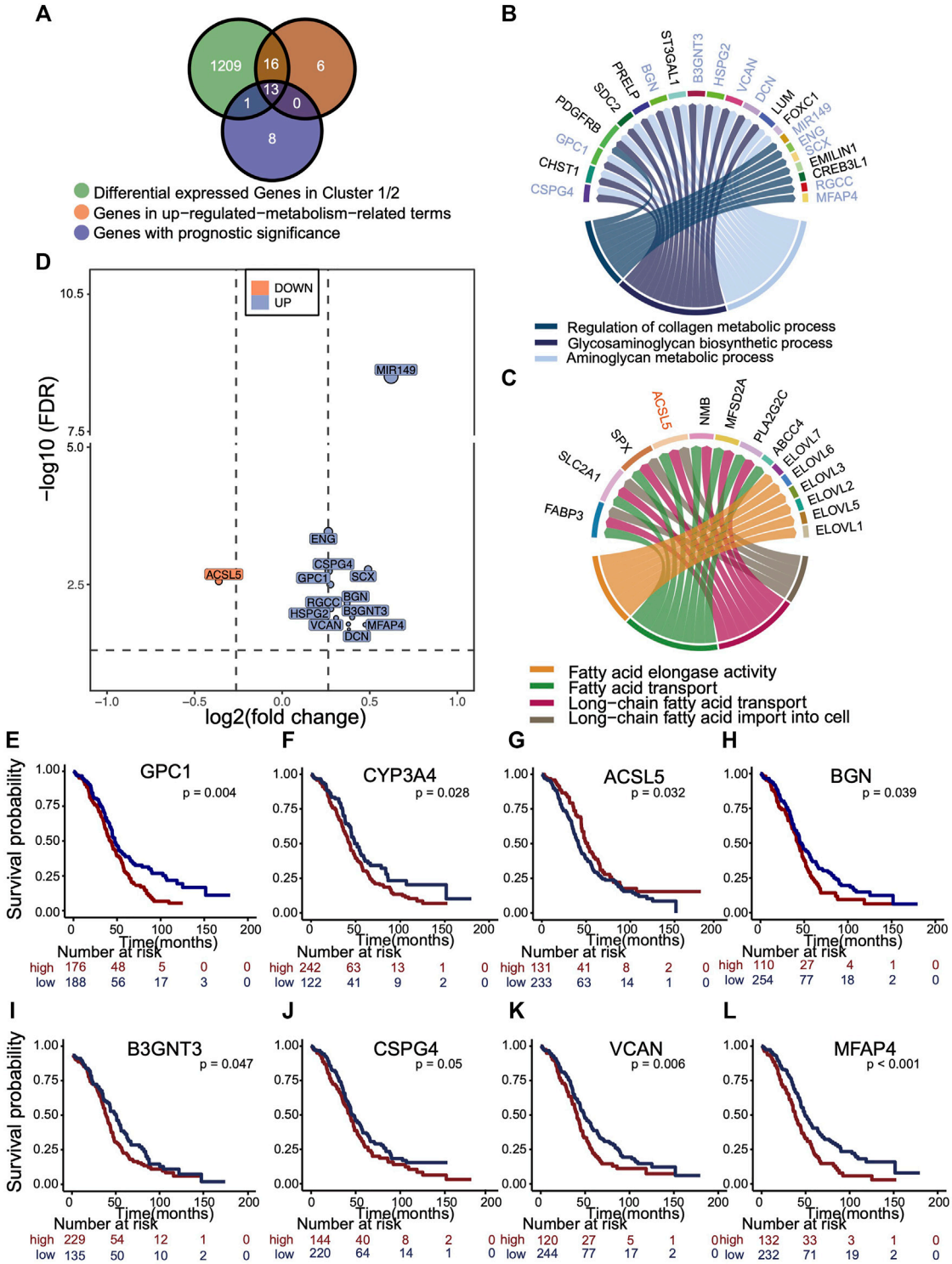

FIGURE 5 | Selection of representative genes differentially expressed in m^{5}C cluster, related to metabolism and with prognostic significance. **(A)** Venn plot showing the overlapping analysis of genes that were differentially expressed (fold change >1.5 and $p < 0.05$) in two clusters, enriched in up-regulated metabolic pathways in each cluster, and had the prognostic significance. **(B,C)** *Circus* plot exhibiting the metabolic pathways up-regulated in each m^{5}C cluster and those 13 genes with prognostic value were marked. Blue, up-regulated in cluster 1. Orange, up-regulated in cluster 2. **(D)** Volcano plot distributes the relative expressions 13 representative genes with log2 (fold change) and log10 (FDR). The reference is gene expression of cluster 1. Blue, up-regulated in cluster 1. Orange, up-regulated in cluster 2. **(E–L)** Kaplan–Meier overall survival curves of eight representative genes.

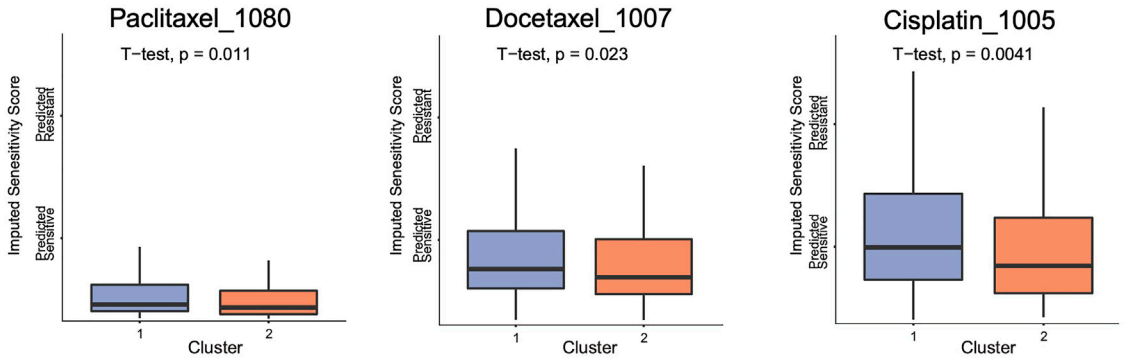

FIGURE 6 | The boxplot of imputed sensitivity score of three chemotherapeutic drugs in two clusters.

and the risk core model is (ALYREF*-0.00349425170618238) + (NOP2*0.0200758391547147) + (TET2*0.145822477408262). Patients were then divided into subgroups of low score and high score according to the cutoff value. The distribution of risk scores in the internal training set and internal testing set is demonstrated in **Figure 7C** and **Supplementary Figure S2C**, and the results suggest the risk score model could distinguish those patients with poor survivals. Patients with high score exhibit poor OS, which were verified in internal training set ($p = 0.016$, hazard ratio [HR] = 3.2), internal testing set ($p = 0.012$, HR = 10), and external testing set ($p = 0.02$, HR = 2.1) (**Figures 7D–F**). The AUCs of ROC curves of the prediction were approximately 0.6 (**Supplementary Figures S2D,E**). To confirm the role of key genes in the risk score signature, *in vitro* experiments were performed. The results showed that knockdown of TET2 in OVC cells could hinder the cell malignant growth, suggesting its potential in the prediction of OS prognosis (**Supplementary Figure S2F**). Furthermore, multivariate analysis of Cox proportional hazards was performed to further confirm the performance of m^5C risk score prediction for OS, and the results showed that the m^5C risk score was an independent prognostic factor ($p = 0.014$, HR = 38.34) (**Figure 7G**).

DISCUSSION

In the present study, the metabolism heterogeneity in two clusters based on m^5C expression profile was annotated through enrichment analyses and found to be significantly correlated with the mRNA levels of m^5C regulators. Then, 13 metabolism-related DEGs of two m^5C clusters related RNA m^5C methylation were identified, which were also associated with OS. Besides metabolism reprogramming, RNA m^5C regulators could also trigger altered chemotherapeutic drug sensitivity and consequently influence survival in OVC. Ultimately, a prognostic model comprising of ALYREF, NOP2, and TET2 for OS was developed for further verifying predictive value of m^5C regulators for prognosis in OVC.

As the present diagnosis and screening program in OVC still have limitations, efforts have been made to seek predictive biomarkers related to cancer occurrence and progression. Through these biomarkers, the distinction of subtypes with different prognoses and molecular characteristics will make the identification of patient subgroups who could well respond to a certain treatment or who had worse survival. In the present study, incorporating mRNA data of ALYREF, NOP2, and TET2 could well stratify those patients with worse survivals, providing evidence for clinical practice. The predictive value of m^5C regulators has also been confirmed in glioma (Wang et al., 2020), breast cancer (Huang et al., 2021), and head and neck squamous cell carcinoma (Xue et al., 2020), and our study made extending support for their predictive role in OVC.

Metabolism reprogramming in OVC has been implicated in the pathogenesis, progression, and target therapy for cancer. In our study, glycosaminoglycan and collagen metabolism–related pathways were activated in cluster 1 and fatty acid metabolism–related pathways were activated in cluster 2. Fatty acids are important components of lipids such as fats, sterol esters, and phospholipids. Lipid metabolism dysregulation has been verified to participate in cancer progression (Li et al., 2021), but it has a more special implication in OVC, as an almost symbiotic relationship exists between OVC and the fat-containing cells in the omentum. FABP4, ELOVL2, and ACSL5 as important genes involved in biosynthesis and transport of fatty acids were found to be up-regulated in cluster 2. FABP4 was highly expressed on the membrane of metastasis OVC cells at the adipocyte–cancer cell interface and mediated lipid accumulation and effect on invasion (Zhao et al., 2019). ELOVL2 has been reported to participate in the biosynthesis of polyunsaturated fatty acids and be involved in tumorigenicity in glioma cancer stem cells (Gimple et al., 2019). ACSL family is responsible for activating long-chain fatty acids, and family members have opposite functions toward carcinogenesis. ACSL5 is nuclear-coded and expressed in the mitochondria and physiologically participates in the proapoptotic sensing of cells acting as a tumor suppressor, which could possibly explain the relatively better prognosis of cluster 2 where ACSL5 was dominantly up-regulated (Quan et al., 2021). The collagen metabolism alteration influences the distribution of collagen and extracellular matrix (ECM)

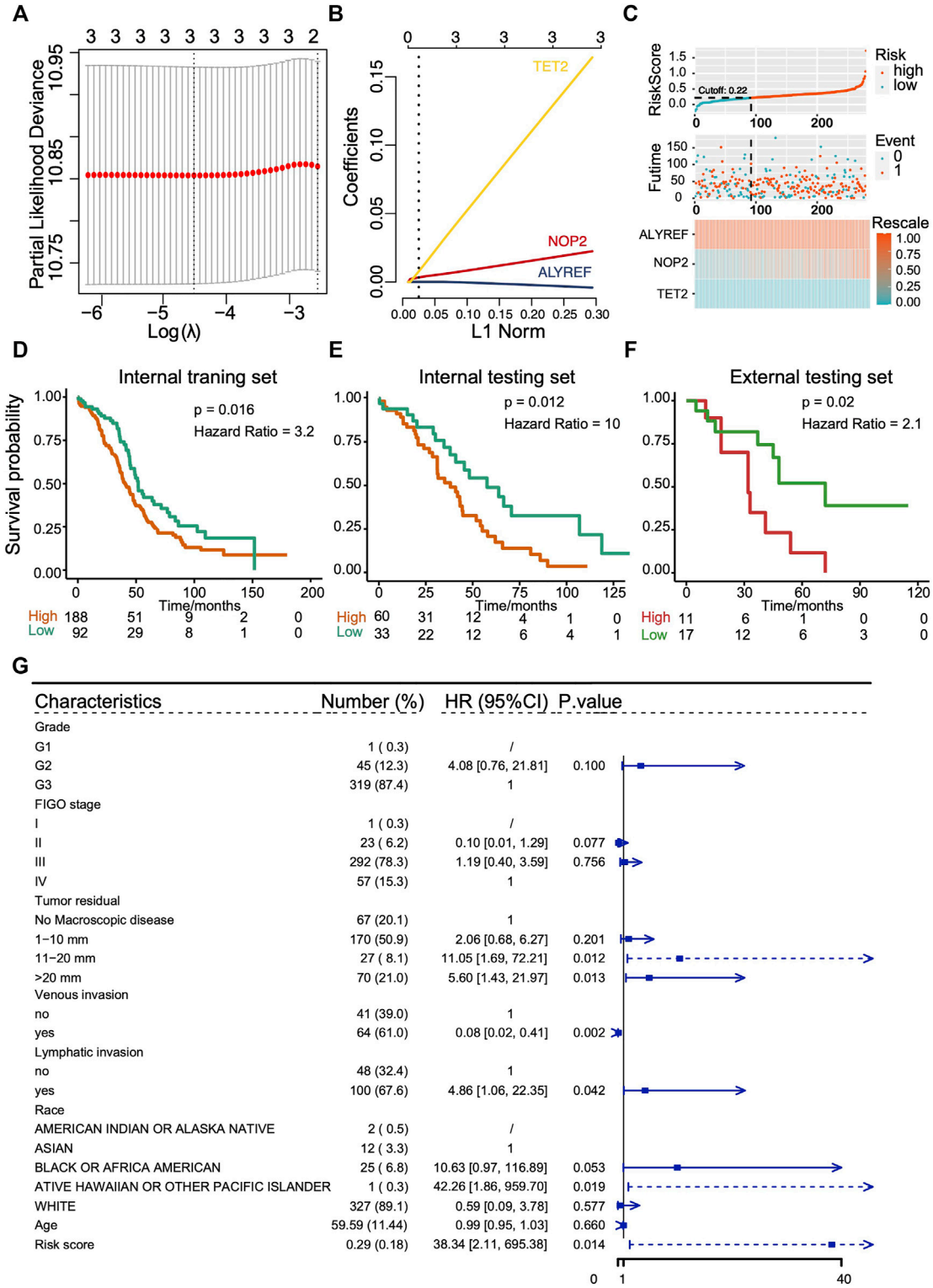

FIGURE 7 | Construction and evaluation of prognostic prediction model with three RNA m^{5}C regulators in TCGA cohort and GEO cohort (GSE19829). **(A,B)** LASSO Cox regression analysis results showing the identification of three prognostic risk signature genes, and the risk score model is (ALYREF*-0.00349425170618238) + (NOP2*0.0200758391547147) + (TET2*0.145822477408262). **(C)** The distribution of prognostic signature-based risk score in internal training set. **(D–F)** The Kaplan–Meier overall survival analysis for patients with high score and low score in internal training set, internal testing set, and external testing set. **(G)** The m^{5}C risk score in Cox multivariate analysis for OS of ovarian cancer patients.

structure, thus affecting cancer progression (Xu et al., 2019). The glycosaminoglycans, another important component of ECM, were found to be involved in multiple signaling pathways related to angiogenesis, cancer invasion, and metastasis (Morla, 2019). VCAN, which is one member of glycosaminoglycan gene sets with leading expression in cluster 1, was previously reported to be up-regulated in ovarian stromal cells and associated with increased microvessel density and poorer survival (Ghosh et al., 2010). In this study, we found the heterogeneity of lipid, glycosaminoglycans, and collagen metabolism in two clusters with distinct m^5C modification. The stepwise accumulation of altered metabolism at mRNA levels in different m^5C clusters eventually resulted in distinct prognoses, indicating that the metabolism alteration has prognostic significance.

The role of epigenetic modifications in cancer metabolism reprogramming has been broadly reported, but there is still a lack of disclosure of how RNA m^5C modification functions in cancer metabolism. It was demonstrated that ALYREF binds the 3′-UTR of PKM2 mRNA and promotes the glucose metabolism of bladder cancer in an m^5C-dependent manner (Wang et al., 2021). In this study, we found 13 representative metabolic genes that were related to m^5C RNA methylation in OVC. All of them have positive or negative correlations with RNA m^5C regulators at the mRNA level (**Supplementary Figure S2G**). Consequently, experimental verification could be done in the future to verify the regulatory role of RNA m^5C methylation of those metabolism genes in cancer.

In conclusion, our study depicted the landscape of genetic variation and gene expression of m^5C regulators in OVC and established a prognostic prediction model formed by ALYRER, NOP2, and TET2 for OS. We also uncovered the indispensable roles of m^5C modification in metabolism heterogeneity and altered sensitivity to chemotherapeutic drugs.

DATA AVAILABILITY STATEMENT

The original contributions presented in the study are included in the article/**Supplementary Material**, further inquiries can be directed to the corresponding author.

AUTHOR CONTRIBUTIONS

PY put forward the ideas of this article. PY, TL, and JX drafted and reviewed the article. JX performed the bio-informatics analysis. YC, YW, and XL helped with acquisition of data and analysis and interpretation of data. All authors read and approved the final manuscript.

FUNDING

This work was sponsored by the National Natural Science Foundation of China (82072886), the Natural Science Foundation of Chongqing (cstc2020jcyj-msxmX0344) and the Natural Science Foundation of Chongqing (cstc2021jcyj-bsh0022).

ACKNOWLEDGMENTS

The authors acknowledge contributions from TCGA databases.

SUPPLEMENTARY MATERIAL

The Supplementary Material for this article can be found online at: https://www.frontiersin.org/articles/10.3389/fcell.2022.807786/full#supplementary-material

REFERENCES

Amort, T., Rieder, D., Wille, A., Khokhlova-Cubberley, D., Riml, C., Trixl, L., et al. (2017). Distinct 5-methylcytosine Profiles in Poly(A) RNA from Mouse Embryonic Stem Cells and Brain. *Genome Biol.* 18 (1), 1. doi:10.1186/s13059-016-1139-1

Blanco, S., Bandiera, R., Popis, M., Hussain, S., Lombard, P., Aleksic, J., et al. (2016). Stem Cell Function and Stress Response Are Controlled by Protein Synthesis. *Nature* 534 (7607), 335–340. doi:10.1038/nature18282

Chai, R. C., Li, Y. M., Zhang, K. N., Chang, Y. Z., Liu, Y. Q., Zhao, Z., et al. (2019a). RNA Processing Genes Characterize RNA Splicing and Further Stratify Lower-Grade Glioma. *JCI Insight* 5, e130591. doi:10.1172/jci.insight.130591

Chai, R. C., Wu, F., Wang, Q. X., Zhang, S., Zhang, K. N., Liu, Y. Q., et al. (2019b). m^6A RNA Methylation Regulators Contribute to Malignant Progression and Have Clinical Prognostic Impact in Gliomas. *Aging* 11, 1204–1225. doi:10.18632/aging.101829

Chen, X., Li, A., Sun, B.-F., Yang, Y., Han, Y.-N., Yuan, X., et al. (2019). 5-methylcytosine Promotes Pathogenesis of Bladder Cancer through Stabilizing mRNAs. *Nat. Cel Biol* 21 (8), 978–990. doi:10.1038/s41556-019-0361-y

Chen, Y. S., Yang, W. L., Zhao, Y. L., and Yang, Y. G. (2021). Dynamic Transcriptomic M5 C and its Regulatory Role in RNA Processing. *Wiley Interdiscip. Rev. RNA* 12 (4), e1639. doi:10.1002/wrna.1639

Cheng, J. X., Chen, L., Li, Y., Cloe, A., Yue, M., Wei, J., et al. (2018). RNA Cytosine Methylation and Methyltransferases Mediate Chromatin Organization and 5-azacytidine Response and Resistance in Leukaemia. *Nat. Commun.* 9 (1), 1163. doi:10.1038/s41467-018-03513-4

Clough, E., and Barrett, T. (2016). The Gene Expression Omnibus Database. *Methods Mol. Biol.* 1418, 93–110. doi:10.1007/978-1-4939-3578-9_5

Freeman, J. W., McGrath, P., Bondada, V., Selliah, N., Ownby, H., Maloney, T., et al. (1991). Prognostic Significance of Proliferation Associated Nucleolar Antigen P120 in Human Breast Carcinoma. *Cancer Res.* 51 (8), 1973–1978.

Gao, J., Aksoy, B. A., Dogrusoz, U., Dresdner, G., Gross, B., Sumer, S. O., et al. (2013). Integrative Analysis of Complex Cancer Genomics and Clinical Profiles Using the cBioPortal. *Sci. Signal.* 6 (269), pl1. doi:10.1126/scisignal.2004088

Ghosh, S., Albitar, L., LeBaron, R., Welch, W. R., Samimi, G., Birrer, M. J., et al. (2010). Up-regulation of Stromal Versican Expression in Advanced Stage Serous Ovarian Cancer. *Gynecol. Oncol.* 119 (1), 114–120. doi:10.1016/j.ygyno.2010.05.029

Gimple, R. C., Kidwell, R. L., Kim, L. J. Y., Sun, T., Gromovsky, A. D., Wu, Q., et al. (2019). Glioma Stem Cell-specific Superenhancer Promotes Polyunsaturated Fatty-Acid Synthesis to Support EGFR Signaling. *Cancer Discov.* 9 (9), 1248–1267. doi:10.1158/2159-8290.cd-19-0061

Heagerty, P. J., and Zheng, Y. (2005). Survival Model Predictive Accuracy and ROC Curves. *Biometrics* 61 (1), 92–105. doi:10.1111/j.0006-341x.2005.030814.x

Huang, Z., Pan, J., Wang, H., Du, X., Xu, Y., Wang, Z., et al. (2021). Prognostic Significance and Tumor Immune Microenvironment Heterogenicity of m5C RNA Methylation Regulators in Triple-Negative Breast Cancer. *Front. Cel Dev. Biol.* 9, 657547. doi:10.3389/fcell.2021.657547

Jemal, A., Murray, T., Samuels, A., Ghafoor, A., Ward, E., and Thun, M. J. (2003). Cancer Statistics, 2003. *CA Cancer J. Clin.* 53, 5–26. doi:10.3322/canjclin.53.1.5

Kaufman, B., Shapira-Frommer, R., Schmutzler, R. K., Audeh, M. W., Friedlander, M., Balmaña, J., et al. (2015). Olaparib Monotherapy in Patients with Advanced Cancer and a Germline BRCA1/2 Mutation. *J. Clin. Oncol.* 33 (3), 244–250. doi:10.1200/JCO.2014.56.2728

Kim, H., Xu, H., George, E., Hallberg, D., Kumar, S., Jagannathan, V., et al. (2020). Combining PARP with ATR Inhibition Overcomes PARP Inhibitor and Platinum Resistance in Ovarian Cancer Models. *Nat. Commun.* 11 (1), 3726. doi:10.1038/s41467-020-17127-2

Kristeleit, R., Shapiro, G. I., Burris, H. A., Oza, A. M., LoRusso, P., Patel, M. R., et al. (2017). A Phase I-II Study of the Oral PARP Inhibitor Rucaparib in Patients with Germline BRCA1/2-Mutated Ovarian Carcinoma or Other Solid Tumors. *Clin. Cancer Res.* 23 (15), 4095–4106. doi:10.1158/1078-0432.ccr-16-2796

Lheureux, S., Braunstein, M., and Oza, A. M. (2019). Epithelial Ovarian Cancer: Evolution of Management in the Era of Precision Medicine. *CA Cancer J Clin.* 69, 280. doi:10.3322/caac.21559

Li, L-Y., Yang, Q., Jiang, Y-Y., Yang, W., Jiang, Y., Li, X., et al. (2021). Interplay and Cooperation between SREBF1 and Master Transcription Factors Regulate Lipid Metabolism and Tumor-Promoting Pathways in Squamous Cancer. *Nat. Commun.* 12 (1), 4362. doi:10.1038/s41467-021-24656-x

Maeser, D., Gruener, R. F., and Huang, R. S. (2021). oncoPredict: an R Package for Predicting *In Vivo* or Cancer Patient Drug Response and Biomarkers from Cell Line Screening Data. *Brief Bioinform* 22. doi:10.1093/bib/bbab260

Moore, K., Colombo, N., Scambia, G., Kim, B.-G., Oaknin, A., Friedlander, M., et al. (2018). Maintenance Olaparib in Patients with Newly Diagnosed Advanced Ovarian Cancer. *N. Engl. J. Med.* 379 (26), 2495–2505. doi:10.1056/nejmoa1810858

Morla, S. (2019). Glycosaminoglycans and Glycosaminoglycan Mimetics in Cancer and Inflammation. *Int. J. Mol. Sci.* 20 (8), 1963. doi:10.3390/ijms20081963

Nombela, P., Miguel-López, B., and Blanco, S. (2021). The Role of m6A, m5C and Ψ RNA Modifications in Cancer: Novel Therapeutic Opportunities. *Mol. Cancer* 20 (1), 18. doi:10.1186/s12943-020-01263-w

Pujade-Lauraine, E., Ledermann, J. A., Selle, F., Gebski, V., Penson, R. T., Oza, A. M., et al. (2017). Olaparib Tablets as Maintenance Therapy in Patients with Platinum-Sensitive, Relapsed Ovarian Cancer and a BRCA1/2 Mutation (SOLO2/ENGOT-Ov21): a Double-Blind, Randomised, Placebo-Controlled, Phase 3 Trial. *Lancet Oncol.* 18 (9), 1274–1284. doi:10.1016/S1470-2045(17)30469-2

Pujade-Lauraine, E. (2017). New Treatments in Ovarian Cancer. *Ann. Oncol.* 28 (Suppl. l_8), viii57–viii60. doi:10.1093/annonc/mdx442

Quan, J., Bode, A. M., and Luo, X. (2021). ACSL Family: The Regulatory Mechanisms and Therapeutic Implications in Cancer. *Eur. J. Pharmacol.* 909, 174397. doi:10.1016/j.ejphar.2021.174397

Ritchie, M. E., Phipson, B., Wu, D., Hu, Y., Law, C. W., Shi, W., et al. (2015). Limma powers Differential Expression Analyses for RNA-Sequencing and Microarray Studies. *Nucleic Acids Res.* 43 (7), e47. doi:10.1093/nar/gkv007

Roundtree, I. A., Evans, M. E., Pan, T., and He, C. (2017). Dynamic RNA Modifications in Gene Expression Regulation. *Cell* 169 (7), 1187–1200. doi:10.1016/j.cell.2017.05.045

Scrucca, L., Santucci, A., and Aversa, F. (2007). Competing Risk Analysis Using R: an Easy Guide for Clinicians. *Bone Marrow Transpl.* 40 (4), 381–387. doi:10.1038/sj.bmt.1705727

Siegel, R. L., Miller, K. D., Fuchs, H. E., and Jemal, A. (2021). Cancer Statistics, 2021. *CA Cancer J. Clinicians* 71 (1), 7, doi:10.3322/caac.21654

Singer, G., Oldt, R., Cohen, Y., Wang, B. G., Sidransky, D., Kurman, R. J., et al. (2003). Mutations in BRAF and KRAS Characterize the Development of Low-Grade Ovarian Serous Carcinoma. *JNCI J. Natl. Cancer Inst.* 95 (6), 484–486. doi:10.1093/jnci/95.6.484

Tang, Y., Gao, C.-C., Gao, Y., Yang, Y., Shi, B., Yu, J.-L., et al. (2020). OsNSUN2-Mediated 5-Methylcytosine mRNA Modification Enhances Rice Adaptation to High Temperature. *Dev. Cel* 53 (3), 272–286. doi:10.1016/j.devcel.2020.03.009

Wang, J. Z., Zhu, W., Han, J., Yang, X., Zhou, R., Lu, H. C., et al. (2021). The Role of the HIF-1α/ALYREF/PKM2 axis in Glycolysis and Tumorigenesis of Bladder Cancer. *Cancer Commun.* 41 (7), 560–575. doi:10.1002/cac2.12158

Wang, P., Wu, M., Tu, Z., Tao, C., Hu, Q., Li, K., et al. (2020). Identification of RNA: 5-Methylcytosine Methyltransferases-Related Signature for Predicting Prognosis in Glioma. *Front. Oncol.* 10, 1119. doi:10.3389/fonc.2020.01119

Wilkerson, M. D., and Hayes, D. N. (2010). ConsensusClusterPlus: a Class Discovery Tool with Confidence Assessments and Item Tracking. *Bioinformatics* 26 (12), 1572–1573. doi:10.1093/bioinformatics/btq170

Xue, M., Shi, Q., Zheng, L., Li, Q., Yang, L., and Zhang, Y. (2020). Gene Signatures of m5C Regulators May Predict Prognoses of Patients with Head and Neck Squamous Cell Carcinoma. *Am. J. Transl Res.* 12, 6841. ISSN:1943-8141/AJTR0116260.

Xu, S., Xu, H., Wang, W., Li, S., Li, H., Li, T., et al. (2019). The Role of Collagen in Cancer: from Bench to Bedside. *J. Transl Med.* 17 (1), 309. doi:10.1186/s12967-019-2058-1

Yang, L., Perrera, V., Saplaoura, E., Apelt, F., Bahin, M., Kramdi, A., et al. (2019). m5C Methylation Guides Systemic Transport of Messenger RNA over Graft Junctions in PlantsC Methylation Guides Systemic Transport of Messenger RNA over Graft Junctions in Plants. *Curr. Biol.* 29 (15), 2465–2476. doi:10.1016/j.cub.2019.06.042

Yang, X., Yang, Y., Sun, B.-F., Chen, Y.-S., Xu, J.-W., Lai, W.-Y., et al. (2017). 5-methylcytosine Promotes mRNA export - NSUN2 as the Methyltransferase and ALYREF as an m5C Reader. *Cell Res* 27 (5), 606–625. doi:10.1038/cr.2017.55

Yu, G., Wang, L.-G., Han, Y., and He, Q.-Y. (2012). clusterProfiler: an R Package for Comparing Biological Themes Among Gene Clusters. *OMICS: A J. Integr. Biol.* 16 (5), 284–287. doi:10.1089/omi.2011.0118

Zhang, B., Wu, Q., Li, B., Wang, D., Wang, L., and Zhou, Y. L. (2020). m6A Regulator-Mediated Methylation Modification Patterns and Tumor Microenvironment Infiltration Characterization in Gastric cancerA Regulator-Mediated Methylation Modification Patterns and Tumor Microenvironment Infiltration Characterization in Gastric Cancer. *Mol. Cancer* 19 (1), 53. doi:10.1186/s12943-020-01170-0

Zhao, G., Cardenas, H., and Matei, D. (2019). Ovarian Cancer-Why Lipids Matter. *Cancers (Basel)* 11 (12), 1870. doi:10.3390/cancers11121870

Conflict of Interest: The authors declare that the research was conducted in the absence of any commercial or financial relationships that could be construed as a potential conflict of interest.

Publisher's Note: All claims expressed in this article are solely those of the authors and do not necessarily represent those of their affiliated organizations, or those of the publisher, the editors, and the reviewers. Any product that may be evaluated in this article, or claim that may be made by its manufacturer, is not guaranteed or endorsed by the publisher.

frontiers | Frontiers in Cell and Developmental Biology

REVIEW
published: 04 July 2022
doi: 10.3389/fcell.2022.935224

RNA N^6-Methyladenine Modification, Cellular Reprogramming, and Cancer Stemness

Huarong Chen[1,2*†], *Yifei Wang*[3†], *Hao Su*[1,2], *Xiaoting Zhang*[1,2], *Hongyan Chen*[1,2] *and Jun Yu*[2*]

[1]Department of Anaesthesia and Intensive Care and Peter Hung Pain Research Institute, The Chinese University of Hong Kong, Hong Kong, China, [2]Institute of Digestive Disease and Department of Medicine and Therapeutics, State Key Laboratory of Digestive Disease, Li Ka Shing Institute of Health Sciences, CUHK Shenzhen Research Institute, The Chinese University of Hong Kong, Hong Kong, China, [3]Department of Anatomical and Cellular Pathology, State Key Laboratory of Oncology in South China, Prince of Wales Hospital, The Chinese University of Hong Kong, Hong Kong, China

OPEN ACCESS

Edited by:
Yanquan Zhang,
University of Kentucky, United States

Reviewed by:
Liu Dabin,
Harbin Medical University, China
Ling-Ling Zheng,
Sun Yat-sen University, China
Yujuan Dong,
The Chinese University of Hong Kong, China

***Correspondence:**
Huarong Chen
hchen2@cuhk.edu.hk
Jun Yu
junyu@cuhk.edu.hk

[†]These authors have contributed equally to this work

Specialty section:
This article was submitted to Signaling, a section of the journal Frontiers in Cell and Developmental Biology

Received: 03 May 2022
Accepted: 26 May 2022
Published: 04 July 2022

Citation:
Chen H, Wang Y, Su H, Zhang X, Chen H and Yu J (2022) RNA N^6-Methyladenine Modification, Cellular Reprogramming, and Cancer Stemness. Front. Cell Dev. Biol. 10:935224. doi: 10.3389/fcell.2022.935224

N^6-Methyladenosine (m^{6}A) is the most abundant modification on eukaryote messenger RNA and plays a key role in posttranscriptional regulation of RNA metabolism including splicing, intracellular transport, degradation, and translation. m^{6}A is dynamically regulated by methyltransferases (writers), RNA-binding proteins (readers), and demethylases (erasers). Recent studies demonstrate that perturbation of m^{6}A regulators remarkably influences cell fate transitions through rewiring various biological processes, such as growth, differentiation, and survival. Moreover, aberrant m^{6}A modification is implicated in a variety of diseases, in particular cancer. In this review, we describe the functional linkage of m^{6}A modifications to cellular reprogramming and cancer stemness properties.

Keywords: RNA metabolism, stemness, tumorigenesis, N^6-methyladenose, reprogramming

INTRODUCTION

N^6-Methyladenosine modification (m^{6}A) refers to the methylation of the adenosine base at the nitrogen-6 position and tends to occur in a consensus sequence RRACH. It was originally discovered in 1970s and now recognized as the most abundant modification present in eukaryotic messenger RNA (mRNA) (Desrosiers et al., 1974; Adams and Cory, 1975; Lavi and Shatkin, 1975; Wei et al., 1975). m^{6}A modification is present in different types of RNAs including mRNAs, transfer RNAs (tRNAs), ribosomal RNAs (rRNAs), circular RNAs (circRNAs), micro RNAs (miRNA), and long non-coding RNAs (lncRNAs) (Liu and Pan, 2016). The process of m^{6}A modification is reversible and regulated by methyltransferases (writers), demethylases (erasers), and RNA-binding proteins (readers). Methyltransferase complex consisting of methyltransferase 3 (METTL3) (Bokar et al., 1997), methyltransferase 14 (METTL14) (Liu et al., 2014), and WT1-associated protein (WTAP) (Ping et al., 2014) catalyzes m^{6}A formation. Other m^{6}A writers such as RNA-binding motif protein 15/15B (RBM15/15B) (Patil et al., 2016), vir-like M6A methyltransferase associated (VIRMA) (Yue et al., 2018), and zinc finger CCCH-type containing 13 (ZC3H13) (Wen et al., 2018) have been identified to facilitate the function of the methyltransferase complex. On the other hand, fat mass and obesity-associated protein (FTO) (Jia et al., 2011) and AlkB homolog H5 (ALKBH5) (Zheng et al., 2013; Alemu et al., 2016), two key demethylases, demethylate m^{6}A modification. Besides, m^{6}A readers, e.g., YTH domain-containing proteins (YTHDF1-3 (Wang et al., 2014a; Wang et al., 2015; Shi et al., 2017) and YTHDC1-2 (Xiao et al., 2016; Wojtas et al., 2017)) and insulin-like growth factor-2 mRNA-binding proteins (IGF2BP1/2/3) (Huang et al., 2018), target m^{6}A marks of

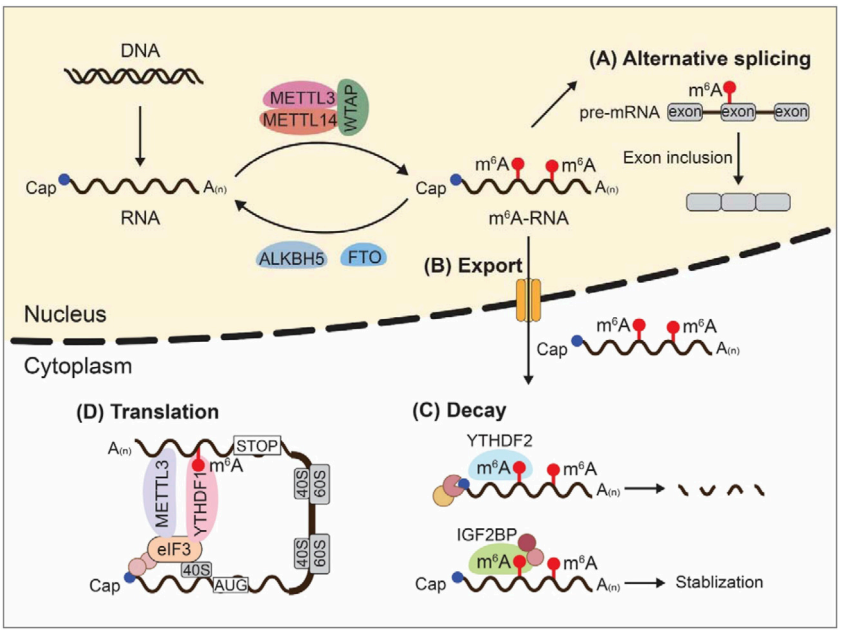

FIGURE 1 | m^{6}A modifications and RNA metabolism. Dynamic m^{6}A modifications inside cells influence almost every step of RNA metabolism including alternative splicing, intracellular transport, degradation, and translation.

transcripts and trigger RNA processing and metabolism such as alternative splicing, intracellular transport, degradation, and translation.

Self-renewal and differentiation are two unique properties of stem cells with the former referring to the capability of stem cells to make more stem cells and maintain the undifferentiated state, while the latter indicating the change of stem cells to a more specialized cell type. Notably, the processes of self-renewal and differentiation are controlled at a transcriptional level wherein epigenetic and epitranscriptomic regulation play critical roles. To date, m^{6}A is proven to be a mark of transcriptome flexibility involved in regulating the function of stem cells. Emerging evidence have demonstrated that m^{6}A modifications are involved in the process of mouse embryonic development (Geula et al., 2015), stem cell self-renewal (Batista et al., 2014; Wang et al., 2014b), spermatogenesis (Zheng et al., 2013), and so on. However, the origins and functions of m^{6}A marks in reprogramming stemness properties are still largely unclear.

Perturbation of m^{6}A regulators strongly affects gene expression patterns and biological functions of cells, leading to a variety of diseases including cancer. Recent evidence reveals a subpopulation of tumor cells, named cancer stem cells (CSCs), responsible for tumor initiation, metastasis, and relapse. The roles of cancer stem cells have been reported in both solid (Visvader and Lindeman, 2008) and hematological cancers (Zagozdzon and Golab, 2015), although the origin of the CSCs remains elusive. They may derive from differentiated cells or tissue-resident stem cells upon tumor initiation. Intriguingly, genes critical for self-renewal of normal stem cells also function as cancer-related genes, e.g., Bmi-1 (Siddique and Saleem, 2012), Nanog (Gawlik-Rzemieniewska and Bednarek, 2016), Notch (Ranganathan et al., 2011), Sox2 (Novak et al., 2020), and Wnt (Zhan et al., 2017). Given that m^{6}A modifications regulate the expression of stemness-related genes, it is not surprising that they also play an important role in CSCs (Zhang et al., 2016; Li et al., 2017; Zhang et al., 2017; Chen et al., 2021).

In this review, we discuss recent studies that underscore the multifaceted role of m^{6}A modifications in controlling gene expression, highlighting key findings that m^{6}A modifications are essential in stem cells reprogramming and cancer stemness properties regulation.

N^6-METHYLADENOSINE AND RNA METABOLISM

m^{6}A controls almost every step of RNA metabolism including alternative splicing, intracellular transport, degradation, and translation (**Figure 1**). In this part, we describe the influences of m^{6}A writers, erasers, and readers on RNA metabolic process through dynamic regulation of m^{6}A.

N^6-Methyladenosine and Alternative Splicing

Alternative splicing (AS) is the process of making messenger RNA (mRNA) from messenger RNA precursor (pre-mRNA) by selecting different combinations of splice sites in pre-mRNA, thus allowing a single gene to code for multiple proteins. AS is essential for generating functional diversity given the limited gene number in eukaryotic organisms. Emerging evidence shows that m^{6}A

writers, METTL3, METTL14, and WTAP, and m^{6}A erasers, ALKBH5 and FTO, are located in nuclear speckles where the AS occurs, indicating a potential role of m^{6}A for controlling pre-mRNA processing. In support of this, treatment of S-adenosylmethionine (SAM) synthesis inhibitors, neplanocin A or cycloleucine, reduced RNA m^{6}A methylation and resulted in nuclear accumulation of unspliced transcripts (Stoltzfus and Dane, 1982; Carroll et al., 1990). Consistently, Dominissini et al. observed a correlation between m^{6}A methylation of multi-isoform genes and isoform switching by analyzing human and mouse transcriptome-wide m^{6}A profiling (Dominissini et al., 2012).

METTL3 was found to colocalize with spliceosomal protein U2 small nuclear ribonucleoprotein B" (U2B′)' in nuclear speckles (Bokar et al., 1997). Silencing of METTL3 could affect AS patterns and gene expressions (Dominissini et al., 2012). WTAP is a regulatory subunit of RNA m^{6}A methyltransferase complex. Localization of METTL3 and METTL14 into nuclear speckles requires interaction with WTAP. Yang et al. showed that WTAP promoted METTL3 and METTL14 accumulation in nuclear speckles and regulated AS of targeted genes (Ping et al., 2014). Knockdown of METTL3 or WTAP led to a remarkable change of transcriptional isoform numbers (Ping et al., 2014). ALKBH5 also colocalized with mRNA-processing factors, including phosphorylated serine/arginine-rich splicing factor 2 (SC35), smith antigen (SM), and alternative splicing factor/splicing factor 2 (ASF/SF2) in nuclear speckles (Zheng et al., 2013). Similarly, FTO was present in nucleoplasm and partially colocalized with splicing factors U4/U6.U5 tri-snRNP-associated protein 1 (SART1), serine/arginine-rich splicing factor 2 (SC35), and RNA polymerase II phosphorylated at Ser2 (Pol II-S2P) (Jia et al., 2011). These two key m^{6}A erasers are both capable of controlling mRNA splicing. ALKBH5 was found to regulate assembly of mRNA processing factors (Zheng et al., 2013); on the other hand, FTO depletion increased the m^{6}A level of target genes, thereby raising the binding capacity of serine/arginine-rich splicing factor 2 (SRSF2) which subsequently increased inclusion of target exons (Zhao et al., 2014). m^{6}A reader YTHDC1 is also engaged in the AS process. YTHDC1 was present in YT bodies near nuclear speckles. Wild type YTHDC1, but not m^{6}A-binding-defective YTHDC1, could recruit pre-mRNA splicing factor SRSF3 (SRp20) but block the binding of SRSF10 (SRp38) to targeted mRNAs in the nucleus, thus promoting exon inclusion (Xiao et al., 2016). All these data indicate an essential regulatory role of m^{6}A in mRNA splicing.

N^6-Methyladenosine and RNA Export

RNAs produced in the nucleus are exported to the cytoplasm through nuclear pore complexes. This is a fundamental step in gene expression process. TREX complex is important for mRNA export. Recent work identified the interactions between TREX subunits (ALYREF, UAP56, THOC5, and CHTOP) and m^{6}A methyltransferases (METTL3, METTL14, WTAP, and KIAA1429) (Lesbirel et al., 2018). The m^{6}A methyltransferase complex could recruit TREX to m^{6}A-modified mRNAs to facilitate their export (Lesbirel et al., 2018). Moreover, depletion of KIAA1429 and WTAP led to an export block for m^{6}A-modified mRNAs (Lesbirel et al., 2018). m^{6}A eraser ALKBH5 also affects mRNA export dependent on its demethylation activity. Cytoplasmic mRNA level was significantly increased after silencing of ALKBH5 because of accelerated nuclear RNA export; re-expression of wild type ALKBH5, but not catalytic inactive mutant H204A, could rescue this phenomenon (Zheng et al., 2013). Binding of YTHDC1 to m^{6}A-modified genes is important for mRNA export. Knockdown of YTHDC1 induced an export block for nuclear m^{6}A-modified mRNA, resulting in accumulation of transcripts in the nucleus (Roundtree et al., 2017). Mechanistically, YTHDC1 interacted with SRSF3, an mRNA export adaptor, to increase RNA binding to SRSF3 (Roundtree et al., 2017).

m^{6}A modifications also participate in circular RNA nuclear export. Depletion of m^{6}A writer METTL3 induced circNSUN2 accumulation in the nucleus, and re-expression of METTL3 could rescue this phenomenon (Chen et al., 2019). Moreover, the m^{6}A reader YTHDC1 was capable of binding to m^{6}A marks of circNSUN2 in the backsplicing junction sites to facilitate the export process (Chen et al., 2019). Together, m^{6}A modifications regulate RNA export.

N^6-Methyladenosine and RNA Decay

RNA decay is the process whereby RNA is enzymatically degraded. RNA decay is important for effective mRNA surveillance and turnover. Accumulating evidence suggest m^{6}A modifications affect RNA stability through dynamic interplays with RNA-binding proteins. In mouse embryonic stem cells, m^{6}A level was found to be negatively correlated with mRNA stability (Wang et al., 2014b). m^{6}A writers METTL3 and METTL14 could form a stable heterodimer to catalyze m^{6}A deposition on RNA. Downregulation of METTL3 and METTL14 reduced the m^{6}A level of mRNA, resulting in more binding of human antigen R (HuR) to mRNA which in turn promoted mRNA stability (Wang et al., 2014b). In line with these findings, depletion of METTL3 in both human and mouse cells led to m^{6}A erasure and prolonged half-life of targeted mRNAs (Batista et al., 2014). Although WTAP lacks m^{6}A catalytic activity, it binds to METTL3-METTL14 complex to enhance m^{6}A deposition. As such, WTAP-mediated m^{6}A modifications were negatively correlated with mRNA stability (Schwartz et al., 2014). Furthermore, silencing of METTL3, METTL14, or WTAP reduced global m^{6}A methylation and increased the lifetime of nascent RNAs (Liu et al., 2014). Therefore, m^{6}A modifications affect RNA stability.

Recent reports state that YTHDF2 is the major decay-inducing reader protein that binds to m^{6}A-modified mRNAs to facilitate RNA degradation (Du et al., 2016; Park et al., 2019). Two distinct mechanisms of YTHDF2-induced mRNA degradation have been identified: RNase P/MRP-mediated endoribonucleolytic-cleavage pathway and carbon catabolite repression 4 (CCR4)-negative on TATA-less (NOT)-mediated deadenylation pathway, depending on whether messenger ribonucleoprotein (mRNP) has heat-responsive protein 12 (HRSP12)-binding site or not (Lee et al., 2020). Showed that m^{6}A-modified RNAs underwent endoribonucleolytic cleavage *via* YTHDF2, HRSP12, and

RNase P/MRP, of which HRSP12 acted as an adaptor to connect YTHDF2 and RNase P/MRP Park et al. (2019). In this case, HRSP12-binding site and RNase P/MRP-directed cleavage site were identified upstream and downstream of YTHDF2-binding site, respectively (Park et al., 2019). Of note, m^{6}A-modified circular RNA could also be degraded through YTHDF2-HRSP12-RNase P/MRP-mediated endoribonucleolytic cleavage (Park et al., 2019). On the other hand, Du et al. reported that YTHDF2 directly recruited CCR4/NOT deadenylase complex to m^{6}A-modified mRNAs, leading to deadenylation of mRNAs (Du et al., 2016). Besides, YTHDF3 was identified to regulate the RNA accessibility of YTHDF2 and enhanced YTHDF2-mediated mRNA decay (Shi et al., 2017). In contrast to YTHDF2-mediated mRNA decay, a recent study revealed that IGF2BP1-3 could recognize m^{6}A markers through their KH domains to stabilize m^{6}A-modified RNA (Huang et al., 2018). Intriguingly, although YTHDF2 and IGF2BP1-3 were all proved to bind to m^{6}A markers, their transcriptome-wide binding sites were distinct (Huang et al., 2018). Therefore, m^{6}A modifications can either enhance or inhibit mRNA stability depending on the binding of specific m^{6}A readers.

N^6-Methyladenosine and Messenger RNA Translation

Translation is the decoding of mRNA by ribosomes to produce polypeptide which later forms a functional protein inside the cells. Recent studies demonstrate that m^{6}A modifications modulate mRNA translation efficiency through different mechanisms. YTHDF1 is known to promote the translation of m^{6}A-modified mRNA. Mechanistically, YTHDF1 could promote ribosome occupancy of targeted mRNA in the cytoplasm by recruiting the initiation factor eukaryotic initiation factor 3 (eIF3) (Wang et al., 2015). In addition, YTHDF3 was reported to facilitate YTHDF1-promoted translation (Shi et al., 2017). METTL3 also enhances mRNA translation. Barbieri et al. found that the transcription factor, CEBPZ, recruited METTL3 to the promoters of select active gene to catalyze m^{6}A methylation in the coding region (CDS) of targeted mRNA, resulting in enhanced translation by relieving ribosome stalling (Barbieri et al., 2017). Consistently, knockdown of METTL3 decreased translational efficiency of m^{6}A-modified transcripts in both human myeloid leukemia and HeLa cell lines (Vu et al., 2017). Surprisingly, METTL3-promoted translation could be independent of m^{6}A catalytic activity (Lin et al., 2016). Gregory and others showed that tethering a wild type or catalytically inactive METTL3 to the 3′UTR of a reporter mRNA exhibited similar translation enhancement (Lin et al., 2016). They further identified a direct physical and functional interaction between METTL3 at 3′UTR near the stop codon and eIF3h at the 5′ untranslated region (5′ UTR) of the mRNA and that METTL3-eIF3h loop may promote translation through ribosome recycling (Choe et al., 2018). Intriguingly, depletion of YTHDF1 did not influence the expression of METTL3 targets (Choe et al., 2018). Thus, METTL3 promotes mRNA translation through diverse mechanisms. It is worth noting that mouse embryonic stem cells (mESCs) with METTL3 knockout exhibited a modest increased translation efficiency (TE) compared to wild type (WT) cells, although this effect was observed for both methylated and unmethylated transcripts with higher GC content (Geula et al., 2015). In this study, loss of m^{6}A could directly enhance mRNA stability of m^{6}A-marked transcripts while indirectly favoring translation of GC-rich transcripts (Geula et al., 2015). Intriguingly, Slobodin et al. reported that transcription rate positively affected the efficiency of mRNA translation which was mediated by m^{6}A modification (Slobodin et al., 2017). Therefore, mRNA m^{6}A could mediate the communication between transcription and translation.

Qian and Jaffrey's team suggested that m^{6}A could enable mRNA translation in a cap- and IRES-independent manner (Meyer et al., 2015; Zhou et al., 2015; Coots et al., 2017; Zhou et al., 2018). They showed that heat shock stress promoted nuclear localization of YTHDF2 which in turn increased 5′ UTR m^{6}A of stress-inducible mRNAs through competing with FTO in preserving m^{6}A modification, leading to enhanced cap-independent translation initiation (Zhou et al., 2015). In addition, eIF3 could bind to 5′ UTR m^{6}A and recruit the 43S complex to initiate translation without the cap-binding factor eIF4E under stress (Meyer et al., 2015). Furthermore, depletion of METTL3 selectively inhibited translation of mRNAs with 5′ UTR m^{6}A, but not mRNAs with 5′ terminal oligopyrimidine (TOP) elements (Coots et al., 2017). Notably, ABCF1 was identified to coordinate with METTL3 in promoting translation of m^{6}A-modified mRNA (Coots et al., 2017). Thus, 5′ UTR m^{6}A facilitates cap-independent translation under stress.

m^{6}A is also thought to facilitate efficient translation of circular RNA (circRNA) (Yang et al., 2017). Initiation factor eIF4G2 and YTHDF3 were identified to be required for m^{6}A-driven circRNAs translation, which were enhanced by METTL3/14-mediated methylation or suppressed by FTO-mediated demethylation (Yang et al., 2017). Consistently, Bozzoni et al. demonstrated that METTL3 and YTHDC1 could direct the back-splicing reaction of circRNAs, and recognition of m^{6}A marks by YTHDF3 and eIF4G2 modulate circRNAs translation (Di Timoteo et al., 2020).

N^6-METHYLADENOSINE AND CELLULAR REPROGRAMMING

Mammalian development is thought to be continuous and unidirectional in which stem cells give rise to specialized differentiated cells through a series of cellular changes. However, recent studies have shown that it is possible to modify cell identity by somatic cell nuclear transfer (SCNT) (Matoba and Zhang, 2018), forced expression of specific transcription factors (Takahashi and Yamanaka, 2016) or micro-RNAs (Judson et al., 2009), and using small signaling molecules (Hou et al., 2013). In 2006, Kazutoshi Takahashi and Shinya Yamanaka successfully reprogrammed mouse embryonic fibroblasts (MEF) and adult mouse tail-tip fibroblasts to generate induced pluripotent stem cells (iPSCs) by ectopic expression of four transcription factors, namely Oct3/4, Sox2, c-Myc, and Klf4 (Takahashi and Yamanaka, 2006). In

2007, they further demonstrated the generation of iPSC from adult human dermal fibroblasts with the same four factors (Takahashi et al., 2007). The fact that terminally differentiated somatic cells can be reprogrammed to generate iPSCs has opened new gateways for therapeutics research. Recent evidence has revealed epigenetic profile changes during the process of cell differentiation and reprogramming and that epigenetic perturbations could affect the efficiency of reprogramming iPSCs (Young, 2011; Liang and Zhang, 2013; Hochedlinger and Jaenisch, 2015; Xu and Xie, 2018). In this part, we describe the influences of m^{6}A modifications on stemness and reprogramming.

N^6-Methyladenosine and Stemness

To maintain self-renewal and pluripotency, stem cells need to stably express pluripotency genes; however, they are also capable of rapidly altering gene expression programming for differentiation. m^{6}A is involved in cell fate determination and is now considered as a mark of transcriptome flexibility required by stem cells. Zhao and others identified that depletion of METTL3 or METTL14 in mESCs suppressed m^{6}A methylation and self-renewal capability (Wang et al., 2014b). Mechanistically, m^{6}A marks blocked the binding of RNA stabilizer protein HuR and protected mRNA from degradation induced by RNA-induced silencing complex (RISC) (Wang et al., 2014b). Consequently, developmental regulators were more enriched than pluripotency genes upon METTL3 or METTL14 knockdown (Wang et al., 2014b). Thus, METTL3/METTL14-mediated m^{6}A modification is required to maintain the pluripotency of ES cells. However, Batista et al. reported that m^{6}A loss promoted ESC self-renewal and hindered differentiation (Batista et al., 2014). In this study, they profiled m^{6}A methylome in mouse and human ESCs, revealing extensive m^{6}A modification of ESC genes, including core pluripotency regulators such as Nanog, Klf4, Myc, Lin28, Med1, Jarid2, and Eed (Batista et al., 2014). They considered m^{6}A as a mark for RNA turnover over in a timely fashion, and knockout of METTL3 improved mESCs self-renewal without affecting cell viability (Batista et al., 2014). The differences in phenotypes between these two studies may partially be explained by the methodology used (RNAi and CRISPR) which may affect downstream m^{6}A-modified RNAs pattern. Another possibility is that the mESCs used in these two studies were at different states. TGFβ signaling is essential for human pluripotent stem cells (hPSCs) to maintain pluripotency (James et al., 2005). Vallier et al. identified a functional interaction between SMAD2/3 transcription factors and METTL3-METTL14-WTAP complex (Bertero et al., 2018). SMAD2/3 could promote the binding of METTL3-METTL14-WTAP to specific SMAD2/3 transcriptional targets involved in early cell fate decisions, e.g., pluripotency factor gene NANOG, leading to increased m^{6}A methylations that facilitate mRNA degradation (Bertero et al., 2018). Consequently, m^{6}A-mediated rapid downregulation of SMAD2/3-targeted genes facilitated timely shut down of pluripotency on differentiation (Bertero et al., 2018). Intriguingly, Filipczyk and others reported that depletion of m^{6}A could both support pluripotency maintenance and exit through activating pAkt and pErk signaling, respectively (Jin et al., 2021).

m^{6}A modification is required for embryo development. Knockout of METTL3 or METTL14 led to early embryonic lethality (Geula et al., 2015; Meng et al., 2019). In *Mettl3*$^{-/-}$ mice, preimplantation epiblasts and naïve embryonic stem cells with loss of m^{6}A were still viable; however, they failed to terminate the naïve state toward lineage differentiation, resulting in early embryonic lethality (Geula et al., 2015). The abnormal expression and location of NANOG caused by METTL3 ablation was regarded as the leading cause (Geula et al., 2015). Meanwhile, METTL14 is indispensable for postimplantation embryonic development. Silencing of METTL14 contributed to abnormal embryo development since embryonic day 6.5 (E6.5), mainly due to resistance to differentiation (Meng et al., 2019). Mechanistically, METTL14 depletion caused dysregulation of genes associated with embryo development pathways (Meng et al., 2019). The m^{6}A readers YTHDF2 and YTHDC1 are also important for mammalian development (Ivanova et al., 2017; Kasowitz et al., 2018). Maternal RNA degradation, which was mediated by YTHDF2, facilitated oocyte maturation; oocytes with YTHDF2 deficiency failed to change metaphase II (MII) transcriptome, leading to female-specific infertility in mice (Ivanova et al., 2017). On the other hand, knockout of YTHDC1 caused massive alternative splicing defects in oocytes, resulting in a block at the primary stage of folliculogenesis (Kasowitz et al., 2018).

N^6-Methyladenosine and Epitranscriptomic Reprogramming

The epigenetic modifications could lock cells into a differentiated state during cell differentiation; therefore, targeting repressive epigenetic marks in differentiated cells improve the efficiency of iPSC formation (Huangfu et al., 2008; Shi et al., 2008). Recent studies also pinpoint m^{6}A as an important player during cellular reprogramming. Chen et al. reported that m^{6}A formation facilitated cell reprogramming to pluripotency (Chen et al., 2015). In this study, lots of cell-type specific markers are m^{6}A-modifed, such as Oct4, Nanog, and DPPA2 for ESCs and iPSCs; POU3F2 and ROBO2 for neural stem cells; and DHH and Sox8 for testicular sertoli cells (Chen et al., 2015). These genes are critical for stem cell maintenance and developmental regulation. Intriguingly, miRNAs could target m^{6}A marks by base pairing and modulate the binding of METTL3, thus leading to the change of cellular m^{6}A abundance (Chen et al., 2015). Deletion of Dicer, an essential endonuclease for producing mature miRNAs, remarkably inhibited the RNA m^{6}A level; in contrast, overexpression of miRNAs increased the binding of METTL3 on mRNAs and enhanced m^{6}A abundance (Chen et al., 2015). To investigate the role of m^{6}A in cell reprogramming, manipulation of METTL3 was conducted in MEFs transduced with four Yamanaka transcription factors. The result indicated that ectopic expression of METTL3 increased colonies of iPSC, enhanced expressions of key pluripotent factors (Oct4, Sox2, and Nanog), and promoted the reprogramming of MEFs to pluripotent stem cells; conversely, depletion of METTL3

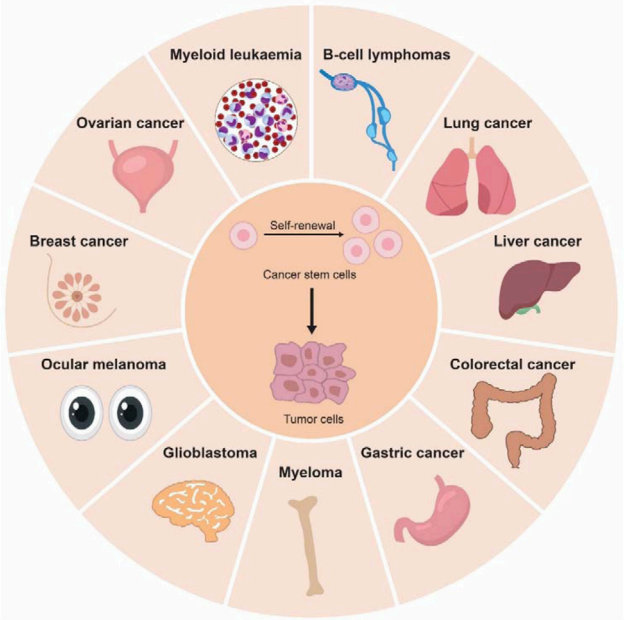

FIGURE 2 | Cancer stem cells are key drivers to tumor initiation and progression. Cancer stem cells (CSCs) have been identified in different type of solid cancers (colorectal cancer, gastric cancer, liver cancer, glioblastoma, melanoma, breast cancer, lung cancer, and ovarian cancer) and hematological cancers (myeloid leukemia, lymphoma, and myeloma).

reduced m^{6}A and led to impeded reprogramming (Chen et al., 2015).

The crosstalk between epigenetic and epitranscriptomic networks is important to cellular reprogramming. Aguilo et al. reported that chromatin-associated zinc finger protein 217 (ZFP217) coordinated epigenetic and epitranscriptomic regulation to ensure ESC self-renewal and somatic cell reprogramming (Aguilo et al., 2015). They identified gradually increased ZFP217 expression along with decreased METTL3 expression during somatic reprogramming (Aguilo et al., 2015). ZFP217 could induce transcription of core reprogramming factors and repress m^{6}A deposition of pluripotency genes by sequestering METTL3 (Aguilo et al., 2015). Depletion of ZFP217 in MEFs increased the m^{6}A level of Nanog, Sox2, Klf4, and c-Myc mRNAs, promoting their degradation and leading to diminished iPSC colonies formation; this phenomenon could be partially rescued by METTL3 knockdown (Aguilo et al., 2015). Therefore, m^{6}A modifications may be a barrier for ZFP217-meidiated somatic cell reprogramming. In support of these, Song et al. demonstrated that ZFP217 suppressed m^{6}A mRNA methylation by promoting FTO expression (Song et al., 2019). Silencing of ZFP217 decreased FTO expression to enhance m^{6}A levels, resulting in retarded adipogenic differentiation (Song et al., 2019).

So, how to understand the conflicting phenomena regarding the role of m^{6}A on somatic cell reprogramming? One possible explanation is that m^{6}A on cell fate choice is context dependent. Geula et al. reported that depletion of METTL3 exerted a divergent effect on naïve and primed PSCs (Geula et al., 2015). In naïve PSCs, pluripotency genes were highly expressed, and silencing of METTL3 could further enhance their expression to boost naïve circuitry stability; by contrast, the expression of pluripotency genes was downregulated while lineage commitment markers were upregulated in primed cells; thus silencing of METTL3 exerted a minor effect on expression of pluripotency genes while it remarkably increased the expression of lineage commitment markers, making the cells tend toward differentiation (Geula et al., 2015). Therefore, epigenetics and epitranscriptomics can form a complex network to regulate stem cell pluripotency and differentiation.

N^6-METHYLADENOSINE AND CANCER STEM CELLS

CSCs or tumor-initiating cells (TICs) are a small subpopulation of cancer cells which could give rise to tumors through processes of self-renewal and differentiation, just like normal stem cell (**Figure 2**). Tumor development and iPSC generation share striking similarities on gene expression programming, implying a potential link between pluripotency and cancer (Wong et al., 2008). Furthermore, recent evidence state that cancer cells could be reprogrammed to retrieve benign cell functions or differentiate into other unrelated cell types by re-expression of lineage-specific genes, opening a new avenue for cancer treatment (Bussard et al., 2010; Pezzolo et al., 2011). Understanding the molecular drivers of CSCs will advance the development of anticancer therapeutics. In this section, we summarize the key findings on how m^{6}A modifications modulate cancer stemness (**Table 1**).

N^6-Methyladenosine and Solid Tumors

Solid tumors refer to an abnormal mass of tissue in "solid" organs. Gastrointestinal (GI) cancer is one of them, referring to cancers that affect the digestive system, e.g., colorectal cancer (CRC), gastric cancer (GC), and liver cancer. Several m^{6}A regulators have been reported to play important roles in GI cancer. Our team recently identified the novel oncogenic epitranscriptome axis of METTL3-m^{6}A-GLUT1-mTORC1 (Chen et al., 2021) and YTHDF1-m^{6}A-ARHGEF2 (Wang et al., 2022) in promoting CRC tumorigenesis. In the former study, METTL3 was found to promote GLUT1 translation in an m^{6}A-dependent manner by integrative m^{6}A sequencing, RNA sequencing, and ribosome profiling analyses, resulting in increased glucose uptake and lactate production which subsequently activated mTORC1 signaling; consequently, depletion of METTL3 impaired the self-renewal capacity of colon cancer-initiating cells (Chen et al., 2021). As to the latter study, knockdown of YTHDF1 suppressed CRC organoids and decreased cell growth; mechanistically, YTHDF1 bind to m^{6}A marks of ARHGEF2 mRNA and enhanced ARHGEF2 translation by multiomic analysis of m^{6}A sequencing, RNA sequencing, YTHDF1 RNA immunoprecipitation sequencing and proteomics (Wang et al., 2022). In line with our findings, Han et al. reported that high expression of YTHDF1 was induced by Wnt signaling in intestinal stem cells (ISCs) which in turn promoted translation

TABLE 1 | M^{6}A-mediated molecular events in different cancer types.

Cancer type	Molecular event
Acute myeloid leukemia	FTO-m^{6}A-ASB2/RARA Li et al. (2017)
	FTO-m^{6}A-MYC/CEBPA Su et al. (2018)
Breast cancer	ALKBH5-m^{6}A-NANOG Zhang et al. (2016)
	METTL14-m^{6}A-DROSHA Peng et al. 2021)
Colorectal cancer	METTL3-m^{6}A-GLUT1-mTORC1 Chen et al. (2021)
	YTHDF1-m^{6}A-ARHGEF2 Wang et al. (2022)
	YTHDF1-m^{6}A-TCF7L2/TCF4-β-catenin Han et al. (2020)
Gastric cancer	YTHDF1-m^{6}A-FZD7-Wnt/β-catenin Pi et al. (2021)
Glioblastoma	YTHDF2-m^{6}A-MYC-IGFBP3 Dixit et al. (2021)
	ALKBH5-m^{6}A-FOXM1 Zhang et al. (2017)
	METTL3/METTL14-m^{6}A-ADAM19 Cui et al. (2017)
	METTL3-m^{6}A-SRSF Li et al. (2019)
Liver cancer	YTHDF2-m^{6}A-OCT4 Zhang et al. (2020)
	METTL14-m^{6}A-HNF3γ Zhou et al. (2020)
	FTO-m^{6}A-TGF-β2 Zhou et al. (2020)
Lung cancer	ALKBH5-m^{6}A-Nanog/Oct4 Liu et al. (2022)
Lymphoma	WTAP-m^{6}A-HK2 Han et al. (2021)
	ALKBH5/FTO-m^{6}A-SPI1/PHF12 Wu et al. (2021)
Multiple myeloma	FTO-m^{6}A-HSF1 Xu et al. (2022)
	ALKBH5-m^{6}A-TRAF1 Qu et al. (2022)
Ovarian cancer	FTO-m^{6}A-PDE1C/PDE4B Huang et al. (2020)

of TCF7L2/TCF4, leading to enhanced β-catenin activity that promoted stemness of ISCs (Han et al., 2020). YTHDF1 also activates Wnt/β-catenin signaling in GC. Pi et al. revealed that YTHDF1 increased translation of frizzled7 (FZD7), a key Wnt receptor, in an m^{6}A-dependent manner; consequently, hyperactivation of the Wnt/β-catenin was induced that facilitated GC tumorigenesis (Pi et al., 2021). Intriguingly, long non-coding RNAs (lncRNAs) could influence the m^{6}A modification process. LNC942 was identified to induce GC stemness and chemoresistance by stabilizing Musashi2 (MSI2), a member of RNA-binding proteins (RBPs); MSI2 then bind to m^{6}A sites of c-Myc mRNA to increase mRNA stability (Zhu et al., 2022).

Current evidence also pinpoints a pivotal role of m^{6}A modifications in liver cancer stem cells (Zhang et al., 2020; Zhou et al., 2020; Bian et al., 2021; Wang et al., 2021). In purified CD133$^+$ liver cancer stem cells, knockdown of YTHDF2 impaired tumor-initiating ability; in contrast, overexpression of YTHDF2 exerted the opposite effect (Zhang et al., 2020). YTHDF2 was capable of binding to m^{6}A sites in the 5′UTR of OCT4 mRNA to promote its translation as determined by luciferase activity assay and polysome profiling assay (Zhang et al., 2020). Meanwhile, METTL14 induced m^{6}A methylation of hepatocyte nuclear factor 3γ (HNF3γ) mRNA, a hepatocyte nuclear factor, leading to reduced HNF3γ expression in hepatocellular carcinoma (HCC) (Zhou et al., 2020). Notably, enforced HNF3γ expression promoted differentiation of HCC cells and liver CSCs, resulting in retarded growth of HCC (Zhou et al., 2020). In addition, HNF3γ expression rendered sensitivity of HCC cells to sorafenib treatment, implying the potential of HNF3γ as a therapeutic target for HCC (Zhou et al., 2020). RALY RNA-binding protein-like (RALYL), a liver progenitor specific gene, was also related with HCC differentiation (Wang et al., 2021). Overexpression of RALYL suppressed the m^{6}A level of TGF-β2 mRNA to enhance its mRNA stability, leading to subsequent activation of TGF-β signaling that contributed to HCC self-renewal and chemoresistance (Wang et al., 2021). In this study, FTO was found to bind to RALYL and thought to be responsible for m^{6}A demethylation of TGF-β2 mRNA (Wang et al., 2021). Furthermore, FTO-mediated RNA demethylation was also involved in S-adenosylmethionine decarboxylase proenzyme (AMD1)-induced cancer stemness in HCC (Bian et al., 2021). AMD1 was capable of stabilizing the interaction between Ras GTPase-activating-like protein 1 (IQGAP1) and FTO, leading to enhanced FTO expression which in turn promoted HCC stemness (Bian et al., 2021). Together, m^{6}A modifications are critical for self-renewal and differentiation of CSCs in GI cancer.

Dysregulated m^{6}A modifications play an important role in lung cancer. Yin et al. identified an lncRNA named RNA Component of Mitochondrial RNA Processing Endoribonuclease (RMRP) which exhibited enriched m^{6}A modifications and increased RNA stability in non-small cell lung cancer (NSCLC) (Yin et al., 2021). Both *in vitro* and *in vivo* experiments in this study revealed that RMRP induced TGFBR1/SMAD2/SMAD3 axis and promoted the cancer stem cell properties of NSCLC (Yin et al., 2021). However, how m^{6}A modifications regulate RMRP stability warrants further investigation. On the other hand, Liu et al. (2022) recently reported that ALKBH5 was highly expressed in CSCs isolated from NSCLC. They revealed that depletion of ALKBH5 increased the global m^{6}A level, suppressed expression of Nanog and Oct4, two essential transcription factors for self-renewal and pluripotency of ESCs, and inhibited stemness of CSCs (Liu et al., 2022). Intriguingly, p53 was reported to regulate malignancies of CSCs partially through transactivating ALKBH5 expression (Liu et al., 2022).

Glioblastoma is a prevalent and malignant cancer that occurs in the brain or spinal cord. m^{6}A modifications could regulate gene expression and cell fate in glioblastoma stem-like cells (GSCs). Compared to normal neural stem cells (NSCs), GSCs preferentially expressed YTHDF2 which was essential for GSCs maintenance (Dixit et al., 2021). Intriguingly, instead of destabilizing mRNAs, YTHDF2 was found to increase MYC and VEGFA mRNA stability in an m^{6}A-dependent manner in GSCs, although the mRNA-stabilizing function of YTHDF2 was unclear (Dixit et al., 2021). YTHDF2-MYC-IGFBP3 axis was further identified to promote glioblastoma growth both *in vitro* and *in vivo* (Dixit et al., 2021). Importantly, administration of linsitinib, an IGF1/IGF1R inhibitor, exerted potent inhibitory effect against YTHDF2-expressing GSCs without affecting NSCs (Dixit et al., 2021). ALKBH5 was also found highly expressed in GSCs, and silencing of ALKBH5 inhibited the growth of patient-derived GSCs (Zhang et al., 2017). Mechanistically, ALKBH5 reduced the m^{6}A level of FOXM1 mRNA, resulting in enhanced FOXM1 expression which in turn promoted GSC tumorigenesis (Zhang et al., 2017). m^{6}A modifications are critical for self-renewal of GSCs. Knockdown of METTL3 or METTL14 promoted growth, self-renewal, and tumorigenesis of human GSC; conversely, overexpression of METTL3 or inhibition of FTO exerted the opposite effect (Cui et al., 2017). ADAM19 was a downstream target of METTL3/METTL14 that exerted critical biological functions in GSCs (Cui et al., 2017). m^{6}A modifications could

influence nonsense-mediated mRNA decay (NMD) in GSCs. Li et al. reported that METTL3 regulated the NMD of splicing factors and AS process in glioblastoma (Li et al., 2019). Depletion of METTL3 inhibited the m^{6}A levels of serine- and arginine-rich splicing factors (SRSF), leading to NMD of SRSF which was mediated by YTHDC1 (Li et al., 2019). Subsequently, downregulated SRSFs significantly changed alternative splicing events of several genes including BCL-X and NCOR2, contributing to suppression of GSCs self-renewal (Li et al., 2019). All these findings establish a critical role of m^{6}A modifications in GSCs.

Breast cancer and ovarian cancer are common cancers in women. m^{6}A modifications exert profound and diverse functions in breast cancer stem cells and ovarian cancer stem cells. In response to hypoxia, hypoxia-inducible factor (HIF)-1α and HIF-2α were stimulated to promote ALKBH5 expression in breast cancer cells; subsequently, ALKBH5 inhibited the m^{6}A level in the 3′UTR of Nanog mRNA and increased NANOG expression, resulting in enhanced breast cancer stem cell phenotype (Zhang et al., 2016). Conversely, ALKBH5 knockdown in human breast cancer cells suppressed tumor initiation capacity (Zhang et al., 2016). Therefore, ALKBH5-mediated m^{6}A modifications play a pivotal role in maintaining breast cancer stemness in the hypoxic environment. Aurora kinase A (AURKA) is a member of serine/threonine kinases family and was reported to stabilize METTL14 protein by preventing its ubiquitylation in breast cancer stem-like cells (Peng et al., 2021). Subsequently, upregulated METTL14 expression induced the m^{6}A level of DROSHA, a Class 2 ribonuclease III enzyme, to stabilize DROSHA mRNA which was meditated by m^{6}A reader IGF2BP2 (Peng et al., 2021). Intriguingly, AURKA could strengthen the binding of IGF2BP2 to DROSHA mRNA, thus promoting DROSHA expression (Peng et al., 2021). Furthermore, DROSHA interacted with β-catenin to transactivate STC1, resulting in enhanced stemness of breast cancer (Peng et al., 2021). In ovarian cancer, FTO is suggested to suppress self-renewal of ovarian CSCs. Huang et al. revealed reduced FTO expression in ovarian tumors and ovarian CSCs (Huang et al., 2020). In this study, ectopic expression of FTO in ovarian cancer cells inhibited the m^{6}A level in the 3′UTR of two phosphodiesterase genes, PDE1C and PDE4B, and reduced their mRNA stability, leading to activation of second messenger 3′, 5′-cyclic adenosine monophosphate (cAMP) signaling and suppression of stemness features (Huang et al., 2020). Furthermore, FTO could suppress self-renewal of ovarian CSCs *in vivo* in an m^{6}A-dependent manner (Huang et al., 2020). All these studies unveil a key role of m^{6}A modifications in regulating stemness phenotype of breast cancer and ovarian cancer.

N^6-Methyladenosine and Hematological Tumors

Hematologic malignancies comprise three main types: leukemia, lymphoma, and multiple myeloma (MM). In acute myeloid leukemia (AML), a subpopulation of AML cells, called leukemia stem cells (LSCs), exert self-renewal capacity and is responsible for the maintenance of the AML phenotype. There have been numerous studies reporting the functional importance of m^{6}A modifications in AML. Li et al. revealed increased expression of FTO in AML (Li et al., 2017). High FTO expression suppressed the m^{6}A levels of ankyrin repeat and SOCS box protein 2 (ASB2) and retinoic acid receptor α (RARA), leading to reduced mRNA stability of these two genes (Li et al., 2017). However, future study is required to identify m^{6}A readers that are responsible for stabilizing FTO target transcripts, such as ASB2 and RARA. Consequently, FTO promoted leukemogenesis and inhibited Tretinoin-induced AML cell differentiation (Li et al., 2017). Given the functional significance of FTO in AML, several FTO inhibitors have been developed. In a subsequent study, Su et al. reported that R-2-hydroxyglutarate (R-2HG), originally thought to be an oncometabolite, strongly inhibited FTO activity, thereby increasing global m^{6}A modifications, resulting in reduced mRNA stability of MYC/CEBPA in R-2HG-sensitive leukemia cells (Su et al., 2018). Of note, R-2HG treatment also increased ASB2 and RARA expressions in R-2HG-sensitive cells, but not in the resistant cells (Su et al., 2018). Importantly, R-2HG exhibited a potent anti-tumor effect against leukemia with high FTO expression by targeting FTO-m^{6}A-MYC/CEBPA axis (Su et al., 2018). However, whether and how R-2HG exerted its effect on cancer metabolism in leukemia was unclear. Accordingly, Qing et al. showed that R-2HG could effectively inhibit aerobic glycolysis in R-2HG-sensitive leukemia cells, but not in normal CD34$^+$ hematopoietic stem/progenitor cells (Qing et al., 2021). Aerobic glycolysis, termed Warburg effect, converts glucose to lactate even without oxygen, thereby providing the energy required by the cancer cells. R-2HG inhibited FTO activity and increased the m^{6}A level of phosphofructokinase platelet (PFKP) and lactate dehydrogenase B (LDHB), two critical glycolytic genes, thereby reducing their mRNA stability which was mediated by YTHDF2 (Qing et al., 2021). Notably, FTO, PFKP, or LDHB depletion recapitulated R-2HG-induced glycolytic inhibition and suppressed leukemogenesis *in vivo* (Qing et al., 2021). Using structure-based rational design, Huang et al. recently developed two FTO inhibitors, FB23 and FB23-2 (derivatives of meclofenamic acid), which could directly bind to FTO and suppress its demethylase activity (Huang et al., 2019). FB23-2 strongly inhibited cell proliferation but induced differentiation/apoptosis of human AML cells both *in vitro* and *in vivo*; moreover, FB23-2 exhibited a promising therapeutic efficacy in patient-derived xeno-transplantation AML mouse model (Huang et al., 2019). Notably, FB23-2 treatment could significantly eliminate LSCs in these mice models, thereby disrupting AML maintenance (Huang et al., 2019). However, the half-maximal inhibitory concentration (IC50) values of FB23 and FB23-2 in suppressing AML are still high: >20 μM and >1 μM for FB23 and FB23-2, respectively (Huang et al., 2019). To develop efficacious inhibitors against FTO, Chen's team conducted a structure-based virtual screening of the 260,000 compounds and validation assays, leading to the identification of two compounds, CS1 and CS2,

which displayed strong inhibitory effects against FTO activity and AML cell viability with 10- to 30-fold lower IC50 (Su et al., 2020). FTO was frequently overexpressed in LSCs, and pharmacological inhibition of FTO by CS1 and CS2 suppressed self-renewal of LSCs (Su et al., 2020). In addition, targeting FTO decreased the expression of immune checkpoints, such as PD-L1, PD-L2, and LILRB, to reverse immune evasion of leukemia cells (Su et al., 2020), highlighting the potential of FTO inhibitors for cancer therapy. Nevertheless, there remains some limitations for small-molecule FTO inhibitors, e.g., toxic side effects, the sensitivity and specificity of inhibitors against LSCs. As such, Cao et al. developed FTO inhibitor-loaded GSH-bioimprinted nanocomposites (GNPIPP12MA) of synergistic FTO inhibition and GSH depletion (Cao et al., 2022). Notably, GNPIPP12MA not only selectively targeted LSCs but also enhanced the efficacy of the PD-L1 blockade, thereby suppressing leukemogenesis (Cao et al., 2022). Other m^{6}A regulators, such as METTL3 (Barbieri et al., 2017; Vu et al., 2017), METTL14 (Weng et al., 2018), YTHDF2 (Paris et al., 2019), YTHDC1 (Cheng et al., 2021; Sheng et al., 2021), and ALKBH5 (Shen et al., 2020; Wang et al., 2020), have also been demonstrated to regulate LSCs features and contribute to leukemogenesis. It is worth noting that Yankova et al. recently developed a highly potent and selective METTL3 inhibitor, named STM2457, that posed a strong effect in suppressing growth while increasing differentiation and apoptosis of AML (Yankova et al., 2021). Together, all these studies suggest that targeting m^{6}A regulators is a potential therapeutic strategy against AML.

Myeloma is a blood cancer of plasma cells derived from bone marrow. Recent evidence implies a functional role of m^{6}A in MM pathogenesis. Upregulated isocitrate dehydrogenase 2 (IDH2) in CD138$^+$ MM cells reduced global RNA m^{6}A modification through activating FTO (Song et al., 2021). The m^{6}A level of WNT7B mRNA was decreased by IDH2, leading to increased WNT7B expression and subsequent activation of Wnt pathway which eventually facilitated tumorigenesis and progression of MM (Song et al., 2021). Consistently, FTO was highly expressed in plasma cells from MM patients, concomitant with decreased RNA m^{6}A level (Xu et al., 2022). FTO inhibited m^{6}A modifications of heat shock factor 1 (HSF1), thereby increasing its mRNA stability in a YTHDF2-dependent manner (Xu et al., 2022). Importantly, FTO-m^{6}A-HSF1 promoted MM cells growth and metastasis (Xu et al., 2022). Similarly, ALKBH5 was overexpressed in MM and promoted MM tumorigenesis (Qu et al., 2022). ALKBH5 inhibited m^{6}A modifications in 3′UTR of TNF receptor-associated factor 1 (TRAF1) and enhanced its mRNA stability, leading to activation of NF-κB and MAPK signaling pathways (Qu et al., 2022).

Lymphoma is cancer of lymphocytes from lymph nodes, spleen, thymus, or bone marrow. Han et al. reported that PIWI-interacting RNAs (piRNAs)-30473 upregulated WTAP and increased the global m^{6}A level in diffuse large B-cell lymphoma (DLBCL) (Han et al., 2021). Hexokinase 2 (HK2) was further identified as the downstream target of piRNA-30473-WTAP-m^{6}A, and upregulated HK2 by piRNA-30473 contributed to DLBCL tumorigenesis (Han et al., 2021). On the other hand, proto-oncogene MYC was found to transcriptionally activate ALKBH5 and FTO and inhibit m^{6}A levels of SPI1 and PHF12 transcripts, thereby suppressing their mRNA translation which was mediated by YTHDF3 (Wu et al., 2021). Furthermore, depletion of ALKBH5 effectively reduced growth of B-cell lymphomas with deregulated MYC expression (Wu et al., 2021).

CONCLUSION AND FUTURE PERSPECTIVES

To date, great efforts have been made to explore the roles of RNA m^{6}A modifications in different biological processes, and improvements have been achieved to advance our understanding of m^{6}A-mediated epitranscriptomic regulation and its potential as therapeutic targets for cancer patients. However, many questions remain elusive: 1) the origins and functions of m^{6}A marks at different stages of human development are still largely unclear; 2) the contribution of m^{6}A modifications in iPSC pluripotency should be further clarified; 3) m^{6}A writers (e.g., METTL3) and erasers (e.g., FTO) both play an oncogenic role in several cancer types (e.g., AML). Thus, m^{6}A regulators likely target different groups of transcripts and regulate different biological processes; 4) the position of m^{6}A sites (e.g., 5′UTR, CDS, or 3′UTR) in transcripts likely influence the recognition of m^{6}A and the subsequent RNA metabolism; 5) m^{6}A readers could exhibit opposite functions. YTHDF2 promotes RNA degradation of m^{6}A-modified mRNAs while IGF2BP1-3 stabilizes them, although they target different transcripts. Besides, more and more m^{6}A readers are being discovered, adding to the complexity of m^{6}A epitranscriptome; and 6) the crosstalk or competition among m^{6}A writers, readers and erasers should be further explored. Although the functions of m^{6}A regulators are context dependent, targeting m^{6}A offers great potential for cancer treatment. Future studies on understanding the context-dependent role of m^{6}A modification in cellular reprogramming and cancer stemness is of utmost importance.

AUTHOR CONTRIBUTIONS

HC and YW wrote the manuscript. HC and JY supervised the study and revised the paper. The remaining authors assisted in editing.

FUNDING

This project was supported by the National Natural Science Foundation of China (NSFC; 82103245, 81972576); RGC-CRF Hong Kong (C4039-19GF); RGC-GRF Hong Kong (14107321, 14110819); Heath and Medical Research Fund (HMRF) (18190951); and CUHK Direct Grant for Research (2020.006).

REFERENCES

Adams, J. M., and Cory, S. (1975). Modified Nucleosides and Bizarre 5′-termini in Mouse Myeloma mRNA. *Nature* 255 (5503), 28–33. doi:10.1038/255028a0

Aguilo, F., Zhang, F., Sancho, A., Fidalgo, M., Di Cecilia, S., Vashisht, A., et al. (2015). Coordination of M 6 A mRNA Methylation and Gene Transcription by ZFP217 Regulates Pluripotency and Reprogramming. *Cell Stem Cell* 17 (6), 689–704. doi:10.1016/j.stem.2015.09.005

Alemu, E. A., He, C., and Klungland, A. (2016). ALKBHs-Facilitated RNA Modifications and De-modifications. *DNA Repair (Amst)* 44, 87–91. doi:10.1016/j.dnarep.2016.05.026

Barbieri, I., Tzelepis, K., Pandolfini, L., Shi, J., Millán-Zambrano, G., Robson, S. C., et al. (2017). Promoter-bound METTL3 Maintains Myeloid Leukaemia by m6A-dependent Translation Control. *Nature* 552 (7683), 126–131. doi:10.1038/nature24678

Batista, P. J., Molinie, B., Wang, J., Qu, K., Zhang, J., Li, L., et al. (2014). m6A RNA Modification Controls Cell Fate Transition in Mammalian Embryonic Stem Cells. *Cell Stem Cell* 15 (6), 707–719. doi:10.1016/j.stem.2014.09.019

Bertero, A., Brown, S., Madrigal, P., Osnato, A., Ortmann, D., Yiangou, L., et al. (2018). The SMAD2/3 Interactome Reveals that TGFβ Controls m6A mRNA Methylation in Pluripotency. *Nature* 555 (7695), 256–259. doi:10.1038/nature25784

Bian, X., Shi, D., Xing, K., Zhou, H., Lu, L., Yu, D., et al. (2021). AMD1 Upregulates Hepatocellular Carcinoma Cells Stemness by FTO Mediated mRNA Demethylation. *Clin. Transl. Med.* 11 (3), e352. doi:10.1002/ctm2.352

Bokar, J. A., Shambaugh, M. E., Polayes, D., Matera, A. G., and Rottman, F. M. (1997). Purification and cDNA Cloning of the AdoMet-Binding Subunit of the Human mRNA (N6-Adenosine)-Methyltransferase. *RNA* 3 (11), 1233–1247.

Bussard, K. M., Boulanger, C. A., Booth, B. W., Bruno, R. D., and Smith, G. H. (2010). Reprogramming Human Cancer Cells in the Mouse Mammary Gland. *Cancer Res.* 70 (15), 6336–6343. doi:10.1158/0008-5472.can-10-0591

Cao, K., Du, Y., Bao, X., Han, M., Su, R., Pang, J., et al. (2022). Glutathione-Bioimprinted Nanoparticles Targeting of N6-Methyladenosine FTO Demethylase as a Strategy against Leukemic Stem Cells. *Small* 18 (13), e2106558. doi:10.1002/smll.202106558

Carroll, S. M., Narayan, P., and Rottman, F. M. (1990). N6-methyladenosine Residues in an Intron-specific Region of Prolactin Pre-mRNA. *Mol. Cell Biol.* 10 (9), 4456–4465. doi:10.1128/mcb.10.9.4456-4465.1990

Chen, H., Gao, S., Liu, W., Wong, C.-C., Wu, J., Wu, J., et al. (2021). RNA N6-Methyladenosine Methyltransferase METTL3 Facilitates Colorectal Cancer by Activating the m6A-GLUT1-mTORC1 Axis and Is a Therapeutic Target. *Gastroenterology* 160 (4), 1284–1300 e16. doi:10.1053/j.gastro.2020.11.013

Chen, R.-X., Chen, X., Xia, L.-P., Zhang, J.-X., Pan, Z.-Z., Ma, X.-D., et al. (2019). N6-methyladenosine Modification of circNSUN2 Facilitates Cytoplasmic Export and Stabilizes HMGA2 to Promote Colorectal Liver Metastasis. *Nat. Commun.* 10 (1), 4695. doi:10.1038/s41467-019-12651-2

Chen, T., Hao, Y.-J., Zhang, Y., Li, M.-M., Wang, M., Han, W., et al. (2015). m6A RNA Methylation Is Regulated by MicroRNAs and Promotes Reprogramming to Pluripotency. *Cell Stem Cell* 16 (3), 289–301. doi:10.1016/j.stem.2015.01.016

Cheng, Y., Xie, W., Pickering, B. F., Chu, K. L., Savino, A. M., Yang, X., et al. (2021). N6-Methyladenosine on mRNA Facilitates a Phase-Separated Nuclear Body that Suppresses Myeloid Leukemic Differentiation. *Cancer Cell* 39 (7), 958–972 e8. doi:10.1016/j.ccell.2021.04.017

Choe, J., Lin, S., Zhang, W., Liu, Q., Wang, L., Ramirez-Moya, J., et al. (2018). mRNA Circularization by METTL3-eIF3h Enhances Translation and Promotes Oncogenesis. *Nature* 561 (7724), 556–560. doi:10.1038/s41586-018-0538-8

Coots, R. A., Liu, X.-M., Mao, Y., Dong, L., Zhou, J., Wan, J., et al. (2017). m6A Facilitates eIF4F-independent mRNA Translation. *Mol. Cell* 68 (3), 504–514 e7. doi:10.1016/j.molcel.2017.10.002

Cui, Q., Shi, H., Ye, P., Li, L., Qu, Q., Sun, G., et al. (2017). m 6 A RNA Methylation Regulates the Self-Renewal and Tumorigenesis of Glioblastoma Stem Cells. *Cell Rep.* 18 (11), 2622–2634. doi:10.1016/j.celrep.2017.02.059

Desrosiers, R., Friderici, K., and Rottman, F. (1974). Identification of Methylated Nucleosides in Messenger RNA from Novikoff Hepatoma Cells. *Proc. Natl. Acad. Sci. U.S.A.* 71 (10), 3971–3975. doi:10.1073/pnas.71.10.3971

Di Timoteo, G., Dattilo, D., Centrón-Broco, A., Colantoni, A., Guarnacci, M., Rossi, F., et al. (2020). Modulation of circRNA Metabolism by m6A Modification. *Cell Rep.* 31 (6), 107641. doi:10.1016/j.celrep.2020.107641

Dixit, D., Prager, B. C., Gimple, R. C., Poh, H. X., Wang, Y., Wu, Q., et al. (2021). The RNA m6A Reader YTHDF2 Maintains Oncogene Expression and Is a Targetable Dependency in Glioblastoma Stem Cells. *Cancer Discov.* 11 (2), 480–499. doi:10.1158/2159-8290.cd-20-0331

Dominissini, D., Moshitch-Moshkovitz, S., Schwartz, S., Salmon-Divon, M., Ungar, L., Osenberg, S., et al. (2012). Topology of the Human and Mouse m6A RNA Methylomes Revealed by m6A-Seq. *Nature* 485 (7397), 201–206. doi:10.1038/nature11112

Du, H., Zhao, Y., He, J., Zhang, Y., Xi, H., Liu, M., et al. (2016). YTHDF2 Destabilizes m6A-Containing RNA through Direct Recruitment of the CCR4-Not Deadenylase Complex. *Nat. Commun.* 7, 12626. doi:10.1038/ncomms12626

Gawlik-Rzemieniewska, N., and Bednarek, I. (2016). The Role of NANOG Transcriptional Factor in the Development of Malignant Phenotype of Cancer Cells. *Cancer Biol. Ther.* 17 (1), 1–10. doi:10.1080/15384047.2015.1121348

Geula, S., Moshitch-Moshkovitz, S., Dominissini, D., Mansour, A. A., Kol, N., Salmon-Divon, M., et al. (2015). m 6 A mRNA Methylation Facilitates Resolution of Naïve Pluripotency toward Differentiation. *Science* 347 (6225), 1002–1006. doi:10.1126/science.1261417

Han, B., Yan, S., Wei, S., Xiang, J., Liu, K., Chen, Z., et al. (2020). YTHDF1-mediated Translation Amplifies Wnt-Driven Intestinal Stemness. *EMBO Rep.* 21 (4), e49229. doi:10.15252/embr.201949229

Han, H., Fan, G., Song, S., Jiang, Y., Qian, C. a., Zhang, W., et al. (2021). piRNA-30473 Contributes to Tumorigenesis and Poor Prognosis by Regulating m6A RNA Methylation in DLBCL. *Blood* 137 (12), 1603–1614. doi:10.1182/blood.2019003764

Hochedlinger, K., and Jaenisch, R. (2015). Induced Pluripotency and Epigenetic Reprogramming. *Cold Spring Harb. Perspect. Biol.* 7 (12), a019448. doi:10.1101/cshperspect.a019448()

Hou, P., Li, Y., Zhang, X., Liu, C., Guan, J., Li, H., et al. (2013). Pluripotent Stem Cells Induced from Mouse Somatic Cells by Small-Molecule Compounds. *Science* 341 (6146), 651–654. doi:10.1126/science.1239278

Huang, H., Wang, Y., Kandpal, M., Zhao, G., Cardenas, H., Ji, Y., et al. (2020). FTO-dependent N6-Methyladenosine Modifications Inhibit Ovarian Cancer Stem Cell Self-Renewal by Blocking cAMP Signaling. *Cancer Res.* 80 (16), 3200–3214. doi:10.1158/0008-5472.can-19-4044

Huang, H., Weng, H., Sun, W., Qin, X., Shi, H., Wu, H., et al. (2018). Recognition of RNA N6-Methyladenosine by IGF2BP Proteins Enhances mRNA Stability and Translation. *Nat. Cell Biol.* 20 (3), 285–295. doi:10.1038/s41556-018-0045-z

Huang, Y., Su, R., Sheng, Y., Dong, L., Dong, Z., Xu, H., et al. (2019). Small-Molecule Targeting of Oncogenic FTO Demethylase in Acute Myeloid Leukemia. *Cancer Cell* 35 (4), 677–691 e10. doi:10.1016/j.ccell.2019.03.006

Huangfu, D., Maehr, R., Guo, W., Eijkelenboom, A., Snitow, M., Chen, A. E., et al. (2008). Induction of Pluripotent Stem Cells by Defined Factors Is Greatly Improved by Small-Molecule Compounds. *Nat. Biotechnol.* 26 (7), 795–797. doi:10.1038/nbt1418

Ivanova, I., Much, C., Di Giacomo, M., Azzi, C., Morgan, M., Moreira, P. N., et al. (2017). The RNA M 6 A Reader YTHDF2 Is Essential for the Post-transcriptional Regulation of the Maternal Transcriptome and Oocyte Competence. *Mol. Cell* 67 (6), 1059–1067 e4. doi:10.1016/j.molcel.2017.08.003

James, D., Levine, A. J., Besser, D., and Hemmati-Brivanlou, A. (2005). TGFβ/Activin/Nodal Signaling Is Necessary for the Maintenance of Pluripotency in Human Embryonic Stem Cells. *Development* 132 (6), 1273–1282. doi:10.1242/dev.01706

Jia, G., Fu, Y., Zhao, X., Dai, Q., Zheng, G., Yang, Y., et al. (2011). N6-methyladenosine in Nuclear RNA Is a Major Substrate of the Obesity-Associated FTO. *Nat. Chem. Biol.* 7 (12), 885–887. doi:10.1038/nchembio.687

Jin, K. X., Zuo, R., Anastassiadis, K., Klungland, A., Marr, C., and Filipczyk, A. (2021). N6-methyladenosine (m(6)A) Depletion Regulates Pluripotency Exit by Activating Signaling Pathways in Embryonic Stem Cells. *Proc. Natl. Acad. Sci. U. S. A.* 118 (51), e2105192118. doi:10.1073/pnas.2105192118

Judson, R. L., Babiarz, J. E., Venere, M., and Blelloch, R. (2009). Embryonic Stem Cell-specific microRNAs Promote Induced Pluripotency. *Nat. Biotechnol.* 27 (5), 459–461. doi:10.1038/nbt.1535

Kasowitz, S. D., Ma, J., Anderson, S. J., Leu, N. A., Xu, Y., Gregory, B. D., et al. (2018). Nuclear m6A Reader YTHDC1 Regulates Alternative Polyadenylation and Splicing during Mouse Oocyte Development. *PLoS Genet.* 14 (5), e1007412. doi:10.1371/journal.pgen.1007412

Lavi, S., and Shatkin, A. J. (1975). Methylated Simian Virus 40-specific RNA from Nuclei and Cytoplasm of Infected BSC-1 Cells. *Proc. Natl. Acad. Sci. U.S.A.* 72 (6), 2012–2016. doi:10.1073/pnas.72.6.2012

Lee, Y., Choe, J., Park, O. H., and Kim, Y. K. (2020). Molecular Mechanisms Driving mRNA Degradation by m6A Modification. *Trends Genet.* 36 (3), 177–188. doi:10.1016/j.tig.2019.12.007

Lesbirel, S., Viphakone, N., Parker, M., Parker, J., Heath, C., Sudbery, I., et al. (2018). The m6A-Methylase Complex Recruits TREX and Regulates mRNA Export. *Sci. Rep.* 8 (1), 13827. doi:10.1038/s41598-018-32310-8

Li, F., Yi, Y., Miao, Y., Long, W., Long, T., Chen, S., et al. (2019). N6-Methyladenosine Modulates Nonsense-Mediated mRNA Decay in Human Glioblastoma. *Cancer Res.* 79 (22), 5785–5798. doi:10.1158/0008-5472.can-18-2868

Li, Z., Weng, H., Su, R., Weng, X., Zuo, Z., Li, C., et al. (2017). FTO Plays an Oncogenic Role in Acute Myeloid Leukemia as a N 6 -Methyladenosine RNA Demethylase. *Cancer Cell* 31 (1), 127–141. doi:10.1016/j.ccell.2016.11.017

Liang, G., and Zhang, Y. (2013). Embryonic Stem Cell and Induced Pluripotent Stem Cell: an Epigenetic Perspective. *Cell Res.* 23 (1), 49–69. doi:10.1038/cr.2012.175

Lin, S., Choe, J., Du, P., Triboulet, R., and Gregory, R. I. (2016). The M 6 A Methyltransferase METTL3 Promotes Translation in Human Cancer Cells. *Mol. Cell* 62 (3), 335–345. doi:10.1016/j.molcel.2016.03.021

Liu, J., Yue, Y., Han, D., Wang, X., Fu, Y., Zhang, L., et al. (2014). A METTL3-METTL14 Complex Mediates Mammalian Nuclear RNA N6-Adenosine Methylation. *Nat. Chem. Biol.* 10 (2), 93–95. doi:10.1038/nchembio.1432

Liu, N., and Pan, T. (2016). N6-methyladenosine-encoded Epitranscriptomics. *Nat. Struct. Mol. Biol.* 23 (2), 98–102. doi:10.1038/nsmb.3162

Liu, X., Wang, Z., Yang, Q., Hu, X., Fu, Q., Zhang, X., et al. (2022). RNA Demethylase ALKBH5 Prevents Lung Cancer Progression by Regulating EMT and Stemness via Regulating P53. *Front. Oncol.* 12, 858694. doi:10.3389/fonc.2022.858694

Matoba, S., and Zhang, Y. (2018). Somatic Cell Nuclear Transfer Reprogramming: Mechanisms and Applications. *Cell Stem Cell* 23 (4), 471–485. doi:10.1016/j.stem.2018.06.018

Meng, T.-G., Lu, X., Guo, L., Hou, G.-M., Ma, X.-S., Li, Q.-N., et al. (2019). Mettl14 Is Required for Mouse Postimplantation Development by Facilitating Epiblast Maturation. *FASEB J.* 33 (1), 1179–1187. doi:10.1096/fj.201800719r

Meyer, K. D., Patil, D. P., Zhou, J., Zinoviev, A., Skabkin, M. A., Elemento, O., et al. (2015). 5′ UTR m6A Promotes Cap-independent Translation. *Cell* 163 (4), 999–1010. doi:10.1016/j.cell.2015.10.012

Novak, D., Hüser, L., Elton, J. J., Umansky, V., Altevogt, P., and Utikal, J. (2020). SOX2 in Development and Cancer Biology. *Seminars Cancer Biol.* 67 (Pt 1), 74–82. doi:10.1016/j.semcancer.2019.08.007

Paris, J., Morgan, M., Campos, J., Spencer, G. J., Shmakova, A., Ivanova, I., et al. (2019). Targeting the RNA m6A Reader YTHDF2 Selectively Compromises Cancer Stem Cells in Acute Myeloid Leukemia. *Cell Stem Cell* 25 (1), 137–148 e6. doi:10.1016/j.stem.2019.03.021

Park, O. H., Ha, H., Lee, Y., Boo, S. H., Kwon, D. H., Song, H. K., et al. (2019). Endoribonucleolytic Cleavage of m6A-Containing RNAs by RNase P/MRP Complex. *Mol. Cell* 74 (3), 494–507 e8. doi:10.1016/j.molcel.2019.02.034

Patil, D. P., Chen, C.-K., Pickering, B. F., Chow, A., Jackson, C., Guttman, M., et al. (2016). m6A RNA Methylation Promotes XIST-Mediated Transcriptional Repression. *Nature* 537 (7620), 369–373. doi:10.1038/nature19342

Peng, F., Xu, J., Cui, B., Liang, Q., Zeng, S., He, B., et al. (2021). Oncogenic AURKA-Enhanced N6-Methyladenosine Modification Increases DROSHA mRNA Stability to Transactivate STC1 in Breast Cancer Stem-like Cells. *Cell Res.* 31 (3), 345–361. doi:10.1038/s41422-020-00397-2

Pezzolo, A., Parodi, F., Marimpietri, D., Raffaghello, L., Cocco, C., Pistorio, A., et al. (2011). Oct-4+/Tenascin C+ Neuroblastoma Cells Serve as Progenitors of Tumor-Derived Endothelial Cells. *Cell Res.* 21 (10), 1470–1486. doi:10.1038/cr.2011.38

Pi, J., Wang, W., Ji, M., Wang, X., Wei, X., Jin, J., et al. (2021). YTHDF1 Promotes Gastric Carcinogenesis by Controlling Translation of FZD7. *Cancer Res.* 81 (10), 2651–2665. doi:10.1158/0008-5472.can-20-0066

Ping, X.-L., Sun, B.-F., Wang, L., Xiao, W., Yang, X., Wang, W.-J., et al. (2014). Mammalian WTAP Is a Regulatory Subunit of the RNA N6-Methyladenosine Methyltransferase. *Cell Res.* 24 (2), 177–189. doi:10.1038/cr.2014.3

Qing, Y., Dong, L., Gao, L., Li, C., Li, Y., Han, L., et al. (2021). R-2-hydroxyglutarate Attenuates Aerobic Glycolysis in Leukemia by Targeting the FTO/m6A/PFKP/LDHB axis. *Mol. Cell* 81 (5), 922–939 e9. doi:10.1016/j.molcel.2020.12.026

Qu, J., Hou, Y., Chen, Q., Chen, J., Li, Y., Zhang, E., et al. (2022). RNA Demethylase ALKBH5 Promotes Tumorigenesis in Multiple Myeloma via TRAF1-Mediated Activation of NF-κB and MAPK Signaling Pathways. *Oncogene* 41 (3), 400–413. doi:10.1038/s41388-021-02095-8

Ranganathan, P., Weaver, K. L., and Capobianco, A. J. (2011). Notch Signalling in Solid Tumours: a Little Bit of Everything but Not All the Time. *Nat. Rev. Cancer* 11 (5), 338–351. doi:10.1038/nrc3035

Roundtree, I. A., Luo, G. Z., Zhang, Z., Wang, X., Zhou, T., Cui, Y., et al. (2017). YTHDC1 Mediates Nuclear Export of N6-Methyladenosine Methylated mRNAs. *Elife* 6, 6. doi:10.7554/eLife.31311

Schwartz, S., Mumbach, M. R., Jovanovic, M., Wang, T., Maciag, K., Bushkin, G. G., et al. (2014). Perturbation of m6A Writers Reveals Two Distinct Classes of mRNA Methylation at Internal and 5′ Sites. *Cell Rep.* 8 (1), 284–296. doi:10.1016/j.celrep.2014.05.048

Shen, C., Sheng, Y., Zhu, A. C., Robinson, S., Jiang, X., Dong, L., et al. (2020). RNA Demethylase ALKBH5 Selectively Promotes Tumorigenesis and Cancer Stem Cell Self-Renewal in Acute Myeloid Leukemia. *Cell Stem Cell* 27 (1), 64–80 e9. doi:10.1016/j.stem.2020.04.009

Sheng, Y., Wei, J., Yu, F., Xu, H., Yu, C., Wu, Q., et al. (2021). A Critical Role of Nuclear m6A Reader YTHDC1 in Leukemogenesis by Regulating MCM Complex-Mediated DNA Replication. *Blood* 138 (26), 2838–2852. doi:10.1182/blood.2021011707

Shi, H., Wang, X., Lu, Z., Zhao, B. S., Ma, H., Hsu, P. J., et al. (2017). YTHDF3 Facilitates Translation and Decay of N6-Methyladenosine-Modified RNA. *Cell Res.* 27 (3), 315–328. doi:10.1038/cr.2017.15

Shi, Y., Tae Do, J., Desponts, C., Hahm, H. S., Schöler, H. R., and Ding, S. (2008). A Combined Chemical and Genetic Approach for the Generation of Induced Pluripotent Stem Cells. *Cell Stem Cell* 2 (6), 525–528. doi:10.1016/j.stem.2008.05.011

Siddique, H. R., and Saleem, M. (2012). Role of BMI1, a Stem Cell Factor, in Cancer Recurrence and Chemoresistance: Preclinical and Clinical Evidences. *Stem Cells* 30 (3), 372–378. doi:10.1002/stem.1035

Slobodin, B., Han, R., Calderone, V., Vrielink, J. A. F. O., Loayza-Puch, F., Elkon, R., et al. (2017). Transcription Impacts the Efficiency of mRNA Translation via Co-transcriptional N6-Adenosine Methylation. *Cell* 169 (2), 326–337 e12. doi:10.1016/j.cell.2017.03.031

Song, S., Fan, G., Li, Q., Su, Q., Zhang, X., Xue, X., et al. (2021). IDH2 Contributes to Tumorigenesis and Poor Prognosis by Regulating m6A RNA Methylation in Multiple Myeloma. *Oncogene* 40 (35), 5393–5402. doi:10.1038/s41388-021-01939-7

Song, T., Yang, Y., Wei, H., Xie, X., Lu, J., Zeng, Q., et al. (2019). Zfp217 Mediates m6A mRNA Methylation to Orchestrate Transcriptional and Post-transcriptional Regulation to Promote Adipogenic Differentiation. *Nucleic Acids Res.* 47 (12), 6130–6144. doi:10.1093/nar/gkz312

Stoltzfus, C. M., and Dane, R. W. (1982). Accumulation of Spliced Avian Retrovirus mRNA Is Inhibited in S -Adenosylmethionine-Depleted Chicken Embryo Fibroblasts. *J. Virol.* 42 (3), 918–931. doi:10.1128/jvi.42.3.918-931.1982

Su, R., Dong, L., Li, C., Nachtergaele, S., Wunderlich, M., Qing, Y., et al. (2018). R-2HG Exhibits Anti-tumor Activity by Targeting FTO/m6A/MYC/CEBPA Signaling. *Cell* 172 (1-2), 90–e23. doi:10.1016/j.cell.2017.11.031

Su, R., Dong, L., Li, Y., Gao, M., Han, L., Wunderlich, M., et al. (2020). Targeting FTO Suppresses Cancer Stem Cell Maintenance and Immune Evasion. *Cancer Cell* 38 (1), 79–96 e11. doi:10.1016/j.ccell.2020.04.017

Takahashi, K., Tanabe, K., Ohnuki, M., Narita, M., Ichisaka, T., Tomoda, K., et al. (2007). Induction of Pluripotent Stem Cells from Adult Human Fibroblasts by Defined Factors. *Cell* 131 (5), 861–872. doi:10.1016/j.cell.2007.11.019

Takahashi, K., and Yamanaka, S. (2016). A Decade of Transcription Factor-Mediated Reprogramming to Pluripotency. *Nat. Rev. Mol. Cell Biol.* 17 (3), 183–193. doi:10.1038/nrm.2016.8

Takahashi, K., and Yamanaka, S. (2006). Induction of Pluripotent Stem Cells from Mouse Embryonic and Adult Fibroblast Cultures by Defined Factors. *Cell* 126 (4), 663–676. doi:10.1016/j.cell.2006.07.024

Visvader, J. E., and Lindeman, G. J. (2008). Cancer Stem Cells in Solid Tumours: Accumulating Evidence and Unresolved Questions. *Nat. Rev. Cancer* 8 (10), 755–768. doi:10.1038/nrc2499

Vu, L. P., Pickering, B. F., Cheng, Y., Zaccara, S., Nguyen, D., Minuesa, G., et al. (2017). The N6-Methyladenosine (m6A)-Forming Enzyme METTL3 Controls Myeloid Differentiation of Normal Hematopoietic and Leukemia Cells. *Nat. Med.* 23 (11), 1369–1376. doi:10.1038/nm.4416

Wang, J., Li, Y., Wang, P., Han, G., Zhang, T., Chang, J., et al. (2020). Leukemogenic Chromatin Alterations Promote AML Leukemia Stem Cells via a KDM4C-ALKBH5-AXL Signaling Axis. *Cell Stem Cell* 27 (1), 81–97 e8. doi:10.1016/j.stem.2020.04.001

Wang, S., Gao, S., Zeng, Y., Zhu, L., Mo, Y., Wong, C. C., et al. (2022). N6-Methyladenosine Reader YTHDF1 Promotes ARHGEF2 Translation and RhoA Signaling in Colorectal Cancer. *Gastroenterology* 162 (4), 1183–1196. doi:10.1053/j.gastro.2021.12.269

Wang, X., Lu, Z., Gomez, A., Hon, G. C., Yue, Y., Han, D., et al. (2014). N6-methyladenosine-dependent Regulation of Messenger RNA Stability. *Nature* 505 (7481), 117–120. doi:10.1038/nature12730

Wang, X., Wang, J., Tsui, Y.-M., Shi, C., Wang, Y., Zhang, X., et al. (2021). RALYL Increases Hepatocellular Carcinoma Stemness by Sustaining the mRNA Stability of TGF-β2. *Nat. Commun.* 12 (1), 1518. doi:10.1038/s41467-021-21828-7

Wang, X., Zhao, B. S., Roundtree, I. A., Lu, Z., Han, D., Ma, H., et al. (2015). N6-methyladenosine Modulates Messenger RNA Translation Efficiency. *Cell* 161 (6), 1388–1399. doi:10.1016/j.cell.2015.05.014

Wang, Y., Li, Y., Toth, J. I., Petroski, M. D., Zhang, Z., and Zhao, J. C. (2014). N6-methyladenosine Modification Destabilizes Developmental Regulators in Embryonic Stem Cells. *Nat. Cell Biol.* 16 (2), 191–198. doi:10.1038/ncb2902

Wei, C.-M., Gershowitz, A., and Moss, B. (1975). Methylated Nucleotides Block 5′ Terminus of HeLa Cell Messenger RNA. *Cell* 4 (4), 379–386. doi:10.1016/0092-8674(75)90158-0

Wen, J., Lv, R., Ma, H., Shen, H., He, C., Wang, J., et al. (2018). Zc3h13 Regulates Nuclear RNA m6A Methylation and Mouse Embryonic Stem Cell Self-Renewal. *Mol. Cell* 69 (6), 1028–1038 e6. doi:10.1016/j.molcel.2018.02.015

Weng, H., Huang, H., Wu, H., Qin, X., Zhao, B. S., Dong, L., et al. (2018). METTL14 Inhibits Hematopoietic Stem/Progenitor Differentiation and Promotes Leukemogenesis via mRNA m6A Modification. *Cell Stem Cell* 22 (2), 191–205 e9. doi:10.1016/j.stem.2017.11.016

Wojtas, M. N., Pandey, R. R., Mendel, M., Homolka, D., Sachidanandam, R., and Pillai, R. S. (2017). Regulation of M(6)A Transcripts by the 3'-->5' RNA Helicase YTHDC2 Is Essential for a Successful Meiotic Program in the Mammalian Germline. *Mol. Cell* 68 (2), 374–387 e12. doi:10.1016/j.molcel.2017.09.021

Wong, D. J., Liu, H., Ridky, T. W., Cassarino, D., Segal, E., and Chang, H. Y. (2008). Module Map of Stem Cell Genes Guides Creation of Epithelial Cancer Stem Cells. *Cell Stem Cell* 2 (4), 333–344. doi:10.1016/j.stem.2008.02.009

Wu, G., Suo, C., Yang, Y., Shen, S., Sun, L., Li, S. T., et al. (2021). MYC Promotes Cancer Progression by Modulating M6 A Modifications to Suppress Target Gene Translation. *EMBO Rep.* 22 (3), e51519. doi:10.15252/embr.202051519

Xiao, W., Adhikari, S., Dahal, U., Chen, Y.-S., Hao, Y.-J., Sun, B.-F., et al. (2016). Nuclear M 6 A Reader YTHDC1 Regulates mRNA Splicing. *Mol. Cell* 61 (4), 507–519. doi:10.1016/j.molcel.2016.01.012

Xu, A., Zhang, J., Zuo, L., Yan, H., Chen, L., Zhao, F., et al. (2022). FTO Promotes Multiple Myeloma Progression by Posttranscriptional Activation of HSF1 in an m6A-YTHDF2-dependent Manner. *Mol. Ther.* 30 (3), 1104–1118. doi:10.1016/j.ymthe.2021.12.012

Xu, Q., and Xie, W. (2018). Epigenome in Early Mammalian Development: Inheritance, Reprogramming and Establishment. *Trends Cell Biol.* 28 (3), 237–253. doi:10.1016/j.tcb.2017.10.008

Yang, Y., Fan, X., Mao, M., Song, X., Wu, P., Zhang, Y., et al. (2017). Extensive Translation of Circular RNAs Driven by N6-Methyladenosine. *Cell Res.* 27 (5), 626–641. doi:10.1038/cr.2017.31

Yankova, E., Blackaby, W., Albertella, M., Rak, J., De Braekeleer, E., Tsagkogeorga, G., et al. (2021). Small-molecule Inhibition of METTL3 as a Strategy against Myeloid Leukaemia. *Nature* 593 (7860), 597–601. doi:10.1038/s41586-021-03536-w

Yin, H., Chen, L., Piao, S., Wang, Y., Li, Z., Lin, Y., et al. (2021). M6A RNA Methylation-Mediated RMRP Stability Renders Proliferation and Progression of Non-small Cell Lung Cancer through Regulating TGFBR1/SMAD2/SMAD3 Pathway. *Cell Death Differ.* doi:10.1038/s41418-021-00888-8 Online ahead of print

Young, R. A. (2011). Control of the Embryonic Stem Cell State. *Cell* 144 (6), 940–954. doi:10.1016/j.cell.2011.01.032

Yue, Y., Liu, J., Cui, X., Cao, J., Luo, G., Zhang, Z., et al. (2018). VIRMA Mediates Preferential m6A mRNA Methylation in 3′UTR and Near Stop Codon and Associates with Alternative Polyadenylation. *Cell Discov.* 4, 10. doi:10.1038/s41421-018-0019-0

Zagozdzon, R., and Golab, J. (2015). Cancer Stem Cells in Haematological Malignancies. *Contemp. Oncol. Pozn.* 19 (1A), A1–A6. doi:10.5114/wo.2014.47127

Zhan, T., Rindtorff, N., and Boutros, M. (2017). Wnt Signaling in Cancer. *Oncogene* 36 (11), 1461–1473. doi:10.1038/onc.2016.304

Zhang, C., Samanta, D., Lu, H., Bullen, J. W., Zhang, H., Chen, I., et al. (2016). Hypoxia Induces the Breast Cancer Stem Cell Phenotype by HIF-dependent and ALKBH5-Mediated m^{6}A-Demethylation of NANOG mRNA. *Proc. Natl. Acad. Sci. U. S. A.* 113 (14), E2047–E2056. doi:10.1073/pnas.1602883113

Zhang, C., Huang, S., Zhuang, H., Ruan, S., Zhou, Z., Huang, K., et al. (2020). YTHDF2 Promotes the Liver Cancer Stem Cell Phenotype and Cancer Metastasis by Regulating OCT4 Expression via m6A RNA Methylation. *Oncogene* 39 (23), 4507–4518. doi:10.1038/s41388-020-1303-7

Zhang, S., Zhao, B. S., Zhou, A., Lin, K., Zheng, S., Lu, Z., et al. (2017). m 6 A Demethylase ALKBH5 Maintains Tumorigenicity of Glioblastoma Stem-like Cells by Sustaining FOXM1 Expression and Cell Proliferation Program. *Cancer Cell* 31 (4), 591–606 e6. doi:10.1016/j.ccell.2017.02.013

Zhao, X., Yang, Y., Sun, B.-F., Shi, Y., Yang, X., Xiao, W., et al. (2014). FTO-dependent Demethylation of N6-Methyladenosine Regulates mRNA Splicing and Is Required for Adipogenesis. *Cell Res.* 24 (12), 1403–1419. doi:10.1038/cr.2014.151

Zheng, G., Dahl, J. A., Niu, Y., Fedorcsak, P., Huang, C.-M., Li, C. J., et al. (2013). ALKBH5 Is a Mammalian RNA Demethylase that Impacts RNA Metabolism and Mouse Fertility. *Mol. Cell* 49 (1), 18–29. doi:10.1016/j.molcel.2012.10.015

Zhou, J., Wan, J., Gao, X., Zhang, X., Jaffrey, S. R., and Qian, S.-B. (2015). Dynamic m6A mRNA Methylation Directs Translational Control of Heat Shock Response. *Nature* 526 (7574), 591–594. doi:10.1038/nature15377

Zhou, J., Wan, J., Shu, X. E., Mao, Y., Liu, X.-M., Yuan, X., et al. (2018). N6-Methyladenosine Guides mRNA Alternative Translation during Integrated Stress Response. *Mol. Cell* 69 (4), 636–647 e7. doi:10.1016/j.molcel.2018.01.019

Zhou, T., Li, S., Xiang, D., Liu, J., Sun, W., Cui, X., et al. (2020). m6A RNA Methylation-Mediated HNF3γ Reduction Renders Hepatocellular Carcinoma Dedifferentiation and Sorafenib Resistance. *Sig Transduct. Target Ther.* 5 (1), 296. doi:10.1038/s41392-020-00299-0

Zhu, Y., Zhou, B., Hu, X., Ying, S., Zhou, Q., Xu, W., et al. (2022). LncRNA LINC00942 Promotes Chemoresistance in Gastric Cancer by Suppressing MSI2 Degradation to Enhance C-Myc mRNA Stability. *Clin. Transl. Med.* 12 (1), e703. doi:10.1002/ctm2.703

Conflict of Interest: The authors declare that the research was conducted in the absence of any commercial or financial relationships that could be construed as a potential conflict of interest.

The reviewer YD declared a shared affiliation with the authors to the handling editor at the time of the review.

frontiers | Frontiers in Cell and Developmental Biology

REVIEW
published: 11 July 2022
doi: 10.3389/fcell.2022.956649

ADAR1-Mediated RNA Editing and Its Role in Cancer

Jizhe Liu[1,2,3], *Fei Wang*[1,4], *Yindan Zhang*[1,2,3], *Jingfeng Liu*[5]* and *Bixing Zhao*[1,4]*

[1]The United Innovation of Mengchao Hepatobiliary Technology Key Laboratory of Fujian Province, Mengchao Hepatobiliary Hospital of Fujian Medical University, Fuzhou, China, [2]College of Life Science, Fujian Agriculture and Forestry University, Fuzhou, China, [3]Fujian Institute of Research on the Structure of Matter, Chinese Academy of Sciences, Fuzhou, China, [4]Mengchao Med-X Center, Fuzhou University, Fuzhou, China, [5]Fujian Medical University Cancer Hospital, Fujian Cancer Hospital, Fuzhou, China

It is well known that the stability of RNA, the interaction between RNA and protein, and the correct translation of protein are significant forces that drive the transition from normal cell to malignant tumor. Adenosine deaminase acting on RNA 1 (ADAR1) is an RNA editing enzyme that catalyzes the deamination of adenosine to inosine (A-to-I), which is one dynamic modification that in a combinatorial manner can give rise to a very diverse transcriptome. ADAR1-mediated RNA editing is essential for survival in mammals and its dysregulation results in aberrant editing of its substrates that may affect the phenotypic changes in cancer. This overediting phenomenon occurs in many cancers, such as liver, lung, breast, and esophageal cancers, and promotes tumor progression in most cases. In addition to its editing role, ADAR1 can also play an editing-independent role, although current research on this mechanism is relatively shallowly explored in tumors. In this review, we summarize the nature of ADAR1, mechanisms of ADAR1 editing-dependent and editing-independent and implications for tumorigenesis and prognosis, and pay special attention to effects of ADAR1 on cancers by regulating non-coding RNA formation and function.

Keywords: ADAR1, RNA editing, cancer, non-coading RNA, adenosine to inosine

OPEN ACCESS

Edited by:
Xiaoxing Li,
The First Affiliated Hospital of Sun Yat-sen University, China

Reviewed by:
Yao Lin,
Fujian University of Traditional Chinese Medicine, China
Heather Hundley,
Indiana University, United States

***Correspondence:**
Jingfeng Liu
drjingfeng@126.com
Bixing Zhao
bixingzhao@gmail.com

Specialty section:
This article was submitted to Signaling, a section of the journal Frontiers in Cell and Developmental Biology

Received: *30 May 2022*
Accepted: *23 June 2022*
Published: *11 July 2022*

Citation:
Liu J, Wang F, Zhang Y, Liu J and Zhao B (2022) ADAR1-Mediated RNA Editing and Its Role in Cancer. Front. Cell Dev. Biol. 10:956649. doi: 10.3389/fcell.2022.956649

INTRODUCTION

A-to-I editing of RNA, a widespread co/post-transcriptional modification in mammals, is catalyzed by adenosine deaminases acting on RNA (ADARs) and has recently been recognized as an essential mechanism of cancer biology (Han et al., 2015; Baker and Slack, 2022). With the continuous increase of next-generation sequencing data, transcriptomics modifications, so-called RNA mutations, are becoming a significant force in promoting the transformation of normal cells into malignant tumors and providing tumor diversity to avoid immune attacks (Nishikura, 2010; Sagredo et al., 2018; Shevchenko and Morris, 2018). ADARs were first discovered in *Xenopus laevis* oocytes and embyros (Bass, 1987; Quin et al., 2021), confirming mediating editing of adenosine-to-inosine (A-to-I) in double-stranded (ds) RNA in mammals (Xu and Öhman, 2018). This edit acts as a functional A-to-G mutation by hydrolytic deamination at C6 of adenosine, changing it to inosine in the region of dsRNA (**Figure 1A**) (Nishikura, 2016).

By hydrolytically deaminating adenosine's 6-position, ADARs catalyze the deamination of adenosine to inosine (Polson et al., 1991). An important target for A-to-I RNA editing is a dsRNA derived from inverted Alu repetitive elements (Alu dsRNA) (Athanasiadis et al., 2004; Bazak et al., 2014). Since cells interpret inosine (I) as guanosine (G), A-to-I editing can lead to non-synonymous codon changes in the transcript and alternative splicing (Walkley and Li, 2017;

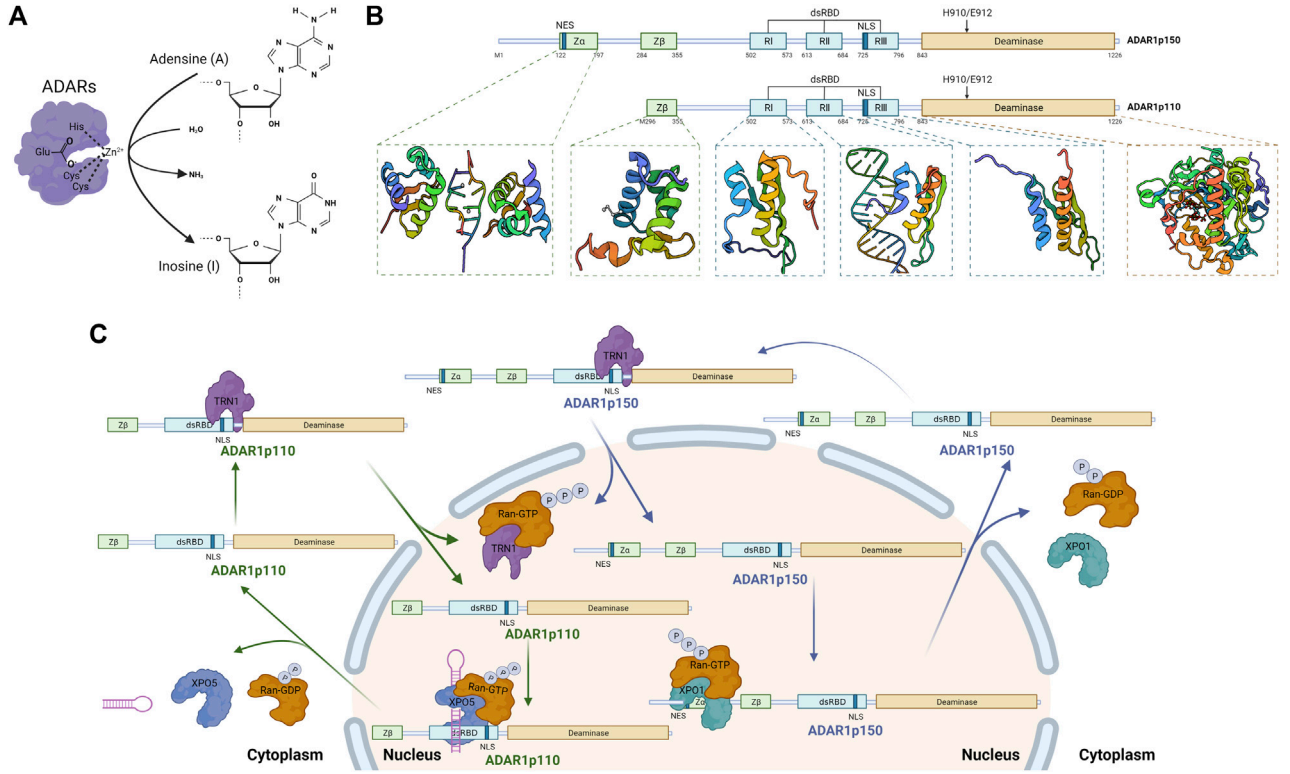

FIGURE 1 | Catalytic function, domain organization, and shuttle mechanism of Adenosine Deaminase Acting on RNA 1 (ADAR1) (Created with BioRender.com). **(A)** RNA editing by ADARs. Alternative RNA editing by C6 deamination of adenosine (A) in the double-stranded RNA region to generate inosine (I), catalyzed by ADARs enzymes. **(B)** Schematic of the domain structure of two isoforms of ADAR1. ADAR1p150 and ADAR1p110 share identical sequence except for an additional N-terminal sequence for ADAR1p150, including an additional Zα domain (PDB: 2GDB) (Placido et al., 2007) and the NES which allows for both cytoplasmic and nuclear localization. Both contain a Zβ domain (PDB: 1XMK) (Athanasiadis et al., 2005) that mainly mediate Z-DNA/RNA binding, three dsRBDs domain (PDB: 2LJH, 2L2K, 2MDR) (Stefl et al., 2010; Barraud et al., 2012; Barraud et al., 2014) that mediate dsRNA binding and homodimerization, and a deaminase domain (PDB: 1ZY7) (Macbeth et al., 2005) that is the catalytic center of ADAR1. **(C)** Cellular localization of ADAR1. XPO1 binds to NES located within the Zα structural domain and regulates nuclear export of ADAR1p150 in the presence of RAN-GTP. Nuclear import of ADAR1p110 is mediated by binding of TRN1 to dsRBD3. NLS located in the third dsRBD, a domain common to both ADAR1 isoforms, binds with TRN1 to assist in the targeting of ADAR1 in the nucleus.

Eisenberg and Levanon, 2018). In addition, ADARs can bind introns or 3′ untranslated regions (UTRs) to regulate the expression level of relative coding regions (Daniel et al., 2015; Sagredo et al., 2018). Still, it also affects targeting and disrupts the maturation of non-coding consequences, mainly microRNA, lncRNA, and circRNA (Velazquez-Torres et al., 2018; de Santiago et al., 2021; Shen et al., 2021). As a result of ADAR-mediated editing, which arises from mismatched A-to-I signatures after reverse transcription, more than 4 million edited positions have been identified (Bazak et al., 2014; Gallo et al., 2017).

Mammals have three ADAR genes, ADAR1 (also called ADAR, DRADA), ADAR2 (also called ADARB1), and ADAR3 (also called ADARB2), with specific structure, location, and function differences (Xu and Öhman, 2018; Shen et al., 2022). Currently, ADAR1 and ADAR2 have been shown to be expressed throughout most tissues and to be catalytically active, and the former mediates more editing events (Hogg et al., 2011). However, ADAR3 is specifically expressed in the brain and its function is only mentioned in a few articles (Melcher et al., 1996; Chen et al., 2000; Walkley and Li, 2017; Samuel, 2019). In glioblastoma, ADAR3 has been reported to be upregulated to competitively inhibit RNA editing at the Q/R site of *GRIA2* by ADAR2 (Oakes et al., 2017; Wang et al., 2018). And these genes of the ADAR family have similar domain structures, mainly composed of a deaminase domain and two or three dsRNA binding domains (dsRBDs) (Erdmann et al., 2021; Quin et al., 2021). The deaminase domain of both ADAR1 and ADAR2 catalyzes the hydrolytic deamination of adenosine to inosine in dsRNA, while the catalytic activity of ADAR3 has not been reported so far (Chen et al., 2000; Nishikura, 2016; Oakes et al., 2017; Samuel, 2019). The dsRBD (~65 amino acids) binds directly to dsRNA through its own structural domain. In spite of the fact that both ADAR1 and ADAR2 had been shown to be associated with tumor progression, editing events regulated by ADAR1 are more strongly correlated with cancer development (Maas et al., 2001; Paz-Yaacov et al., 2015). There could be two main reasons for this result. One is that the enrichment of ADAR1 far exceeds that of ADAR2. ADAR1 expression was seen in nearly all tissues, while ADAR2 was most expressed in the brain, but more minor in other tissues (Paz-Yaacov et al., 2015). Significantly, ADAR1 is absolutely required, and ADAR1-null

mice die during embryonic life due to extensive apoptosis and defective hematopoiesis (Hartner et al., 2004; Wang et al., 2004). Furthermore, two is that human Adar1 maps to a single locus on chromosome 1q21, whose amplification is the most common cytogenetic abnormalities in multiple types of cancer and a poor prognostic factor (Knuutila et al., 1998; Jiang et al., 2012; Teoh et al., 2018).

ADARs editing is critical for survival in mammals, and its dysregulation may contribute to cancer development (Ramírez-Moya et al., 2021). The function of ADAR1-mediated RNA editing in immunity, especially innate immunity, has been summarized in many reviews (Lamers et al., 2019; Quin et al., 2021; Song et al., 2022), so this article will not address this aspect of the function. In addition to its editing role, ADAR1 can also play an editing-independent role. Regardless of whether the stability of ADARs regulatory RNAs is dependent on RNA editing, RNA binding is essential for their action (Wang I. X et al., 2013). Still, it will focus on the role of ADAR1 in cancer. For example, ADAR1 is more abundant in lung, liver, esophageal and chronic myelogenous leukemia, and with few exceptions, it promotes cancer progression (Jiang et al., 2012; Qin et al., 2014; Zhang et al., 2018; Sun et al., 2020). This review will focus on the structure and regulatory mechanisms of the ADAR1 enzymes and the relationship between aberrant editing of specific substrates and tumorigenesis, especially non-coding RNA.

NATURE OF ADENOSINE DEAMINASE ACTING ON RNA 1

The human ADAR1 gene spans approximately 40 kb and includes 17 exons, and the transcript level of ADAR1 is increased by IFN or pathogen stimulation (George et al., 2011). ADAR1 has two protein isoforms, full-length ADAR1p150 (150 kDa) and shorter ADAR1p110 (110 kDa) (**Figure 1B**) (Sun et al., 2021). Both contain a nuclear localization signal (NLS), allowing nuclear localization (Nishikura, 2016; Baker and Slack, 2022). In addition, ADAR1p150 contains a nuclear export signal (NES), accordingly shuttles between the nucleus and cytoplasm and is predominantly cytoplasmic (Xu and Öhman, 2018; Sun et al., 2021; Baker and Slack, 2022). Both isoforms contain a Zβ domain, three dsRNA-binding domains and a deaminase catalytic domain (George et al., 2011). 1) Zβ domain is a Z-DNA/RNA binding domain which NLS locates in (Athanasiadis et al., 2005); 2) dsRNA-binding domains (RI, RII, and RIII, ~65 amino acids), which have an α-β-β-β-α configuration, make direct contact with dsRNA (Thomas and Beal, 2017); 3) deaminase domain is the catalytic center of ADAR1, in which the E912A point mutation in ADAR1p150 (E617A for ADAR1p110) disrupts catalytic deaminase activity (Wang I. X et al., 2013; Lamers et al., 2019; Baker and Slack, 2022). Moreover, besides Zβ domain, ADAR1p150 contains Zα domain, another Z-DNA/RNA binding domain, which may have affected its bonding preferences (Nishikura, 2016; Sun et al., 2021). Notably, shorter ADAR1p110 is constitutively expressed in ubiquitous types of cells, whereas full-length ADAR1p150 is expressed only when some activators stimulate cells, such as type I and type II IFN (Rice et al., 2012; Li et al., 2016). Among the inverted retrotransposon repeats of the long spacer nuclear element (LINE) and short spacer nuclear element (SINE) families are a number of endogenous long dsRNAs that are thought to be key-acting substrate RNAs for ADAR1 (Liddicoat et al., 2015). Moreover, the Alu motif mentioned above is a member of the SINE family and is also one of the sites found to be subject to the greatest extent and number of ADAR1 edits (Nishikura, 2010; Liddicoat et al., 2015; Nishikura, 2016).

Although ADAR1p150 is primarily localized in the cytoplasm and ADAR1p110 is predominantly localized in the nucleus, both ADAR1p150 and ADAR1p110 shuttle between the nucleus and cytoplasm (**Figure 1C**) (Strehblow et al., 2002; Desterro et al., 2003). The nuclear export factor exportin 1 (XPO1, also known as CRM1) binds to the nuclear export signal (NES) located within the Zα structural domain and regulates nuclear export of ADAR1p150 in the presence of RAN-GTP (Poulsen et al., 2001). The binding of transport protein 1 (TRN1) to dsRBD3 mediates nuclear import of ADAR1p110, a process that is inhibited by dsRNA binding (Barraud et al., 2014). The nuclear localization signal (NLS) located in the third dsRBD, a domain common to both ADAR1 isoforms, binds with TRN1 to assist in the targeting of ADAR1 in the nucleus (Fritz et al., 2009).

RNA EDITING-DEPENDENT OF ADENOSINE DEAMINASE ACTING ON RNA 1 AND TUMORIGENESIS AND PROGRESSION MECHANISMS

ADAR1 is frequently amplified in many diverse types of cancers with elevated activity (Fritzell et al., 2018), including hepatocellular carcinoma, non-small cell lung cancer, thyroid cancer, pancreatic cancer, esophageal cancer, cervical cancer, and multiple myeloma, and consistent with increased RNA editing levels of its substrates (Chen et al., 2013; Han et al., 2015; Paz-Yaacov et al., 2015; Chen Y et al., 2017; Hu et al., 2017; Sun et al., 2020). Conversely, decreased ADAR1 expression was observed in metastatic melanoma, invasive breast cancer, and kidney cancers (Shoshan et al., 2015; Gumireddy et al., 2016). Most RNA editing sites are located in noncoding regions or noncoding sequences and therefore do not result in changes in protein sequence or expression (Fritzell et al., 2018; Quin et al., 2021). However, a small number of coding events still occur in the coding region, thus affecting gene expression, or even if RNA editing occurs in non-coding sequences, it may indirectly regulates gene expression through mechanisms such as affecting the function of non-coding RNAs. The focus of this section is on this particular editing events by ADAR1 catalyzed, which contribute significantly to cancer development and metastasis. And the content of this section is divided into four main parts according to the differences in catalytic substrates, coding gene, intron, 3′ UTR, and three non-coding RNAs, including microRNA, lncRNA and circRNA. In most cases, increased ADAR1 expression and/or

TABLE 1 | ADAR1 edits specific substrates involved in cancer progression.

Gene	Substrate type	Editing residues	Cancer	Hallmark	References
ADAR1 promoting cancer					
AZIN1	Coding gene	S/G	LIHC[a]	Growth, colony formation, invasion, migration	Chen et al. (2013)
			ESCC[a]		Qin et al. (2014)
			NSCLC[a]		Hu et al. (2017)
			CRC[a]	Growth, colony formation, invasion, migration, stemness	Shigeyasu et al. (2018), Takeda et al. (2019)
BLCAP	Coding gene	Y/C	LIHC[a]	Proliferation, invasion, migration	Hu et al. (2015)
		Y/C; Q/R; K/R	CESC[a]	Invasion, migration	Chen W et al. (2017)
NEIL1	Coding gene	K/R	MM[a]	Growth, metastasis, colony formation	Jiang et al. (2012)
GLI1	Coding gene	R/G	MM[a]	Growth, colony formation, self-renewal	Shimokawa et al. (2013), Lazzari et al. (2017)
ITGA2	Coding gene	NA[a]	LIHC[a]	Invasion, migration	Yu et al. (2019)
CDK13	Coding gene	Q/R	TC[a]	Proliferation, viability, invasion	Dong et al. (2018), Ramírez-Moya et al. (2021)
FAK	Intron	Intron	LUAD[a]	Growth, metastasis, colony formation	Amin et al. (2017)
ARHGAP26	3′ UTR	3′ UTR	BRCA[a]	Growth, malignant transformation	Wang Q et al. (2013)
DHFR	3′ UTR	3′ UTR	BRCA[a]	Proliferation	Nakano et al. (2017)
miR-200b	MiRNA	MiRNA	TC[a]	Proliferation, invasion, migration	Ramírez-Moya et al. (2020)
miRNA-149-3p	MiRNA	MiRNA	MM[a]	Proliferation, growth	Yujie Ding et al. (2020)
LINC00944	LncRNA	LncRNA	BRCA[a]	Growth, colony formation	de Santiago et al. (2021)
PCA3	LncRNA	Duplex with PRUNE2	PRAD[a]	Growth, adhesion, migration	Bussemakers et al. (1999)
circNEIL3	CircRNA	CircRNA	PDAC[a]	Proliferation, metastasis	Olive et al. (2009), Shen et al. (2021)
circARSP91	CircRNA	CircRNA	LIHC[a]	Growth	You et al. (2015), Shi et al. (2017)
hsa_circ_0004872	CircRNA	CircRNA	GC[a]	Metastasis, colony formation	Ma et al. (2020)
ADAR1 suppressing cancer					
GABRA3	Coding gene	I/M	BRCA[a]	Migration/invasion	Gumireddy et al. (2016)
CCNI	Coding gene	R/G	MEL[a]	Activates of TIL	Zhang et al. (2018)
DFFA	3′ UTR	3′ UTR	BRCA[a]	Invasion	Roberts et al. (2018)
miR-455-5p	MiRNA	MiRNA	MM[a]	Growth, metastasis	Shoshan et al. (2015)
miR-378a-3p	MiRNA	MiRNA	MM[a]	Invasion, migration	Velazquez-Torres et al. (2018)
miR-222	MiRNA	MiRNA	MM[a]	Growth and metastasis, invasion	Galore-Haskel et al. (2015)

[a]*NA, not available; LIHC, liver hepatocellular carcinoma; ESCC, esophageal squamous cell carcinoma; NSCLC, non-small-cell lung cancer; CRC, colorectal carcinoma; CESC, cervical squamous cell carcinoma and endocervical adenocarcinoma; MM, multiple myeloma; TC, thyroid cancer; LUAD, lung adenocarcinoma; BRCA, breast invasive carcinoma; PRAD, prostate adenocarcinoma; PDAC, pancreatic ductal adenocarcinoma; GC, gastric cancer; MEL, melanoma.*

activity promotes cancer generation and progression; while in a few cancers, low expression and/or activity of ADAR1 mediating cancer phenotypes (Shoshan et al., 2015; Gumireddy et al., 2016). We have compiled and summarized the prior literature that experimentally confirms the substrate, editing site, and effects of ADAR1 editing on cancer phenotypes (**Table 1**).

Coding Genes

Early mechanistic studies on ADARs focused on causing protein recoding, which potentially modifies the amino acid sequence, thereby leading to decreased activity or acquisition of the encoded protein (**Figure 2A**). The coding sequence has a double-stranded structure on the exon, which is the region that may be subject to ADAR1-mediated A to I editing. Most A-to-I editing sites are generally found in introns and 3' UTRs of coding genes, with 1% or fewer occurring in coding exons (Bahn et al., 2012; Wang I. X et al., 2013; Picardi et al., 2015).

Antizyme inhibitor 1 (AZIN1) is the most widely studied ADAR1 substrate in cancer, and edited AZIN1 promotes the development of hepatocellular carcinoma, non-small cell lung cancer, colorectal cancer, esophageal squamous cell carcinoma, and other cancers (Chen et al., 2013; Qin et al., 2014; Hu et al., 2017; Shigeyasu et al., 2018; Xu and Öhman, 2018). For instance, Under the action of deaminase of ADAR1, the serine (S) transforms glycine (G) substitution at residue 367, located in β-strand 15 of AZIN1 in HCC, resulting to its conformational change, inducing a cytoplasmic-to-nuclear translocation, and conferred "gain-of-function" phenotype, such as growth, colony formation, invasion, and migration (Chen et al., 2013). ADAR1 over-edited AZIN1 RNA is an independent risk factor for lymph node and distant metastasis and may serve as a prognostic basis for overall survival and disease-free survival (Shigeyasu et al., 2018). In several of these cancers, AZIN1 has the same editing site and causes similar phenotypic changes in cancer cells (Qin et al., 2014; Hu et al., 2017; Shigeyasu et al., 2018). However, in colorectal cancer, in addition to the above phenotypes, changes in cell stemness are also involved (Shigeyasu et al., 2018; Takeda et al., 2019).

Bladder cancer-associated protein (BLCAP) is a highly conserved gene that plays a tumor-suppressive role in different

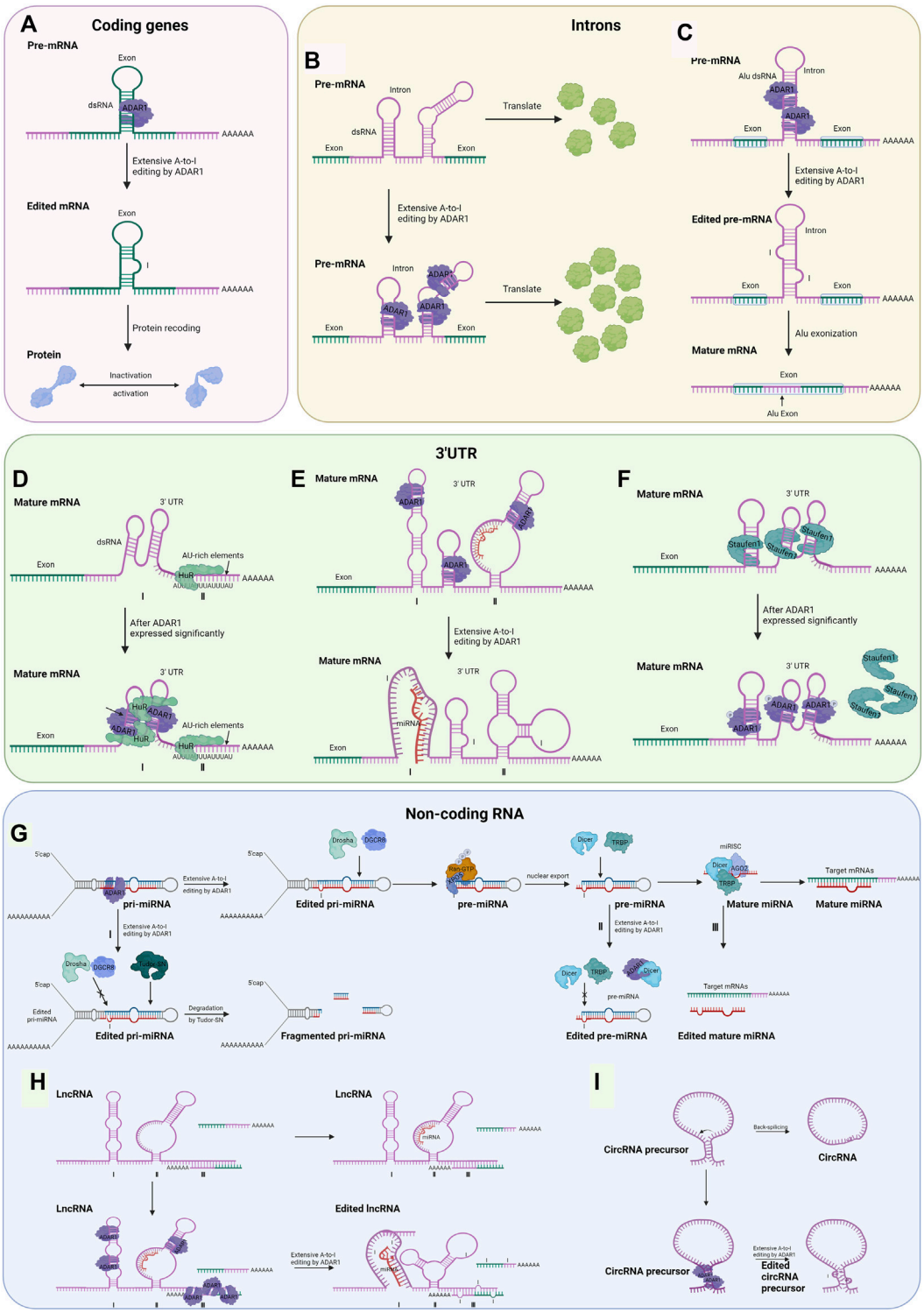

FIGURE 2 | Possible regulatory mechanisms for RNA editing-dependent and editing-independent of ADAR1 involved in tumorigenesis and progression (Created with BioRender.com). **(A)** The dsRNA hairpin structures formed in the exonic region of the encoded gene are recognized by ADAR1. It undergoes A-to-I editing, and splicing machinery interprets inosine as guanosine, which leads to inactivation or activation of the final translation product. **(B)** ADAR1 binds to the intron of pre-mRNA, resulting in increased abundance of exon. **(C)** By editing intronic fold-back dsRNAs with A-to-I editing, splice sites could be created or deleted, leading to the inclusion or exclusion of Alu exons. **(D)** ADAR1 interacts with HuR proteins to coregulate common transcripts. **(E)** Editing of the 3′UTR can change the stability of the mRNA by creating or destroying the binding site of the miRNA. I: acquired the ability to bind miRNA; II: loss of the ability to bind miRNA. **(F)** ADAR1 competes with

(*Continued*)

FIGURE 2 | Staufen1 protein for the dsRNA binding site, thereby excluding Staufen1 binding and subsequent decaying of antiapoptotic genes in an editing-independent manner. **(G)** The Drosha/DGCR8 complex digests ADAR1-edited pri-miRNAs in the nucleus, generating approximately 70 nt of pre-miRNA intermediates that are translocated to the cytoplasm mediated by exportin-5 (Exp5) and Ran-GTP. The Dicer/TRBP complex undergoes a second cleavage to generate mature miRNAs which target and regulate downstream mRNAs. Because of the editing effect of ADAR1, the process may be aborted at three points. **I**: in pri-mRNA, editing occurs at the RNA site that binds to Drosha and DGCR8, which causes the formation of fragmented pri-miRNA in the action of Tudor-SN; **II**: in pre-miRNA, editing occurs at the RNA site that binds to Dicer and TRBP, or ADAR1 interacts with Dicer; **III**: in mature miRNA, editing occurs at the RNA site that binds to mRNA. The mechanism of miRNA editing by ADAR1 is also applicable to the other two non-coding RNAs and will not be described below. **(H)** Regulatory mechanisms of ADAR1 Editing for dsRNA on lncRNA. **I**: acquired the ability to bind miRNA; **II**: loss of the ability to bind miRNA; **III**: lncRNAs are recognized and edited by ADAR1 after complementary pairing with mRNA bases. **(I)** Editing of Alu repeats can antagonize circRNA formation.

cancers and is a novel ADAR-mediated editing substrate in hepatocellular carcinoma and cervical cancer (Hu et al., 2015; Chen W et al., 2017). Over-editing of BLCAP was found in 40.1% HCCs compared to adjacent liver tissues. And RNA-edited BLCAP may stably promote cell proliferation by activating AKT/mTOR signal pathway (Hu et al., 2015). In cervical cancers, editing events by ADAR1 alter the genetically coded amino acid in BLCAP YXXQ motif, inducing BLCAP to lose the inhibition to signal transducer and activator of transcription 3 (STAT3) activation, which drives the carcinogenesis progression (Chen W et al., 2017). However, compared with the related normal tissues, BLCAP edited isoforms were reduced in astrocytoma, bladder cancer and colorectal cancer, indicating that the RNA editing level of BLCAP differs in different tumors (Meng et al., 2017).

However, in contrast to the above examples, in some cancers, such as breast cancer, melanoma, RNA editing of ADAR1 inhibits cancer development. In other words, low levels of ADAR1 editing in certain cancers lead to poor prognosis of patients (Gumireddy et al., 2016; Nishikura, 2016; Zhang et al., 2018; Baker and Slack, 2022). ADAR1-edited Gabra3 was only in non-invasive breast cancer and showed that edited Gabra3 reduced the abundance of wild-type Gabra3 on the cell surface and inhibited AKT activation, thereby suppressing breast cancer cell invasion and metastasis (Gumireddy et al., 2016). In melanoma, the ADAR1-edited cell cycle protein I (CCNI)^{R75G} peptide activates tumor-infiltrating lymphocytes (TIL) and promotes TIL killing of cancer cells (Zhang et al., 2018).

To summarize, the above findings suggest that the expression of ADAR1 varies depending on the coding gene and cancer type. Whether ADAR1 overexpression or over-editing promotes or prevents cancer progression depends on the type of editing substrates, their level of expression, and how they participate respectively in regulating malignant changes in cancer cells.

Intron

The intron in certain coding regions has also been shown to recognize and bind to ADAR1 before being spliced and promote exon expression in an editing-dependent manner. A few articles have reported this approach, and the mechanisms have not been explored in detail (**Figure 2B**). ADAR1 post-transcriptionally increased the abundance of focal adhesion kinase (FAK) protein by binding and editing to a specific intronic site on chr8: 141,702,274 in FAK transcript, resulting in the increased stabilization of FAK mRNA, thereby promoting mesenchymal properties, migration, and invasion of lung adenocarcinoma (Amin et al., 2017).

RNA editing of Alu-rich intron regions may lead to Alu exonization, which controls mRNA levels and translation efficiency and potentially leads to disease (**Figure 2C**) (Lev-Maor et al., 2007; Sakurai et al., 2010). However, this modality is only found in G protein-coupled receptor 107 (Athanasiadis et al., 2004), nuclear prelamin A (Lev-Maor et al., 2007) and seryl-tRNA synthetase (Sakurai et al., 2010). However, there is no evidence that ADAR1 mediates cancer-associated gene exonization.

3′ Untranslated Region

There are two main ways ADAR1-catalyzed editing on the 3′ UTR influences gene expression regulation. A relatively common one is editing of Alu dsRNA on the 3′ UTR, which binds to and is regulated by microRNA when unedited. The other is dependent on editing to alter the stability of the mature mRNA, mainly achieved by the recruitment of HuR proteins with ADAR1 (**Figure 2D**) (Song et al., 2016). RNA editing events that occur in the 3′UTR of mRNAs may alter their interactions with miRNAs. Within the 3′ UTRs of mRNAs from nine different types of cancer, Pinto et al. identified over 63,000 editing sites that harbor Alu dsRNAs that serve as recruitment signals for ADAR (Pinto et al., 2018). Several studies have established that RNA editing that occurs in the 3′UTR can create or disrupt miRNA binding sites, thereby altering the mRNA stability of cancer-related genes (**Figure 2E**) (Liang and Landweber, 2007; Borchert et al., 2009).

For instance, 3′ UTR of Rho GTPase activating protein 26 (ARHGAP26) transcript undergoes ADAR1-catalyzed extensive A-to-I RNA editing (Wang Q et al., 2013). Known as a cancer suppressor, ARHGAP26 activates Rho GTPases (Zhong et al., 2019). Undergone A-to-I editing, the 3′ UTR of ARHGAP26 failed to pair with miR-30b-3p and miR-573, thus translating without interference, thereby promoting breast cancer growth and malignant transformation (Wang Q et al., 2013). As a counterexample, ADAR1, which is much less expressed in breast cancer, targets the 3′ UTR of DNA fragmentation factor subunit alpha (DFFA) transcript, therefore promoting cancer cell invasion (Roberts et al., 2018). DFFA is an inhibitor of caspase-activated DNase (ICAD) that triggers DNA fragmentation during apoptosis (Fawzy et al., 2017). In non-invasive, hormone-responsive breast cancer cell lines, editing of DFFA mRNA by ADFA1 rendered the mRNA unrecognized by miR-140-3p, thereby increasing DFFA levels and inducing

apoptosis, whereas lack of editing in highly invasive, triple-negative breast cancer cell lines prevented DFFA from being regulated by miR-1403p (Roberts et al., 2018).

Altered RNA stability is an essential mechanism for ADAR1-mediated regulation of gene expression. ADAR1 recruits and interacts with human antigen R (HuR, gene name *ELAVL1*), a family of RNA-binding proteins selectively binds to single-stranded AU-rich RNA sequences (de Silanes et al., 2003; Meisner et al., 2004), to increase transcript stability (**Figure 2D**) (Wang I. X et al., 2013). It is estimated that 3′ UTR of up to 8% of all mRNAs contain AU-rich elements, including genes for cancer progression (Shaw and Kamen, 1986; Shaw et al., 2006). Among the 775 genes whose expression levels decreased after ADAR1 knockdown, the genes containing HuR binding sites showed significantly higher expression than the others (Wang I. X et al., 2013), such as MCM4 (Bagley et al., 2012), TMPO(Li et al., 2020), and GSR (McLoughlin et al., 2019).

Non-Coding RNA

Currently, dysregulated levels of non-coding RNAs (ncRNAs) appear to be reported for every type of cancer, and non-coding transcripts are expected to be the next class of diagnostic and therapeutic tools in oncology (Song et al., 2016; Shen et al., 2022). In addition to RNA editing mediated amino acid substitutions in specific genes contributing to cancer, elevated ADAR1 editing of non-coding RNAs, can also promote cancer progression (Qi et al., 2014; Ramírez-Moya et al., 2020). ADARs can also bind and edit some non-coding genes that contain inverted Alu repeats or LINE of non-coding genes, such as microRNA (miRNA), long non-coding RNA (lncRNA), and circular RNA (circRNA) to suppress non-coding RNA maturation (Torsin et al., 2021).

MicroRNA

According to their binding sites along with RNA transcripts, ADAR1 protects mRNA from degradation, regulates miRNA processing, and alters splicing patterns (Xu and Öhman, 2018).

It has been shown that ADAR1 interacts with Dicer or DCGR8 to mediate processing of pre-miRNAs, ultimately leading to microRNA destabilization (Bahn et al., 2015). In this way, the editing of certain microRNA precursors results in lower levels of expression or altered function of mature miRNAs, thereby leading to alterations in certain cancer phenotypes (**Figure 2G**). In thyroid cancer cells, ADAR1-dependent editing miR-200b exhibits a lower activity against its target ZEB1-3′ UTR, which facilitates the epithelial–mesenchymal transition, thus resulting in proliferation, invasion, and migration of thyroid tumor cells (Ramírez-Moya et al., 2020). In melanoma cells, ADAR1p150 directly interacted with Dicer, an enzyme cleave precursor miRNA (usually 70 nt) to form mature miRNA (around 22 nt), which increased the cleavage rate of pre-miRNA and promoted the loading and maturing of miRNA (Chiosea et al., 2006), thereby promoting the biosynthesis and function of miRNA-149-3p (Yujie Ding et al., 2020). The expression of GSK3α, a direct target of miR-149-3p, is decreased, eventually resulting in proliferation of melanoma cells and inhibited cell apoptosis (Yujie Ding et al., 2020).

Likewise, modification of certain microRNAs by ADAR1 can exert a suppressive effect on cancer, and such miRNAs tend to be less expressed in cancerous tissues with a high metastatic capacity (Shoshan et al., 2015; Velazquez-Torres et al., 2018; Xu and Öhman, 2018). For example, with high levels of A-to-I editing in low metastatic melanoma but not in high metastatic melanoma, edited miR-455-5p lost the binding site of its downstream cancer suppressor protein CPEB1, which resulted in the suppression of melanoma growth and metastasis (Shoshan et al., 2015). Only in non-metastatic melanoma cells, edited miR-378a-3p predominantly binds to and represses the expression of the 3′-UTR of the PARVA oncogene, thereby inhibiting the progression of melanoma to a malignant phenotype (Velazquez-Torres et al., 2018).

Long Non-Coding RNA

Recently, LncRNAs have been shown to be central regulators of gene expression in a variety of genes (Guo et al., 2020). The lncRNAs involved in oncogenes and tumor suppressors are modified by A-to-I RNA editing machinery, with modifications that are drastically altered in cancer cells (Silvestris et al., 2020). ADAR1 can change RNA expression levels by interacting with other RNA-binding proteins, such as Dicer (Deng et al., 2019) and HuR (Stellos et al., 2016), the same mechanism as the 3′ UTR and the miRNA described previously. In addition, editing of dsRNA on lncRNA by ADAR1 changes its structure, which affects the binding of downstream target miRNAs (**Figure 2H**). Exceptional cases are reported in the literature where lncRNAs are recognized and edited by ADAR1 after complementary pairing with mRNA bases (**Figure 2H**) (Bussemakers et al., 1999).

The expression of ADAR1-regulated lncRNA LINC00944 is immune-related in breast cancer cells. LINC00944 expression was positively correlated to tumor infiltrating T lymphocytes, the age at diagnosis, tumor size, and poor prognosis (de Santiago et al., 2021). In spite of the variations in LINC00944 expression corresponding to up and down regulation of ADAR1, it is unknown the regulatory mechanism of ADAR1 for this lncRNA (de Santiago et al., 2021).

Prostate cancer antigen 3 (PCA3), a long non-coding RNA, is upregulated in human prostate cancer (Bussemakers et al., 1999). PCA3 regulates the level of PRUNE2 through a unique regulatory mechanism that involves the formation of PRUNE2/ADAR1-edited PCA3 double-stranded RNA. Editing by ADAR1 at multiple sites in the PCA3/PRUNE2 duplex results in a reduction of PRUNE2, and an increase in PCA3 expression, therefore increasing in cancer cell the ability of cancer cell, such as proliferation, adhesion and migration (Bussemakers et al., 1999).

Circular RNA

As mentioned above, ADAR1 interacts with by binding to the inverse complementary dsRNA, such as Alu repeat region; circRNAs can also interact with it in this way (Chen and Yang, 2015). ADAR1 creates or disrupts splice sites by acting on dsRNA editing, thereby inhibiting circRNA cyclization (**Figure 2I**) (Zhang and Carmichael, 2001; Fritz et al., 2009; Shevchenko and Morris, 2018).

CircNEIL3 and ADAR1 are upregulated in pancreatic ductal adenocarcinoma (PDAC) cells and tissues, and circNEIL3 as a

miRNA sponge leads to down-regulation of miR-432-5p, thereby suppressing the down-regulation effect caused by the 3′UTR interaction of this microRNA with ADAR1 (Xu et al., 2020; Shen et al., 2021). Subsequently, ADAR1 enhances GLI1 editing, which promotes the transcription of target genes, including cyclin D1, cyclin E and Snail, and the cyclin-dependent kinases CDK2, CDK4 and CDK6 afterward decreased (Olive et al., 2009; Wang et al., 2020; Shen et al., 2021). In summary, the circNEIL3/miR-432-5p/ADAR1/GLI1/cyclin D1/CDK axis regulates the proliferation and metastasis of PDAC *via* the downstream GLI1/cyclin D1 and EMT pathway (Olive et al., 2009; Shen et al., 2021).

In addition, ADAR1 has been described to repress circRNA production intensely, and its A-I editing process usually occurs near reverse complementary matches (RCMs) in circRNA flanking introns, A structure essential for circRNA cyclization (Shi et al., 2017; Ma et al., 2020). Through this editing, secondary structures between RCMs could be stronger or weaker respectively depending on whether correcting A:C was mismatched to I(G)-C pairs or I(G) U pairs (Shen et al., 2022).

Androgen receptor (AR), a transcriptional activator of ADAR1 promoter, could suppress circARSP91 expression by upregulating ADAR1 p110, eventually leading to HCC tumor growth both *in vitro* and *in vivo* (You et al., 2015; Shi et al., 2017). Circular RNA hsa_circ_0004872, dramatically downregulated in gastric cancer, molecular sponges miR-224 to upregulate the expression of the miR-224 downstream targets p21 and Smad4 by targeting the 3′-UTR (Ma et al., 2020). Smad4, as a transcription factor, could inhibit ADAR1 expression level by directly binding to the promoter region of ADAR1, thereby further upregulating hsa_circ_0004872 levels. In other words, Smad4/ADAR1/hsa_circ_0004872/miR-224/Smad4 axis regulated tumor size and local lymph node metastasis in gastric cancer (Hansen et al., 2013; Zhu et al., 2017; Ma et al., 2020).

ADAR1 can edit reverse complementary matches (RCM) of ADAR1-regulated circRNAs, altering the secondary structure formed between RCMs within the flanking introns and enhancing the binding of RNA-binding proteins (RBPs) to the site of action (Kristensen et al., 2019; Shen et al., 2022). And the different expression of ADAR1 leads to editing dysregulation of A-to-I RNA editome in multiple cancers, such as HCC, ESCC, CRC, and GC (Qin et al., 2014; Han et al., 2020; Song et al., 2021). These ADAR1-regulated circRNAs are not byproducts of reverse splicing but important molecules that influence cancer development and progression.

RNA EDITING-INDEPENDENT OF ADENOSINE DEAMINASE ACTING ON RNA 1 AND TUMORIGENESIS AND PROGRESSION MECHANISMS

The most direct role of ADAR1 relies on A-to-I editing, which can alter coding sequences, binding motifs, RNA structure, etc., to regulate substrate abundance. However, ADARs have also been shown to have an editing-independent role, as they can also function as RNA-binding proteins independent of catalytic activity (Nishikura, 2016).

In melanoma, ADAR1 controls the expression of integrin beta 3 (ITGB3), a cell surface protein associated with tumor invasion (Pinon and Wehrle-Haller, 2011; Orgaz and Sanz-Moreno, 2013), *via* miR-22 and PAX6 transcription factor at the post-transcriptional and transcriptional levels. The expression and functional output of both FOXD1, which controls miR-22 expression, and PAX6 are independent of RNA editing, therefore promoting growth and invasion of melanoma (Nemlich et al., 2018).

In cytoplasm, binding of the targeted 3′ UTR allows phosphorylated ADAR1p110 to preclude binding of Staufen1 and subsequent decay of the anti-apoptotic gene, thereby promoting survival of stressed cells in an editorially independent manner (**Figure 2F**) (Sakurai et al., 2017). It has been reported in the literature that Staufen1 has positive or negative effects on disease progression: in some malignancies, upregulated Staufen1 may act as an oncogene and promote cancer progression (Boulay et al., 2014; Xu et al., 2015; Crawford Parks et al., 2017); while in other cancers, Staufen1 may act as a tumor suppressor and inhibit disease progression (Gong and Maquat, 2011; Boulay et al., 2014; Su et al., 2020). Nevertheless, reports on the mechanism of ADAR1 for Staufen1 have not yet appeared in cancer. Interaction of lncRNA with Staufen1 has also been reported in a variety of cancers (Sakurai et al., 2017); however again no mechanism of action of ADAR1 for Staufen1 in tumors has been reported. In HCC, ADAR1 was detected to interact directly with Dicer without editing, resulting in the processing of pre-miR-27a (Qi et al., 2017). Mature miR-27a binds to the 3′-UTR of methyltransferase 7A (METTL7A), a known tumor suppressor, decreasing its expression level (Qi et al., 2017). In addition, ADAR1 can regulate miRNA processing in an RNA-binding but editing-independent manner. ADAR1 can indirectly affect miRNA biogenesis by regulating Dicer expression at the translational level through the Letal-7 gene (let-7) (Zipeto et al., 2016).

CONCLUDING REMARKS AND FUTURE PERSPECTIVES

In conclusion, we show the structure and regulatory mechanisms of the ADAR1, and the significant role of ADAR1 in regulating many aspects of RNA function in cancers, including regulating the biogenesis of coding gene, intron, 3′ UTR, and three prevalent non-coding RNA, such as miRNA, lncRNA, circRNA. However, many important questions remain in the field including: 1) What are the factors that influence altered ADAR1 expression in cancer, and how do they play a role? 2) There are many editing-independent mechanisms of action in cancer that exist only in theory and for which there is no clear experimental evidence. 3) Up-regulation of ADAR1 expression promotes cancer development and progression in most cases, and down-regulation of ADAR1 in some cases can also achieve cancer progression. How do cancer cells control the abundance of ADAR1 so precisely to enhance their progression? Future investigation of these issues may lead to further discoveries in A-to-I RNA editing.

AUTHOR CONTRIBUTIONS

BZ and JzL conceived the content and wrote the manuscript. FW and YZ contributed to the figures and the literature collection. BZ and JfL supervised the overall project and edited the manuscript. All authors contributed to the article and approved the submitted version.

FUNDING

This work was supported by National Key R&D Program of China (SQ2020YFF0426513), the Scientific Foundation of Fuzhou Municipal Health commission (2021-S-wp1), the Backbone Talents Training Project of Fujian provincial Health Commission (2020GGA072).

REFERENCES

Amin, E. M., Liu, Y., Deng, S., Tan, K. S., Chudgar, N., Mayo, M. W., et al. (2017). The RNA-Editing Enzyme ADAR Promotes Lung Adenocarcinoma Migration and Invasion by Stabilizing FAK. *Sci. Signal.* 10, eaah3941. doi:10.1126/scisignal.aah3941

Athanasiadis, A., Placido, D., Maas, S., Brown, B. A., Lowenhaupt, K., and Rich, A. (2005). The Crystal Structure of the Zβ Domain of the RNA-Editing Enzyme ADAR1 Reveals Distinct Conserved Surfaces Among Z-Domains. *J. Mol. Biol.* 351, 496–507. doi:10.1016/j.jmb.2005.06.028

Athanasiadis, A., Rich, A., and Maas, S. (2004). Widespread A-To-I RNA Editing of Alu-Containing mRNAs in the Human Transcriptome. *PLoS Biol.* 2, e391. doi:10.1371/journal.pbio.0020391

Bagley, B. N., Keane, T. M., Maklakova, V. I., Marshall, J. G., Lester, R. A., Cancel, M. M., et al. (2012). A Dominantly Acting Murine Allele of Mcm4 Causes Chromosomal Abnormalities and Promotes Tumorigenesis. *PLoS Genet.* 8, e1003034. doi:10.1371/journal.pgen.1003034

Bahn, J. H., Ahn, J., Lin, X., Zhang, Q., Lee, J.-H., Civelek, M., et al. (2015). Genomic Analysis of ADAR1 Binding and its Involvement in Multiple RNA Processing Pathways. *Nat. Commun.* 6, 6355. doi:10.1038/ncomms7355

Bahn, J. H., Lee, J.-H., Li, G., Greer, C., Peng, G., and Xiao, X. (2012). Accurate Identification of A-To-I RNA Editing in Human by Transcriptome Sequencing. *Genome Res.* 22, 142–150. doi:10.1101/gr.124107.111

Baker, A. R., and Slack, F. J. (2022). ADAR1 and its Implications in Cancer Development and Treatment. *Trends Genet.* doi:10.1016/j.tig.2022.03.013

Bakheet, T., Kamen, R., and Bakheet, T. (2006). ARED 3.0: the Large and Diverse AU-Rich Transcriptome. *Nucleic Acids Res.* 34, D111–D114. doi:10.1093/nar/gkj052

Barraud, P., Banerjee, S., Mohamed, W. I., Jantsch, M. F., and Allain, F. H.-T. (2014). A Bimodular Nuclear Localization Signal Assembled via an Extended Double-Stranded RNA-Binding Domain Acts as an RNA-Sensing Signal for Transportin 1. *Proc. Natl. Acad. Sci. U.S.A.* 111, E1852–E1861. doi:10.1073/pnas.1323698111

Barraud, P., Heale, B. S. E., O'Connell, M. A., and Allain, F. H.-T. (2012). Solution Structure of the N-Terminal dsRBD of Drosophila ADAR and Interaction Studies with RNA. *Biochimie* 94, 1499–1509. doi:10.1016/j.biochi.2011.12.017

Bass, B. (1987). A Developmentally Regulated Activity that Unwinds RNA Duplexes. *Cell* 48, 607–613. doi:10.1016/0092-8674(87)90239-X

Bazak, L., Haviv, A., Barak, M., Jacob-Hirsch, J., Deng, P., Zhang, R., et al. (2014). A-to-I RNA Editing Occurs at over a Hundred Million Genomic Sites, Located in a Majority of Human Genes. *Genome Res.* 24, 365–376. doi:10.1101/gr.164749.113

Borchert, G. M., Gilmore, B. L., Spengler, R. M., Xing, Y., Lanier, W., Bhattacharya, D., et al. (2009). Adenosine Deamination in Human Transcripts Generates Novel microRNA Binding Sites. *Hum. Mol. Genet.* 18, 4801–4807. doi:10.1093/hmg/ddp443

Boulay, K., Ghram, M., Viranaicken, W., Trépanier, V., Mollet, S., Fréchina, C., et al. (2014). Cell Cycle-dependent Regulation of the RNA-Binding Protein Staufen1. *Nucleic Acids Res.* 42, 7867–7883. doi:10.1093/nar/gku506

Bussemakers, M. J., van Bokhoven, A., Verhaegh, G. W., Smit, F. P., Karthaus, H. F., Schalken, J. A., et al. (1999). DD3: a New Prostate-specific Gene, Highly Overexpressed in Prostate Cancer. *Cancer Res.* 59, 5975–5979.

Chen, C.-X., Cho, D.-S. C., Wang, Q., Lai, F., Carter, K. C., and Nishikura, K. (2000). A Third Member of the RNA-specific Adenosine Deaminase Gene Family, ADAR3, Contains Both Single- and Double-Stranded RNA Binding Domains. *RNA* 6, 755–767. doi:10.1017/S1355838200000170

Chen, L.-L., and Yang, L. (2015). Regulation of circRNA Biogenesis. *RNA Biol.* 12, 381–388. doi:10.1080/15476286.2015.1020271

Chen, L., Li, Y., Lin, C. H., Chan, T. H. M., Chow, R. K. K., Song, Y., et al. (2013). Recoding RNA Editing of AZIN1 Predisposes to Hepatocellular Carcinoma. *Nat. Med.* 19, 209–216. doi:10.1038/nm.3043

Chen, W., He, W., Cai, H., Hu, B., Zheng, C., Ke, X., et al. (2017). A-to-I RNA Editing of BLCAP Lost the Inhibition to STAT3 Activation in Cervical Cancer. *Oncotarget* 8, 39417–39429. doi:10.18632/oncotarget.17034

Chen, Y., Wang, H., Lin, W., and Shuai, P. (2017). ADAR1 Overexpression Is Associated with Cervical Cancer Progression and Angiogenesis. *Diagn Pathol.* 12, 12. doi:10.1186/s13000-017-0600-0

Chiosea, S., Jelezcova, E., Chandran, U., Acquafondata, M., McHale, T., Sobol, R. W., et al. (2006). Up-Regulation of Dicer, a Component of the MicroRNA Machinery, in Prostate Adenocarcinoma. *Am. J. Pathology* 169, 1812–1820. doi:10.2353/ajpath.2006.060480

Crawford Parks, T. E., Marcellus, K. A., Langill, J., Ravel-Chapuis, A., Michaud, J., Cowan, K. N., et al. (2017). Novel Roles for Staufen1 in Embryonal and Alveolar Rhabdomyosarcoma via C-myc-dependent and -independent Events. *Sci. Rep.* 7, 42342. doi:10.1038/srep42342

Daniel, C., Lagergren, J., and Öhman, M. (2015). RNA Editing of Non-coding RNA and its Role in Gene Regulation. *Biochimie* 117, 22–27. doi:10.1016/j.biochi.2015.05.020

de Santiago, P. R., Blanco, A., Morales, F., Marcelain, K., Harismendy, O., Sjöberg Herrera, M., et al. (2021). Immune-related lncRNA LINC00944 Responds to Variations in ADAR1 Levels and it Is Associated with Breast Cancer Prognosis. *Life Sci.* 268, 118956. doi:10.1016/j.lfs.2020.118956

de Silanes, I. L., Fan, J., Yang, X., Zonderman, A. B., Potapova, O., Pizer, E. S., et al. (2003). Role of the RNA-Binding Protein HuR in Colon Carcinogenesis. *Oncogene* 22, 7146–7154. doi:10.1038/sj.onc.1206862

Deng, S.-J., Chen, H.-Y., Zeng, Z., Deng, S., Zhu, S., Ye, Z., et al. (2019). Nutrient Stress-Dysregulated Antisense lncRNA GLS-AS Impairs GLS-Mediated Metabolism and Represses Pancreatic Cancer Progression. *Cancer Res.* 79, 1398–1412. doi:10.1158/0008-5472.CAN-18-0419

Desterro, J. M. P., Keegan, L. P., Lafarga, M., Berciano, M. T., O'Connell, M., and Carmo-Fonseca, M. (2003). Dynamic Association of RNA-Editing Enzymes with the Nucleolus. *J. Cell Sci.* 116, 1805–1818. doi:10.1242/jcs.00371

Dong, X., Chen, G., Cai, Z., Li, Z., Qiu, L., Xu, H., et al. (2018). CDK13 RNA Over-editing Mediated by ADAR1 Associates with Poor Prognosis of Hepatocellular Carcinoma Patients. *Cell Physiol. Biochem.* 47, 2602–2612. doi:10.1159/000491656

Eisenberg, E., and Levanon, E. Y. (2018). A-to-I RNA Editing - Immune Protector and Transcriptome Diversifier. *Nat. Rev. Genet.* 19, 473–490. doi:10.1038/s41576-018-0006-1

Erdmann, E. A., Mahapatra, A., Mukherjee, P., Yang, B., and Hundley, H. A. (2021). To Protect and Modify Double-Stranded RNA - the Critical Roles of ADARs in Development, Immunity and Oncogenesis. *Crit. Rev. Biochem. Mol. Biol.* 56, 54–87. doi:10.1080/10409238.2020.1856768

Fawzy, M. S., Toraih, E. A., Ibrahiem, A., Abdeldayem, H., Mohamed, A. O., and Abdel-Daim, M. M. (2017). Evaluation of miRNA-196a2 and Apoptosis-Related Target Genes: ANXA1, DFFA and PDCD4 Expression in Gastrointestinal Cancer Patients: A Pilot Study. *PLoS ONE* 12, e0187310. doi:10.1371/journal.pone.0187310

Fritz, J., Strehblow, A., Taschner, A., Schopoff, S., Pasierbek, P., and Jantsch, M. F. (2009). RNA-regulated Interaction of Transportin-1 and Exportin-5 with the Double-Stranded RNA-Binding Domain Regulates Nucleocytoplasmic Shuttling of ADAR1. *Mol. Cell Biol.* 29, 1487–1497. doi:10.1128/MCB.01519-08

Fritzell, K., Xu, L.-D., Lagergren, J., and Öhman, M. (2018). ADARs and Editing: The Role of A-To-I RNA Modification in Cancer Progression. *Seminars Cell & Dev. Biol.* 79, 123–130. doi:10.1016/j.semcdb.2017.11.018

Gallo, A., Vukic, D., Michalík, D., O'Connell, M. A., and Keegan, L. P. (2017). ADAR RNA Editing in Human Disease; More to it Than Meets the I. *Hum. Genet.* 136, 1265–1278. doi:10.1007/s00439-017-1837-0

Galore-Haskel, G., Nemlich, Y., Greenberg, E., Ashkenazi, S., Hakim, M., Itzhaki, O., et al. (2015). A Novel Immune Resistance Mechanism of Melanoma Cells Controlled by the ADAR1 Enzyme. *Oncotarget* 6, 28999–29015. doi:10.18632/oncotarget.4905

George, C. X., Gan, Z., Liu, Y., and Samuel, C. E. (2011). Adenosine Deaminases Acting on RNA, RNA Editing, and Interferon Action. *J. Interferon & Cytokine Res.* 31, 99–117. doi:10.1089/jir.2010.0097

Gong, C., and Maquat, L. E. (2011). lncRNAs Transactivate STAU1-Mediated mRNA Decay by Duplexing with 3′ UTRs via Alu Elements. *Nature* 470, 284–288. doi:10.1038/nature09701

Gumireddy, K., Li, A., Kossenkov, A. V., Sakurai, M., Yan, J., Li, Y., et al. (2016). The mRNA-Edited Form of GABRA3 Suppresses GABRA3-Mediated Akt Activation and Breast Cancer Metastasis. *Nat. Commun.* 7, 10715. doi:10.1038/ncomms10715

Guo, C.-J., Ma, X.-K., Xing, Y.-H., Zheng, C.-C., Xu, Y.-F., Shan, L., et al. (2020). Distinct Processing of lncRNAs Contributes to Non-conserved Functions in Stem Cells. *Cell* 181, 621. doi:10.1016/j.cell.2020.03.006

Han, J., An, O., Hong, H., Chan, T. H. M., Song, Y., Shen, H., et al. (2020). Suppression of Adenosine-To-Inosine (A-To-I) RNA Editome by Death Associated Protein 3 (DAP3) Promotes Cancer Progression. *Sci. Adv.* 6, eaba5136. doi:10.1126/sciadv.aba5136

Han, L., Diao, L., Yu, S., Xu, X., Li, J., Zhang, R., et al. (2015). The Genomic Landscape and Clinical Relevance of A-To-I RNA Editing in Human Cancers. *Cancer Cell* 28, 515–528. doi:10.1016/j.ccell.2015.08.013

Hansen, T. B., Jensen, T. I., Clausen, B. H., Bramsen, J. B., Finsen, B., Damgaard, C. K., et al. (2013). Natural RNA Circles Function as Efficient microRNA Sponges. *Nature* 495, 384–388. doi:10.1038/nature11993

Hartner, J. C., Schmittwolf, C., Kispert, A., Müller, A. M., Higuchi, M., and Seeburg, P. H. (2004). Liver Disintegration in the Mouse Embryo Caused by Deficiency in the RNA-Editing Enzyme ADAR1. *J. Biol. Chem.* 279, 4894–4902. doi:10.1074/jbc.M311347200

Hogg, M., Paro, S., Keegan, L. P., and O'Connell, M. A. (2011). RNA Editing by Mammalian ADARs. *Adv. Genet.* 73, 87–120. doi:10.1016/B978-0-12-380860-8.00003-3

Hu, X., Chen, J., Shi, X., Feng, F., Lau, K. W., Chen, Y., et al. (2017). RNA Editing of AZIN1 Induces the Malignant Progression of Non-small-cell Lung Cancers. *Tumour Biol.* 39, 101042831770000. doi:10.1177/1010428317700001

Hu, X., Wan, S., Ou, Y., Zhou, B., Zhu, J., Yi, X., et al. (2015). RNA Over-editing of BLCAP Contributes to Hepatocarcinogenesis Identified by Whole-Genome and Transcriptome Sequencing. *Cancer Lett.* 357, 510–519. doi:10.1016/j.canlet.2014.12.006

Jiang, A., Reece, D., and Chang, H. (2012). Genomic Stratification of Multiple Myeloma Treated with Novel Agents. *Leukemia Lymphoma* 53, 202–207. doi:10.3109/10428194.2011.608449

Knuutila, S., Björkqvist, A. M., Autio, K., Tarkkanen, M., Wolf, M., Monni, O., et al. (1998). DNA Copy Number Amplifications in Human Neoplasms: Review of Comparative Genomic Hybridization Studies. *Am. J. Pathol.* 152, 1107–1123.

Kristensen, L. S., Andersen, M. S., Stagsted, L. V. W., Ebbesen, K. K., Hansen, T. B., and Kjems, J. (2019). The Biogenesis, Biology and Characterization of Circular RNAs. *Nat. Rev. Genet.* 20, 675–691. doi:10.1038/s41576-019-0158-7

Lamers, M. M., van den Hoogen, B. G., and Haagmans, B. L. (2019). ADAR1: "Editor-In-Chief" of Cytoplasmic Innate Immunity. *Front. Immunol.* 10, 1763. doi:10.3389/fimmu.2019.01763

Lazzari, E., Mondala, P. K., Santos, N. D., Miller, A. C., Pineda, G., Jiang, Q., et al. (2017). Alu-dependent RNA Editing of GLI1 Promotes Malignant Regeneration in Multiple Myeloma. *Nat. Commun.* 8, 1922. doi:10.1038/s41467-017-01890-w

Lev-Maor, G., Sorek, R., Levanon, E. Y., Paz, N., Eisenberg, E., and Ast, G. (2007). RNA-editing-mediated Exon Evolution. *Genome Biol.* 8, R29. doi:10.1186/gb-2007-8-2-r29

Li, L., Qian, G., Zuo, Y., Yuan, Y., Cheng, Q., Guo, T., et al. (2016). Ubiquitin-dependent Turnover of Adenosine Deaminase Acting on RNA 1 (ADAR1) Is Required for Efficient Antiviral Activity of Type I Interferon. *J. Biol. Chem.* 291, 24974–24985. doi:10.1074/jbc.M116.737098

Li, Z., Feng, Y., Zhang, Z., Cao, X., and Lu, X. (2020). TMPO-AS1 Promotes Cell Proliferation of Thyroid Cancer via Sponging miR-498 to Modulate TMPO. *Cancer Cell Int.* 20, 294. doi:10.1186/s12935-020-01334-4

Liang, H., and Landweber, L. F. (2007). Hypothesis: RNA Editing of microRNA Target Sites in Humans? *RNA* 13, 463–467. doi:10.1261/rna.296407

Liddicoat, B. J., Piskol, R., Chalk, A. M., Ramaswami, G., Higuchi, M., Hartner, J. C., et al. (2015). RNA Editing by ADAR1 Prevents MDA5 Sensing of Endogenous dsRNA as Nonself. *Science* 349, 1115–1120. doi:10.1126/science.aac7049

Ma, C., Wang, X., Yang, F., Zang, Y., Liu, J., Wang, X., et al. (2020). Circular RNA Hsa_circ_0004872 Inhibits Gastric Cancer Progression via the miR-224/Smad4/ADAR1 Successive Regulatory Circuit. *Mol. Cancer* 19, 157. doi:10.1186/s12943-020-01268-5

Maas, S., Patt, S., Schrey, M., and Rich, A. (2001). Underediting of Glutamate Receptor GluR-B mRNA in Malignant Gliomas. *Proc. Natl. Acad. Sci. U.S.A.* 98, 14687–14692. doi:10.1073/pnas.251531398

Macbeth, M. R., Schubert, H. L., VanDemark, A. P., Lingam, A. T., Hill, C. P., and Bass, B. L. (2005). Inositol Hexakisphosphate Is Bound in the ADAR2 Core and Required for RNA Editing. *Science* 309, 1534–1539. doi:10.1126/science.1113150

McLoughlin, M. R., Orlicky, D. J., Prigge, J. R., Krishna, P., Talago, E. A., Cavigli, I. R., et al. (2019). TrxR1, Gsr, and Oxidative Stress Determine Hepatocellular Carcinoma Malignancy. *Proc. Natl. Acad. Sci. U.S.A.* 116, 11408–11417. doi:10.1073/pnas.1903244116

Meisner, N.-C., Hackermüller, J., Uhl, V., Aszódi, A., Jaritz, M., and Auer, M. (2004). mRNA Openers and Closers: Modulating AU-Rich Element-Controlled mRNA Stability by a Molecular Switch in mRNA Secondary Structure. *ChemBioChem* 5, 1432–1447. doi:10.1002/cbic.200400219

Melcher, T., Maas, S., Herb, A., Sprengel, R., Higuchi, M., and Seeburg, P. H. (1996). RED2, a Brain-specific Member of the RNA-specific Adenosine Deaminase Family. *J. Biol. Chem.* 271, 31795–31798. doi:10.1074/jbc.271.50.31795

Meng, S., Zhou, H., Feng, Z., Xu, Z., Tang, Y., Li, P., et al. (2017). CircRNA: Functions and Properties of a Novel Potential Biomarker for Cancer. *Mol. Cancer* 16, 94. doi:10.1186/s12943-017-0663-2

Nakano, M., Fukami, T., Gotoh, S., and Nakajima, M. (2017). A-to-I RNA Editing Up-Regulates Human Dihydrofolate Reductase in Breast Cancer. *J. Biol. Chem.* 292, 4873–4884. doi:10.1074/jbc.M117.775684

Nemlich, Y., Baruch, E. N., Besser, M. J., Shoshan, E., Bar-Eli, M., Anafi, L., et al. (2018). ADAR1-mediated Regulation of Melanoma Invasion. *Nat. Commun.* 9, 2154. doi:10.1038/s41467-018-04600-2

Nishikura, K. (2016). A-to-I Editing of Coding and Non-coding RNAs by ADARs. *Nat. Rev. Mol. Cell Biol.* 17, 83–96. doi:10.1038/nrm.2015.4

Nishikura, K. (2010). Functions and Regulation of RNA Editing by ADAR Deaminases. *Annu. Rev. Biochem.* 79, 321–349. doi:10.1146/annurev-biochem-060208-105251

Oakes, E., Anderson, A., Cohen-Gadol, A., and Hundley, H. A. (2017). Adenosine Deaminase that Acts on RNA 3 (ADAR3) Binding to Glutamate Receptor Subunit B Pre-mRNA Inhibits RNA Editing in Glioblastoma. *J. Biol. Chem.* 292, 4326–4335. doi:10.1074/jbc.M117.779868

Olive, K. P., Jacobetz, M. A., Davidson, C. J., Gopinathan, A., McIntyre, D., Honess, D., et al. (2009). Inhibition of Hedgehog Signaling Enhances Delivery of Chemotherapy in a Mouse Model of Pancreatic Cancer. *Science* 324, 1457–1461. doi:10.1126/science.1171362

Orgaz, J. L., and Sanz-Moreno, V. (2013). Emerging Molecular Targets in Melanoma Invasion and Metastasis. *Pigment. Cell Melanoma Res.* 26, 39–57. doi:10.1111/pcmr.12041

Paz-Yaacov, N., Bazak, L., Buchumenski, I., Porath, H. T., Danan-Gotthold, M., Knisbacher, B. A., et al. (2015). Elevated RNA Editing Activity Is a Major Contributor to Transcriptomic Diversity in Tumors. *Cell Rep.* 13, 267–276. doi:10.1016/j.celrep.2015.08.080

Picardi, E., Manzari, C., Mastropasqua, F., Aiello, I., D'Erchia, A. M., and Pesole, G. (2015). Profiling RNA Editing in Human Tissues: towards the Inosinome Atlas. *Sci. Rep.* 5, 14941. doi:10.1038/srep14941

Pinon, P., and Wehrle-Haller, B. (2011). Integrins: Versatile Receptors Controlling Melanocyte Adhesion, Migration and Proliferation. *Pigment Cell & Melanoma Res.* 24, 282–294. doi:10.1111/j.1755-148X.2010.00806.x

Pinto, Y., Buchumenski, I., Levanon, E. Y., and Eisenberg, E. (2018). Human Cancer Tissues Exhibit Reduced A-To-I Editing of miRNAs Coupled with Elevated Editing of Their Targets. *Nucleic Acids Res.* 46, 71–82. doi:10.1093/nar/gkx1176

Placido, D., Brown, B. A., Lowenhaupt, K., Rich, A., and Athanasiadis, A. (2007). A Left-Handed RNA Double Helix Bound by the Zα Domain of the RNA-Editing Enzyme ADAR1. *Structure* 15, 395–404. doi:10.1016/j.str.2007.03.001

Polson, A. G., Crain, P. F., Pomerantz, S. C., McCloskey, J. A., and Bass, B. L. (1991). The Mechanism of Adenosine to Inosine Conversion by the Double-Stranded RNA Unwinding/modifying Activity: a High-Performance Liquid Chromatography-Mass Spectrometry Analysis. *Biochemistry* 30, 11507–11514. doi:10.1021/bi00113a004

Poulsen, H., Nilsson, J., Damgaard, C. K., Egebjerg, J., and Kjems, J. (2001). CRM1 Mediates the Export of ADAR1 through a Nuclear Export Signal within the Z-DNA Binding Domain. *Mol. Cell Biol.* 21, 7862–7871. doi:10.1128/MCB.21.22.7862-7871.2001

Qi, L., Chan, T. H. M., Tenen, D. G., and Chen, L. (2014). RNA Editome Imbalance in Hepatocellular Carcinoma. *Cancer Res.* 74, 1301–1306. doi:10.1158/0008-5472.CAN-13-3485

Qi, L., Song, Y., Chan, T. H. M., Yang, H., Lin, C. H., Tay, D. J. T., et al. (2017). An RNA editing/dsRNA Binding-independent Gene Regulatory Mechanism of ADARs and its Clinical Implication in Cancer. *Nucleic Acids Res.* 45, 10436–10451. doi:10.1093/nar/gkx667

Qin, Y.-R., Qiao, J.-J., Chan, T. H. M., Zhu, Y.-H., Li, F.-F., Liu, H., et al. (2014). Adenosine-to-Inosine RNA Editing Mediated by ADARs in Esophageal Squamous Cell Carcinoma. *Cancer Res.* 74, 840–851. doi:10.1158/0008-5472.CAN-13-2545

Quin, J., Sedmík, J., Vukić, D., Khan, A., Keegan, L. P., and O'Connell, M. A. (2021). ADAR RNA Modifications, the Epitranscriptome and Innate Immunity. *Trends Biochem. Sci.* 46, 758–771. doi:10.1016/j.tibs.2021.02.002

Ramírez-Moya, J., Baker, A. R., Slack, F. J., and Santisteban, P. (2020). ADAR1-mediated RNA Editing Is a Novel Oncogenic Process in Thyroid Cancer and Regulates miR-200 Activity. *Oncogene* 39, 3738–3753. doi:10.1038/s41388-020-1248-x

Ramírez-Moya, J., Miliotis, C., Baker, A. R., Gregory, R. I., Slack, F. J., and Santisteban, P. (2021). An ADAR1-dependent RNA Editing Event in the Cyclin-dependent Kinase CDK13 Promotes Thyroid Cancer Hallmarks. *Mol. Cancer* 20, 115. doi:10.1186/s12943-021-01401-y

Rice, G. I., Kasher, P. R., Forte, G. M. A., Mannion, N. M., Greenwood, S. M., Szynkiewicz, M., et al. (2012). Mutations in ADAR1 Cause Aicardi-Goutières Syndrome Associated with a Type I Interferon Signature. *Nat. Genet.* 44, 1243–1248. doi:10.1038/ng.2414

Roberts, J., Patterson, D., King, V., Amin, S., Polska, C., Houserova, D., et al. (2018). ADAR Mediated RNA Editing Modulates MicroRNA Targeting in Human Breast Cancer. *Processes* 6, 42. doi:10.3390/pr6050042

Sagredo, E. A., Blanco, A., Sagredo, A. I., Pérez, P., Sepúlveda-Hermosilla, G., Morales, F., et al. (2018). ADAR1-mediated RNA-Editing of 3′UTRs in Breast Cancer. *Biol. Res.* 51, 36. doi:10.1186/s40659-018-0185-4

Sakurai, M., Shiromoto, Y., Ota, H., Song, C., Kossenkov, A. V., Wickramasinghe, J., et al. (2017). ADAR1 Controls Apoptosis of Stressed Cells by Inhibiting Staufen1-Mediated mRNA Decay. *Nat. Struct. Mol. Biol.* 24, 534–543. doi:10.1038/nsmb.3403

Sakurai, M., Yano, T., Kawabata, H., Ueda, H., and Suzuki, T. (2010). Inosine Cyanoethylation Identifies A-To-I RNA Editing Sites in the Human Transcriptome. *Nat. Chem. Biol.* 6, 733–740. doi:10.1038/nchembio.434

Samuel, C. E. (2019). Adenosine Deaminase Acting on RNA (ADAR1), a Suppressor of Double-Stranded RNA-Triggered Innate Immune Responses. *J. Biol. Chem.* 294, 1710–1720. doi:10.1074/jbc.TM118.004166

Shaw, G., and Kamen, R. (1986). A Conserved AU Sequence from the 3′ Untranslated Region of GM-CSF mRNA Mediates Selective mRNA Degradation. *Cell* 46, 659–667. doi:10.1016/0092-8674(86)90341-7

Shen, H., An, O., Ren, X., Song, Y., Tang, S. J., Ke, X.-Y., et al. (2022). ADARs Act as Potent Regulators of Circular Transcriptome in Cancer. *Nat. Commun.* 13, 1508. doi:10.1038/s41467-022-29138-2

Shen, P., Yang, T., Chen, Q., Yuan, H., Wu, P., Cai, B., et al. (2021). CircNEIL3 Regulatory Loop Promotes Pancreatic Ductal Adenocarcinoma Progression via miRNA Sponging and A-To-I RNA-Editing. *Mol. Cancer* 20, 51. doi:10.1186/s12943-021-01333-7

Shevchenko, G., and Morris, K. V. (2018). All I's on the RADAR : Role of ADAR in Gene Regulation. *FEBS Lett.* 592, 2860–2873. doi:10.1002/1873-3468.13093

Shi, L., Yan, P., Liang, Y., Sun, Y., Shen, J., Zhou, S., et al. (2017). Circular RNA Expression Is Suppressed by Androgen Receptor (AR)-regulated Adenosine Deaminase that Acts on RNA (ADAR1) in Human Hepatocellular Carcinoma. *Cell Death Dis.* 8, e3171. doi:10.1038/cddis.2017.556

Shigeyasu, K., Okugawa, Y., Toden, S., Miyoshi, J., Toiyama, Y., Nagasaka, T., et al. (2018). AZIN1 RNA Editing Confers Cancer Stemness and Enhances Oncogenic Potential in Colorectal Cancer. *JCI Insight* 3, e99976. doi:10.1172/jci.insight.99976

Shimokawa, T., Rahman, M. F.-U., Tostar, U., Sonkoly, E., Ståhle, M., Pivarcsi, A., et al. (2013). RNA Editing of the GLI1 Transcription Factor Modulates the Output of Hedgehog Signaling. *RNA Biol.* 10, 321–333. doi:10.4161/rna.23343

Shoshan, E., Mobley, A. K., Braeuer, R. R., Kamiya, T., Huang, L., Vasquez, M. E., et al. (2015). Reduced Adenosine-To-Inosine miR-455-5p Editing Promotes Melanoma Growth and Metastasis. *Nat. Cell Biol.* 17, 311–321. doi:10.1038/ncb3110

Silvestris, D. A., Scopa, C., Hanchi, S., Locatelli, F., and Gallo, A. (2020). De Novo A-to-I RNA Editing Discovery in lncRNA. *Cancers* 12, 2959. doi:10.3390/cancers12102959

Song, B., Shiromoto, Y., Minakuchi, M., and Nishikura, K. (2022). The Role of RNA Editing Enzyme ADAR1 in Human Disease. *WIREs RNA* 13, e1665. doi:10.1002/wrna.1665

Song, C., Sakurai, M., Shiromoto, Y., and Nishikura, K. (2016). Functions of the RNA Editing Enzyme ADAR1 and Their Relevance to Human Diseases. *Genes* 7, 129. doi:10.3390/genes7120129

Song, Y., An, O., Ren, X., Chan, T. H. M., Tay, D. J. T., Tang, S. J., et al. (2021). RNA Editing Mediates the Functional Switch of COPA in a Novel Mechanism of Hepatocarcinogenesis. *J. Hepatology* 74, 135–147. doi:10.1016/j.jhep.2020.07.021

Stefl, R., Oberstrass, F. C., Hood, J. L., Jourdan, M., Zimmermann, M., Skrisovska, L., et al. (2010). The Solution Structure of the ADAR2 dsRBM-RNA Complex Reveals a Sequence-specific Readout of the Minor Groove. *Cell* 143, 225–237. doi:10.1016/j.cell.2010.09.026

Stellos, K., Gatsiou, A., Stamatelopoulos, K., Perisic Matic, L., John, D., Lunella, F. F., et al. (2016). Adenosine-to-inosine RNA Editing Controls Cathepsin S Expression in Atherosclerosis by Enabling HuR-Mediated Post-transcriptional Regulation. *Nat. Med.* 22, 1140–1150. doi:10.1038/nm.4172

Strehblow, A., Hallegger, M., and Jantsch, M. F. (2002). Nucleocytoplasmic Distribution of Human RNA-Editing Enzyme ADAR1 Is Modulated by Double-Stranded RNA-Binding Domains, a Leucine-Rich Export Signal, and a Putative Dimerization Domain. *Mol. Biol. Cell* 13, 3822–3835. doi:10.1091/mbc.e02-03-0161

Su, R., Ma, J., Zheng, J., Liu, X., Liu, Y., Ruan, X., et al. (2020). PABPC1-induced Stabilization of BDNF-AS Inhibits Malignant Progression of Glioblastoma Cells through STAU1-Mediated Decay. *Cell Death Dis.* 11, 81. doi:10.1038/s41419-020-2267-9

Sun, T., Yu, Y., Wu, X., Acevedo, A., Luo, J.-D., Wang, J., et al. (2021). Decoupling Expression and Editing Preferences of ADAR1 P150 and P110 Isoforms. *Proc. Natl. Acad. Sci. U.S.A.* 118, e2021757118. doi:10.1073/pnas.2021757118

Sun, Y., Fan, J., Wang, B., Meng, Z., Ren, D., Zhao, J., et al. (2020). The Aberrant Expression of ADAR1 Promotes Resistance to BET Inhibitors in Pancreatic Cancer by Stabilizing C-Myc. *Am. J. Cancer Res.* 10, 148–163.

Takeda, S., Shigeyasu, K., Okugawa, Y., Yoshida, K., Mori, Y., Yano, S., et al. (2019). Activation of AZIN1 RNA Editing Is a Novel Mechanism that Promotes Invasive Potential of Cancer-Associated Fibroblasts in Colorectal Cancer. *Cancer Lett.* 444, 127–135. doi:10.1016/j.canlet.2018.12.009

Teoh, P. J., An, O., Chung, T.-H., Chooi, J. Y., Toh, S. H. M., Fan, S., et al. (2018). Aberrant Hyperediting of the Myeloma Transcriptome by ADAR1 Confers Oncogenicity and Is a Marker of Poor Prognosis. *Blood* 132, 1304–1317. doi:10.1182/blood-2018-02-832576

Thomas, J. M., and Beal, P. A. (2017). How Do ADARs Bind RNA? New Protein-RNA Structures Illuminate Substrate Recognition by the RNA Editing ADARs. *BioEssays* 39, 1600187. doi:10.1002/bies.201600187

Torsin, L. I., Petrescu, G. E. D., Sabo, A. A., Chen, B., Brehar, F. M., Dragomir, M. P., et al. (2021). Editing and Chemical Modifications on Non-coding RNAs in Cancer: A New Tale with Clinical Significance. *Int. J. Mol. Sci.* 22, 581. doi:10.3390/ijms22020581

Velazquez-Torres, G., Shoshan, E., Ivan, C., Huang, L., Fuentes-Mattei, E., Paret, H., et al. (2018). A-to-I miR-378a-3p Editing Can Prevent Melanoma Progression via Regulation of PARVA Expression. *Nat. Commun.* 9, 461. doi:10.1038/s41467-018-02851-7

Walkley, C. R., and Li, J. B. (2017). Rewriting the Transcriptome: Adenosine-To-Inosine RNA Editing by ADARs. *Genome Biol.* 18, 205. doi:10.1186/s13059-017-1347-3

Wang, F., Wu, P., Gong, S., Chen, Y., Gao, J., Wang, S., et al. (2020). Aberrant TRPM4 Expression in MLL-Rearranged Acute Myeloid Leukemia and its Blockade Induces Cell Cycle Arrest via AKT/GLI1/Cyclin D1 Pathway. *Cell. Signal.* 72, 109643. doi:10.1016/j.cellsig.2020.109643

Wang I. X., I. X., So, E., Devlin, J. L., Zhao, Y., Wu, M., and Cheung, V. G. (2013). ADAR Regulates RNA Editing, Transcript Stability, and Gene Expression. *Cell Rep.* 5, 849–860. doi:10.1016/j.celrep.2013.10.002

Wang Q, Q., Hui, H., Guo, Z., Zhang, W., Hu, Y., He, T., et al. (2013). ADAR1 Regulates *ARHGAP26* Gene Expression through RNA Editing by Disrupting miR-30b-3p and miR-573 Binding. *RNA* 19, 1525–1536. doi:10.1261/rna.041533.113

Wang, Q., Miyakoda, M., Yang, W., Khillan, J., Stachura, D. L., Weiss, M. J., et al. (2004). Stress-induced Apoptosis Associated with Null Mutation of ADAR1 RNA Editing Deaminase Gene. *J. Biol. Chem.* 279, 4952–4961. doi:10.1074/jbc.M310162200

Wang, R., Zhang, S., Chen, X., Li, N., Li, J., Jia, R., et al. (2018). CircNT5E Acts as a Sponge of miR-422a to Promote Glioblastoma Tumorigenesis. *Cancer Res.* 78, 4812–4825. doi:10.1158/0008-5472.CAN-18-0532

Xu, L.-D., and Öhman, M. (2018). ADAR1 Editing and its Role in Cancer. *Genes* 10, 12. doi:10.3390/genes10010012

Xu, T.-p., Liu, X.-x., Xia, R., Yin, L., Kong, R., Chen, W.-m., et al. (2015). SP1-induced Upregulation of the Long Noncoding RNA TINCR Regulates Cell Proliferation and Apoptosis by Affecting KLF2 mRNA Stability in Gastric Cancer. *Oncogene* 34, 5648–5661. doi:10.1038/onc.2015.18

Xu, T., Lei, T., Li, S.-Q., Mai, E.-H., Ding, F.-H., and Niu, B. (2020). DNAH17-AS1 Promotes Pancreatic Carcinoma by Increasing PPME1 Expression *via* Inhibition of miR-432-5p. *World J. Gastroenterol.* 26, 1745–1757. doi:10.3748/wjg.v26.i15.1745

You, X., Vlatkovic, I., Babic, A., Will, T., Epstein, I., Tushev, G., et al. (2015). Neural Circular RNAs Are Derived from Synaptic Genes and Regulated by Development and Plasticity. *Nat. Neurosci.* 18, 603–610. doi:10.1038/nn.3975

Yu, J., Zhang, C., Yu, Q., Yu, H., and Zhang, B. (2019). ADAR1 P110 Enhances Adhesion of Tumor Cells to Extracellular Matrix in Hepatocellular Carcinoma via Up-Regulating ITGA2 Expression. *Med. Sci. Monit.* 25, 1469–1479. doi:10.12659/MSM.911944

Yujie Ding, M. M., Shi, X., Ji, J., and Su, Y. (2020). ADAR1p150 Regulates the Biosynthesis and Function of miRNA-149* in Human Melanoma. *Biochem. Biophysical Res. Commun.* 523, 900–907. doi:10.1016/j.bbrc.2019.12.110

Zhang, M., Fritsche, J., Roszik, J., Williams, L. J., Peng, X., Chiu, Y., et al. (2018). RNA Editing Derived Epitopes Function as Cancer Antigens to Elicit Immune Responses. *Nat. Commun.* 9, 3919. doi:10.1038/s41467-018-06405-9

Zhang, Z., and Carmichael, G. G. (2001). The Fate of dsRNA in the Nucleus. *Cell* 106, 465–476. doi:10.1016/s0092-8674(01)00466-4

Zhong, H., Wangxia, L., Fang, Y., Liu, Y., Zhao, Y., and Shi, Z. (2019). Circular RNA ARHGAP26 Is Over-expressed and its Downregulation Inhibits Cell Proliferation and Promotes Cell Apoptosis in Gastric Cancer Cells. *Saudi J. Gastroenterol.* 25, 119. doi:10.4103/sjg.SJG_283_18

Zhu, J., Ye, J., Zhang, L., Xia, L., Hu, H., Jiang, H., et al. (2017). Differential Expression of Circular RNAs in Glioblastoma Multiforme and its Correlation with Prognosis. *Transl. Oncol.* 10, 271–279. doi:10.1016/j.tranon.2016.12.006

Zipeto, M. A., Court, A. C., Sadarangani, A., Delos Santos, N. P., Balaian, L., Chun, H.-J., et al. (2016). ADAR1 Activation Drives Leukemia Stem Cell Self-Renewal by Impairing Let-7 Biogenesis. *Cell Stem Cell* 19, 177–191. doi:10.1016/j.stem.2016.05.004

Conflict of Interest: The authors declare that the research was conducted in the absence of any commercial or financial relationships that could be construed as a potential conflict of interest.

Publisher's Note: All claims expressed in this article are solely those of the authors and do not necessarily represent those of their affiliated organizations, or those of the publisher, the editors and the reviewers. Any product that may be evaluated in this article, or claim that may be made by its manufacturer, is not guaranteed or endorsed by the publisher.

frontiers | Frontiers in Cell and Developmental Biology

TYPE Original Research
PUBLISHED 31 August 2022
DOI 10.3389/fcell.2022.954214

OPEN ACCESS

EDITED BY
Xiaoxing Li,
The First Affiliated Hospital of Sun Yat-sen University, China

REVIEWED BY
Ming-an Sun,
Yangzhou University, China
Shitao Rao,
Fujian Medical University, China

*CORRESPONDENCE
Liang Zhao,
liangsmu@foxmail.com
Rui Zhou,
yaruisunny@sina.com

†These authors have contributed equally to this work

SPECIALTY SECTION
This article was submitted to Signaling, a section of the journal Frontiers in Cell and Developmental Biology

RECEIVED 27 May 2022
ACCEPTED 08 August 2022
PUBLISHED 31 August 2022

CITATION
Liu W, Liu C, You J, Chen Z, Qian C, Lin W, Yu L, Ye L, Zhao L and Zhou R (2022), Pan-cancer analysis identifies YTHDF2 as an immunotherapeutic and prognostic biomarker.
Front. Cell Dev. Biol. 10:954214.
doi: 10.3389/fcell.2022.954214

Pan-cancer analysis identifies YTHDF2 as an immunotherapeutic and prognostic biomarker

Weiwei Liu[1,2†], Chaoqun Liu[1,2†], Jia You[2†], Zilin Chen[1,2], Cheng Qian[1,2], Wandie Lin[1,2], Lina Yu[1,2], Lele Ye[2], Liang Zhao[1,2*] and Rui Zhou[1,2*]

[1]Department of Pathology, Nanfang Hospital, Southern Medical University, Guangzhou, China, [2]Guangdong Province Key Laboratory of Molecular Tumor Pathology, Department of Pathology, School of Basic Medical Sciences, Southern Medical University, Guangzhou, China

Background: N^6-methyladenosine (m6A) modification is a dynamic and reversible post-transcriptional RNA modification prevalent in eukaryotic cells. YT521-B homology domain family 2 (YTHDF2) has been identified as a member of m6A reader protein involving in many vital biological processes, whereas its role and functional mechanisms in cancers remain unclear.

Methods: Bioinformatics analyses were performed on multiple databases including GTEx, TCGA, GEO and Cbioportal to explore the connection between YTHDF2 expression and its genomic changes including tumor mutation burden, microsatellite instability and mismatch repair in 33 different cancer types. We also investigated the association of YTHDF2 expression with prognosis, immune infiltration, tumor microenvironment, immune checkpoints and chemokines. Besides, the correlation of YTHDF2 expression with copy number variation and promoter methylation was also studied in tumors compared with normal tissues. At last, we analyzed the protein-protein interacting network and related genes of YTHDF2 to enrich its potential functional mechanism in tumor development and progression. Real-time qPCR was used to verify the expression of YTHDF2-related genes in colorectal cancer cells, and immunohistochemical staining was adopted to verify immune infiltration in tissue sections from 51 hepatocellular carcinoma patients.

Results: YTHDF2 was overexpressed in a majority of tumor types and associated with their poor overall survival, progression-free interval, and disease-specific survival. The correlation of YTHDF2 expression with tumor mutation burden, microsatellite instability and mismatch repair was also detected in most of the tumor types. Moreover, YTHDF2 might participate in the immune regulation through influencing the expression of immune checkpoint genes and the infiltration of immunocytes in tumor microenvironment. Notably, we demonstrated a positive correlation between YTHDF2 expression and the infiltration of $CD8^+$ T cells and macrophages in many tumors, and it was verified in 51 clinic hepatocellular carcinoma tissues. In addition, the involvement of YTHDF2 in "Spliceosome" and "RNA degradation" were two

potential functional mechanisms underlying its influence on tumor progression. The regulation of YTHDF2 on predicted genes has been verified in CRC cells.

Conclusion: YTHDF2 might be a new therapeutic target and a potential biomarker of cancer immune evasion and poor prognosis.

KEYWORDS

YTHDF2, prognosis, immunotherapy, immune cell infiltration, tumor microenvironment

Introduction

Cancer is one of the leading causes of mortality worldwide and a serious threat to human health (Bray et al., 2018). Although there is no absolute cure for cancer, proper treatments can effectively alleviate the pain and prolong the survival time of cancer patients. In recent years, the emerging cancer immunotherapy shows its potential as a revolutionizing cancer treatment, among which the immune checkpoint blockage therapy has been proven to be a prominent approach (Ribas and Wolchok, 2018). With the help of various public cancer databases and the user-friendly analysis software and platforms, it is possible to predict new immunotherapy targets and evaluating their potential as prognosis biomarkers by performing pan-cancer expression analysis (Blum et al., 2018).

N^6-methyladenosin (m6A) is one of the pervasive mRNA modifications that is intensively studied in eukaryotes (Zhao et al., 2017a; Roundtree et al., 2017), and has been reported involving in many biological processes, such as mRNA stability (Wang et al., 2014), protein translation (Lin et al., 2016), embryonic development (Zhao et al., 2017b), and immunoregulation (Zhang et al., 2019). It has also been demonstrated that the dysregulation of m6A modification and aberrant expression of m6A-associated proteins were associated with tumor initiation and progression (Deng et al., 2018; He et al., 2018). For instance, the aberrant high expression of fat mass and obesity-associated protein (FTO), a demethylase that can decrease the systemic m6A level, played a stimulatory role in chronic myeloid leukemia (Li et al., 2017a). The upregulation of another demethylase, α-ketoglutarate-dependent dioxygenase alkB homolog 5 (ALKBH5), could stimulate cancer progression probably by stabilizing stemness-related transcripts (Zhang et al., 2016; Zhang et al., 2017). Moreover, the increased RNA methylation catalyzed by methyltransferase-like 3 (METTL3) was required for cancer development (Barbieri et al., 2017; Chen et al., 2018). The fate of m6A-modified mRNAs was dependent on the m6A selective binding proteins (Meyer and Jaffrey, 2017). YTH-Domain Family Member 2 (YTHDF2) is the first identified m^6A-binding protein and its function in mRNA stabilization has been well-studied [18]. A dual role of YTHDF2 in pancreatic cancer has been reported that it could promote proliferation, whereas suppress migration and invasion at the same time (Chen et al., 2017). YTHDF2 might function as a tumor suppressor through inhibiting cell growth and proliferation in HCC (Zhong et al., 2019). On the contrary, YTHDF2 could also play an oncogenic role in prostate cancer cell proliferation and migration (Li et al., 2018). So far, the existing evidence is insufficient to conclude a consistent pathogenic role of YTHDF2 in tumor development and progression, let alone its functional mechanism in regulating the immune microenvironment and modulating therapeutic responses. Therefore, we adopted numerous databases and tried to explore the associations between YTHDF2 expression and prognosis, tumor mutation load (TMB), microsatellite instability (MSI), immune checkpoint (ICP) genes, tumor microenvironment (TME), immune cell infiltration, and immune-related genes, hoping to uncover the underlying mechanisms.

Materials and methods

Expression and biological function analysis of YT521-B homology domain family 2 in tumors

Gene Expression Profiling Interactive Analysis (GEPIA) (http://gepia.cancer-pku.cn/index.html) (Topalian et al., 2015; Li et al., 2017b; Tang et al., 2017) is an interactive web server that provides RNA sequencing results analysis of 9,736 tumor and 8,587 normal samples from the TCGA and the GTEx projects, using a standard processing pipeline. In this study, we analyzed the expression of YTHDF2 in different cancer types via different expression modules. GEPIA was adopted to analyze the expression of YTHDF2 in 33 different cancer types.

Correlation analysis of YT521-B homology domain family 2 expression and prognosis

Survival data of clinical samples was extracted and downloaded from the TCGA database. Three indicators, including overall survival (OS), disease-specific survival (DSS), and progression-free interval (PFI), were selected to study the relationship between YTHDF2 expression and the prognosis of cancer patients. The Kaplan-Meier method and log-rank test were used for survival analyses ($p < 0.05$) of each cancer type. Survival curves were plotted using the "survival" and "survminer" in R packages. Moreover, Cox analysis was conducted using "survival"

and "forestplot" in R packages to determine the relationship between YTHDF2 expression and the survival in various cancers.

Correlation analysis of YT521-B homology domain family 2 expression and immune infiltration

The Tumor Immune Estimation Resource (TIMER) database (https://cistrome.shinyapps.io/timer/) (Li et al., 2017b) includes 10,897 samples covering 32 cancer types from TCGA and provides systematical analysis of immune infiltration in various cancer types. The TIMER2 server was used to analyze the correlations between the expression of YTHDF2 and infiltration of six different kinds of immune cells, including B cells, $CD8^+$ T cells, $CD4^+$ T cells, macrophages, neutrophils, and dendritic cells (DCs). The correlation analysis was conducted using the Partial Spearman's correlation coefficient and the purity-corrected partial Spearman's rho value along with the corresponding p values ($p < 0.05$).

We also explored the relationship between the expression of YTHDF2 and TMB, MSI, ICP genes, as well as the ESTIMATE score in the TME *via* the SangerBox website (http://sangerbox.com/Tool).

Clinical samples and cell lines

Tissue chips of human hepatocellular carcinoma were made from clinical samples obtained after elective surgery in Nanfang Hospital during 2007 and 2010. Correlation between YTHDF2 expression and immune infiltration was verified by IHC staining. All experiments performed are endorsed by the Ethics Committee of Southern Medical University and complied with the Declaration of Helsinki.

Colorectal cancer cell line HCT116 was brought from Cell Bank of Chinese Academy of Science (Shanghai, China) and maintained in Dulbecco's modified Eagle's medium (Gibco, United States) supplemented with 10% fetal bovine serum (NEWZERUM, China) at 37°C with 5% CO_2. The primer sequences of YTHDF2 related genes were listed in Supplementary Table S1. YTHDF2-pcDNA 3.1 and siYTHDF2 were adopted to overexpress or silence the expression of YTHDF2 using Lipo3000 (Invitrogen, United States) transfection reagent.

Immunohistochemistry staining

Immunohistochemistry (IHC) staining was conducted on tissue chips of human hepatocellular carcinoma. Firstly, sections were dewaxed and rehydrated by ethanol series, which was followed by a high-pressure antigen repair using TRIS-EDTA buffer for 7 min. Secondly, slices were blocked with 5% normal goat serum at room temperature for 60 min after incubating in 3% H_2O_2 for 15 min to block endogenous peroxidase. Thirdly, the slices were incubated with appropriate primary antibody of YTHDF2 (1:1,000, A15616, Abclonal), CD3 (ZA-0503, ZSGB-BIO), CD8 (ZA-0508, ZSGB-BIO) and CD68 (ZM-0060, ZSGB-BIO) at 4°C overnight. Finally, IHC staining was performed using Horseradish peroxidase (HRP) conjugated with DAB. The semi-quantitative analyses of IHC staining were examined and scored by two senior pathologists under double-blind condition, according to the scores of intensity and degree. The intensity scores were defied as 0 (no staining), 1 (weak), 2 (medium) and 3 (strong). The percentage of positive staining area was defined as 0 (no staining), 1 (1%–25%), 2 (26%–50%), 3 (51%–75%), and 4 (≥75%). The final IHC score was calculated by multiplying the intensity score by degree score of each sample (scale range from 0 to 12). The expression of YTHDF2 was divided into "low YTHDF2" group (score <6) and "high YTHDF2" group (score ≥6).

Real-time qPCR

Total RNA was extracted from HCT116 CRC cells using RNAiso-Plus (TAKARA), and the following reverse transcription into cDNA was completed using qRT-PCR cDNA synthesis kit (TAKARA). The real-time quantitative PCR was performed to confirm the expression of YTHDF2 interacting proteins using TransStart Tip Green qPCR SuperMix (+Dye II) (TransGen Biotech) on the Applied Biosystems 7500 Sequence Detection system. The program of real-time qPCR followed the following cycling conditions: 95°C 5 min for 1 cycle; 95°C 4 s, 60°C 30 s, 72°C 35 s for 40 cycles and followed a melting curve stage. The primers sequences are shown in Table1. The mRNA levels of target genes were normalized to housekeeping gene GAPDH and calculated via the 2-ΔΔCT method.

Statistical analysis

Statistical analyses of the results generated by the on-line interactive web servers using public databases were automatically computed. These results were considered as statistically significant at $^*p < 0.05$, $^{**}p < 0.01$, $^{***}p < 0.001$. The statistical results of GO and KEGG analyses derived from multiple cancer types were corrected by multiple testing using Bonferroni, Holm and FDR to avoid potential false positive results.

Results

The expression of YT521-B homology domain family 2 in different cancer types

We studied the differential expression of YTHDF2 in tumor tissues and adjacent normal tissues derived from TCGA database.

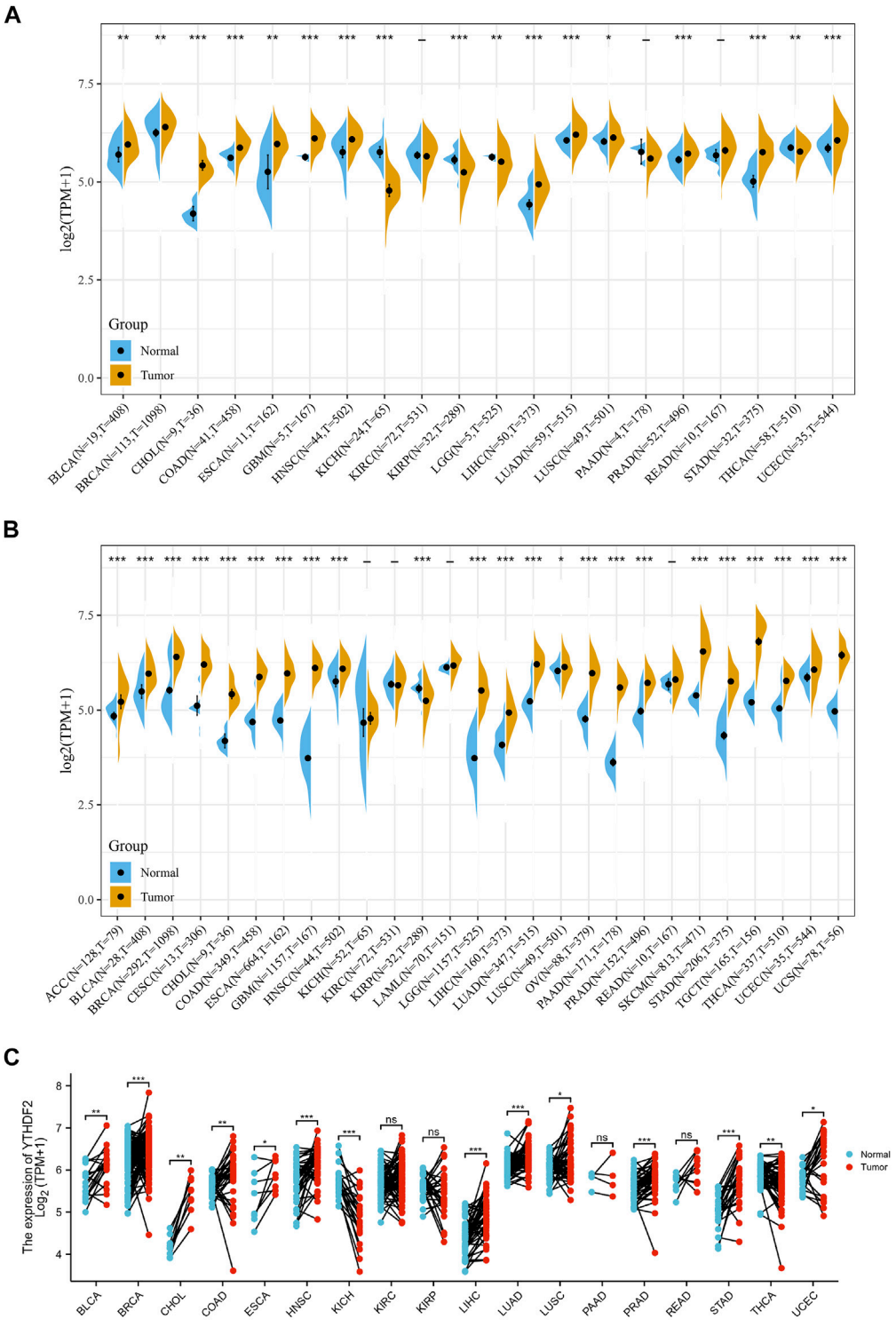

FIGURE 1
Differential expression of YTHDF2 across cancers. **(A)** The expression of YTHDF2 in tumor and adjacent normal tissues using the TCGA data. **(B)** The differential expression of YTHDF2 in tumor and normal tissues of 27 cancer types using the combined data of TCGA and GTEx. **(C)** The expression of YTHDF2 in tumors and paired adjacent normal tissues. *$p < 0.05$, **$p < 0.01$, ***$p < 0.001$.

Figure 1A showed that YTHDF2 was overexpressed in bladder urothelial carcinoma (BLCA), breast invasive carcinoma (BRCA), cholangiocarcinoma (CHOL), colon adenocarcinoma (COAD), esophageal carcinoma (ESCA), glioblastoma multiforme (GBM), head and neck squamous cell carcinoma (HNSC), liver hepatocellular carcinoma (LIHC), lung adenocarcinoma (LUAD), lung squamous cell carcinoma (LUSC), prostate adenocarcinoma (PRAD), stomach adenocarcinoma (STAD), and uterine corpus endometrial carcinoma tissues (UCEC), compared with that in the adjacent normal tissues. On the contrary, the expression of YTHDF2 was lower in renal tumors including kidney chromophobe carcinoma (KICH) and renal papillary cell carcinoma (KIRP), brain lower grade glioma (LGG) and thyroid carcinoma (THCA), than that in the adjacent non-tumorous tissues. Moreover, there was no expression difference of YTHDF2 in kidney renal clear cell carcinoma (KIRC), pancreatic adenocarcinoma (PAAD) and rectum adenocarcinoma (READ).

As normal samples in the TCGA database are limited, we combined the normal samples from GTEx with the tumor samples from TCGA, and evaluated the expression of YTHDF2 in 27 different cancer types. Compared with the normal tissues, except for the lower YTHDF2 expression in KIRP tissues and similar YTHDF2 expression in KICH, KIRC and LAML tissues, YTHDF2 was overexpressed in all the left 23 cancer types (Figure 1B). Expression analysis of the paired tumor and normal samples also demonstrated that the expression of YTHDF2 was dramatically upregulated in 16 cancer types including BLCA, BRCA, CHOL, COAD, ESCA, HNSC, LIHC, LUAD, LUSC, PRAD, STAD, THCA and UCEC, whereas downregulated only in KICH (Figure 1C).

In order to identify the major cell types that express YTHDF2, we carried out YTHDF2 single-cell analyses using single-cell data from 79 tumor samples. The results showed that YTHDF2 was mainly expressed in malignant cells and immune cells, especially in monocytes/macrophages (Supplementary Figures S1A,B). Moreover, YTHDF2 was comprehensively expressed in immune cells including T cells, dendritic cells, NK cells and monocytes in the TME of CRC (GSE146711, Supplementary Figure S1A). A single-cell study of 3321 cells from six patients with glioma demonstrated that YTHDF2 was overexpressed in malignant glioma cells and monocytes/macrophages in the TME (GSE102130, Supplementary Figure S1D).

YT521-B homology domain family 2 gene mutation and promoter methylation analysis

Firstly, the mutation frequency of YTHDF2 across cancers was analyzed using the cBioPortal database, and the highest mutation frequency of YTHDF2 was detected in Uterine Carcinosarcoma (Figure 2A). Then, we mapped the mutation data of 15 different cancers from TCGA to further analyze the specific types of YTHDF2 mutation. We found that the "missense mutation" is the major type of YTHDF2 mutation (Figure 2B). Subsequently, we explored the copy number variations (CNVs) of YTHDF2, and found that a high frequency of CNVs was detected in LGG, CESC, LUAD, COAD, BRCA, ESCA, SARC, STAD, UCEC, HNSC, KIRC, LUSC, LIHC, MESO, READ, PAAD, OV, TGCT, SKCM, and BLCA (Figure 2C). Finally, we detected the promoter methylation level of YTHDF2 across cancers using UALCAN database. The results demonstrated that the promoter methylation level of YTHDF2 was higher in BRCA, CHOL, HNSC, KIRC, PRAD, KIRP, LUSC, LIHC and ESCA compared with normal tissues, while lower in LUAD, READ, COAD, THC and UE (Supplementary Figure S2). We also analyzed the correlation between the expression of YTHDF2 and its promoter methylation in various tumor types. We found that the abnormal YTHDF2 expression was negatively correlated with the promoter methylation values of CpG dinucleotides in most of the tumor types including BLCA, BRCA, CHOL, DLBC, ESCA, GBM, KICH, KIRP, LAML, LGG, LIHC, LUAD, LUSC, MESO, PAAD, PCPG, PRAD, READ, SARC, TGCT, UCEC and UVM, while positively correlated only in COAD, HNSC and THYM (Supplementary Figure S3).

Prognostic analysis of YT521-B homology domain family 2 in cancers

To study the association between YTHDF2 expression and prognosis, we performed a series of survival-associated analyses, including OS, DSS, and PFI. Cox proportional hazards model analysis showed that the expression of YTHDF2 was associated with OS in LIHC ($p = 0.005$), KIRC ($p = 0.023$), KICH ($p = 0.038$), ACC ($p = 0.028$), LGG ($p < 0.001$), READ ($p = 0.05$), and SARC ($p < 0.001$) (Figure 3A). Furthermore, YTHDF2 was a high-risk factor in LIHC, LGG, ACC, SARC, and KICH, while a low-risk gene in other cancer types, particularly in READ. Kaplan-Meier survival analysis also demonstrated a significant negative correlation between YTHDF2 expression and OS in patients with LIHC ($p = 0.005$), KICH ($p = 0.043$), ACC ($p = 0.013$), LGG ($p < 0.001$), and SARC ($p = 0.029$), whereas high YTHDF2 expression was associated with a longer survival time in patients with KIRC ($p = 0.02$) and READ ($p = 0.05$) (Figure 3B).

Moreover, the PFI analyses in Supplementary Figure S4A revealed a negative correlation between YTHDF2 expression and prognosis in patients with LIHC ($p = 0.016$), KIRC ($p = 0.008$), KICH ($p = 0.034$), ACC ($p = 0.002$), LGG ($p < 0.001$) and KIRP ($p = 0.027$). However, in patients with CHOL ($p = 0.017$) and KIRC ($p = 0.008$), such a relationship could not be detected.

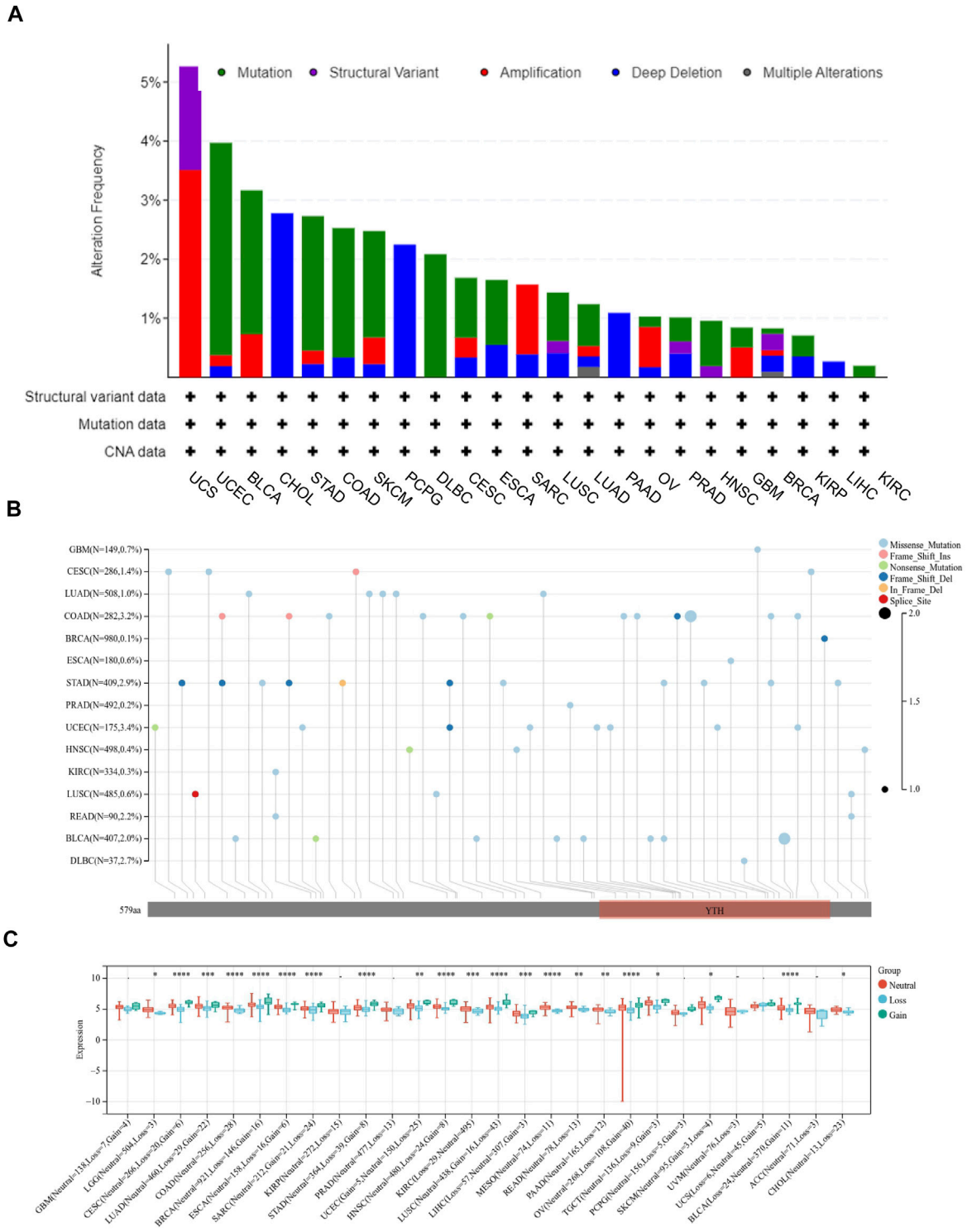

FIGURE 2
The mutation of YTHDF2 in cancers analyzed using TCGA data. **(A)** The mutation frequency and types of YTHDF2 in different cancer types. **(B)** The mutation information of YTHDF2 in different cancers. **(C)** The correlation between YTHDF2 expression and CNV. *$p < 0.05$, **$p < 0.01$, ***$p < 0.001$.

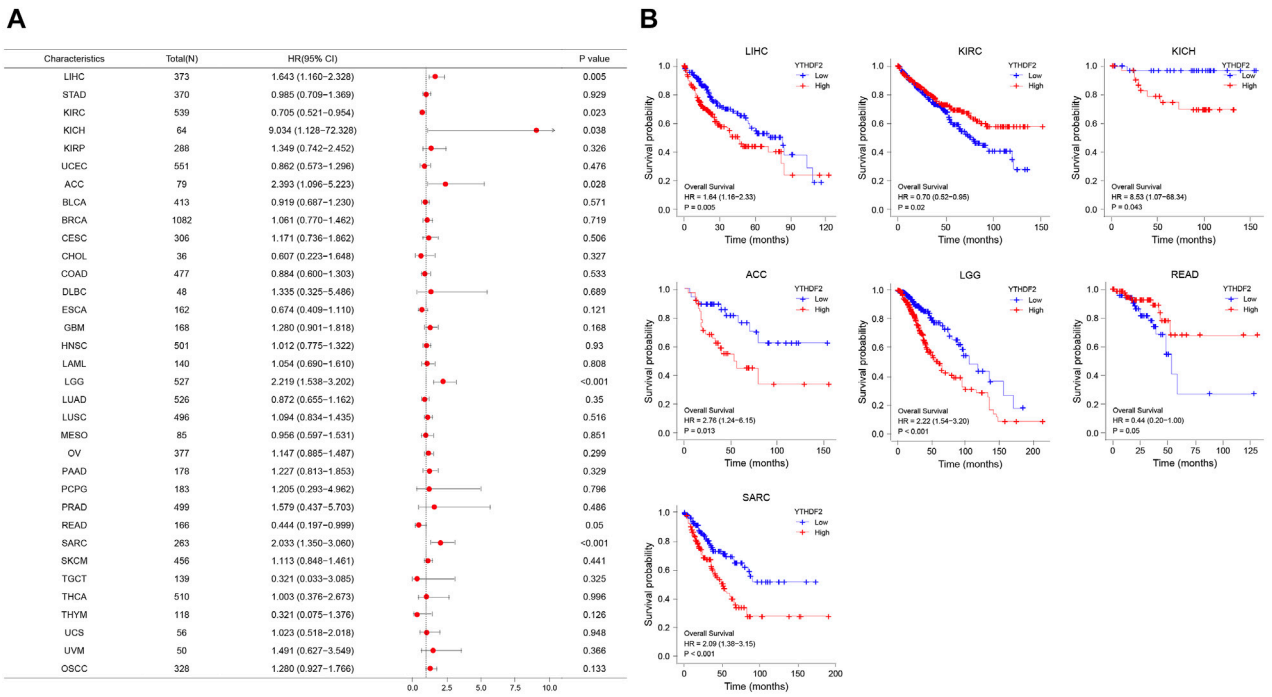

FIGURE 3
YTHDF2 expression is associated with overall survival time (OS). **(A)** Forest plot of OS associations in 34 cancer types. **(B)** Kaplan-Meier analysis of the association between YTHDF2 expression and OS.

Kaplan-Meier survival analysis revealed a negative correlation between YTHDF2 expression and prognosis in patients with ACC ($p = 0.001$), KICH ($p = 0.04$), KIRP ($p = 0.03$), LIHC ($p = 0.016$) and LGG ($p < 0.001$) (Supplementary Figure S4B).

The forest plots showed hazard ratio (HR) > 1 was detected in ACC ($p = 0.031$), LGG ($p < 0.001$) and SARC ($p = 0.001$), while HR < 1 in KIRC ($p = 0.007$) (Supplementary Figure S4C). Kaplan-Meier analysis showed that individuals with ACC ($p = 0.014$), LGG ($p < 0.001$) and SARC ($p = 0.002$) had a high YTHDF2 expression level, but a poor DSS. On the contrary, patients with a high YTHDF2 expression level had a longer survival time in KIRC ($p = 0.006$) (Supplementary Figure S4D).

In addition, in order to further explore the predictive value of YTHDF2 for the prognosis of patients with LIHC, KIRC, KICH, ACC, LGG, READ, SARC, and CHOL, we conducted the ROC analysis and found that YTHDF2 had a better predictive ability for the prognosis of patients with CHOL, KICH, LGG and READ, and a good predictive ability for patients with LIHC (Figure 4A). Subsequently, we performed a time-dependent ROC analysis, and the results showed that YTHDF2 had a high predictive ability for the 1-year, 3-year and 5-year survival rates of KICH patients (AUC = 0.983, 0.814, 0.870 respectively), whereas a low predictive ability for patients with LGG, LIHC and SARC (Figure 4B).

Immune aspects of YT521-B homology domain family 2 in tumor microenvironment

The biological significance of YTHDF2 was conducted in different cancers. As shown in Supplementary Figure S5, the GO functional annotation and KEGG pathway analysis indicated that YTHDF2 could positively regulate cell adhesion, cell cycle, and several immune-related functions. As TME plays an important role in regulating tumor progression and could affect the response of immunotherapy, we calculated the correlation between YTHDF2 expression and immune scores (Supplementary Figure S6A), stromal scores (Supplementary Figure S6B), estimated scores (Supplementary Figure S6C) and tumor purity (Supplementary Figure S6D) in 32 cancers based on the ESTIMATE algorithm to assess the relationship between YTHDF2 expression and TME composition. As a result, there was a negative correlation between YTHDF2 expression and immune scores, stromal scores and estimated scores, and a positive correlation with tumor purity in most cancers except LGG and PPAD (Supplementary Figures S6A–D). ACC, UCEC, and SKCM-P are the top three cancers with significant correlation between YTHDF2 expression and immune scores (Figure 5A). TGCT, ACC and UCEC are the top three cancers with significant correlation between YTHDF2 expression and

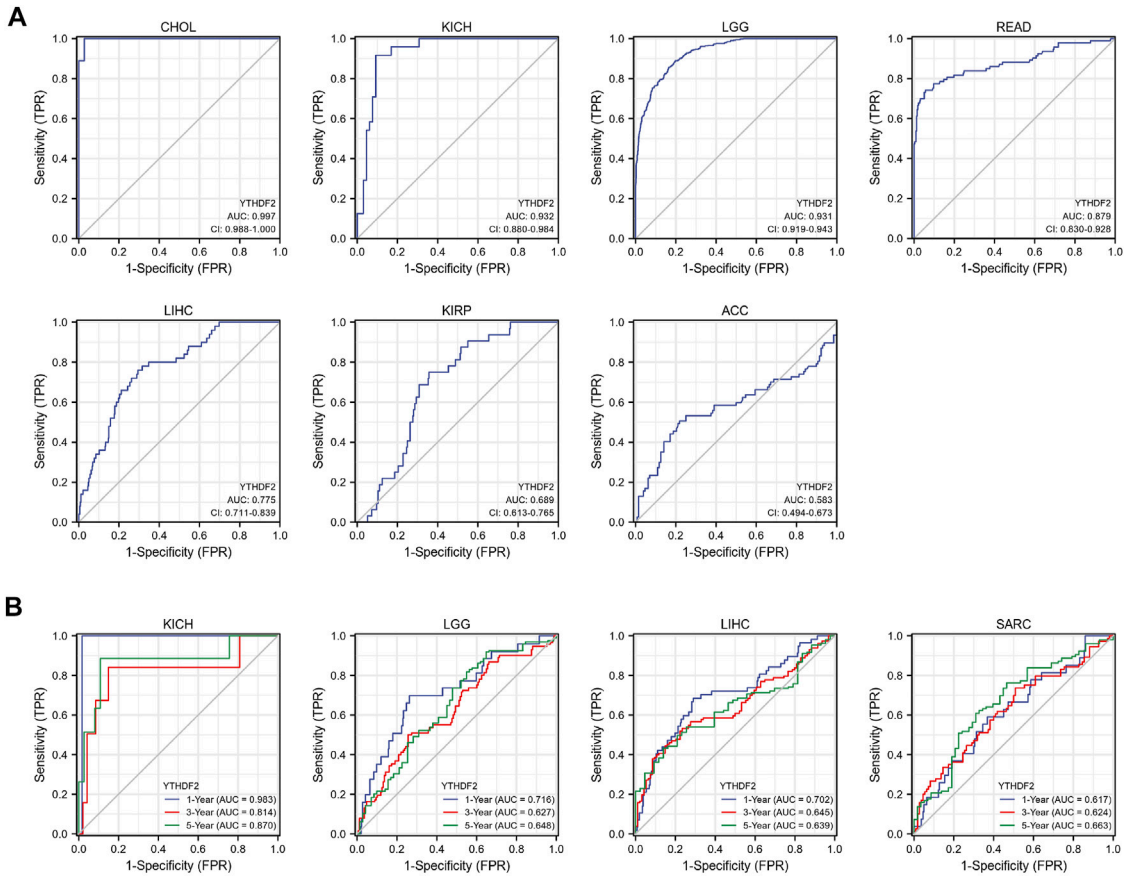

FIGURE 4
The predictive potential of YTHDF2 on prognosis. **(A)** ROC analysis demonstrates the predictive potential of YTHDF2 on prognosis in CHOL, KICH, LGG, READ, LIHC, KIRP, and ACC. **(B)** Time-dependent ROC analysis demonstrates the predictive potential of YTHDF2 on 1-year, 3-year, and 5-year survival rate of patients with KICH, LGG, LIH, and KIRC.

stromal scores (Figure 5B). Similarly, ACC, UCEC, and TGCT are the top three cancers with significant correlation between YTHDF2 expression and estimate scores (Figure 5C). The above results indicated that the YTHDF2 expression in tumors is closely related to the composition of TME.

Correlation between YT521-B homology domain family 2 expression and immune infiltration in tumor microenvironment

It has been confirmed that immune cells in the TME could affect the survival of cancer patients. As the prognostic role of YTHDF2 has been discovered in the pan-cancer research, it is meaningful to explore the relationship between YTHDF2 expression and immune infiltration. Here, we calculated the correlation between YTHDF2 expression and immune infiltration in 39 different tumors by TIMER. The results indicated that YTHDF2 expression was significantly correlated with tumor purity in 12 tumors, and significantly correlated with the infiltration of B cells, $CD4^+$ T cells, $CD8^+$ T cells, dendritic cells, macrophages and neutrophils in 19, 18, 20, 22, 13, and 23 tumors respectively (Supplementary Figure S7A), among which COAD, KIRC and LGG were the top three significantly correlated cancers (Figure 6A). In order to better understand the relationship between YTHDF2 expression and the differential infiltration of immune cells, TIMER database was adopted to analyze the correlation between the expression of YTHDF2 and different immune cell marker genes in KICH, KIRP, LGG, LIHC, PPAD, THYM, UVM, KIRC, READ, ACC and SARC. After tumor purity adjustment, we found that the expression of YTHDF2 was positively correlated with that of majority immune cell marker genes (Supplementary Figure S7B). The conclusion was also confirmed by the IHC staining of YTHDF2 in clinical HCC samples, in which a positively correlation with the infiltration of $CD3^+$ T cells, $CD8^+$ T cells

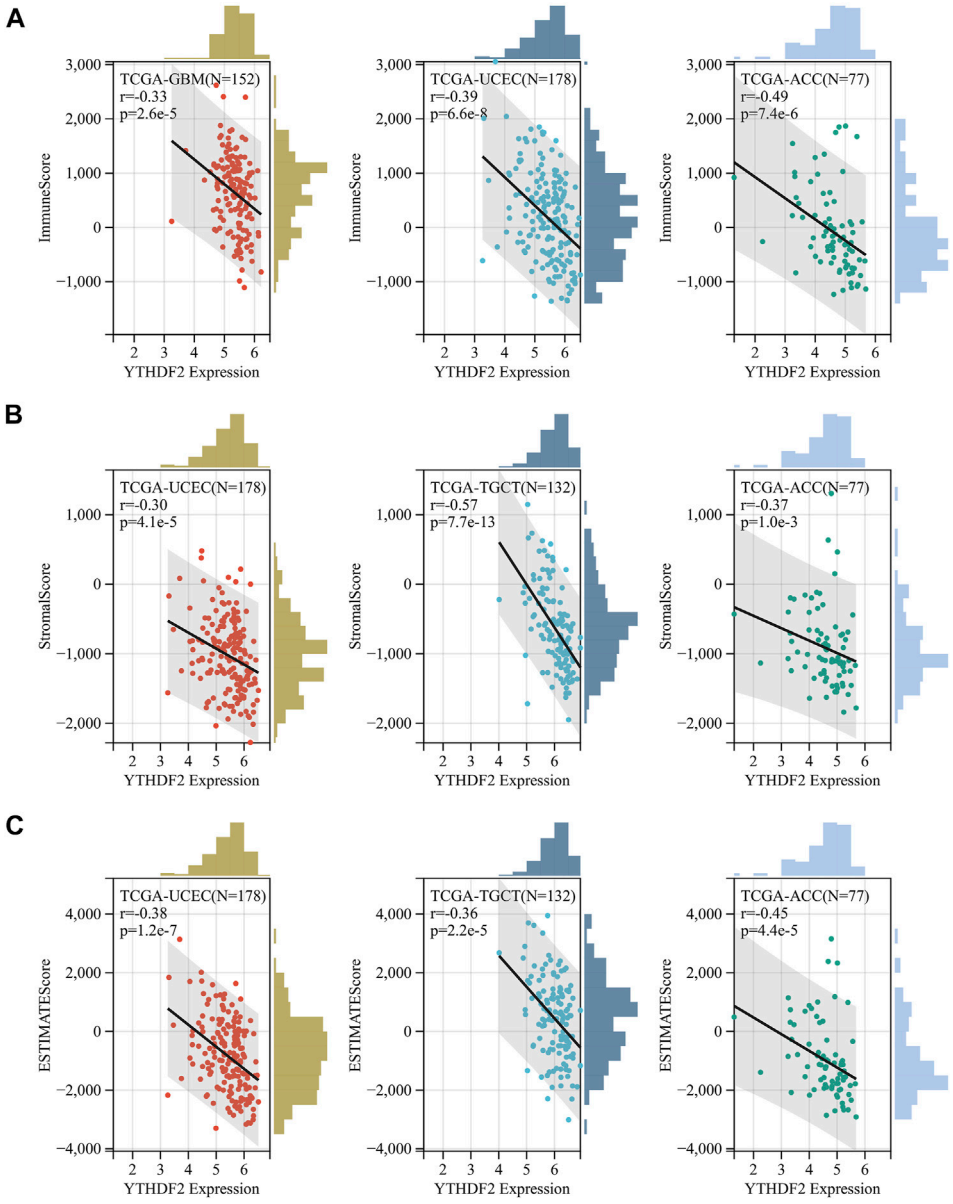

FIGURE 5
The correlation between YTHDF2 expression and immuneScore, stromalscore and estimatescore in GBM, UCEC and ACC. **(A)** the correlation between YTHDF2 expression and Immunescore in UCEC, TGCT, and ACC. **(B)** The correlation between YTHDF2 expression and stromalscore in UCEC, TGCT and ACC. **(C)** The correlation between YTHDF2 expression and estimatescore in GBM, UCEC and ACC.

and CD68$^+$ macrophages was detected (Figures 6B,C). In addition, we also found a positive correlation between the CNVs of YTHDF2 and the tumor infiltrating lymphocytes (TILs) (Supplementary Figure S8A), immunostimulants (Supplementary Figure S8B), immunosuppressants (Supplementary Figure S8C), MHC (Supplementary Figure S8D), chemokines (Supplementary Figure S8E), and chemokine receptors (Supplementary Figure S8F), especially in CHOL, KICH, and LGG.

The correlation between the expression of YT521-B homology domain family 2 and immune checkpoint genes in human cancers

ICP genes have been demonstrated to have significant influences on immune cells infiltration and outcomes of immunotherapy (Topalian et al., 2015). Hence, we explored the association between the expression of YTHDF2 and ICP

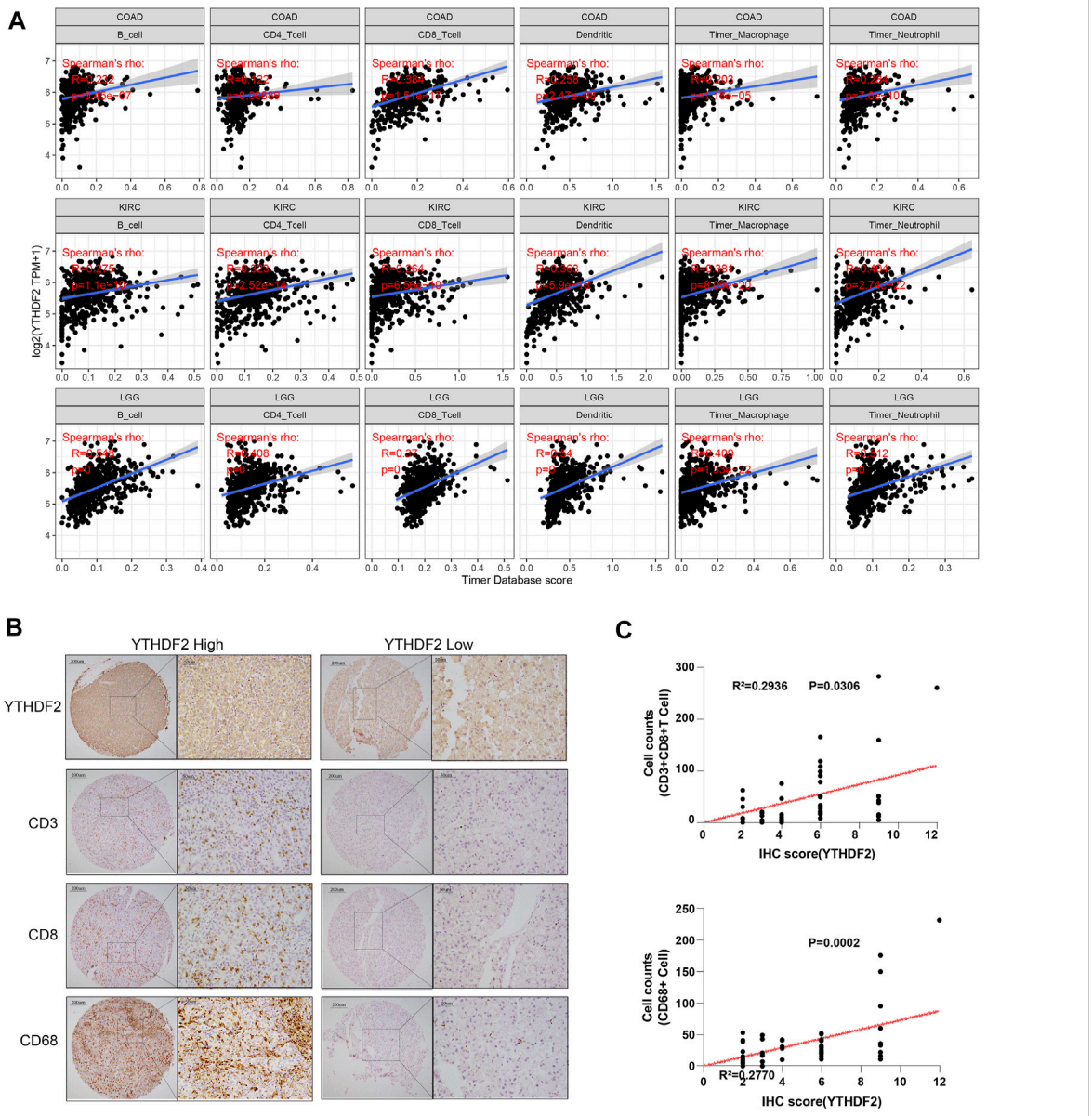

FIGURE 6
The correlation between YTHDF2 expression and immune infiltration in different cancer types. **(A)** The correlation between YTHDF2 expression and immune infiltration in the top three tumors. **(B)** Immunohistochemical images of hepatocellular carcinoma show intra-tissue characteristics of $CD3^+CD8^+$ T cells/CD68 macrophages with high and low expression of YTHDF2. **(C)** The correlation analysis of YTHDF2 expression with $CD3^+CD8^+$ T cells and CD68 macrophage infiltration in hepatocellular carcinoma validation cohort.

genes in human cancers to explore the potential role of YTHDF2 in immunotherapy. The correlation between YTHDF2 expression and 47 ICP genes were verified in most cancer types (Figure 7). The results showed that the expression of YTHDF2 was positively correlated with immune checkpoint genes in COAD, KICH, KIRC, KIRP, LGG, LIHC, PAAD, PRAD, PCPG, and UVM, especially in KICH, LGG, LIHC, and UVM. The above results indicated that high YTHDF2 expression obtained a predictive potential of immunotherapies through targeting ICP genes. However, YTHDF2 expression is reversely correlated with the ICP genes in BLCA, BRCA, GBM, LUAD, LUSC, and THYM, suggesting a poor immunotherapy outcome in YTHDF2 overexpression patients with those tumors.

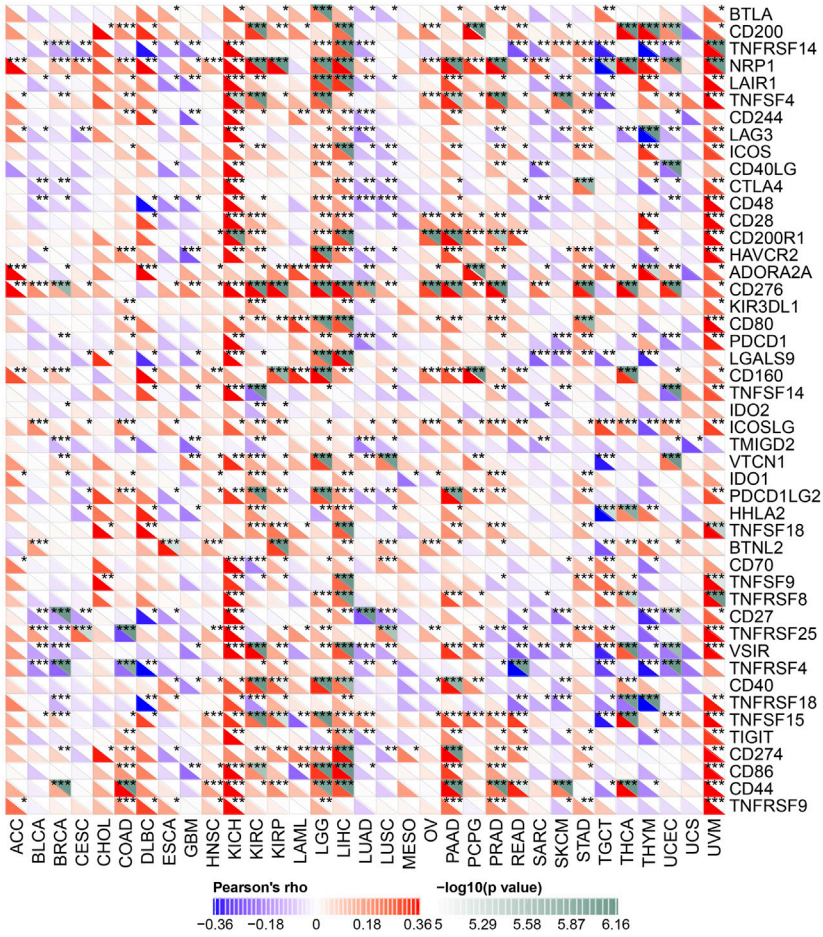

FIGURE 7
The correlation between YTHDF2 expression and pan-cancer immune checkpoint genes. *$p < 0.05$; **$p < 0.01$; ***$p < 0.001$.

Correlations between YT521-B homology domain family 2 expression and mismatch repair, tumor mutation burden, and microsatellite instability in cancers

Microsatellites (MS) are simple repetitive sequences of nucleotide bases that are liable to make errors during DNA replication, which could be recognize and repair by mismatch repair (MMR) genes. Tumors with defective MMR systems are susceptible to microsatellite mutations, which lead to high microsatellite instability (MSI) levels, and in turn cause the accumulated mutations in cancer-related genes and the aggravated tumor mutation burden (TMB). Therefore, we investigated the relationship between YTHDF2 expression and several MMR genes, including MLH1, MSH2, MSH6, PMS2 and EPCAM. As a result, YTHDF2 was positively correlated with MMR gene expression in all the cancer types, excluding CHOL and UCS (Figure 8A). As TMB has been proven to be an immune-response biomarker that can effectively predict the immunotherapeutic effects of immune checkpoint blockers (ICBs), we examined the association between YTHDF2 expression and TMB in different cancers. The results showed that YTHDF2 expression and TMB were positively correlated in GBMLGG, COAD, COADREAD, STAD, and LIHC, while negatively correlated in THCA (Figure 8B). We also studied the association between the expression of YTHDF2 and MSI, and found that they are positively correlated in GBM, CESC, and STAD, while negatively correlated in BRCA, PRAD, HNSC, THCA, and DLBC (Figure 8C). As MMR, TMB, and MSI are all promising immunotherapeutic biomarkers for ICP-based immunotherapy, the above results further confirmed the potential of YTHDF2 as a predictor of ICI therapeutic response.

Enrichment analysis of YT521-B homology domain family 2-Related partners

To further explore the mechanism underlying YTHDF2 mediated tumor development and progression, we

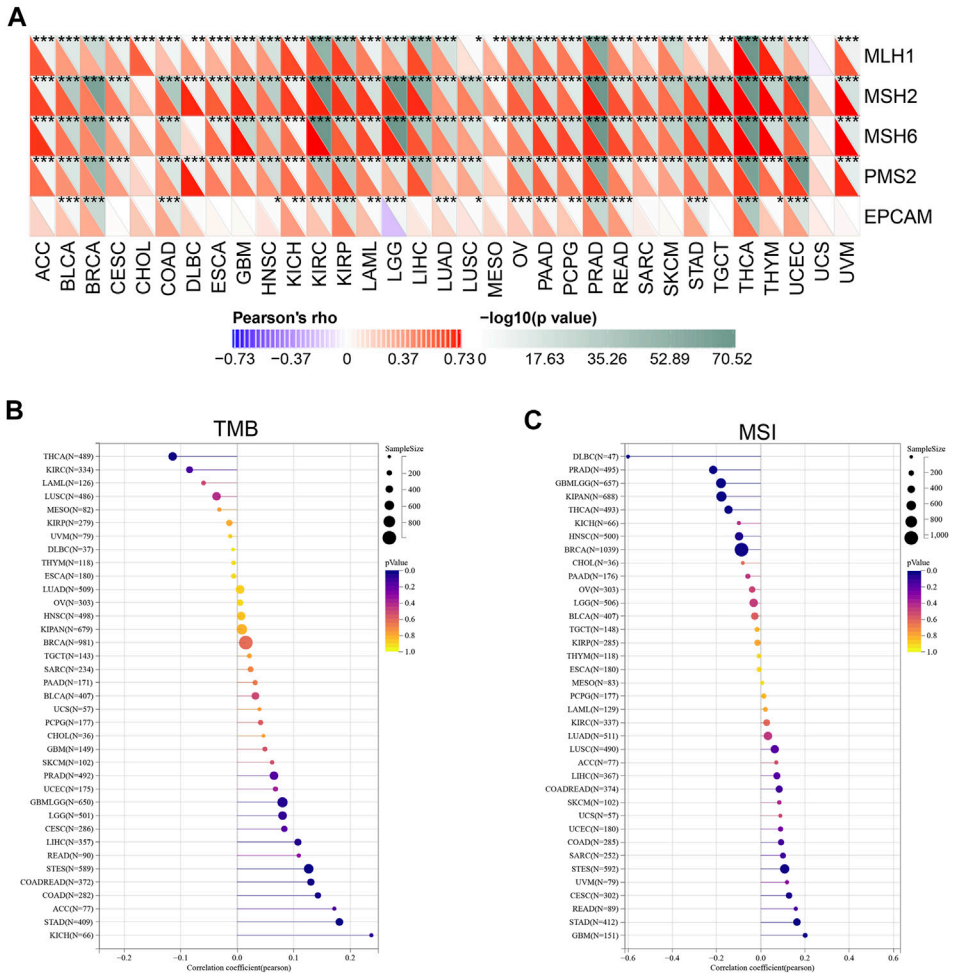

FIGURE 8
The correlation between YTHDF2 expression and the MMR **(A)**, TMB **(B)**, and MSI **(C)**. *$p < 0.05$; **$p < 0.01$; ***$p < 0.001$.

carried out a series of pathway enrichment analyses on YTHDF2 interacting proteins and related genes based on STRING and GEPIA2. In this study, we obtained 48 YTHDF2 interacting proteins predicted from the PPI network (Figure 9A), and gained the top 100 YTHDF2-related genes (Supplementary Table S2), among which nuclear inhibitor of protein phosphatase 1(PPP1R8, R = 0.77), histone-binding protein RBBP4 (RBBP4, R = 0.75), KH domain-containing, RNA-binding, signal transduction-associated protein 1 (KHDRBS1, R = 0.73), glucocorticoid modulatory element-binding protein 1 (GMEB1, R = 0.74) and heterogeneous nuclear ribonucleoprotein R (HNRNPR, R = 0.71) are the top five genes (Figure 9B). The corresponding heat map also demonstrated a significant positive correlation between the expression of YTHDF2 and the top five genes in all the tumor types from the TCGA (Figure 9C). Through analyzing the direct YTHDF2-interacting proteins and cross analyzing the YTHDF2-related genes, 7 YTHDF2-regulated genes were confirmed. As shown in Figure 9D, they were ELAV-like protein 1 (ELAVL1), Ras GTPase-activating protein-binding protein 1 (G3BP1), Pumilio homolog 1 (PUM1), CCR4-NOT transcription complex subunit 9 (RQCD1), Serine/arginine-rich splicing factor 3 (SRSF3), Ubiquitin-associated protein 2-like (UBAP2L) and Caprin-1 (CAPRIN1). Subsequently, we overexpressed and silenced the expression of YTHDF2 respectively in HCT116 cells to detect its influence on the expression of the above 7 YTHDF2-regulated genes. The results showed that YTHDF2 could upregulate the expression of G3BP1, SRSF3, PUM1, and UBAP2L, but downregulate that of ELAVL1. We failed to confirm the regulation of YTHDF2 on CAPRIN1 and RQCD1. Consistently, silenced the expression of YTHDF2 dramatically enhanced the expression of ELAVL1 and CAPRIN1, but suppressed that of SRSF3, PUM1 and UBAP2L (Supplementary Figures S9A,B). The GO enrichment analysis of the combined two data sets showed that "regulation of mRNA

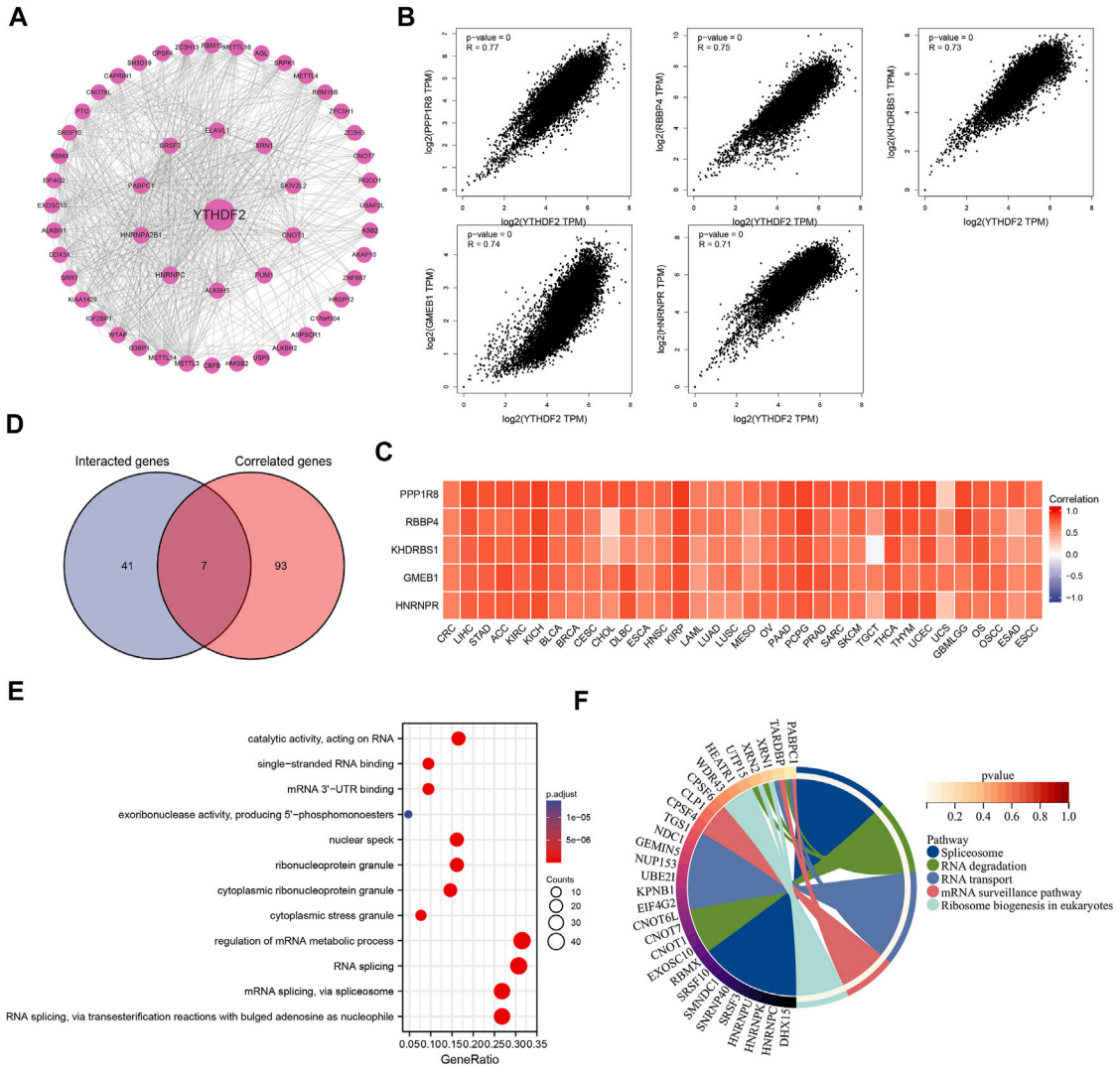

FIGURE 9
The protein-protein interactions network, Go enrichment analysis and KEGG pathway analysis. **(A)** The YTHDF2 interacting proteins that screened by the online STRING tools. **(B)** The top 100 YTHDF2-related genes in TCGA database, among which the top five targeting genes are screened out. **(C)** The heatmap showed the expression of the top five YTHDF2 targeting genes in different cancer types. **(D)** The cross analysis of YTHDF2-interacting and YTHDF2-related genes. **(E)** GO enrichment analysis based on the YTHDF2-interacting and YTHDF2-related genes. **(F)** The KEGG pathway analysis based on YTHDF2-interacting and YTHDF2-related genes.

metabolic process" and "RNA splicing" are the top two enriched pathways, which might involve in the YTHDF2-regulated tumor development and progression (Figure 9E). The KEGG pathway enrichment analysis further demonstrated that YTHDF2 was correlated with "Spliceosome" and "RNA degradation" (Figure 9F).

Discussion

As the m6A mRNA modification involves in many biological processes, its dysregulation and/or the aberrant expression of related proteins have been demonstrated associating with tumor initiation and progression. YTHDF2 is an m6A reader protein involving in many vital biological processes. In the present study, we performed a pan-cancer analysis and tried to investigate the expression of YTHDF2 and its predictive value on prognosis across various tumors. Single-cell sequencing analyses revealed that expression of YTHDF2 could be detected not only in malignant tumor cells, but also in the surrounding immune cells. A series of survival-associated analyses including OS, DSS, and PFI were conducted to evaluate the predictive potential of YTHDF2 for prognosis across cancers. Although the disparities existed in different tumor types, the aberrant

expression of YTHDF2 has been proposed to be a promising prognosis predictive factor in some cancer types, including ACC, LGG, KICH, KIRP, LIHC, KIRC, and READ, based on both single-factor Cox regression analysis and Kaplan-Meier survival analyses.

It has been demonstrated that the mutation of vital genes could drive the tumorigenesis and convert normal somatic cells into cancer cells (Martincorena and Campbell, 2015). Hence, we analyzed the YTHDF2 genome using cBioportal database to disclose its mutation frequency and types. The results showed that high YTHDF2 mutation frequency was detected in various tumors, and the missense mutation was the most common mutation type in 15 different tumors. Moreover, we also investigated that YTHDF2 expression was correlated with its CNVs and promoter methylation in most cancer types. The high mutation potential, CNVs and methylation of YTHDF2 in cancers might all contribute to the development and progression of various tumors.

The following GO functional annotation and KEGG pathway analysis in various cancers indicated that YTHDF2 could positively regulate cell adhesion, cell cycle, and immune-related functions. As somatic mutations in the cancer cells could contribute significantly to immune evasion and poor responses to therapies (Zacharakis et al., 2018), we proposed that the genomic changes of YTHDF2 might contribute to tumor development and progression, as well as influence the tumor therapy effects, partially through regulating immune reactions.

The development of ICIs is a revolutionary milestone in the field of cancer therapy. Tumor cells can evade immunosurveillance to achieve malignant progression through different mechanisms, one of which is to active the immune checkpoints to suppress antitumor immune responses (Darvin et al., 2018). Notably, we found that YTHDF2 expression was positively correlated with some ICP genes in most tumors, especially in KICH, LGG, LIHC and UVM. These results suggest that YTHDF2 had a potential to promote immune escape. MMR is an important factor related to genome stability and integrity (Fishel, 2015; Russo et al., 2019). Besides NMR, TMB and MSI are two new sensitive predictors of immunotherapy (Boland and Goel, 2010; Yarchoan et al., 2017; Lee et al., 2019). Our study found that YTHDF2 expression was positively correlated with MMR genes in all cancers excluding CHOL and UCS. In addition, YTHDF2 is also positively correlated with TMB and MSI in some cancer types. Our results suggested that YTHDF2 might play an important role in tumor immunity and serve as a predictive marker for immunotherapy. Moreover, TME plays an important role in tumor genesis, development, metastasis and clinical treatment, as well as affects tumor immune escape and angiogenesis (Lyssiotis and Kimmelman, 2017; Han et al., 2021; Hiam-Galvez et al., 2021). It has been reported that the aberrant infiltration of immune cells in normal tissues could enhance tumor development and progression (Pagès et al., 2005; Man et al., 2013). Some oncogenic proteins can also regulate the infiltration of immune cells in the TME. Our results showed that the expression of YTHDF2 was negatively correlated with estimate scores, stromal scores, and immune scores in human generalized cancers, but positively correlated with tumor purity in the majority of tumor types, suggesting an important role of YTHDF2 in TME composition. We also investigated the role of YTHDF2 on immune infiltration levels across cancers. The results demonstrated that YTHDF2 was associated with immune cells infiltration in BLCA, BRCA, COAD, KICH, LGG, LICH, PPAD, PCPG, KIRP, PRAD, SKCM, and THCA. In addition, the co-expression of YTHDF2 and immune cell-related genes in those cancer types further confirmed the correlation between YTHDF2 and tumor immune infiltration. The IHC staining of YTHDF2 in clinic HCC samples was consistent with that derived from the database, the result of which further confirmed the correlation between YTHDF2 and immune infiltration in TME. As the disparities exist in different tumor types, the role of YTHDF2 in immune infiltration needs to be further validated.

Here, we also combined the YTHDF2 interacting proteins and related genes, the pathway enrichment of which suggested that RNA splicing and degradation were the top two events and possible mechanisms involving in YTHDF2-mediated tumor development and progression. Since the conclusion was based on the bioinformatics analysis of TCGA or GEO data sets, we overexpressed and silenced the expression of YTHDF2 to confirm the regulation of YTHDF2 on 7 predicted genes in HCT116 CRC cells by real-time qPCR. Further biological experiments conducted on various tumor cells are still required to verify the YTHDF2-regulated genes.

In summary, we tried to provide a comprehensive bioinformatics analysis on the expression, mutation and promoter methylation of YTHDF2 across cancers, and investigated its predictive value on prognosis. Our results suggested a correlation between YTHDF2 and TME composition, as well as its vital role in immune infiltration and immunotherapeutic response in a majority of tumor types. Moreover, we also screened the YTHDF2-related genes and YTHDF2-interacting proteins to predict its functional mechanisms. In short, YTHDF2 might serve as a potential biomarker for tumor detection, therapeutic response and prognostic analysis.

Data availability statement

The datasets presented in this study can be found in online repositories. The names of the repository/repositories and accession number(s) can be found in the article/ Supplementary Material.

Ethics statement

The studies involving human participants were reviewed and approved by the Ethics Committee of Southern Medical University. The patients/participants provided their written informed consent to participate in this study.

Author contributions

Conceptualization, WL and CL; methodology, LZ; software, WL and LY; validation, ZC, WL, LY, and CQ; formal analysis, RZ; investigation, WL and JY; resources, LZ; data curation, RZ; writing—original draft preparation, WL; writing—review and editing, RZ; visualization, WL; supervision, LZ; project administration, LZ; All authors have read and agreed to the published version of the manuscript.

Funding

This work was supported by the National Natural Science Foundation of China (Nos. 81972813, 82073026), Guangdong Basic and Applied Basic Research Foundation (2018B030311036, 2019A1515010974, 2020A1515011389, 2020A1515011236), Fork Ying Tung Education Foundation (161035) and Special Funds for Guangdong Scientific and Technological Innovation Strategy (pdjh2020a011). This work is also supported by the Bejing Xisike Clinical Oncology Research Foundation (Y-Roche2019/2-0025).

Acknowledgments

The authors thank all of the research staffs and students who participated in this study.

Conflict of interest

The authors declare that the research was conducted in the absence of any commercial or financial relationships that could be construed as a potential conflict of interest.

Publisher's note

All claims expressed in this article are solely those of the authors and do not necessarily represent those of their affiliated organizations, or those of the publisher, the editors and the reviewers. Any product that may be evaluated in this article, or claim that may be made by its manufacturer, is not guaranteed or endorsed by the publisher.

Supplementary material

The Supplementary Material for this article can be found online at: https://www.frontiersin.org/articles/10.3389/fcell.2022.954214/full#supplementary-material

References

Barbieri, I., Tzelepis, K., Pandolfini, L., Shi, J., Millán-Zambrano, G., Robson, S. C., et al. (2017). Promoter-bound METTL3 maintains myeloid leukaemia by m6A-dependent translation control. *NATURE* 552 (7683), 126–131. doi:10.1038/nature24678

Blum, A., Wang, P., and Zenklusen, J. C. (2018). SnapShot: TCGA-analyzed tumors. *Cell* 173 (2), 530. doi:10.1016/j.cell.2018.03.059

Boland, C. R., and Goel, A. (2010). Microsatellite instability in colorectal cancer. *GASTROENTEROLOGY* 138 (6), 2073–2087. doi:10.1053/j.gastro.2009.12.064

Bray, F., Ferlay, J., Soerjomataram, I., Siegel, R. L., Torre, L. A., and Jemal, A. (2018). Global cancer statistics 2018: GLOBOCAN estimates of incidence and mortality worldwide for 36 cancers in 185 countries. *CA A Cancer J. Clin.* 68 (6), 394–424. doi:10.3322/caac.21492

Chen, J., Sun, Y., Xu, X., Wang, D., He, J., Zhou, H., et al. (2017). YTH domain family 2 orchestrates epithelial-mesenchymal transition/proliferation dichotomy in pancreatic cancer cells. *Cell CYCLE* 16 (23), 2259–2271. doi:10.1080/15384101.2017.1380125

Chen, M., Wei, L., Law, C. T., Tsang, F. H., Shen, J., Cheng, C. L., et al. (2018). RNA N6-methyladenosine methyltransferase-like 3 promotes liver cancer progression through YTHDF2-dependent posttranscriptional silencing of SOCS2. *HEPATOLOGY* 67 (6), 2254–2270. doi:10.1002/hep.29683

Darvin, P., Toor, S. M., Sasidharan Nair, N. V., and Elkord, E. (2018). Immune checkpoint inhibitors: Recent progress and potential biomarkers. *Exp. Mol. Med.* 50 (12), 1–11. doi:10.1038/s12276-018-0191-1

Deng, X., Su, R., Weng, H., Huang, H., Li, Z., and Chen, J. (2018). RNA N6-methyladenosine modification in cancers: Current status and perspectives. *Cell Res.* 28 (5), 507–517. doi:10.1038/s41422-018-0034-6

Fishel, R. (2015). Mismatch repair. *J. Biol. Chem.* 290 (44), 26395–26403. doi:10.1074/jbc.r115.660142

Han, Z., Dong, Y., Lu, J., Yang, F., Zheng, Y., and Yang, H. (2021). Role of hypoxia in inhibiting dendritic cells by VEGF signaling in tumor microenvironments: Mechanism and application. *Am. J. CANCER Res.* 11 (8), 3777–3793.

He, L., Li, J., Wang, X., Ying, Y., Xie, H., Yan, H., et al. (2018). The dual role of N6-methyladenosine modification of RNAs is involved in human cancers. *J. Cell Mol. Med.* 22 (10), 4630–4639. doi:10.1111/jcmm.13804

Hiam-Galvez, K. J., Allen, B. M., and Spitzer, M. H. (2021). Systemic immunity in cancer. *Nat. Rev. CANCER* 21 (6), 345–359. doi:10.1038/s41568-021-00347-z

Lee, D. W., Han, S. W., Bae, J. M., Jang, H., Han, H., Kim, H., et al. (2019). Tumor mutation burden and prognosis in patients with colorectal cancer treated with adjuvant fluoropyrimidine and oxaliplatin. *Clin. CANCER Res.* 25 (20), 6141–6147. doi:10.1158/1078-0432.ccr-19-1105

Li, J., Meng, S., Xu, M., Wang, S., He, L., Xu, X., et al. (2018). Downregulation of N6-methyladenosine binding YTHDF2 protein mediated by miR-493-3p suppresses prostate cancer by elevating N6-methyladenosine levels. *Oncotarget* 9 (3), 3752–3764. doi:10.18632/oncotarget.23365

Li, T., Fan, J., Wang, B., Traugh, N., Chen, Q., Liu, J. S., et al.TIMER (2017). Timer: A web server for comprehensive analysis of tumor-infiltrating immune cells. *CANCER Res.* 77 (21), e108–e110. doi:10.1158/0008-5472.can-17-0307

Li, Z., Weng, H., Su, R., Weng, X., Zuo, Z., Li, C., et al. (2017). FTO plays an oncogenic role in acute myeloid leukemia as a N 6 -methyladenosine RNA demethylase. *CANCER Cell* 31 (1), 127–141. doi:10.1016/j.ccell.2016.11.017

Lin, S., Choe, J., Du, P., Triboulet, R., and Gregory, R. I. (2016). The m 6 A methyltransferase METTL3 promotes translation in human cancer cells. *Mol. Cell* 62 (3), 335–345. doi:10.1016/j.molcel.2016.03.021

Lyssiotis, C. A., and Kimmelman, A. C. (2017). Metabolic interactions in the tumor microenvironment. *Trends Cell Biol.* 27 (11), 863–875. doi:10.1016/j.tcb.2017.06.003

Man, Y. G., Stojadinovic, A., Mason, J., Avital, I., Bilchik, A., Bruecher, B., et al. (2013). Tumor-infiltrating immune cells promoting tumor invasion and metastasis: Existing theories. *J. Cancer* 4 (1), 84–95. doi:10.7150/jca.5482

Martincorena, I., and Campbell, P. J. (2015). Somatic mutation in cancer and normal cells. *SCIENCE* 349 (6255), 1483–1489. doi:10.1126/science.aab4082

Meyer, K. D., and Jaffrey, S. R. (2017). Rethinking m6A readers, writers, and erasers. *Annu. Rev. Cell Dev. Biol.* 33, 319–342. doi:10.1146/annurev-cellbio-100616-060758

Pagès, F., Berger, A., Camus, M., Sanchez-Cabo, F., Costes, A., Molidor, R., et al. (2005). Effector memory T cells, early metastasis, and survival in colorectal cancer. *N. Engl. J. Med.* 353 (25), 2654–2666. doi:10.1056/nejmoa051424

Ribas, A., and Wolchok, J. D. (2018). Cancer immunotherapy using checkpoint blockade. *SCIENCE* 359 (6382), 1350–1355. doi:10.1126/science.aar4060

Roundtree, I. A., Evans, M. E., Pan, T., and He, C. (2017). Dynamic RNA modifications in gene expression regulation. *Cell* 169 (7), 1187–1200. doi:10.1016/j.cell.2017.05.045

Russo, M., Crisafulli, G., Sogari, A., Reilly, N. M., Arena, S., Lamba, S., et al. (2019). Adaptive mutability of colorectal cancers in response to targeted therapies. *SCIENCE* 366 (6472), 1473–1480. doi:10.1126/science.aav4474

Tang, Z., Li, C., Kang, B., Gao, G., Li, C., and Zhang, Z. (2017). Gepia: A web server for cancer and normal gene expression profiling and interactive analyses. *NUCLEIC ACIDS Res.* 45 (1), W98–W102. doi:10.1093/nar/gkx247

Topalian, S. L., Drake, C. G., and Pardoll, D. M. (2015). Immune checkpoint blockade: A common denominator approach to cancer therapy. *CANCER Cell* 27 (4), 450–461. doi:10.1016/j.ccell.2015.03.001

Wang, X., Lu, Z., Gomez, A., Hon, G. C., Yue, Y., Han, D., et al. (2014). N6-methyladenosine-dependent regulation of messenger RNA stability. *NATURE* 505 (7481), 117–120. doi:10.1038/nature12730

Yarchoan, M., Hopkins, A., and Jaffee, E. M. (2017). Tumor mutational burden and response rate to PD-1 inhibition. *N. Engl. J. Med.* 377 (25), 2500–2501. doi:10.1056/nejmc1713444

Zacharakis, N., Chinnasamy, H., Black, M., Xu, H., Lu, Y. C., Zheng, Z., et al. (2018). Immune recognition of somatic mutations leading to complete durable regression in metastatic breast cancer. *Nat. Med.* 24 (6), 724–730. doi:10.1038/s41591-018-0040-8

Zhang, C., Fu, J., and Zhou, Y. (2019). A review in research progress concerning m6A methylation and immunoregulation. *Front. Immunol.* 10, 922. doi:10.3389/fimmu.2019.00922

Zhang, C., Samanta, D., Lu, H., Bullen, J. W., Zhang, H., Chen, I., et al. (2016). Hypoxia induces the breast cancer stem cell phenotype by HIF-dependent and ALKBH5-mediated m^{6}A-demethylation of NANOG mRNA. *Proc. Natl. Acad. Sci. U. S. A.* 113 (14), E2047–E2056. doi:10.1073/pnas.1602883113

Zhang, S., Zhao, B. S., Zhou, A., Lin, K., Zheng, S., Lu, Z., et al. (2017). m 6 A demethylase ALKBH5 maintains tumorigenicity of glioblastoma stem-like cells by sustaining FOXM1 expression and cell proliferation ProgramA demethylase ALKBH5 maintains tumorigenicity of glioblastoma stem-like cells by sustaining FOXM1 expression and cell proliferation program. *CANCER Cell* 31 (4), 591–606. doi:10.1016/j.ccell.2017.02.013

Zhao, B. S., Roundtree, I. A., and He, C. (2017). Post-transcriptional gene regulation by mRNA modifications. *Nat. Rev. Mol. Cell Biol.* 18 (1), 31–42. doi:10.1038/nrm.2016.132

Zhao, B. S., Wang, X., Beadell, A. V., Lu, Z., Shi, H., Kuuspalu, A., et al. (2017). m6A-dependent maternal mRNA clearance facilitates zebrafish maternal-to-zygotic transitionA-dependent maternal mRNA clearance facilitates zebrafish maternal-to-zygotic transition. *NATURE* 542 (7642), 475–478. doi:10.1038/nature21355

Zhong, L., Liao, D., Zhang, M., Zeng, C., Li, X., Zhang, R., et al. (2019). YTHDF2 suppresses cell proliferation and growth via destabilizing the EGFR mRNA in hepatocellular carcinoma. *Cancer Lett.* 442, 252–261. doi:10.1016/j.canlet.2018.11.006

Glossary

ACC Adrenocortical carcinoma

BLCA Bladder urothelial carcinomaBladder urothelial carcinoma

BLCA Bladder urothelial carcinomaBladder urothelial carcinoma

BRCA Breast invasive carcinoma

CECS Cervical squamous cell carcinoma and endocervical adenocarcinoma

CHOL Cholangial carcinoma

COAD Colon adenocarcinoma

DLBC Lymphoid Neoplasm Diffuse Large B-cell Lymphoma

DSS Disease-specific survival

ESCA Esophageal carcinoma

GBM Glioblastoma multiforme

GEO Gene Expression Omnibus

GEPIA Gene Expression Profiling Interactive Analysis

GSEA Gene Set Enrichment Analysis

GTEx The Genotype-Tissue Expression

HNSC Head and neck squamous cell carcinoma

ICP Immune Checkpoint

IHC Immunohistochemistry

KICH Kidney chromophobe

KIRC Kidney renal clear cell carcinoma

KIRP Kidney renal papillary cell carcinoma

LAML Acute Myeloid Leukemia

LGG Lower Grade Glioma

LIHC Liver hepatocellular carcinoma

LUAD Lung adenocarcinoma

LUSC Lung squamous cell carcinoma

m6A N6-methyladenosine

MESO Mesothelioma

MMR Mismatch Repair

MSI Myeloid-derived suppressor cells suppressor cells

OS Overall survival

OSCC Oral squamous cell carcinoma

OV Mesothelioma, Ovarian Serous Cystadenocarcinoma

PAAD Pancreatic adenocarcinoma

PCPG Pheochromocytoma and Paraganglioma

PFI Progress Free Interval

PRAD Prostate adenocarcinoma

READ Rectum adenocarcinoma

STAD Stomach adenocarcinoma

TCGA The Cancer Genome Atlas

THCA Thyroid carcinoma

THYM Thymoma

TIMER Tumor Immune Estimation Resource

TMB Tumor mutation burden

TME Tumor Microenvironment

UCEC Uterine corpus endometrial carcinomaUterine corpus endometrial carcinoma

UCEC Uterine corpus endometrial carcinomaUterine corpus endometrial carcinoma

UCS Uterine Carcinosarcoma

UVM Uveal Melanoma

YTHDF2 YT521-B homology domain family 2

frontiers | Frontiers in Cell and Developmental Biology

TYPE Original Research
PUBLISHED 02 September 2022
DOI 10.3389/fcell.2022.954769

OPEN ACCESS

EDITED BY
Liang Zhou,
Southern Medical University, China

REVIEWED BY
Juan Jin,
Anhui Medical University, China
Fang Fang,
Peking Union Medical College Hospital (CAMS), China

*CORRESPONDENCE
Jianxin Wu,
cipbiolab@163.com

†These authors share first authorship

SPECIALTY SECTION
This article was submitted to Signaling, a section of the journal Frontiers in Cell and Developmental Biology

RECEIVED 27 May 2022
ACCEPTED 08 August 2022
PUBLISHED 02 September 2022

CITATION
Liu K, Ju W, Ouyang S, Liu Z, He F, hao J, Guan H and Wu J (2022), Exercise training ameliorates myocardial phenotypes in heart failure with preserved ejection fraction by changing N6-methyladenosine modification in mice model.
Front. Cell Dev. Biol. 10:954769.
doi: 10.3389/fcell.2022.954769

Exercise training ameliorates myocardial phenotypes in heart failure with preserved ejection fraction by changing N6-methyladenosine modification in mice model

Kai Liu[1,2,3†], Wenhao Ju[2,3,4†], Shengrong Ouyang[2,3], Zhuo Liu[2,3], Feng He[2,3], Jingyi hao[5], Hongyan Guan[2,3] and Jianxin Wu[1,2,3,4,5*]

[1]Department of Biochemistry and Immunology, Capital Institute of Pediatrics-Peking University Teaching Hospital, Beijing, China, [2]Department of Biochemistry and Immunology, Capital Institute of Pediatrics, Beijing, China, [3]Beijing Municipal Key Laboratory of Child Development and Nutriomics, Beijing, China, [4]Graduate School of Peking Union Medical College, Beijing, China, [5]Beijing TongRen Hospital, Capital Medical University, Beijing, China

Heart failure with preserved ejection fraction (HFpEF) shows complicated and not clearly defined etiology and pathogenesis. Although no pharmacotherapeutics have improved the survival rate in HFpEF, exercise training has become an efficient intervention to improve functional outcomes. Here, we investigated N6-methyladenosine (m^6A) RNA methylation modification in a "two-hit" mouse model with HFpEF and HFpEF with exercise (HFpEF + EXT). The manner of m^6A in HFpEF and HFpEF + EXT hearts was explored *via* m^6A-specific methylated RNA immunoprecipitation followed by high-throughput and RNA sequencing methods. A total amount of 3992 novel m^6A peaks were spotted in HFpEF + EXT, and 426 differently methylated sites, including 371 hypermethylated and 55 hypomethylated m^6A sites, were singled out for further analysis (fold change >2, $p < 0.05$). According to gene ontology (GO) and Kyoto Encyclopedia of Genes and Genomes (KEGG) pathway analyses, unique m^6A-modified transcripts in HFpEF + EXT were associated with apoptosis-related pathway and myocardial energy metabolism. HFpEF + EXT had higher total m^6A levels and downregulated fat mass and obesity-related (FTO) protein levels. Overexpression of FTO cancels out the benefits of exercise in HFpEF + EXT mice by promoting myocyte apoptosis, myocardial fibrosis and myocyte hypertrophy. Totally, m^6A is a significant alternation of epitranscriptomic processes, which is also a potentially meaningful therapeutic target.

KEYWORDS

HFPEF, m^6A, apoptosis, FTO, myocardial energy metabolism

Introduction

Heart failure (HF) with preserved ejection fraction (HFpEF) is a complicated clinical syndrome associated with poor quality of life, extensive utilization of medical resources and premature death (Dunlay et al., 2017; Mishra and Kass, 2021; Omote et al., 2022). HFpEF affects 50% of patients with HF worldwide and has been increasing in prevalence largely connected with the aging of the population (Mishra and Kass, 2021; Omote et al., 2022). HFpEF is an aging disease characterized by cardiac hypertrophy, myocardial interstitial fibers, and cardiac diastolic dysfunction (Prandi et al., 2022). Considering the complex pathogenesis of HFpEF, it is the most significant unmet medical need in cardiovascular disease (Mishra and Kass, 2021). Previous studies have suggested that HFpEF is a hemodynamic disorder characterized by hypertension, myocardial hypertrophy, myocardial fibrosis and diastolic dysfunction. However, current studies believe that HFpEF is a syndrome with abnormal function of multiple organs, including diseases caused by the comprehensive effects on the heart, lung, kidney, immunity, inflammation, metabolism and others (Figtree et al., 2021; Mishra and Kass, 2021; Omote et al., 2022; Prandi et al., 2022). Cardiac molecular and cellular mechanisms with HFpEF include cardiac hypertrophy, myocardial fibrosis, inflammation, cardiomyocyte sarcomere disfunction and mitochondrial and metabolic defects (Schiattarella et al., 2021a). However, the etiology and pathogenesis of HFpEF are unclear. At present, the effective treatment of HFpEF is very limited and cannot prevent the development of the disease. Urgent problems and effective solutions are needed.

Recent studies have shown that exercise training (EXT) is an important means of nonpharmacological intervention and prevention of cardiovascular diseases. EXT can improve exercise ability and quality of life, and is related to reducing the risk of hospitalization and cardiovascular death (Leggio et al., 2020; Jaconiano and Moreira-Gonçalves, 2022). However, its positive influence basically lacks a physiological explanation in HFpEF. In patients with heart failure with reduced ejection fraction (HFrEF), physical exercise is already a class I level A recommendation (Ho et al., 2019). Concerning HFpEF, systematic reviews and meta-analysis offer a high level of evidence that EXT is a safe and effective strategy improving upon peak VO_2, 6 min walk, cardiorespiratory fitness, diastolic function, quality of life, and general health (Ismail et al., 2013; Dieberg et al., 2015; Fukuta et al., 2019). Another research supported that EXT significantly improves the exercise capacity and left ventricular diastolic function, indicating an improvement in ventricular stiffness and filling pressures (Edelmann et al., 2011; Fukuta et al., 2019). Nevertheless, this evidence is not consensual. Therefore, we use a new "two-hit" mouse model of HFpEF (Schiattarella et al., 2019; Schiattarella et al., 2021b), which simulates concomitant metabolic and hypertensive stress in mice to explore the effect mechanism of EXT on HFpEF.

Epigenetic regulation includes DNA methylation, histone modifications, and noncoding RNAs. Their important role in HFpEF has been widely researched, and the effect of RNA alternation on the control of gene expression in HFpEF will be clarified (Handy et al., 2011; Feil and Fraga, 2012; Poller et al., 2018; Zhang et al., 2021a; Hamdani et al., 2021). N6-methyladenosine (m^6A) methylation is the most common internal mRNA alternation, which affects the metabolism of RNA throughout its life cycle (Wang et al., 2014a; Wang et al., 2014b; Alarcón et al., 2015). The latest evidence shows that m^6A modification not only participates in normal biological processes, but also serves vital functions in the occurrence and progression of different heart diseases (Dorn et al., 2019; Mathiyalagan et al., 2019; Mo et al., 2019; Berulava et al., 2020; Gao et al., 2020; Krüger et al., 2020; Lin et al., 2020). But the reversal of myocardial dysfunction in HFpEF by EXT through m^6A modification has not been studied.

The modification of m^6A is related to different types of cardiovascular diseases, including cardiac fibrosis, cardiac hypertrophy, myocardial infarction, atherosclerosis, abdominal aortic aneurysm, heart failure and HFpEF (Dorn et al., 2019; Mathiyalagan et al., 2019; Berulava et al., 2020; Gao et al., 2020; Lin et al., 2020). Nevertheless, the transcriptome-wide distribution of m^6A in HFpEF + EXT heart samples remains largely unknown. This research tried to clarify the m^6A methylation profiles of heart tissue samples from HFpEF + EXT and control (HFpEF) mice and give evidence of highly diverse m^6A-modified patterns in both groups. It is displayed that abnormal m^6A RNA alternations in HFpEF + EXT samples are possible for modulating myocardial apoptosis and myocardial energy metabolism, close to the cardiac aging phenotype. Our outcomes offer evidence that exercise-induced m^6A alternation is closely related to the pathogenesis of HFpEF in the new model and will promote further research on the potential drug targets of m^6A alternation in the treatment of HFpEF.

Materials and methods

Animals

The contents of this study had been reviewed and approved by the ethics committee of Capital Institute of Pediatrics, whose approved license number was DWLL2019003. This study's routines were all in accordance with corresponding ethical standards. C57BL/6J male mice were adopted for wild-type studies. All mice used in the trials were 8 weeks old (Schiattarella et al., 2019) and kept in cages at 24°C with a 12 h alternating light/dark cycle. The HFpEF model was constructed using mice with unrestricted access to HFD (High Fat Diet) food (D12492, Research Diet) and water for 16 weeks. N^{ω}-nitro-l-arginine methyl ester (l-NAME) (0.5 g/L, Sigma-Aldrich) was added in the water, and the pH of the mixture

was adjusted to 7.4. Mice in the control group were fed unlimited normal food and water. At the eighth week, mice began to do moderate-intensity running on a treadmill at a 10° gradient for 8 weeks (5 times a week, running for 5 days and rest for 2 days, with 5 min of running and 2 min of rest for 10 cycles, a total of 50 min of running and speed with 10 m/min). After the mice were euthanized, we collected hearts with 1.5 ml RNase-free centrifuge tubes, and stored them immediately at 4°C for 12 h. Samples were finally placed at −80°C for long-term storage to prevent RNA degradation.

Echocardiographic assessment

At 28 weeks of age, cardiac function by echocardiography in all mice in a scrambled order was assessed with a VEVO 3100 instrument, by dedicated personnel. Anesthesia mice were induced by continuous inhalation using 2% isoflurane +2 L/min air flow rate. The probe was placed in the center of the heart to observe the short axis of the heart. Observe the long axis of the heart during the slitting and adjust the heart rate to maintain 415–460 beats/min. Coefficients gathered included: left ventricular end-diastolic diameter, left ventricular end-systolic diameter, heart rate, left ventricular shortening, LVEF, peak doppler flow velocity in early mitral valve diastolic, peak doppler flow velocity across late mitral valve diastolic. All measurements were averages of at least three beats.

Western blotting and antibodies

Our western blotting assays were performed strictly following the standard protocols of our laboratory. Firstly, mouse heart tissues were ground using the tissue crusher with the tissue lysate, and lysates were prepared with RIPA lysis buffer from Beyotime Biotechnology, where protease inhibitor were added. Blots were screened using specific antibodies: GAPDH (5174, 1:10000; CST), Mettl3 (ab195352, 1:1000; Abcam), FTO (ab92821, 1:1000; Abcam), ALKBH5 (ab69325, 1:1000; Abcam), Mettl14 (HPA038002, 1:1000; Sigma), and m^{6}A (ab208577, 1: 500; Abcam).

Histological analysis

Mouse hearts were fixed with freshly made 4% paraformaldehyde overnight, dehydrated by a dehydrator, embedded in paraffin, sliced by a paraffin slicer, 7 μm for each section, and stained with hematoxylin and eosin. Furthermore, we previously sectioned frozen heart tissue samples from mice at 7 μm slices, followed by incubation with wheat germ agglutinin (1:100) for 1 h in the dark, and finally washed three times with PBS. Cell nuclei were stained with DAPI (1:1000, 10 min) and washed thrice with PBS. Firstly, we dropped a water-soluble antifade mounting medium on the samples, then we covered the samples with glass cover slips, and finally we investigated the samples with a confocal microscope (Leica Sp8). Using the Image-Pro Plus 6.0 software to calculate the cross-sectional areas of cardiomyocytes. To detect fibrosis in the murine cardiac, we stained heart sections with the usual Masson's trichrome procedure.

Overexpression of fat mass and obesity-related

Empty adeno-associated virus (AAV-EV) and adeno-associated virus expressing FTO (AAV-FTO) were manufactured by Hanbio Biotechnology Ltd. (Shanghai, China). The viruses were under the control of a heart-specific *cTNT* promoter with an EGFP tag. The virus titer we used to do the experiment was approximately 1×10^{12} V g/ml. At 8 weeks, we injected 120 μL of AAV-EV and AAV-FTO viruses *via* tail vein for each mouse.

m^{6}A dot blot assay

We extracted total RNA from experimental mouse hearts with Trizol (Invitrogen). Total RNA was diluted to 1000 ng/μL and denaturated for 3 min at 95°C to break the RNA secondary structure into single strands. Immediately placed on ice to prevent the re-formation of RNA secondary structures. 2 μL RNA was directly dropped onto the Hybond-N+ membrane (GE Healthcare) and incubated at 80°C using an 80°C hybridizer for 1 h. Uncrosslinked RNA was washed with PBS with 0.01% Tween-20 for 5 min. We incubated membranes with anti-m^{6}A antibody (1: 500 in PBS with 0.01% Tween-20) at 4°C for 12 h after blocking with 5% skim milk (in PBS with 0.01% Tween-20) for 1 h. We used horseradish peroxidase-conjugated anti-rabbit IgG secondary antibody to treat membranes for 1 h at room temperature, and rinsed 4 times for 10 min each with PBS followed by chemiluminescence development. To ensure that repeated dots contained the same amount of total RNA, methylene blue staining was utilized.

MeRIP-seq

After three mice in HFpEF and HFpEF + EXT groups were euthanized, the total RNA samples were extracted from heart tissue specimens and quantitatively analyzed applying the NanoDrop ND-1000 (Thermo Fisher Scientific, MA, United States). Next, 20 μg total RNA was collected for interruption and purification to obtain the product after fragmentation treatment, and the Zymo RNA Clean and

Concentrator-5 kit was used for the purification and recovery of the fragmented RNA. The resulting product was added with anti-m^{6}A antibody (Sigma-Aldrich: ABE572), protein A-magnetic beads (Invitrogen: 10002D), protein G-magnetic beads (Invitrogen: 10004D); mixed; and incubated overnight. The mixture was subjected to magnetic separation. The supernatant was collected and added with 5× precipitation buffer and RNA enzyme inhibitor, and the mixture was reacted at 4°C for 1–3 h, washed 2–3 times with low-salt precipitation buffer, and washed 2–3 times with high-salt buffer. The RNA was extracted from chloroform lysate to obtain the purified product. Ribosomal RNA removed the obtained products, and the SMART principle synthesized the first-strand cDNA. We amplified enriched library fragments by PCR and purified the library fragments by magnetic beads with DNA to obtain an RNA methylation m^{6}A detection library. Finally, we employed the bioptic qsep100 analyzer to quality check the libraries. The NovaSeq high-throughput sequencing platform and PE150 sequencing mode were adopted for sequencing.

Adapters and filters were trimed with the Cutadapt (v2.5) for sequences, and the Hisat2 aligner (v2.1.0) was adopted to align remaining reads to the human Ensemble genome GRCh38 (mouse Ensemble genome GRCm38). The exomePeak R package was adopted to identify differential m^{6}A peaks. We used the clusterProfiler R package (v3.6.0) for GO and KEGG analyses. And we used the Guitar R package (v1.16.0) to visualize m^{6}A-RNA-related genomic features. We subjected m^{6}A peaks with p value <0.05 for the *de novo* motif analysis with homer (v4.10.4).

RNA-seq

Total RNA samples were taken from heart tissue specimens after three mice in the HFpEF and HFpEF + EXT groups were euthanized. Trimming adapters and filtering for sequences was done with Cutadapt (v2.5), and the Hisat2 aligner (v2.1.0) was adopted to align the remaining reads to the human Ensemble genome GRCh38 (mouse Ensemble genome GRCm38). The feature Counts were used to determine the reads that mapped the genome (v1.6.3). Differential gene expression analysis was made with the DESeq2 R-package.

Single-base elongation and ligation-based qPCR amplification method validation

The Single-base elongation and ligation-based qPCR amplification method (SELECT) assay was used to monitor site-specific m^{6}A levels, as previously described (Xiao et al., 2018). Briefly, total RNA (2 μg) was combined with 1 μL of dNTP, 2 μL of 10 × CutSmart buffer, and 2 μL of every 400 nmol/L up and down primer (Table.1). RNA free water to the final volume 17 μL. The combination of RNA and primers was annealed at the following temperatures: 90°C for 1 min, 80°C for 1 min, 70°C for 1 min, 60°C for 1 min, 50°C for 1 min, and 40°C for 6 min. Then add 3 μL solution with 0.01 U DNA polymerase, 0.5 U SplintR ligase and 10 nmol ATP. After incubation at 40°C for 20 min and 80°C for 20 min, template abundance was quantified by taking 2 μL of reaction solution for real-time qPCR analysis.

Real-time PCR (RT-PCR)

We picked 10 genes with differentially methylated sites based on MeRIP-seq, and tested these genes with Real-time PCR using SYBR-green and standard amplification protocols. The ΔΔCt technique was used to calculate expression levels. Table 2 shows the primer sequences.

Exercise exhaustion test

After 3 days of treadmill adaptation, experimental mice were tested for fatigue. Mice ran upward (20°) on a treadmill at a warm-up rate of 5 m/min for 4 min, which was grown to 14 m/min for 2 min. Subsequently, the speed was grown by 2 m/min every 2 min until the mice were exhausted. Exhaustion was defined as the inability of the mouse to resume running within 10 s of direct contact with the electrical stimulus net. While measuring the running time, the running distance was calculated.

Transferase-mediated dUTP nick-end labeling

TUNEL experiments were made with the *In Situ* Cell Death Detection Kit (Cat. No.11684795910, Roche). The tissue section was fixed with fixation solution (4% paraformaldehyde in PBS, pH 7.4, freshly prepared) for 20 min at +15°C to +25°C and washed for 30 min with PBS. The 2-minute incubation of slides was made in permeabilization solution (0.1% Triton X-100, 0.1% sodium citrate, freshly prepared) on ice. Next, slides were added with 50 μL TUNEL reaction mixture and incubated in a humidified atmosphere for 60 min at +37°C in the dark. Finally, samples were directly analyzed under a confocal microscope.

Transmission electron microscopy

Mouse hearts were fixed in 2.5% cacodylate buffer with glutaraldehyde, embedded with 2% agarose, fixed in 1%

TABLE 1 The gene-specific SELECT-PCR primers used were as follows.

Gene	Forward and reverse primer
Fas_	tagccagtaccgtagtgcgtgACAGCCCAGATCCACAGCATG
	5phos/CTGCAGCAAGGGAAAACAGCcagaggctgagtcgctgcat
Capn2	tagccagtaccgtagtgcgtgCCCCTCGGCCGCTTCGCGG
	5phos/CCTTGGCCAGCTTTATCGCGATGCcagaggctgagtcgctgcat
Casp12	tagccagtaccgtagtgcgtgGTCATCAAAAACCCCATCCAGCATG
	5phos/CCTTGGCCAAACCTTTGATCTcagaggctgagtcgctgcat
Mef2a	tagccagtaccgtagtgcgtgGCTGCTGGAGCTGCTCAGACTG
	5phos/CCACAGGGGAGCGCCCCcagaggctgagtcgctgcat
Casp7	tagccagtaccgtagtgcgtgGAGCCTGGCTCCAATCACCATAG
	5phos/CCATGGTTCTAGTCTCTAGAAGGCTGCcagaggctgagtcgctgcat
Jun	tagccagtaccgtagtgcgtgCCCGGCCACTTGTTACCGG
	5phos/CCTCTGGGTCAGGAAAGTTGCTGcagaggctgagtcgctgcat
Pdia3	tagccagtaccgtagtgcgtgTGGTTTTGCCTTCTCTGGTGTAAGAG
	5phos/CCTTTTATAAAGTGGTGCATTTGGCTcagaggctgagtcgctgcat
Tnnt2	tagccagtaccgtagtgcgtgGACTGCACACAGGTCTTGAGGTATCTG
	5phos/TCAGCCTCAGCAGGGACTGGCcagaggctgagtcgctgcat
Adrb1	tagccagtaccgtagtgcgtgCGTCCAGGCTCGAATCGCTG
	5phos/CCACAGTGGTTGTCCCGCCTcagaggctgagtcgctgcat
Agtr1a	tagccagtaccgtagtgcgtgGTCCTTTGGTCGTGAGCCATTTAG
	5phos/CCGATGCTGCCCTGGTTTCTcagaggctgagtcgctgcat

TABLE 2 The gene-specific PCR primers used were as follows.

Gene	Forward and reverse primer
Fas	F: 5′-AACATGGAACCCTTGAGCCA-3′
	R:5′ AGGCGATTTCTGGGACTTTGT 3′
Caspase-12	F:5′ -TGCGAGTTTCATCCTGAACAAGGCTG 3′
	R:5′ -AACACCAGGAATGTGCTGTCTGAGGACT 3′
Mef2a	F:5′ GGTGGTGGCAGTCTTG 3′
	R:5′ TATCCTTTGGGCATTCA 3′
Jun	F:5′ CGCACGCTCCTAAACAAACT 3′
	R:5′ GTCATAGAACGGTCCGTCACTT 3′
Tnnt2	F:5′ GCCCACATGCCTGCTT 3′
	R:5′ CACCTCCTCGGCGTCA 3′
Agtr1a	F:5′ CTGAGGTGGAGTGACAGGTT 3′
	R:5′ TTTGGTCGTGAGCCATTTA 3′

osmium tetroxide buffer, stained in 2% uranyl acetate, dehydrated with ethanol, embedded in resin, sliced by an ultrafine slicing machine, and stained with 2% uranyl acetate and lead citrate. Images for experimental use were obtained on the FEI Tecnai G2 Spirit electron microscope equipped with LaB6.

Statistical analysis

All data for all experiments are from three or more independent experimental manipulations and are shown as mean ± SEM. The GraphPad Prism 6.0 program was used to conduct the statistical analysis. Differences with two groups were used two tailed unpaired Student's t-test analysis and three or more groups were analyzed with a one- or two-way analysis of variance. Differences with a significance level of $p < 0.05$ were of statistical significance.

Results

Exercise reverses heart failure with preserved ejection fraction phenotypes by suppressing myocardial fibrosis and improving cardiac dysfunction with the changes in global m^{6}A levels

In our study, HFpEF + EXT mice evidently ameliorated myocardial fibrosis and myocardial hypertrophy compared with the control (Figures 1A,B) and had evidently decreased heart weight to tibia length proportions (HW/TL, $n = 6$, $p = 0.0005$; Figure 1B). Furthermore, EXT clearly ameliorated

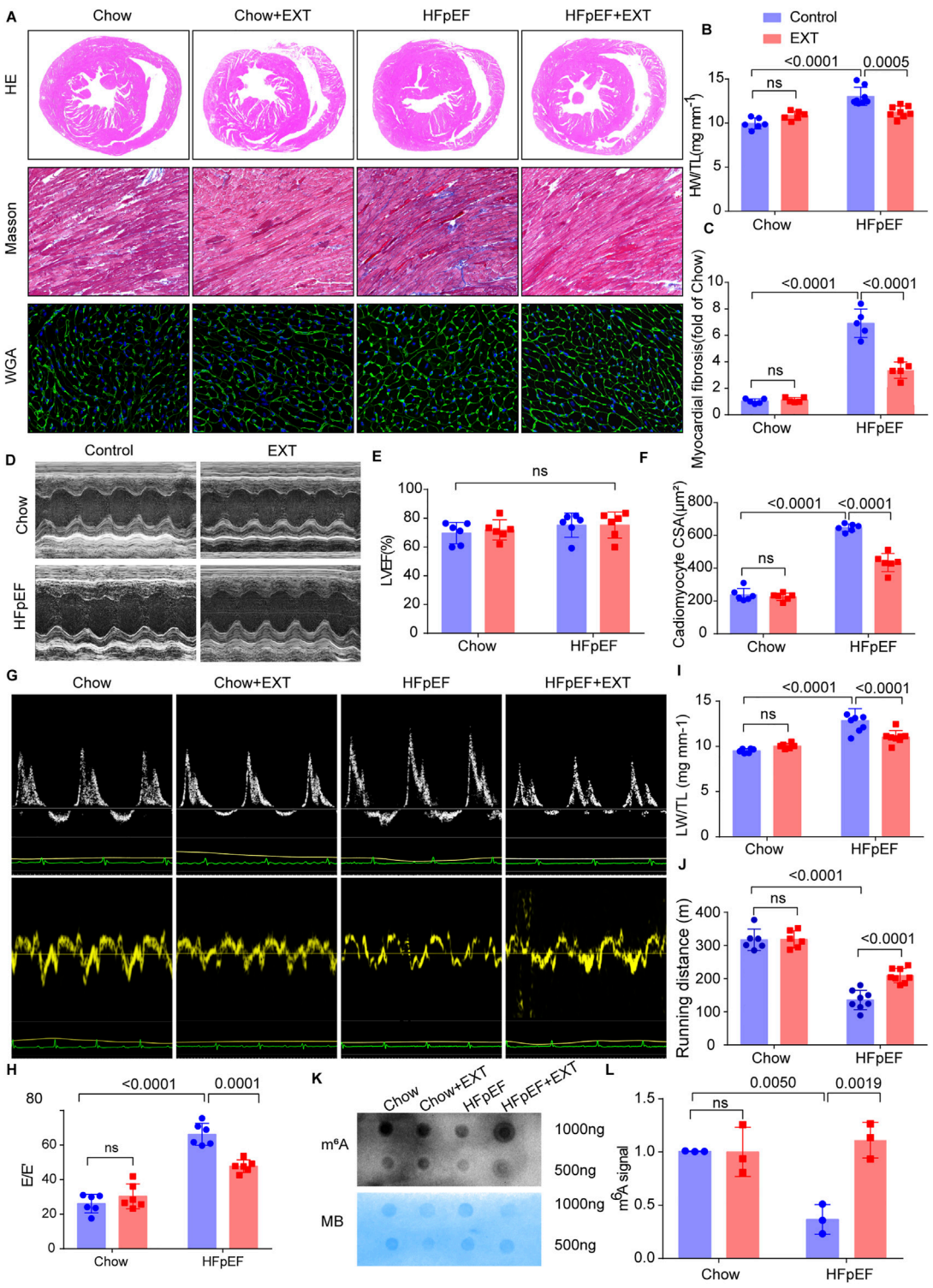

FIGURE 1
Exercise training reverses HFpEF phenotypes by suppressing myocardial fibrosis and improving cardiac dysfunction with the changes in global m^{6}A levels. **(A)** Gross morphology of hearts stained with HE, cardiac fibrosis stained with Masson, and cardiomyocyte area stained with wheat germ agglutinin (WGA). Scale bar = 1 mm with HE, 100 μm with Masson, and 50 μm with WGA. **(B)** Proportion of heart weight to tibia length (n = 6 mice per group). **(C)** Quantitative analysis of cardiac fibrosis (n = 6 mice per group). **(D)** Representative M-mode echocardiography images. **(E)** Left ventricular ejection fraction (LVEF) (n = 6 mice per group). **(F)** Quantitative analysis of cardiomyocyte area (n = 6 mice per group). **(G,H)** Representative Doppler echocardiography images and E/E′ ratio (n = 6 mice per group). **(I)** Ratio of lung weight to tibia length (n = 6 mice per group).
(*Continued*)

FIGURE 1
(J) Running distance during exercise exhaustion test (n = 6 mice per group). **(K,L)** Representative dot blot showing global m^{6}A modification levels in hearts and methylene blue (MB) staining and quantification of global m^{6}A modification levels (n = 3 mice per group). Data are mean ± SEM, with all individual data points plotted. Two-way ANOVA and Tukey's multiple comparison test were used. Numbers above square brackets show significant p values.

myocardial interstitial fibrosis (n = 6, p < 0.0001; Figures 1A,C) and markedly reduced the cardiomyocyte cross-sectional region (n = 6, p < 0.0001; Figures 1A,F). In order to prove the improvement of cardiac function in mice, we performed serial echocardiography in HFpEF + EXT mice. Longitudinal echocardiographic evaluation revealed the persistent preservation of LVEF in all groups (n = 6, ns; Figures 1D,E), coupled with significant alterations in degrees of diastolic dysfunction and left ventricular filling pressure in mice exposed to the EXT (n = 6, p < 0.0001; Figures 1G,H). Consistent with the increase of filling pressures reported in the literature, mice exposed to EXT specifically exhibited a significant decrease in lung weight to tibia length ratios (LW/TL, n = 6, p < 0.0001; Figure 1I), indicating improvement in pulmonary function. Furthermore, the running distance was further in HFpEF + EXT mice compared with HFpEF mice (n = 6, p < 0.0001; Figure 1J). Overall, these data demonstrated that EXT reversed HFpEF phenotypes by suppressing myocardial fibrosis and improving cardiac dysfunction.

The global m^{6}A level is an important feature of m^{6}A modification. Therefore, the global m^{6}A levels of mouse hearts in different groups were detected. Dot blot examination of cardiac samples from separate groups revealed that HFpEF + EXT mice had higher total m^{6}A levels than HFpEF mice. (Figures 1K,L, p = 0.0019). Next, we performed transcriptome-wide MeRIP-seq and mRNA-Seq to analyze the effect of EXT on the m^{6}A methylation of HFpEF.

Exercise training demonstrates differential m^{6}A modification patterns in heart failure with preserved ejection fraction mouse hearts

HFpEF + EXT mouse hearts had specific m^{6}A alternation patterns which were different from those of HFpEF mouse heart samples. We found 26401 m^{6}A peaks, corresponding to 13832 gene transcripts in the HFpEF + EXT group by the model-based analysis through exomePeak v2.13.2 (Figures 2A,B). In the HFpEF group, 27085 m^{6}A peaks, representing 14122 gene transcripts (Figures 2A,B), were confirmed. Compared with the HFpEF group, HFpEF + EXT hearts had 3992 novel peaks, and 4676 peaks were absent. This result indicated that the global m^{6}A alternation types in the HFpEF + EXT group were different from those in the HFpEF group (Figure 2B). We identified a map of m^{6}A methylation using the MEME-ChIP software and confirmed the top consensus motif in m^{6}A peaks as GGACU (Figure 2C). The GGACU was parallel to the previously confirmed RRACH motif (where R = G or A; A = m^{6}A, and H = U, A, or C) (Dominissini et al., 2012; Meyer et al., 2012).

We found that m^{6}A peak in the HEpEF + EXT group was mainly increased in the 5′ untranslated region (5′ UTR) and decreased in the 3′ untranslated region (3′ UTR) compared with the HFpEF group. (Figure 2D). According to their precise positions in RNA transcripts, we categorized the total and unique m^{6}A peaks in HFpEF + EXT and HFpEF whole-transcriptome data into 5′ UTR, transcription start site region, coding sequence (CDS), stop codon, and 3′ UTR. Our results showed that the enrichment of m^{6}A peak was mainly concentrated in the region near CDS, 3′ UTR, and stop codon vicinity regions (Figure 2E), which was similar to previous m^{6}A-seq results (Dominissini et al., 2012). HFpEF + EXT-specific m^{6}A peak distributional patterns showed a different style from HFpEF-specific peaks, and which was with a relative increase in CDS, TSS and Start codon regions (33.3% vs. 33.6%, 3.3% vs 2.9%; 7.7% vs. 6.4%; Figure 2E) and a relative decrease in Stop codon and 3′ UTR, (20.4% vs. 21.4%, 32.4% vs. 33.5%; Figure 2E).

Kyoto encyclopedia of genes and genomes pathways enriched for differential m^{6}A methylation transcripts in heart failure with preserved ejection fraction + Exercise training group are mainly concentrated in apoptosis, RNA degradation, and MAPK signaling pathways

Differential methylation transcripts were identified and analyzed using GO and KEGG pathway analyses. By comparing the abundance of m^{6}A peaks between HFpEF + EXT and HFpEF samples, we found that there were 22409 m^{6}A peaks in both samples. We detected a total of 426 differentially methylated sites and took them as the research target for further research. Among these differentially methylated sites, 371 hypermethylated and 55 hypomethylated m^{6}A sites were observed in the HFpEF + EXT group compared with HFpEF (fold change [FC] > 2, p < 0.05; Figure 2F). When we analyzed the differentially methylated places in both groups using the Integrative Genomics Viewer software, we found

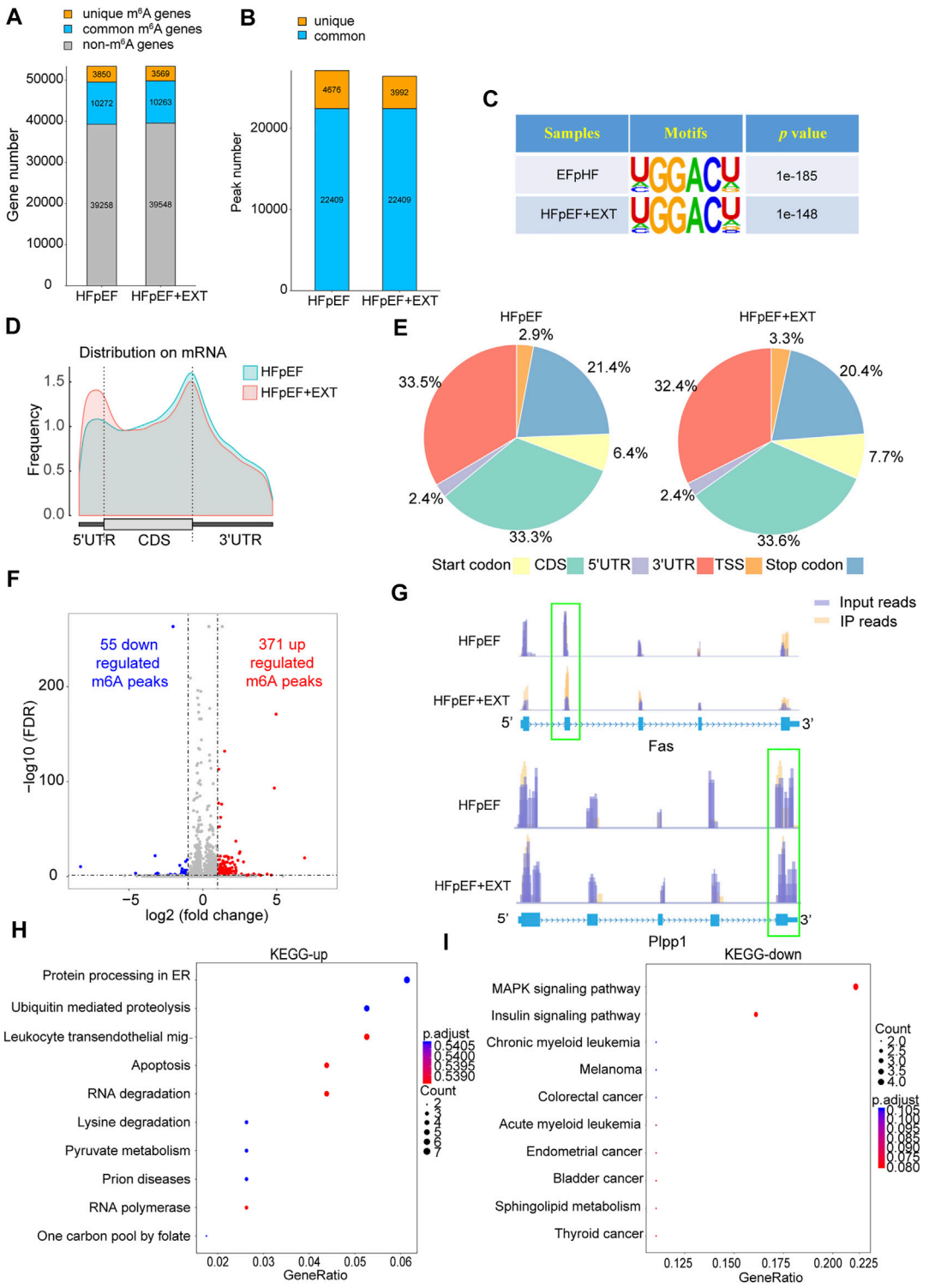

FIGURE 2
Exercise training demonstrates differential m^{6}A modification patterns in HFpEF mouse hearts. **(A,B)** Summary of genes with identified m6A modification present at m^{6}A-seq. **(C)** Sequence logo standing for the consensus motif identified by Discriminative Regular Expression Motif Elicitation in the two groups.**(D)** Distribution of N6-methyladenosine peaks across the length of mRNAs in two groups.**(E)** Venn diagram showing distribution of m^{6}A peaks in the indicated regions in HFpEF and HFpEF + EXT groups.**(F)** Identification of 371 hypermethylated and 55 hypomethylated m^{6}A peaks.**(G)** N6-methyladenosine abundance in Fas and Plpp1 mRNA transcripts in HFpEF and HFpEF + EXT samples **(H,I)** The top 10 enriched pathways terms from MeRIR-seq for upregulated and downregulated m^{6}A peaks. Leukocyte transendothelial mig-: Leukocyte transendothelial migration.

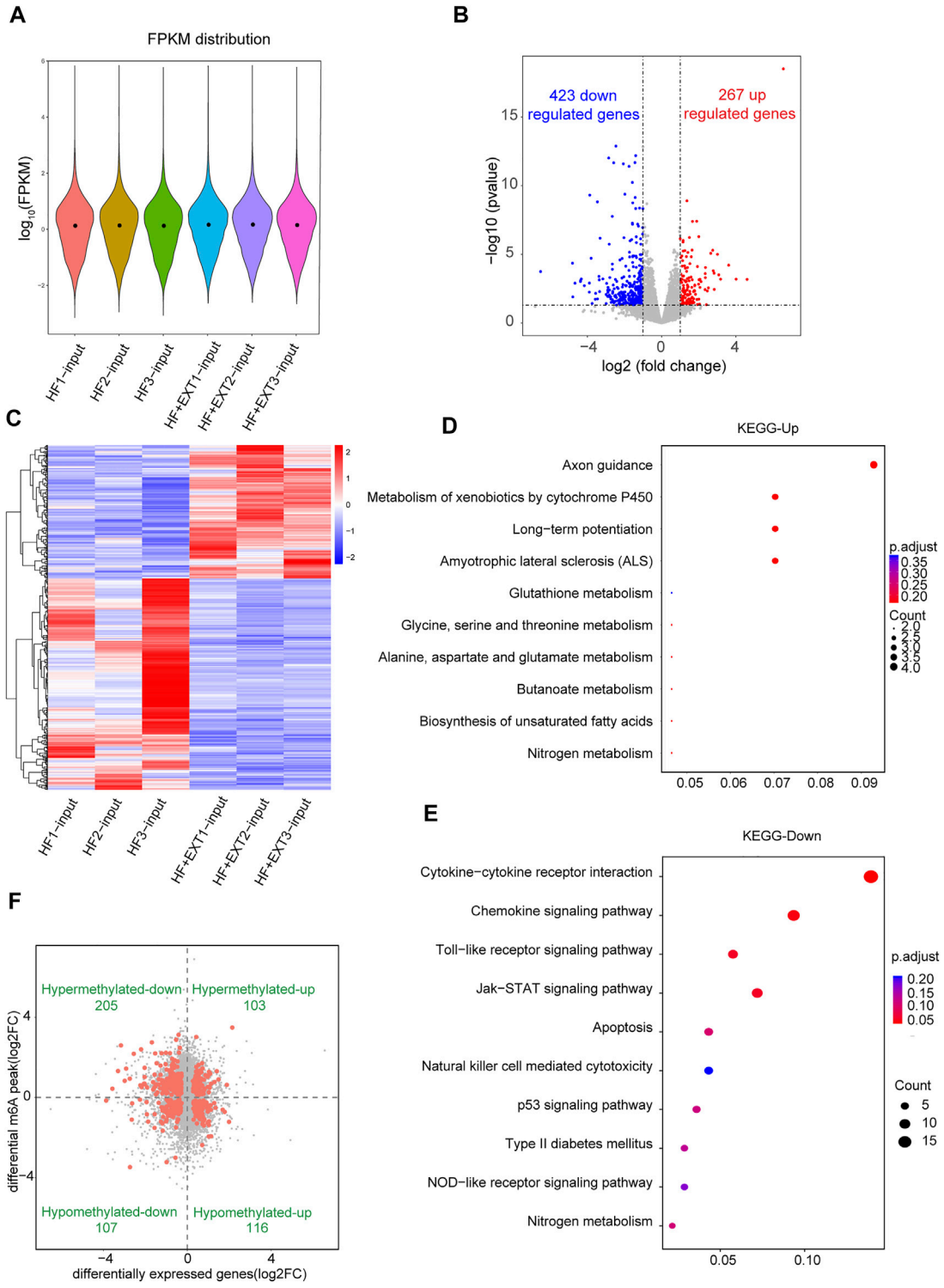

FIGURE 3
Combined analysis of RNA-seq and MeRIP-seq data comparing HFpEF with HFpEF + EXT heart samples. **(A)** FPKM distribution of two groups. **(B)** Volcano plots showing different expression mRNAs between HFpEF and HFpEF + RE samples (fold change >2 and $p < 0.05$). **(C)** Clustering analysis of differentially expressed mRNAs. **(D,E)** The top 10 enriched KEGG pathways of differentially mRNA for upregulated and downregulated mRNA. **(F)** The distribution of transcripts with significantly changed in m^{6}A-modification level and corresponding mRNA expression ($p < 0.05$) by four-quadrant graph. Red dots represent significant differences in RNA expression and m^{6}A modification, and gray dots do not meet the conditions.

that there was significantly altered intensity in the HFpEF + EXT group. Figure 2G showed the representative m^{6}A-methylated mRNA peaks in the Fas/APO-1 receptors (*Fas*) and phospholipid phosphatase-1 (*Plpp1*) genes, which were the sites with reduced and grown m^{6}A levels, respectively.

In order to explore the potential biological significance of exercise-related m^{6}A methylation changes in HFpEF, we performed the GO analysis of differentially methylated RNAs. Compared with those in HFpEF mice, our results revealed that hypermethylated and hypomethylated RNAs in HFpEF + EXT mice were especially related to energy metabolism terms, e.g., regulation of carbohydrate catalog, regulation of glycolytic process and carbohydrate catabolic process, suggesting that differentially methylated RNAs were mainly concentrated in energy metabolism (Supplementary Figure S2). Furthermore, the KEGG pathway analysis of differentially methylated RNAs in HFpEF + EXT mice were predominantly concentrated in myocardial cell death and myocardial energy metabolism, e.g., apoptosis, pyruvate metabolism, MAPK signaling pathway, insulin signaling pathway and sphingolipid metabolism pathway, which are mainly and strongly connected with myocardial apoptosis (Figures 2H,I). In conclusion, our findings suggested that these differentially methylated RNAs might take part in the myocardial energy metabolism and apoptosis pathway.

Overall, the transcripts of HFpEF + EXT-specific m^{6}A peaks were mainly concentrated on myocardial cell death and myocardial energy metabolism, which were the main pathological features of HFpEF.

Conjoint analysis of m^{6}A-seq and RNA-Seq data shows that specific m^{6}A-modified transcripts were extremely correlated with the myocardial remodeling pathological characteristics of heart failure with preserved ejection fraction

The reads per kilobase per million mapped reads (FRKM distribution) indicated no difference in gene expression between samples (Figure 3A). RNA-Seq results indicated that 690 mRNAs, including 423 downregulated and 267 upregulated mRNAs, in HFpEF + EXT samples were significantly dysregulated compared with those in HFpEF samples (FC > 2, $p < 0.05$; Figure 3B). The tendency of differing gene expression between the groups was contemporaneous among individual samples within every group, according to further hierarchical clustering analysis of RNA-Seq data. ($n = 3$ per group, Figure 3C). Importantly, GO and KEGG pathway analysis displayed that differentially expressed genes were closely connected with apoptosis pathway and myocardial energy metabolism pathway (Figures 3D,E; Supplementary Figure S3), and this finding was coincident with the involvement in myocardial remodeling pathology (Dunlay et al., 2017; Figtree et al., 2021; Mishra and Kass, 2021; Omote et al., 2022; Prandi et al., 2022).

In order to further study the target genes modified by m^{6}A, target genes were idenfieid by the conjoint analysis of m^{6}A-seq and RNA-Seq data. Through bioinformatics analysis, we confirmed 308 hypermethylated m^{6}A peaks in mRNA transcripts, of which 103 and 205 were significantly upregulated and downregulated respectively (Figure 3F). Furthermore, 223 hypomethylated m^{6}A peaks were confirmed in mRNA transcripts, of which 116 and 107 peaks were downregulated and upregulated, respectively (Figure 3F). Furthermore, the integrated analysis of MeRIP-seq and RNA-Seq data and KEGG pathway analysis showed that specific m^{6}A-modified transcripts were closely associated with myocardial energy metabolism, especially myocardial apoptosis. Hence, we identified genes that were critical to these processes and further validated them, including *Fas, Capn2, Casp12, Casp7, Jun, Pdia3, Tnnt2, Mef2a, Adrb1* and *Agtr1a* (Figure 4A; Table 3).

We used SELECT-PCR to validate the m6A levels of those different critical genes *Fas, Capn2, Casp12, Casp7, Jun, Pdia3, Tnnt2, Mef2a, Adrb1* and *Agtr1a*, which were associated with myocardial apoptosis and myocardial energy metabolism. We found that the m^{6}A methylation levels of *Fas*, *Casp12, Tnnt2, Mef2a* and *Agtr1a* were significantly increased and the m^{6}A methylation of *Jun* was significantly decreased (Figure 4A). Furthermore, the mRNA levels of *Fas, Casp12, Jun, Tnnt2, Mef2a* and *Agtr1a* were measured in HFpEF + EXT and HFpEF hearts (Figure 4B), and results showed that *Jun, Tnnt2, Mef2a* and *Agtr1a* had similar mRNA expression tendencies in keeping with their m^{6}A methylation levels, but *Fas* had opposite mRNA expression tendencies in keeping with their m^{6}A methylation levels (Figure 4A).

Exercise training ameliorates myocardial apoptosis in heart failure with preserved ejection fraction by decreasing apoptosis pathway and increasing myocardial energy metabolism

Apoptosis is one of the most important characteristics of pathological cardiac remodeling, and exercise training is an effective method to reduce cardiomyocyte apoptosis. To investigate the effect of exercise on cardiomyocyte apoptosis in the HFpEF heart, we used terminal deoxynucleotidyl transferase-mediated dUTP nick-end labeling (TUNEL) to stain cardiac pathological sections. The representative fluorescence photos of TUNEL positive nuclei in the HFpEF heart after exercise are shown in Figure 4C. In the myocardium of HFpEF mice, the proportion of TUNEL positive cardiomyocytes

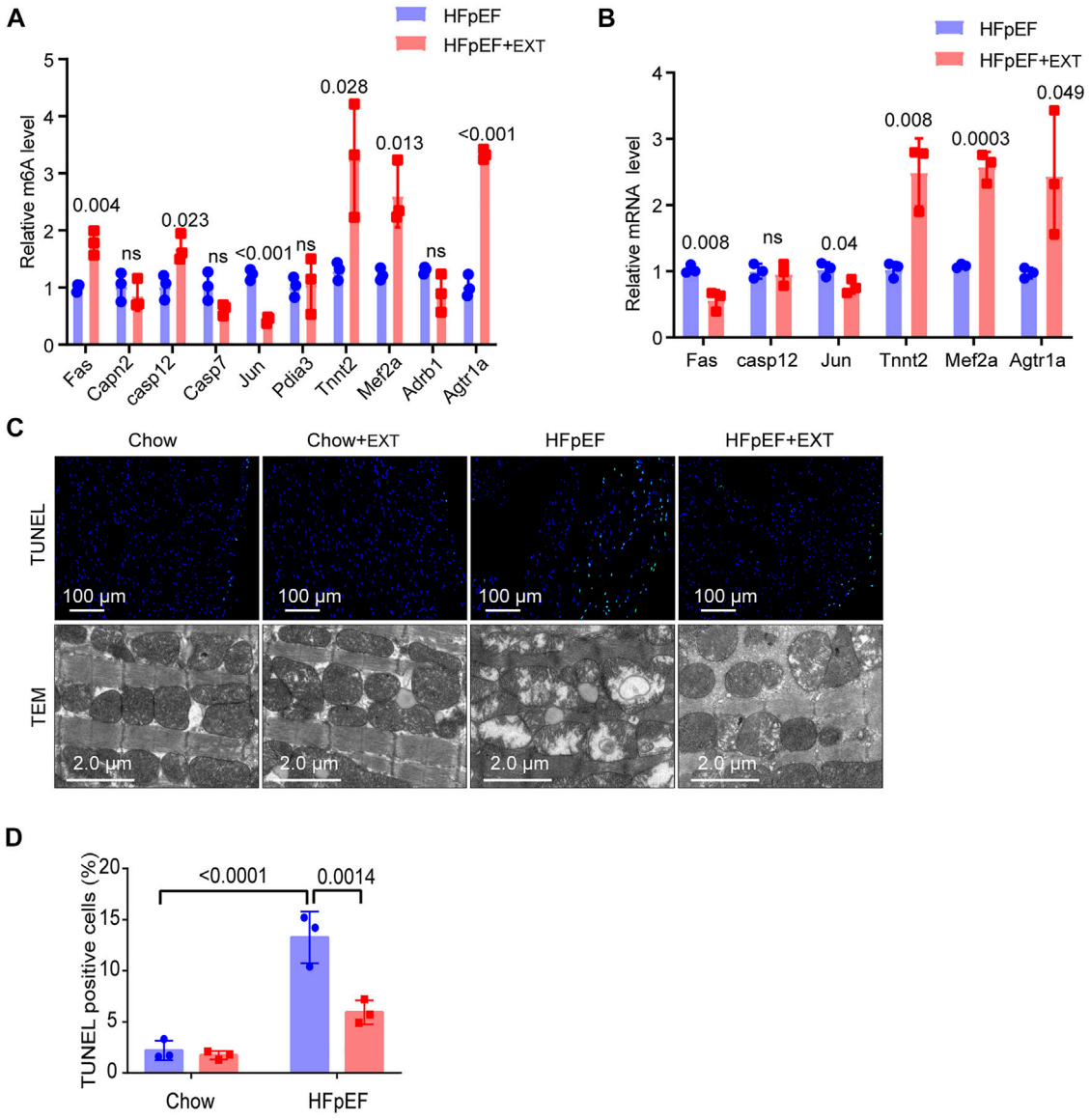

FIGURE 4
Identification of the downstream target genes and mechanisms of exercise improvement of HFpEF. **(A)** Single-base elongation and ligation-based qPCR amplification method (SELECT) validation of m^{6}A level changes of ten related genes. **(B)** The relative mRNA levels of six genes determined by real-time PCR in HFpEF and HFpEF + EXT samples. n = 3 mice per group. Data are presented as mean ± SEM. Multiple unpaired t tests were used. **(C,D)** Representative images of TUNEL and TEM and quantitative analysis of TUNEL-positive cells. n = 3 mice per group. Data are presented as mean ± SEM. Two-way ANOVA and Tukey's multiple comparison test were used. Numbers above square brackets display great p values.

was greatly higher than that of control mice, while a smaller number of TUNEL positive cells could be detected in the myocardium of control or HFpEF mice after exercise (Figures 4C,D).

In order to verify whether exercise can exert its cardioprotective function by maintaining the integrity and function of mitochondria, we measured and detected the mitochondrial structure of the heart of control group and HFpEF mice with or without exercise using an electron microscope. The ultrastructure of heart sections of control group and HFpEF mice with or without exercise was analyzed by an electron microscope to determine the integrity of mitochondria (Figure 4C). In the normal mouse myocardium, mitochondria were well aligned between the longitudinally oriented myocardial myofibrils, and no difference was observed after exercise. However, the abundance of mitochondria in HFpEF appeared to be significantly altered, and the arrangement of mitochondria in HFpEF mice was

TABLE 3 The ranking of the top 10 genes in each quadrant graph.

Gene name	Pattern	Chromosome	m^{6}A level change				mRNA level change			
			Peak region	Peak start	Peak end	fold_enrchment	diff. lg. p	Strand	log2FC	*p* value
Casp12	Hyper-down	9	CDS	5345459	5346656	1.72	−9.81	+	−1.27477	0.000628688
Capn2	Hyper-down	1	five_prime_utr	182517278	182517608	22.6	−6.37	−	−0.30561	0.032386574
Fas	Hyper-down	19	CDS	34290658	34309091	1.79	−17.3	+	−1.03262	0.002731876
Casp7	Hypo-down	19	three_prime_utr	56441600	56441809	3.37	−2.04	+	−0.53649	0.022176301
Jun	Hypo-down	4	CDS	95049867	95052222	34.9	−1.45	−	−0.98579	5.99E-08
Pdia3	Hypo-down	2	three_prime_utr	121435993	121437910	3.93	−4.47	+	−0.50359	0.005265144
Tnnt2	Hyper-up	1	exon	135836353	135836534	2.41	−8.85	+	0.730282	0.001676025
Mef2a	Hyper-up	7	five_prime_utr	67349856	67372858	2.8	−5.61	−	0.439723	0.005269679
Adrb1	Hypo-up	19	CDS	56723142	56724091	72.7	−5.32	+	0.530445	0.01782968
Agtr1a	Hypo-up	13	CDS	30381099	30382388	14.5	−1.97	+	0.5337	0.033615285

disorganized, and the mitochondria were swollen and aggregated, and cristae were slightly loosened (Figure 4C). After 2 months of exercise, there was evidence that damage to cardiac mitochondria and disrupted cristae were restored in HFpEF + EXT hearts (Figure 4C).

Overexpression of fat mass and obesity-related cancels out the benefits of exercise in heart failure with preserved ejection fraction + Exercise training mice by promoting myocyte apoptosis, myocardial fibrosis and myocyte hypertrophy

On basis of the analysis outcomes of unique genes in HFpEF + EXT and HFpEF hearts by GO/KEGG, we suspected that the FTO is closely related to the regulation of energy metabolism and might exert a significant effect on the pathogenesis of HFpEF. Therefore, we explored the mechanism of FTO in HFpEF through experiments. The protein level of FTO in HFpEF + EXT mice was downregulated in comparison with that in HFpEF mice. The FTO protein level detected by Western blotting was greatly lower than that in the HFpEF + EXT group in comparison with the HFpEF group ($p = 0.001$; $n = 6$ per group; Figures 5A,B). We also looked at the expression of other key methyltransferases and demethylases during m^{6}A modification, including Mettl3, Mettl14, and ALKBH5. Mettl3 was increased, and no significant difference was observed in Mettl4 and ALKBH5 (Figures 5A,C–E).

Overexpression of FTO cancels out the benefits of exercise in HFpEF + EXT mice by promoting myocyte apoptosis, myocardial fibrosis and myocyte hypertrophy. At the age of 16 weeks, we injected the AAV vector encoding FTO into the HFpEF + EXT mice through the tail vein, and detected the expression of FTO after 8 weeks. After injection of AAV-FTO for 8 weeks, expression of myocardial FTO increased by approximately 7.5-fold in HFpEF + EXT mouse hearts (Supplementary Figures S1A,B). After 8 weeks of adenovirus injection, we found overexpression of FTO increased interstitial fibrosis in HFpEF + EXT mouse hearts (Figures 6A,B, $p = 0.0089$). Furthermore, the overexpression of FTO efficiently augmented cardiomyocyte hypertrophy, as demonstrated by the increase in cross-sectional area of cardiomyocyte in HFpEF + EXT mouse hearts (Figures 6A,C, $p < 0.0001$). Moreover, the overexpression of FTO accelerated apoptosis in myocytes and increased the proportion of TUNEL-positive cells in the myocardium (Figures 6A,D, $p = 0.0306$). The overexpression of FTO significantly destroyed mitochondrial integrity and function by disorganized mitochondrial arrays and aggregates of swollen mitochondria with slight lysis of the cristae (Figure 5A). Furthermore, the doppler echocardiography showed that FTO overexpression exacerbated diastolic dysfunction in HFpEF + EXT mice by increasing the E/E′ ratio (Figure 6E). The overexpression of FTO reduced LW/TL and running distance ($n = 6$, $p = 0.0444$ and $p < 0.0001$; Figures 6F,G). Overexpression of FTO reduced the mRNA levels of Tnnt2, Mef2a and Agtr1a, and increased the mRNA levels of Fas and Jun (Figure 6H). Overall, these data indicated that the overexpression of FTO cancels out the benefits of exercise in

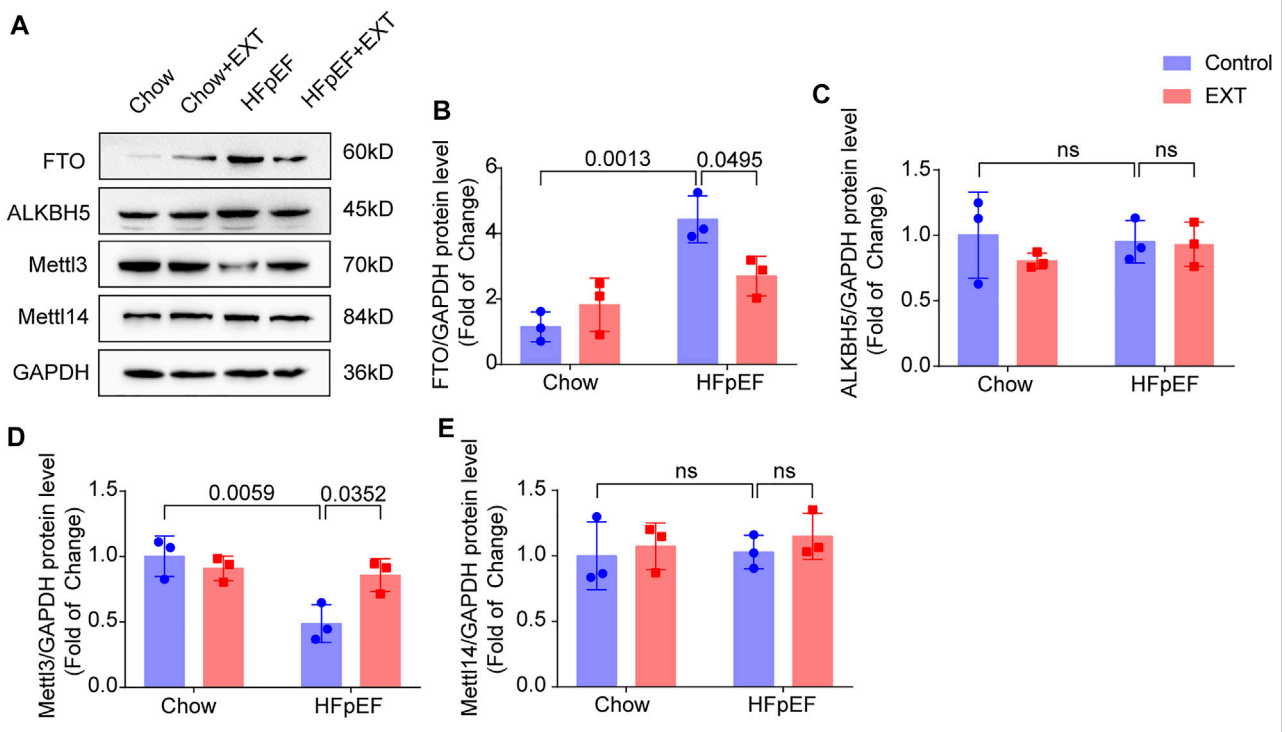

FIGURE 5
FTO is Downregulated in HFpEF + EXT compared to HFpEF. **(A–E)** Representative Western blots plots of FTO, Mettl3, ALKBH5 and Mettl14, and quantitative analysis of FTO/GAPDH, Mettl3/GAPDH protein, ALKBH5/GAPDH and Mettl14/GAPDH expressions. *n* = 3 per group. Data are presented as mean ± SEM. Two-way ANOVA and Tukey's multiple comparison test were used. Numbers above square brackets show significant *p* values.

HFpEF + EXT mice by promoting myocyte apoptosis, myocardial fibrosis and myocyte hypertrophy.

Discussion

HFpEF is an aging disease characterized by cardiac hypertrophy, myocardial interstitial fibers, and cardiac diastolic dysfunction (Prandi et al., 2022). Due to inadequate understanding of the pathophysiology and animal models of HFpEF, it is difficult to develop methods to treat this more prevalent and lethal disease (Schiattarella et al., 2019; Deng et al., 2021). Unlike HFrEF, patients with HFpEF constitute a highly heterogenous population. HFpEF patients usually do not trace back to a primary lesions and injuries of cardiomyocytes but rather to a complex of series of systemic abnormalities, e.g., metabolic dysfunction, hypertension, hyperlipidemia, renal dysfunction and pulmonary dysfunction (Dunlay et al., 2017; Deng et al., 2021; Mishra and Kass, 2021). There are many reasons for the lack of effective therapies of HFpEF, but it is largely because of incompletely understanding its complex pathophysiology and the lack of appropriate animal models to study its pathogenesis. EXT is an important nonpharmacological treatment, which can reduce the risk of hospitalization and cardiovascular mortality risk (Jaconiano and Moreira-Gonçalves, 2022). Although the significance of epigenetic regulation in the control of gene expression to diagnose and treat HFpEF has been widely examined (Hamdani et al., 2021), the effect of RNA alternation on the control of gene expression to affect HFpEF has only recently been investigated. Previous studies demonstrated that the mRNA of m^{6}A writers Mettl3 and Mettl4; m^{6}A eraser FTO; and reader YTHDF2 are elevated in patients with HFpEF (Zhang et al., 2021a). In HFpEF mice, the mRNA of FTO and YTHDC1 is upregulated but Mettl3 is downregulated (Zhang et al., 2021a). In elderly HFpEF mice, EXT could improve exercise capacity, diastolic function, and systolic reserves and reduce pulmonary congestion (Roh et al., 2020). However, the distribution of m^{6}A within transcriptome-wide in HFpEF + EXT samples is still mostly unknown. Our research showed that m^{6}A RNA methylation is changed in HFpEF + EXT mice, indicating specific m^{6}A alternation patterns on the transcriptome-wide and gene-specific scales that were distinct from those of in HFpEF mice. GO and KEGG analyses demonstrated that m^{6}A RNA methylation differential genes between HFpEF + EXT and HFpEF mice are specifically associated with myocardial energy metabolism. HFpEF + EXT mice are observed with downregulated FTO compared with HFpEF mice, and the

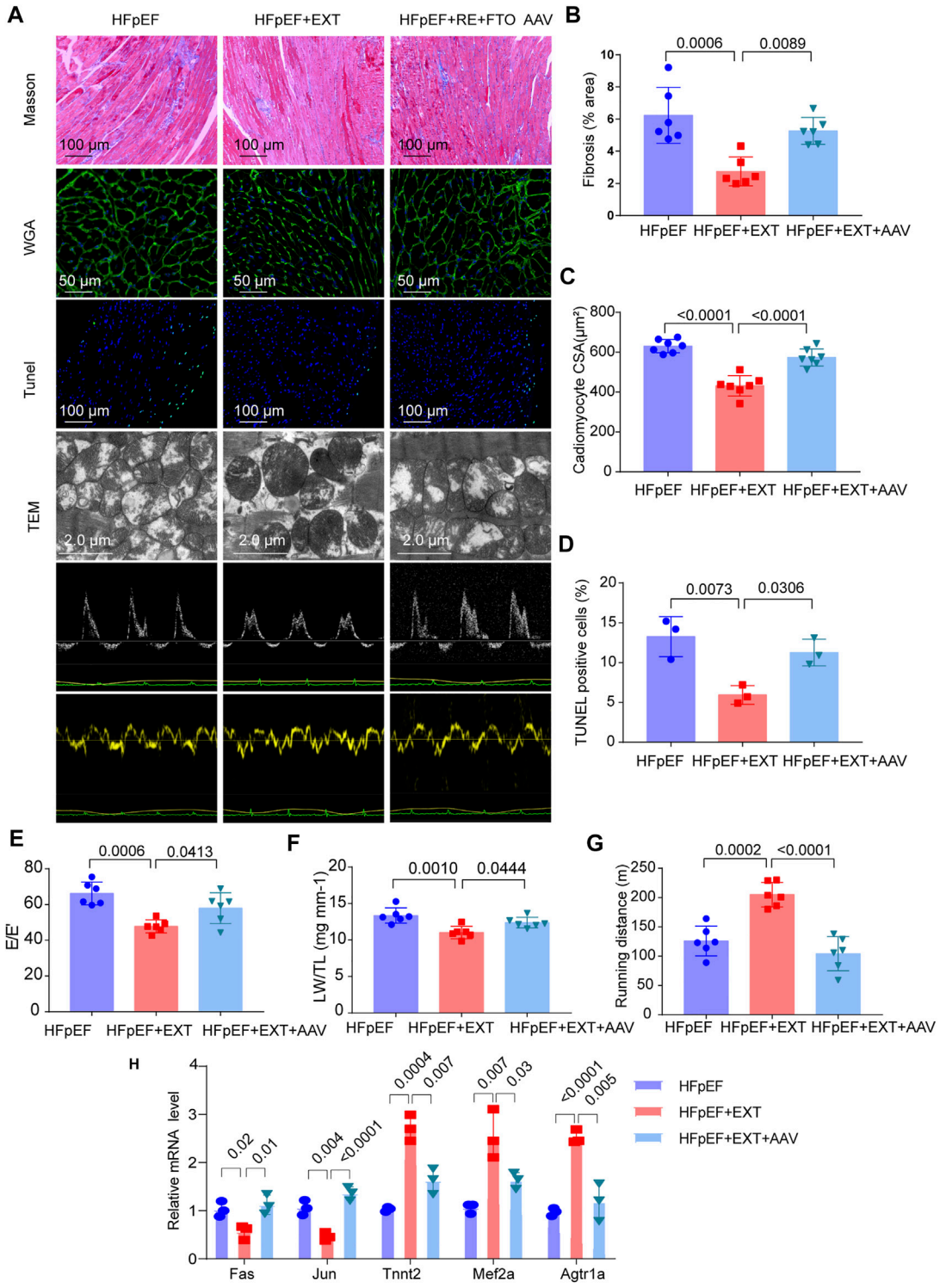

FIGURE 6
Overexpression of FTO cancels out the benefits of exercise in HFpEF + EXT mice. **(A)** Gross morphology of hearts stained with Masson, WGA, TUNEL, TEM, and Doppler echocardiography from HFpEF, HFpEF + EXT and HFpEF + EXT + AAV9 mice. **(B)** Quantitative analysis of interstitial fibrosis (n = 6 mice per group). **(C)** Quantitative analysis of cardiomyocyte cross-sectional area (n = 6 mice per group). **(D)** Quantitative analysis of TUNEL-positive cells (n = 3 per group). **(E)** Quantitative analysis of E/E′ ratio (n = 6 mice per group). **(F)** Ratio of lung weight to tibia length (n = 6 mice per group). **(G)** Running distance during exercise exhaustion test (n = 6 mice per group). **(H)** The relative mRNA levels of six genes determined by real-time PCR in HFpEF, HFpEF + EXT and HFpEF + EXT + AAV9 mice (n = 3 mice per group). Data are presented as mean ± SEM. One-way ANOVA and Tukey's multiple comparison test were used. Numbers above square brackets show significant p values.

overexpression of FTO cancels out the benefits of exercise in HFpEF + EXT mice by promoting myocyte apoptosis, myocardial fibrosis and myocyte hypertrophy. FTO is a key m^{6}A demethylase that may regulate cardiomyocyte function through catalyzing the demethylation of m^{6}A on particular mRNAs, such as *Fas, Jun, Tnnt2, Mef2a* and *Agtr1a*.

Exercise modifies the m^{6}A profile of HFpEF, and these differential modification genes are closely associated with myocardial energy metabolism. The pattern of m^{6}A modification in HFpEF + EXT mice was different from those of HFpEF mice on both transcriptome-wide and gene-specific scales. 22 409 m^{6}A peaks in HFpEF + EXT mice were determined, indicating that m^{6}A is a widespread post transcriptional RNA alternation in various heart disorders. In addition, we investigated that differentially methylated m^{6}A peaks in HFpEF + EXT mice are primarily present in 5′UTR, which may promote mRNA translation. Importantly, in our research, we found that in HFpEF + EXT mice, the Fas m^{6}A-modified site is primarily present in the 5′UTR. Therefore, we speculated that the differential methylation of RNAs in HFpEF + EXT might affect post-transcriptional translation levels and translation efficiency of RNA. We found that genes with differential m^{6}A methylation and mRNA expression in HFpEF + EXT mice were mainly enriched in processes and pathways related to myocardial energy metabolism and apoptosis pathway, such as MAPK signaling pathway, insulin signaling pathway, sphingolipid metabolism, pyruvate metabolism, apoptosis, and regulation of intrinsic apoptotic signaling pathway processes (Figures 2H,I). HFpEF is a complex disease that includes cardiac hypertrophy, myocardial fibrosis, inflammation, cardiomyocyte sarcomere disfunction and mitochondrial and metabolic defects, which lead to mitochondrial dysfunction, inflammation and myocardial cardiac diastolic dysfunction (Figtree et al., 2021; Jaconiano and Moreira-Gonçalves, 2022). Recent clinical studies found that a year of committed EXT reverses abnormal left ventricular myocardial stiffness in patients with stage B HFpEF (Hieda et al., 2021). However, because of limited access to cardiac tissue, the molecular mechanisms of HFpEF remained largely unknown. Here, our study indicated that exercise induces similar functional benefits in HFpEF mouse, and the Conjoint analysis of MeRIP-seq and RNA-Seq data revealed that exercise alters the metabolic phenotype of cardiomyocytes and improves the apoptosis of myocardial cells for HFpEF. Indeed, our findings suggested that while EXT only ameliorated the HFpEF phenotypes in this “two-hit” model, it improved the overall cardiac performance and exercise capacity. We propose that, from the mice “two-hit” model with HFpEF, EXT confers benefits. The mechanism of epigenetic regulation thus provides a new therapeutic target for HFpEF and a new approach to studying HFpEF.

Exercise improves mitochondrial function in HFpEF and affects the myocardial energy metabolism phenotype (Vega et al., 2017). Post-exercise hearts exhibited a higher capacity for fatty acid oxidation and ATP generation than non-exercise hearts in response to the stimulation of increased cardiac workload by b EXT (Moreira et al., 2020). The transcriptional coactivator PGC-1α is a core molecule in the regulation of cardiomyocyte metabolism, and it was originally recognized as a cold inducible element in mitochondrial biogenesis and necessary for the metabolic adaptations of the heart to exercise (Moreira et al., 2020). In our study, an important target gene for improving the myocardial phenotype of HFpEF during exercise is Fas. Fas ligand (FasL) is a cell surface molecule of the tumor necrosis factor family binding to its receptor Fas to induce apoptosis of Fas bearing cells (Wajant, 2002). In our study, Fas m^{6}A methylation expression levels are upregulated, but the mRNA and protein expression levels are downregulated, indicating that m^{6}A modification of *Fas* may influence mRNA degradation.

FTO is downregulated in HFpEF + EXT samples, and overexpression of FTO cancels out the benefits of exercise in HFpEF + EXT mice by promoting myocyte apoptosis, myocardial fibrosis and myocyte hypertrophy. In 2007, the *FTO* gene was identified in a type II diabetes genome-wide relationship research (Dina et al., 2007). Furthermore, a population cohort research showed that the effect of FTO genes was closely associated with energy intake (Scuteri et al., 2007). However, it is not clear how FTO affects the mechanisms of obesity and energy metabolism. Our KEGG pathway analysis showed that differentially methylated RNAs are predominantly associated with the MAPK and insulin signaling pathways in cardiomyocytes. In conclusion, the FTO is critical for energy metabolism. FTO expression is downregulated in mammalian heart failure hearts and hypoxic cardiomyocytes, with higher m^{6}A levels in RNA and impaired cardiomyocyte contractile performance, according to recent investigations (Mathiyalagan et al., 2019). Additionally, in mice with heart failure, the m^{6}A demethylase FTO improves cardiac function *via* controlling glucose absorption and glycolysis (Zhang et al., 2021b). In this research, the overexpression of FTO deteriorates heart function by growing E/E′ and LW/TL and decreasing the running distance. Furthermore, overexpression of FTO cancels out the benefits of exercise in HFpEF + EXT mice by promoting myocyte apoptosis, myocardial fibrosis and myocyte hypertrophy.

The present study has limitations. Firstly, we did not find human heart samples to validate our experimental results. Therefore, we will next seek human heart samples to validate the important role of m^{6}A modification in the pathogenesis of HFpEF. Secondly, although we found the target genes were modified by m^{6}A, the mechanism of how the binding proteins control the target genes has not been explored. Next, how binding proteins affect target gene stability, translational efficiency, or degradation will be explored. Thirdly, although we demonstrated that overexpressing FTO in the heart worsened cardiac function, future research with cardiac specific knockout FTO mice and HFpEF models will investigate the actual mechanism by which FTO mediates HFpEF.

Consequently, m^{6}A RNA methylation was modified in HFpEF + EXT mice, who displayed distinct m^{6}A alternation patterns at the transcriptome and gene levels compared to HFpEF mice. Differentially methylated genes were found to be linked with myocardial fibrosis, myocyte hypertrophy, myocardial apoptosis, and myocardial energy metabolism in GO and KEGG studies. Exercise improved mitochondrial function in HFpEF and myocardial energy metabolism phenotype to reverse the myocardial phenotypes. FTO was downregulated in HFpEF + EXT mice compared with that in HFpEF mice, and the overexpression of FTO cancels out the benefits of exercise in HFpEF + EXT mice by promoting myocyte apoptosis, myocardial fibrosis and myocyte hypertrophy. FTO is a key m^{6}A demethylase that may regulate cardiomyocyte function through catalyzing the demethylation of m^{6}A on particular mRNAs, such as *Fas*, *Jun*, *Tnnt2*, *Mef2a* and *Agtr1a*.

Data availability statement

The datasets presented in this study can be found in online repositories. The names of the repository/repositories and accession number(s) can be found below: Gene Expression Omnibus accession number: GSE208354.

Ethics statement

The animal study was reviewed and approved by Capital Institute of Pediatrics.

Author contributions

KL and JW designed the experiments and wrote the manuscript. KL, WJ, FH, and JH carried out experiments, and SO analyzed the data. JW, HG and ZL supervised this project. KL and WJ contributed equally to this study. All authors have finally been approved for publication.

Funding

This work is supported by grants from CAMS Innovation Fund for Medical Sciences (CIFMS, 2016-I2M-1-008); Public service development and reform pilot project of Beijing Medical Research Institute (BMR2019-11); The Special Fund of the Pediatric Medical Coordinated Development Center of Beijing Hospitals Authority (No. XTZD20180402); the National Key Research and Development Program of China (2018YFC1002503).

Conflict of interest

The authors declare that the research was conducted in the absence of any commercial or financial relationships that could be construed as a potential conflict of interest.

Publisher's note

Supplementary material

The Supplementary Material for this article can be found online at: https://www.frontiersin.org/articles/10.3389/fcell.2022.954769/full#supplementary-material

SUPPLEMENTARY FIGURE S1
Flow chart and adeno-associated virus overexpression FTO. . Flow chart of HFpEF modeling and running method in mice. **(B,C)** Representative Western blots and quantitative analysis of overexpression of FTO. n = 3 Data are presented as mean ± SEM. One-way ANOVA and Tukey's multiple comparison test were used. Numbers above square brackets show significant p values.

SUPPLEMENTARY FIGURE S2
GO analysis of Differential m^{6}A modification genes. Biological Process analysis of up-regulated and down-regulated m^{6}A methylation genes. **(C,D)** Cellular Component analysis of up-regulated and down-regulated m^{6}A methylation genes. **(E,F)** Molecular Function analysis of up-regulated and down-regulated m^{6}A methylation genes.

SUPPLEMENTARY FIGURE S3
GO analysis of Differential mRNA genes. Biological Process analysis of upregulated and downregulated mRNA genes. **(C,D)** Cellular Component analysis of upregulated and downregulated m6A mRNA genes. **(E,F)** Molecular Function analysis of upregulated and downregulated mRNA genes.

References

Alarcón, C. R., Lee, H., Goodarzi, H., Halberg, N., and Tavazoie, S. F. (2015). N6-methyladenosine marks primary microRNAs for processing. *Nature* 519 (7544), 482–485. doi:10.1038/nature14281

Berulava, T., Buchholz, E., Elerdashvili, V., Pena, T., Islam, M. R., Lbik, D., et al. (2020). Changes in m6A RNA methylation contribute to heart failure progression by modulating translation. *Eur. J. Heart Fail* 22 (1), 54–66. doi:10.1002/ejhf.1672

Deng, Y., Xie, M., Li, Q., Xu, X., Ou, W., Zhang, Y., et al. (2021). Targeting mitochondria-inflammation circuit by β-hydroxybutyrate mitigates HFpEF. *Circ. Res.* 128 (2), 232–245. doi:10.1161/circresaha.120.317933

Dieberg, G., Ismail, H., Giallauria, F., and Smart, N. A. (2015). Clinical outcomes and cardiovascular responses to exercise training in heart failure patients with preserved ejection fraction: A systematic review and meta-analysis. *J. Appl. Physiol. (1985)* 119 (6), 726–733. doi:10.1152/japplphysiol.00904.2014

Dina, C., Meyre, D., Gallina, S., Durand, E., Körner, A., Jacobson, P., et al. (2007). Variation in FTO contributes to childhood obesity and severe adult obesity. *Nat. Genet.* 39 (6), 724–726. doi:10.1038/ng2048

Dominissini, D., Moshitch-Moshkovitz, S., Schwartz, S., Salmon-Divon, M., Ungar, L., Osenberg, S., et al. (2012). Topology of the human and mouse m6A RNA methylomes revealed by m6A-seq. *Nature* 485 (7397), 201–206. doi:10.1038/nature11112

Dorn, L. E., Lasman, L., Chen, J., Xu, X., Hund, T. J., Medvedovic, M., et al. (2019). The N 6 -methyladenosine mRNA methylase METTL3 controls cardiac homeostasis and hypertrophy. *Circulation* 139 (4), 533–545. doi:10.1161/circulationaha.118.036146

Dunlay, S. M., Roger, V. L., and Redfield, M. M. (2017). Epidemiology of heart failure with preserved ejection fraction. *Nat. Rev. Cardiol.* 14 (10), 591–602. doi:10.1038/nrcardio.2017.65

Edelmann, F., Gelbrich, G., Düngen, H. D., Fröhling, S., Wachter, R., Stahrenberg, R., et al. (2011). Exercise training improves exercise capacity and diastolic function in patients with heart failure with preserved ejection fraction: Results of the ex-DHF (exercise training in diastolic heart failure) pilot study. *J. Am. Coll. Cardiol.* 58 (17), 1780–1791. doi:10.1016/j.jacc.2011.06.054

Feil, R., and Fraga, M. F. (2012). Epigenetics and the environment: Emerging patterns and implications. *Nat. Rev. Genet.* 13 (2), 97–109. doi:10.1038/nrg3142

Figtree, G. A., Broadfoot, K., Casadei, B., Califf, R., Crea, F., Drummond, G. R., et al. (2021). A call to action for new global approaches to cardiovascular disease drug solutions. *Eur. Heart J.* 42 (15), 1464–1475. doi:10.1093/eurheartj/ehab068

Fukuta, H., Goto, T., Wakami, K., Kamiya, T., and Ohte, N. (2019). Effects of exercise training on cardiac function, exercise capacity, and quality of life in heart failure with preserved ejection fraction: A meta-analysis of randomized controlled trials. *Heart Fail Rev.* 24 (4), 535–547. doi:10.1007/s10741-019-09774-5

Gao, X. Q., Zhang, Y.-H., Liu, F., Ponnusamy, M., Zhao, X.-M., Zhou, L.-Y., et al. (2020). The piRNA CHAPIR regulates cardiac hypertrophy by controlling METTL3-dependent N6-methyladenosine methylation of Parp10 mRNA. *Nat. Cell Biol.* 22 (11), 1319–1331. doi:10.1038/s41556-020-0576-y

Hamdani, N., Costantino, S., Mügge, A., Lebeche, D., Tschöpe, C., Thum, T., et al. (2021). Leveraging clinical epigenetics in heart failure with preserved ejection fraction: A call for individualized therapies. *Eur. Heart J.* 42 (20), 1940–1958. doi:10.1093/eurheartj/ehab197

Handy, D. E., Castro, R., and Loscalzo, J. (2011). Epigenetic modifications. *Circulation* 123 (19), 2145–2156. doi:10.1161/circulationaha.110.956839

Hieda, M., Sarma, S., Hearon, C. M., MacNamara, J. P., Dias, K. A., Samels, M., et al. (2021). One-year committed exercise training reverses abnormal left ventricular myocardial stiffness in patients with stage B heart failure with preserved ejection fraction. *Circulation* 144 (12), 934–946. doi:10.1161/circulationaha.121.054117

Ho, J. E., Zern, E. K., Wooster, L., Bailey, C. S., Cunningham, T., Eisman, A. S., et al. (2019). Differential clinical profiles, exercise responses, and outcomes associated with existing HFpEF definitions. *Circulation* 140 (5), 353–365. doi:10.1161/circulationaha.118.039136

Ismail, H., McFarlane, J. R., Nojoumian, A. H., Dieberg, G., and Smart, N. A. (2013). Clinical outcomes and cardiovascular responses to different exercise training intensities in patients with heart failure. *JACC Heart Fail.* 1 (6), 514–522. doi:10.1016/j.jchf.2013.08.006

Jaconiano, E., and Moreira-Gonçalves, D. (2022). Unveiling the role of exercise training in targeting the inflammatory paradigm of heart failure with preserved ejection fraction: A narrative review. *Heart Fail Rev.* 27 (1), 163–190. doi:10.1007/s10741-021-10138-1

Krüger, N., Biwer, L. A., Good, M. E., Ruddiman, C. A., Wolpe, A. G., DeLalio, L. J., et al. (2020). Loss of endothelial FTO antagonizes obesity-induced metabolic and vascular dysfunction. *Circ. Res.* 126 (2), 232–242. doi:10.1161/circresaha.119.315531

Leggio, M., Fusco, A., Loreti, C., Limongelli, G., Bendini, M. G., Mazza, A., et al. (2020). Effects of exercise training in heart failure with preserved ejection fraction: An updated systematic literature review. *Heart Fail Rev.* 25 (5), 703–711. doi:10.1007/s10741-019-09841-x

Lin, J., Zhu, Q., Huang, J., Cai, R., and Kuang, Y. (2020). Hypoxia promotes vascular smooth muscle cell (VSMC) differentiation of adipose-derived stem cell (ADSC) by regulating Mettl3 and paracrine factors. *Stem Cells Int.* 2020, 2830565. doi:10.1155/2020/2830565

Mathiyalagan, P., Adamiak, M., Mayourian, J., Sassi, Y., Liang, Y., Agarwal, N., et al. (2019). FTO-dependent N 6 -methyladenosine regulates cardiac function during remodeling and repair. *Circulation* 139 (4), 518–532. doi:10.1161/circulationaha.118.033794

Meyer, K. D., Saletore, Y., Zumbo, P., Elemento, O., Mason, C. E., and Jaffrey, S. R. (2012). Comprehensive analysis of mRNA methylation reveals enrichment in 3′ UTRs and near stop codons. *Cell* 149 (7), 1635–1646. doi:10.1016/j.cell.2012.05.003

Mishra, S., and Kass, D. A. (2021). Cellular and molecular pathobiology of heart failure with preserved ejection fraction. *Nat. Rev. Cardiol.* 18 (6), 400–423. doi:10.1038/s41569-020-00480-6

Mo, X. B., Lei, S.-F., Zhang, Y.-H., and Zhang, H. (2019). Examination of the associations between m6A-associated single-nucleotide polymorphisms and blood pressure. *Hypertens. Res.* 42 (10), 1582–1589. doi:10.1038/s41440-019-0277-8

Moreira, J. B. N., Wohlwend, M., and Wisløff, U. (2020). Exercise and cardiac health: Physiological and molecular insights. *Nat. Metab.* 2 (9), 829–839. doi:10.1038/s42255-020-0262-1

Omote, K., Verbrugge, F. H., and Borlaug, B. A. (2022). Heart failure with preserved ejection fraction: Mechanisms and treatment strategies. *Annu. Rev. Med.* 73, 321–337. doi:10.1146/annurev-med-042220-022745

Poller, W., Dimmeler, S., Heymans, S., Zeller, T., Haas, J., Karakas, M., et al. (2018). Non-coding RNAs in cardiovascular diseases: Diagnostic and therapeutic perspectives. *Eur. Heart J.* 39 (29), 2704–2716. doi:10.1093/eurheartj/ehx165

Prandi, F. R., Evangelista, I., and Sergi, D. (2022). *Mechanisms of cardiac dysfunction in diabetic cardiomyopathy: Molecular abnormalities and phenotypical variants*. Dordrecht, Netherlands: Heart Fail Rev. doi:10.1007/s10741-021-10200-y

Roh, J. D., Houstis, N., Yu, A., Chang, B., Yeri, A., Li, H., et al. (2020). Exercise training reverses cardiac aging phenotypes associated with heart failure with preserved ejection fraction in male mice. *Aging Cell* 19 (6), e13159. doi:10.1111/acel.13159

Schiattarella, G. G., Altamirano, F., Kim, S. Y., Tong, D., Ferdous, A., Piristine, H., et al. (2021). Xbp1s-FoxO1 axis governs lipid accumulation and contractile performance in heart failure with preserved ejection fraction. *Nat. Commun.* 12 (1), 1684. doi:10.1038/s41467-021-21931-9

Schiattarella, G. G., Altamirano, F., Tong, D., French, K. M., Villalobos, E., Kim, S. Y., et al. (2019). Nitrosative stress drives heart failure with preserved ejection fraction. *Nature* 568 (7752), 351–356. doi:10.1038/s41586-019-1100-z

Schiattarella, G. G., Sequeira, V., and Ameri, P. (2021). Distinctive patterns of inflammation across the heart failure syndrome. *Heart Fail Rev.* 26 (6), 1333–1344. doi:10.1007/s10741-020-09949-5

Scuteri, A., Sanna, S., Chen, W.-M., Uda, M., Albai, G., Strait, J., et al. (2007). Genome-wide association scan shows genetic variants in the FTO gene are associated with obesity-related traits. *PLoS Genet.* 3 (7), e115. doi:10.1371/journal.pgen.0030115

Vega, R. B., Konhilas, J. P., Kelly, D. P., and Leinwand, L. A. (2017). Molecular mechanisms underlying cardiac adaptation to exercise. *Cell Metab.* 25 (5), 1012–1026. doi:10.1016/j.cmet.2017.04.025

Wajant, H. (2002). The Fas signaling pathway: More than a paradigm. *Science* 296 (5573), 1635–1636. doi:10.1126/science.1071553

Wang, X., Lu, Z., Gomez, A., Hon, G. C., Yue, Y., Han, D., et al. (2014). N6-methyladenosine-dependent regulation of messenger RNA stability. *Nature* 505 (7481), 117–120. doi:10.1038/nature12730

Wang, Y., Li, Y., Toth, J. I., Petroski, M. D., Zhang, Z., and Zhao, J. C. (2014). N6-methyladenosine modification destabilizes developmental regulators in embryonic stem cells. *Nat. Cell Biol.* 16 (2), 191–198. doi:10.1038/ncb2902

Xiao, Y., Wang, Y., Tang, Q., Wei, L., Zhang, X., and Jia, G. (2018). An elongation- and ligation-based qPCR amplification method for the radiolabeling-free detection of locus-specific N 6 -methyladenosine modification. *Angew. Chem. Int. Ed.* 57 (49), 15995–16000. doi:10.1002/anie.201807942

Zhang, B., Jiang, H., Wu, J., Cai, Y., Dong, Z., Zhao, Y., et al. (2021). m6A demethylase FTO attenuates cardiac dysfunction by regulating glucose uptake and glycolysis in mice with pressure overload-induced heart failure. *Sig Transduct. Target Ther.* 6 (1), 377. doi:10.1038/s41392-021-00699-w

Zhang, B., Xu, Y., Cui, X., Jiang, H., Luo, W., Weng, X., et al. (2021). Alteration of m6A RNA methylation in heart failure with preserved ejection fraction. *Front. Cardiovasc. Med.* 8, 647806. doi:10.3389/fcvm.2021.647806

frontiers | Frontiers in Cell and Developmental Biology

TYPE Review
PUBLISHED 12 September 2022
DOI 10.3389/fcell.2022.982606

OPEN ACCESS

EDITED BY
Xichen Bao,
Guangzhou Institutes of Biomedicine and Health (CAS), China

REVIEWED BY
Baofa Sun,
Nankai University, China
Jiangbo Wei,
The University of Chicago, United States

*CORRESPONDENCE
Simon Siu Man Ng,
simonng@surgery.cuhk.edu.hk
Yujuan Dong,
yjdong@surgery.cuhk.edu.hk

SPECIALTY SECTION
This article was submitted to Signaling, a section of the journal Frontiers in Cell and Developmental Biology

RECEIVED 30 June 2022
ACCEPTED 22 August 2022
PUBLISHED 12 September 2022

CITATION
Cheung JCT, Deng G, Wong N, Dong Y and Ng SSM (2022), More than a duologue: In-depth insights into epitranscriptomics and ferroptosis. *Front. Cell Dev. Biol.* 10:982606. doi: 10.3389/fcell.2022.982606

More than a duologue: In-depth insights into epitranscriptomics and ferroptosis

Justin Chak Ting Cheung[1], Guangzheng Deng[1], Nathalie Wong[1], Yujuan Dong[1,2]* and Simon Siu Man Ng[1]*

[1]Department of Surgery, Prince of Wales Hospital, The Chinese University of Hong Kong, Shatin, Hong Kong SAR, China, [2]CUHK-Shenzhen Research Institute, The Chinese University of Hong Kong, Shatin, Hong Kong SAR, China

Beyond transcription, RNA molecules are enzymatically modified to influence the biological functions of living organisms. The term "epitranscriptomics" describes the changes in RNA strands aside from altering the innate sequences. Modifications on adenosine (A) are the most widely characterized epitranscriptomic modification, including N^6-methyladenosine (m^6A), N^1-methyladenosine (m^1A), polyadenylation, and adenosine-to-inosine (A-to-I) RNA editing, and modifications on other nucleotides seem to be fewer, such as N^7-methylguanosine (m^7G), 5-methylcytosine (m^5C), and pseudouridine (Ψ). These changes on the RNA strand surface, exclusively by their RNA-modifying proteins (RMPs), are reported in various biological phenomena, including programmed cell death (PCD). One necro-biological phenomenon that has been observed for long but has started to gain heed in recent years is "*ferroptosis*." The phospholipid peroxidation by polyunsaturated-fatty-acid-containing-phospholipid hydroperoxyl (PLOOH) radicals destroys membrane integrity due to a series of mechanisms. The Fenton reaction, constituting the final Haber–Weiss reaction that is less recognized, collaboratively leading to the conversion of polyunsaturated fatty acid (PUFA) to PLOOH, is the etymological origin of ferroptosis. However, it is with increasing evidence that ferroptotic signaling is also intervened by epitranscriptomic modifications, although the truth is still ambiguous. We attempted to delineate some up-to-date discoveries on both epitranscriptomics and ferroptosis, bringing up the fundamentals to address any potential connection between the two. Next, we discussed whether a duologal relationship, or more, exists between the two, taking the ROS level and iron status into consideration. Lastly, we surveyed future perspectives that would favor the understanding of these topics.

KEYWORDS

ferroptosis, epitranscriptomics, iron metabolism, lipid peroxidation, reactive oxygen species

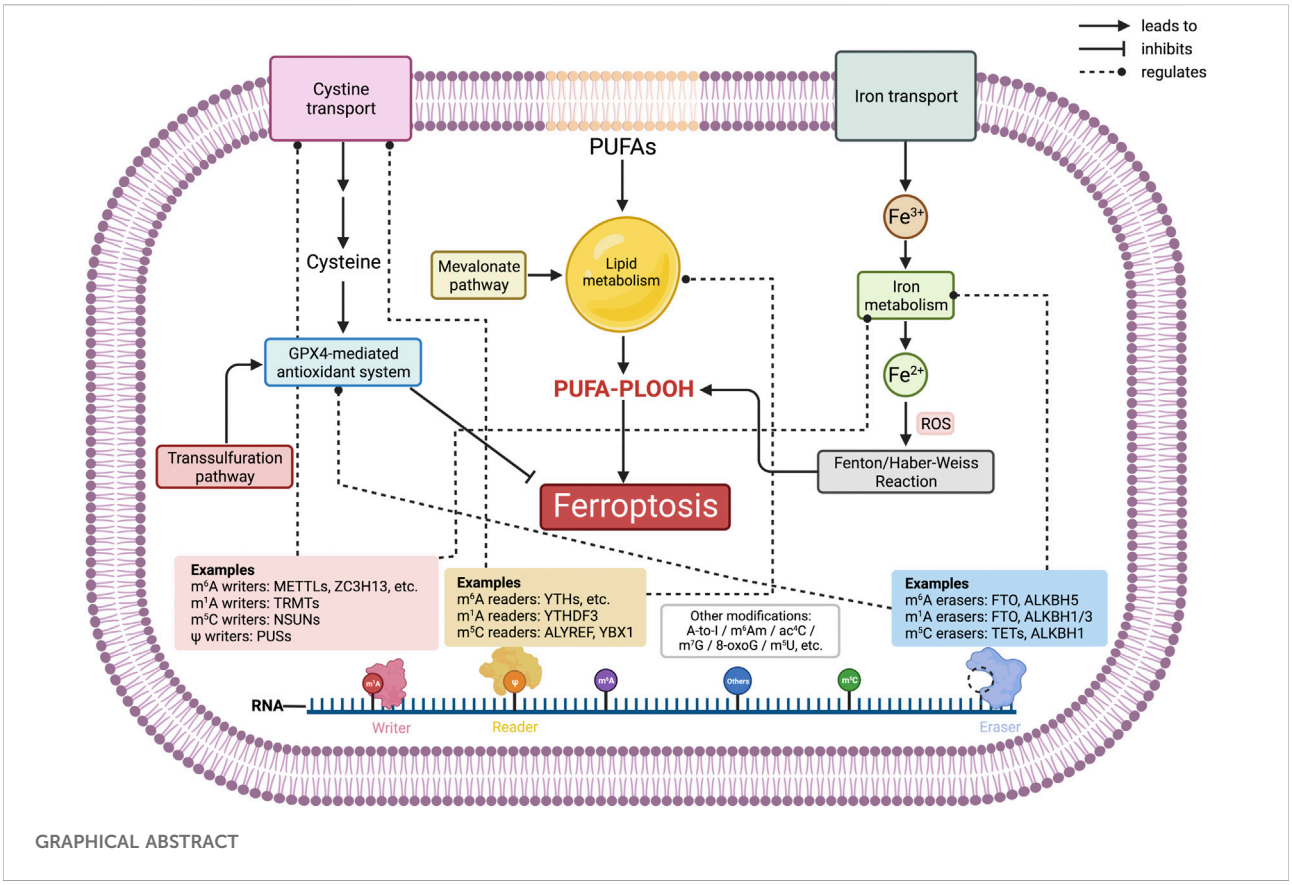

GRAPHICAL ABSTRACT

Introduction

The RNA world theory hypothesized that every living matter originated from RNA as the entity of evolutionary heredity, in lieu of DNA (Rana & Ankri, 2016). After that, a myriad of scientists have boosted our awareness of RNA through their work and established the principles underlining the *Central Dogma* of molecular biology. Nevertheless, beyond transcription, RNA molecules can also be enzymatically modified, building a new field of epitranscriptomics that is currently under intense interest. These modifications are reported in various physiological and pathological processes, which are reviewed brilliantly elsewhere, such as tRNA modifications in the role of development (Frye et al., 2018) and transcriptional and chromatin regulation by m^{6}A (Wei & He, 2021) (Shi et al., 2019). Moreover, their respective RNA-modifying proteins (RMPs) are also the targets for the investigation of epitranscriptomic regulations (Shi et al., 2019). Specific to oncological research, these RNA-modifying processes are often hijacked in cancers to acquire pro-survival advantages, and aberrant epitranscriptomic modifications have been implicated in resistance to programmed cell death (PCD). Ferroptosis, a new type of PCD denoted by an iron-dependent lethal accumulation of lipid peroxides, has started to gain heed in recent years. The complexity in ferroptotic signaling has indeed offered more opportunities for potential therapeutic manipulations in treating cancer. We attempted to delineate the up-to-date discoveries on both epitranscriptomics and ferroptosis, bringing up the fundamentals to address any potential connection between the two. Next, we discussed whether a duologal relationship, or more, exists between the two, taking the ROS level and iron status into consideration. Lastly, we surveyed future perspectives that would favor the understanding of these topics.

Beyond transcriptomics: epitranscriptomics

RNA comprises several kinds of modifications on the transcripts that constitute the epitranscriptome. The enzyme-mediated covalent modifications on RNA, also termed epitranscriptomic modifications, experienced an arduous period after the pioneering discovery of pseudouridine (ψ) in 1951 by Davis and Ellen as the first epitranscriptomic modification (Davis & Allen, 1957). After the early work from Perry & Kelley, (1974) proving the existence of an mRNA epitranscriptomic modification in mouse L-cells, it has then

TABLE 1 Examples of RNA-modifying proteins and associated epitranscriptomic modifications.

Nucleoside execution-on	Type of epitranscriptomic modification	Location (s)	Writer	Reader	Eraser
Adenosine (A)	N6-Methyladenosine (m^6A)	mRNA, rRNA, snRNA, and tRNA	METTL family members: METTL3-METTL14 heterodimer (assisted by WTAP interacting with VIRMA), METTL4, METTL5–TRMT112 complex, and METTL16	YTHs (YTHDF1/2/3, YTHDC1 with SRSF3, and NXF1 and YTHDC2)	FTO (guided by SFPQ)
			ZC3H13 corporation: ZC3H13-RBM15/RBM15B ZC3H13-WTAP	HNRNP (HNRNPA2B1/C/G)	ALKBH5
			VIRMA/KIAA1429	IGF2BPs (IGF2BP1/2/3)	
			CBLL1/HAKAI	NKAP	
			ZCCHC4		
	N1-Methyladenosine (m1A)	tRNA, mRNA, and rRNA	TRMT family members: TMRT10C and TRMT6-TRMT61A orthologs	YTHDF3	ALKBH1 and ALKBH3
			m1A58 MTase		FTO
	A-to-I editing	mRNA	ADARs (ADAR1/2/3)	—	—
	N6,2′-O-Dimethyladenosine (m^6Am)	mRNA	PCIF1	—	FTO
Cytidine (C)	5-methylcytosine (m5C)	mRNA, tRNA, rRNA, and ncRNA	NSUNs (NSUN1/2/3/4/5/6/7)	ALYREF	TETs (TET1/2/3)
			DNMT2		
			TRDMT1	YBX1	ALKBH1
			TRM4A/4B		
	N4-Acetylcytosine (ac^4C)	rRNA and tRNA	NAT10	—	—
	3-Aethylcytidine (m^3C)	rRNA, tRNA, and mRNA	METTL2/6 (tRNA)	—	ALKBH1
			METTL8 (mRNA)		
Uridine (U)	Pseudouridine (Ψ)	rRNA, tRNA, mRNA, and snRNA	PUS1/2/3/4/6/7/9	—	—
			TRUB1		
			DKC1		
Guanine (G)	7-Methylguanosine (m7G)	mRNA, tRNA, rRNA, and miRNA	METTL1/WDR4	—	—
	N2-methylguanosine (m^2G)	tRNA and rRNA	rRNA (guanine-N2-)-methyltransferase	—	—
	Queuine (Q)	tRNA	TGT	—	—

become clearer that the life cycle of an mRNA transcript does not merely experience transcription but also posttranscriptional processing such as 5′-capping, poly-adenylation, and most importantly in the context of this article, epitranscriptomic modifications.

Epitranscriptomic modifications are observed in both coding mRNA transcripts (Frye et al., 2018) (Gilbert et al., 2016) and non-coding RNA, such as long non-coding RNA (lncRNA) (Yin et al., 2021), microRNA (miRNA) (Konno et al., 2019), and transfer RNA (tRNA) (Pereira et al., 2018). Dysregulated epitranscriptomic modifications on both coding mRNA and tRNA have been intuitively considered signatures in pathologies (Destefanis et al., 2021) (Suzuki, 2021) (Yang et al., 2020). Specifically, posttranscriptional editing determines the RNA fate through mediating cellular processes, including alternative splicing (Xue et al., 2021), nonsense-mediated mRNA decay (Li et al., 2019a), and translation (Ranjan & Leidel, 2019). Extending to biological functions, the epitranscriptome has built its niche in physiological regulation, which is exemplified by circadian rhythm regulation by A-to-I editing catalyzing the ADAR enzyme family (Terajima et al., 2017), GBM-associated protein expression upregulated by METTL3 via SOX2 (Visvanathan et al., 2018), and poor prognostic characterization through the IGF2BP/SOX2/METTL3 axis in CRC (Li et al., 2019b).

Epitranscriptomic signatures and RNA-modifying proteins

According to MODOMICS, an RNA modification database constructed by Boccaletto et al. few years ago, documented RNA modifications have now raised to 144 (Dunin-Horkawicz et al., 2006), and the upsurge continues due to improved sequencing techniques and other technological advancements. To date, discussions on RNA modifications mainly revolve around the

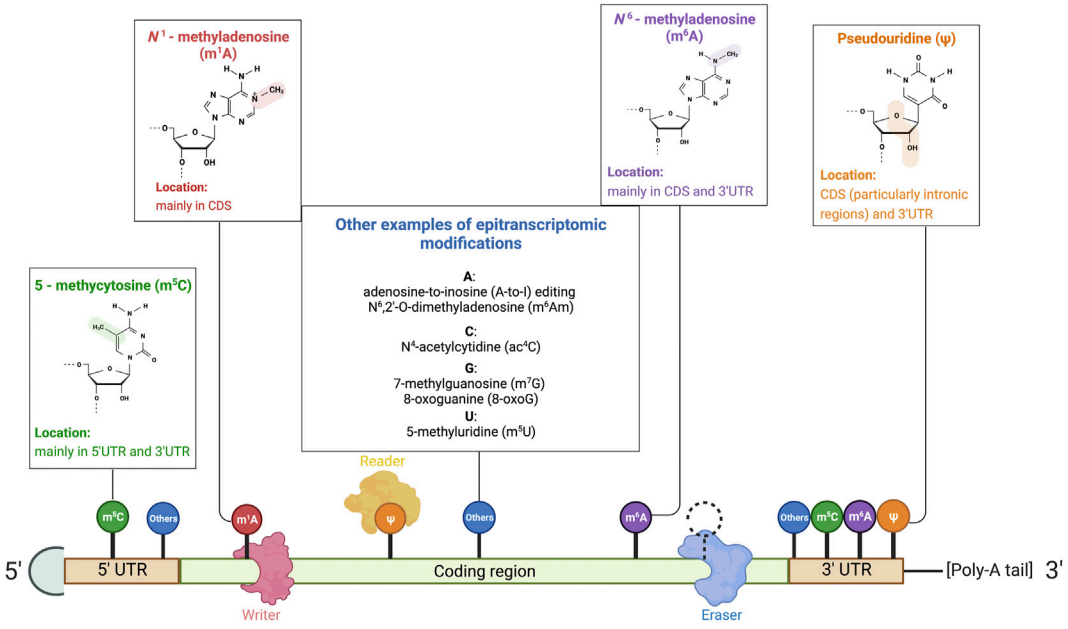

FIGURE 1
Illustration of RNA-modifying proteins on mRNA and common RNA modifications. Common base modifications include N^6−methyladenosine (m^6A), N^1−methyladenosine (m^1A), pseudouridine (ψ), and 5−methycytosine (m^5C), to name but a few. Less common modifications are also listed in the illustration. RNA-modifying proteins that govern the expression of the mRNA transcript by manipulating epitranscriptomic sites include (1) writers that deposit RNA modifications, (2) erasers that remove the epitranscriptomics modifications, and (3) readers that are recruited and recognize the modifications to alter the fate of transcripts. Reprinted from "Common eukaryotic mRNA modifications", by BioRender.com (2020). Retrieved from https://app.biorender.com/biorender-templates.

well-characterized ones, including N^6-methyladenosine (m^6A), 5-methylcytosine in RNA (m^5C), N^1-methyladenosine (m^1A), and pseudouridine (Ψ). Others like 5-hydroxymethylcytosine (5-hmC), N^4-acetylcytidine (ac^4C), and adenosine-to-inosine editing (A-to-I) are only registered with unknown or unspecified functions. Moreover, MODOMICS covers the related diseases and pathways (Dunin-Horkawicz et al., 2006), with sequential updates at regular intervals (Machnicka et al., 2013) (Boccaletto et al., 2018), leading to more attention directed to the rising role of RNA modifications contributing to the nuanced transcriptomic homeostasis from clinicians and scientists (Song et al., 2020).

The fate of an mRNA transcript is determined by a series of events posttranscriptionally, and one of such crucial processes is epitranscriptomic modifications. In general, the process of mRNA epitranscriptomic editing relies on three major types of RNA-modifying proteins (RMPs):

1) writers that deposit RNA modifications, for e.g., methyltransferase-like (METTL) enzyme family members, zinc finger CCCH-type containing 13 (ZC3H13), and VIRMA/KIAA1429 for m^6A, TRMT family members for m^1A, ADARs for A-to-I editing, and NSUNs for m^5C;
2) erasers that remove the epitranscriptomic modifications, for e.g., fat mass- and obesity-associated protein (FTO) for m^6A and AlkB homologs (ALKBH) for m^1A, m^6A, and m^5C;
3) readers that are recruited and recognize the modifications to alter the fate of mRNA transcripts, for e.g., YT521-B homology (YTH) domain family members for m^6A and Aly/REF export factor (ALYREF) for m^5C.

RNAWRE, which was constructed in 2020 by Nie et al. (2020) and apropos to mention, comprises more than 2000 manually curated writers, erasers, and readers. RMP regulation determines whether the previously mentioned epitranscriptomic signatures are installed, removed, or recognized. By dint of Table 1 summary and Figure 1 illustration, types of epitranscriptomic marks and their respective RMPs will not be outlined thoroughly in paragraphs. The concept of how these epitranscriptomic marks and RMP expression affect the existence and severity of ferroptosis will be discussed in later parts and illustrated in the compiled figures.

Detecting epitranscriptomics modifications

Even though the adjustments on nucleotides seem slight and minuscule, finding a way to elucidate the epitranscriptomic marks is never simple and uncomplicated. Consecutive efforts

are required owing to these nanoscopic modifications down to nucleotides. This review will not focus on the in-depth discussion of epitranscriptomic mark detection, given that such an issue has already been brilliantly reviewed elsewhere (Helm & Motorin, 2017) (Sarkar et al., 2021). Nevertheless, we shall highlight the important ones, including NGS-based techniques or mass spectrometry-based techniques.

Next-generation sequencing-based techniques

AlkB-facilitated RNA methylation sequencing (ARM-seq) (Cozen et al., 2015), combines reverse transcription (RT) and enzymatic demethylation and relies on detecting truncations due to existing methylated nucleosides during RT. Localization of truncations from high-throughput sequencing navigates the potential methylated sites in RNA transcripts, except when the reaction reaches RT-silent bases such as pseudouridine, ribothymidine, or m^5C. Aside from RT-methods, antibody-dependent assays like m^6A-seq (for m^6A) or m^1A-seq (for m^1A), MeRIP-seq (Dominissini et al., 2015), CLIP-based strategies (Ke et al., 2015), PAR-CLIP–MeRIP (Liu et al., 2015), miCLIP (for methylated nucleosides in RNA) (Hawley & Jaffrey, 2019), and suicide enzyme trap (for identification of methyltransferase targets on RNA strands) (Khoddami & Cairns, 2013) have also revolutionized the epitranscriptomic mark detection. By eliminating the possibility of having RT-arrest and mis-incorporation of nucleosides during RT like RT-based detection, enrichment-based methods stand out with their superb specificity to methylated nucleosides.

Mass spectrometry-based techniques

Dating back to 1977, McCloskey and Nishimura were the first to utilize MS to detect tRNA modifications down to nucleoside resolution. The RNA MS regimen relies on enzymatic digestion/reduction of RNA strands to nucleosides/nucleotides with the nucleic acid backbone being eliminated, and the downward workflow is analogous to metabolite MS, including ionizing the compound and deflecting the molecule in an electric field, followed by a magnetic field. The determination of an m/z ratio greatly depends on retention time, molecular mass, and fragmentation patterns in tandem mass spectrometry (MS/MS) for the identification of modification residues (Helm & Motorin, 2017). Variations of MS include combination with liquid chromatography purification on RNA fragments *a posteriori* nuclease such as RNase T1 and MC1, followed by electrospray ionization (ESI) and MS/MS, entitled LC-ESI-MS/MS (Yuan, 2017). Two years ago, Wein et al. (2020) constructed an open-source database for documenting RNA MS data named NucleicAcidSearchEngine (NASE). Heiss et al. (2021) have also recreated LC-MS/MS by combining nucleic acid isotope labeling (NAIL) and MS, entitled NAIL-MS, to address the dynamic nature of epitranscriptomic modifications that the currently available MS protocols lack the ability to tackle. Nonetheless, despite the comprehensiveness offered by MS, respective localization of modifications in the RNA environment will be completely lost and irretrievable.

Ironing out the iron: investigating ferroptosis

The first observation on erastin-induced lethality in engineered Ras-mutant human foreskin fibroblasts discovered distinctive morphological features and biochemical machineries compared to traditional programmed cell death (PCD). *Ferroptosis*, coined in 2012 under the work of Dixon et al. (2012), has shed light on the field of PCD and has, henceforth, attracted heed from cell biologists. Devoid of apoptotic morphological features, such as apoptotic body formation or nuclear fragmentation, ferroptotic cells are characterized by increased mitochondrial densities and reduction of mitochondrial crista that are not observed in the conventional PCD (Li et al., 2020). The discovery of iron chelation also denoted an unprecedented biochemical pathway in regulating ferroptosis. Even so, much of our knowledge in ferroptosis is still not complete nor is satisfactory enough to intervene this mechanistic pathway in the current clinical settings.

In the history of ferroptosis characterization, the pioneering finding of erastin has led to the comprehensive dissection of ferroptosis in recent years. Large-scale screening experiments in surveying the killing effects of a multitude of compounds exerted on cancer cells *via* mitochondrial voltage-dependent anion channels, conducted by Dolma et al. (2003), have directed the very first discovery of erastin. Few years afterward, erastin treatment was investigated, and the results of lipid-related oxidative stress were noticed by Yagoda et al. (2007). The RAS-selective lethal 3 (RSL3) was brought up in 2008 from another large-scale synthetic lethal screening by Yang & Stockwell (2008) in the presence of RAS (therefore, the nomenclature). Dixon et al. (2012) officially entitled this iron-dependent cell death as "*ferroptosis*". Successful characterization has then propagated more in-depth discoveries, including ferrostatin-1 (fer-1) inhibition of ferroptosis, mitochondria independency (Gaschler et al., 2018), sorafenib induction of ferroptosis (Lachaier et al., 2014) (Louandre et al., 2013), system X_c^- being inhibited by erastin (Dixon et al., 2014) (grounded in the fact that cystine deprivation leads to glutathione-dependent cell death long before the characterization of ferroptosis (Eagle, 1955) (Hinson et al., 2010)), glutathione peroxidase 4 (GPX4) participation (Yang et al., 2014), and enormous regulatory ferroptotic inducers (other than erastin, e.g., DPIs, FIN56, and FINO2) and inhibitors (e.g., iron chelators, vitamin E, SRS8-24, and CA-1).

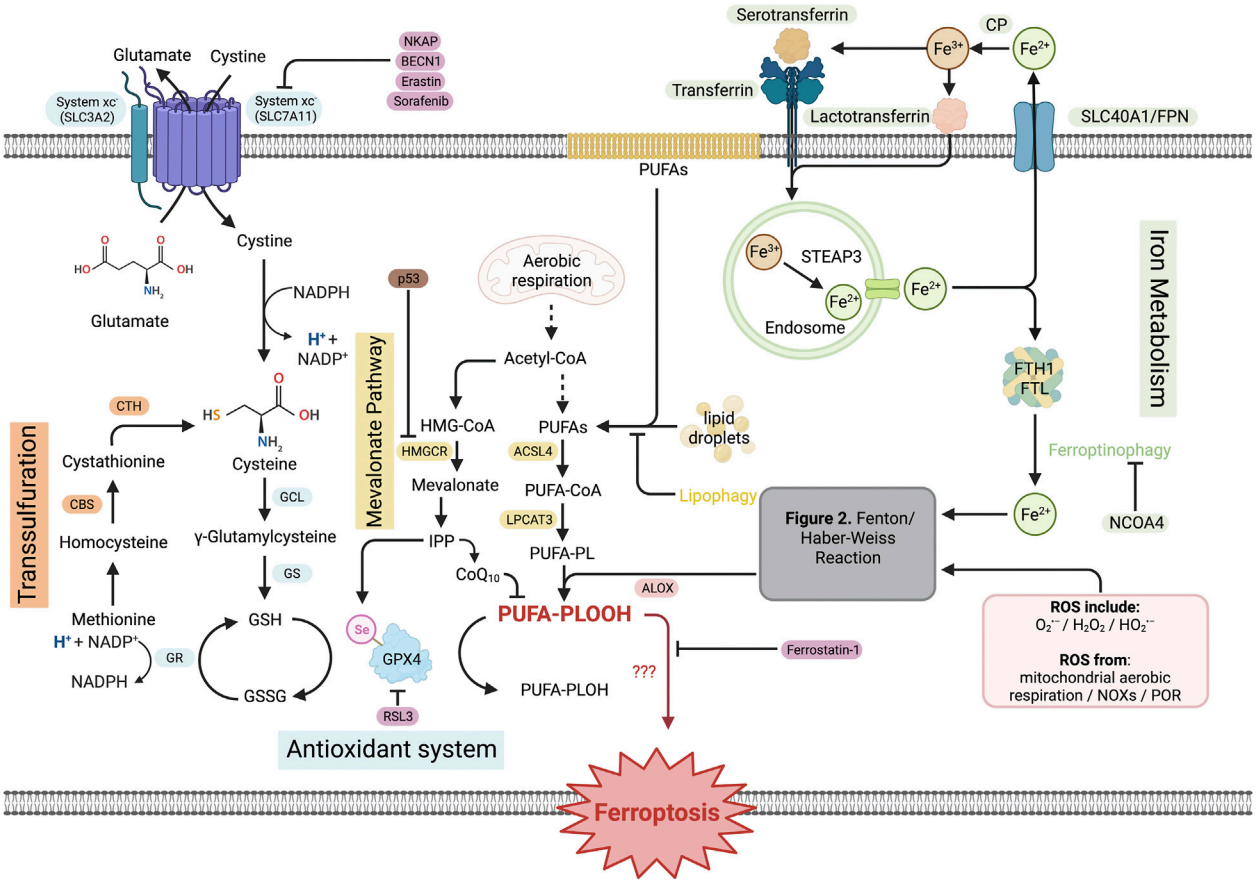

FIGURE 2
Pathways of ferroptosis. The entirety of ferroptosis signaling is complex and orchestrated by different sub-pathways, along with a multitude of regulatory proteins or substances. The antioxidant system starts with system xc^- activity that assists the exchange of cystine and glutamate. Intracellular cystine is converted, in multi-step reactions, to GSH. The transsulfuration reaction starts with conversion of intracellular methionine to cysteine and joins the antioxidant system to enhance GSH production. Lipid ROS production from membrane PUFAs, intracellular lipid droplets, and acetyl-CoA resulted from mitochondrial aerobic respiration, which is negatively regulated by lipophagy, provides predominant lipid source to produce lipid ROS by joining the Fenton/Haber–Weiss reaction. Iron metabolism starts with Fe^{3+} endocytosis initiated by a transferrin receptor, and STEAP3-mediated reduction to Fe^{2+} takes place in endosome. Fe^{2+} joins LIP by FTH1/FTL. Ferritinophagy triggers the release of Fe^{2+} to join intracellular ROS pool and proceeds to the Fenton/Haber–Weiss reaction to produce lipid ROS. Taken together, the PUFA-PLOOH resulting from the reactions induces ferroptotic damage with the mechanism that lacks exactitude. Created with BioRender.com.

Delineating the mechanisms of ferroptosis

Ferroptosis starts with the production of lipid peroxides as a general cellular suicidal program with an iron-mediated oxidative mechanism. Cellular reactions exhibit redox equilibrium, and disruption of redox equilibrium is attributed to the synthesis and accumulation of reactive oxygen species. Definitive ROS, including superoxide anion ($O_2^{-}\bullet$), hydrogen peroxide (H_2O_2), hydroxyl radicals (HO•), hydroperoxides (ROOH), and hydroxyl radicals (ROO•), are formed by partial reduction of oxygen. ROS are generated inevitably from oxidative phosphorylation in mitochondria to cellular respiration, and the endogenous antioxidant system is instrumental to remove the oxidative stress. It has been held as an axiom that ROS accumulation also lays the groundwork of multiple pathologies, given its roles in cellular damage in diabetic cardiomyopathy (Kaludercic & Di Lisa, 2020), atherosclerosis (Yang et al., 2017), neurological complications (Manoharan et al., 2016), and in cell growth, especially in cancers (Aggarwal et al., 2019) (Dias Amoedo et al., 2020) (Tien Kuo & Savaraj, 2006) (Zeng et al., 2021). A detailed mechanistic overview of ferroptosis is illustrated in Figure 2.

What lies at the cardiac part of this cellular iron-mediated killing is lipid ROS. The most abundant ROS, superoxide, is generated by cytochrome P450 and NADPH oxidases (NOXs) partial reduction, forming H_2O_2 by superoxide dismutase (SOD), and the anions proceed to the production of hydroxyl radicals with the catalytic role of iron. In fact, published articles only

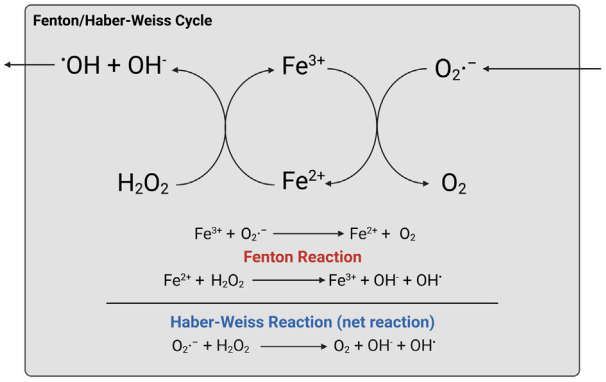

FIGURE 3
Fenton/Haber–Weiss reaction. Created with BioRender.com.

documented the iron participation as the Fenton reaction, and the final Haber–Weiss reaction, obtained after balancing chemical equations from Fenton and the others, was less recognized than the Fenton reaction. Ferrous ions (Iron (II) or Fe^{2+}) are mainly produced from the labile iron pool (LIP) and upon radical attack to heme groups with iron–sulfur (Fe–S) clusters (Gomez et al., 2014). Oxidation of ferrous to ferric ion (iron (III) or Fe^{3+}) facilitates free radical formation from H_2O_2, whilst the O_2^{-}• radicals are also oxidized to harmless O_2 as a net Haber–Weiss reaction. Taken together, the iron-mediated production of hydroxyl radicals is a "superoxide-driven Fenton-catalyzing Haber–Weiss reaction," or Fenton/Haber–Weiss reaction, as illustrated in Figure 3.

After the Paleoproterozoic Great Oxygenation Event (GOE), lives on the earth were subjected to oxidation readily, especially for polyunsaturated lipids with bis-allylic carbons (Wagner et al., 1994). The victim of such ROS attack in ferroptosis after all the aforementioned series of events is, therefore, polyunsaturated fatty acids (PUFAs). Under normal physiology, PUFAs, including arachidonic acid, eicosapentaenoic acid (EPA), and docosahexaenoic acid (DHA), are situated in the cell membrane. The attack from accumulating free radicals to PUFAs, otherwise named peroxidation reaction, generates phospholipid free radicals (PL•) and, therefore, PUFA-containing-phospholipid hydroperoxides (PL-PUFA (PE)-OOH, PLOOH in short) (Forcina & Dixon, 2019), facilitated by different lipoxygenases (LOXs). It was also demonstrated that depletion of an acyl-CoA synthetase ACSL4 and LPCAT3 esterification enzyme inhibited ferroptosis (Doll et al., 2017) (Yuan et al., 2016). PLOOHs execute the unelucidated last hit to the cell membrane and initiate disruption to cellular integrity, leading to ferroptosis.

The transmembrane cystine/glutamate exchanger commences the work to initiate a ferroptosis-specific antioxidant system. System x_c^-, which was found to be inhibited by erastin, serves as an amino acid homeostatic control with the exchange of extracellular L-cystine and intracellular L-glutamate. Dissecting the antiporter, it consists of two subunits, a light chain solute carrier family 7 member 11 (SLC7A11) and a heavy chain subunit SLC family 3 member 2 (SLC3A2), which are targeted by respective inhibitors. Intracellular cysteine from cystine reduction facilitates the production of glutathione (GSH) that is catalyzed by glutamate–cysteine ligase catalytic subunit (GCLC) (which is inhibited by buthionine sulfoximine (BSO)) and then by glutathione synthetase (GSS). The classical redox-associated glutathione system (GSH and oxidized GSH disulfide (GSSG)) comes in to play a role in antioxidant defense, proven back in the 90s (Ceballos-Picot et al., 1996). Glutathione peroxidase 4 (GPX4) protects the cells from ferroptotic death by reducing toxic PLOOHs to PUFA-containing-phospholipid hydroxides (PL-PUFA (PE)-OH, PLOH in short), with the presence of selenium (Liu et al., 2021) and GSH (Ursini & Maiorino, 2020). While PLOHs appear to be non-ferroptogenic (not ferroptosis-inducing), this marks the end of the brief ferroptosis mechanisms as the homeostasis is achieved.

Ferroptosis has been observed in different pathologies. For example, in Alzheimer's disease that is characterized by prominent brain cell death, β-amyloid plaques and neurofibrillary tangles were investigated, and excess iron accumulation and downregulation of iron exporter, ferroportin1, were observed, thereby explaining the oxidative stress exerted and promoting the AD cognitive impairment (Bao et al., 2021). In renal ischemia/reperfusion injury (IRI), ferroptosis is proven in the mediation of renal tubule-synchronized necrosis, and a novel third-generation ferrostatin 16–86 could rescue or protect the tubular damage that contributes to IRI (Linkermann et al., 2014). In cancer, particularly in colorectal cancer, it was evident that ferroptosis promotes metabolic rewiring, or the Warburg effect, which favors cancer cell growth, as well as suppresses ferroptosis sensitivity by inducing ROS production and activating nuclear factor erythroid 2-related factor 2 (NRF2) (Yuan et al., 2021). These are just few examples that ferroptosis correlates with disease progression, and more details about various pathologies can be found in other good articles such as Jiang et al. (2021b) and Yan et al. (2021) for readers' reference.

Ferroptosis and epitranscriptomics: neither two monologues nor a mere duologue

Due to technological advancements in investigating epitranscriptomics and firmer theoretical bedrock on the principle of ferroptosis, both topics are gaining escalating heed from scientists. However, the association between epitranscriptomics and ferroptosis has yet been organized. Thence, with reference to the preliminary background

TABLE 2 Discovered epitranscriptomic marks on ferroptosis-related proteins.

Disease model	Mechanisms in ferroptosis	Epitranscriptomic mark-associated protein	Discovery	Reference
Lung cells (A549)	Lipoxygenase pathway, arachidonic acid metabolic process, and response to selenium ion	m6A reader–YTHDF2	BPQDs increase the global m6A level and decrease ALKBH5 to promote ferroptosis-related pathways	Ruan et al. (2021)
Acute myeloid leukemia cell line (TF-1)	GPX4 antioxidant	m6A eraser–FTO	In-house GNRa-CSP12 sensitized AML cells to TKIs by FTO-m^{6}A hypomethylation on GPX4 to promote ferroptosis	Du et al. (2021)
AC16 cardiomyocytes and neonatal rat ventricle cardiomyocytes	Iron uptake ROS production	m^{6}A writer–METTL14	Doxorubicin induced METTL14 and lncRNA KCNQ1OT1 to inhibit miR-7-5p, triggering the TFRC increase to promote ferroptosis	Zhuang et al. (2021)
Human hepatic malignant and normal cell lines	Cysteine import	m^{6}A writer–METTL14; m^{6}A reader–YTHDF2	METTL14 suppression in SLC7A11 and thereafter degradation relied on the YTHDF2-dependent pathway were observed under hypoxia	Fan et al. (2021)
Malignant and normal lung cell lines	Cysteine import	m6A writer–METTL3; m6A reader–YTHDF1	METTL3 modifies the m^{6}A level in SLC7A11 by recruiting YTHDF1 to promote ferroptosis in LUAD.	Xu et al. (2022)
Human liver tissues	Cysteine import	m^{6}A writer–METTL4; m6A reader–YTHDF1; m6A eraser–FTO	METTL4 upregulation and FTO downregulation increase global m^{6}A level in BECN1 mRNA that originally inhibit SLC7A11, and the YTHDF1 increase promotes BECN1 stability to inhibit cysteine intake and promote ferroptosis in HSCs	Shen et al. (2021)
Mice HSCs	Cysteine import	m6A reader–YTHDF1; m6A eraser–FTO	DHA downregulated FTO to increase m^{6}A in BECN1 mRNA, leading to YTHDF1-dependent enhanced stability to inhibit SLC7A11 cysteine–glutamate exchange, promoting HSC ferroptosis	Shen et al. (2022)
Human glioblastoma cell lines (U87MG and U251)	Cysteine import	m^{6}A reader–NKAP	NKAP binds to m^{6}A in SLC7A11 transcripts and promotes transcriptional splicing and maturation to suppress ferroptosis in glioblastoma cells	Sun et al. (2022)
CRC and adenoma tissues	Ferritinophagy	m6A eraser–ALKBH5	CircRNA cIARS interacts with ALKBH5 to positively regulate ferritinophagy in SF-treated HCC cells	Liu et al. (2020)
BMSCs in mice	Erastin-induced ferroptotic cysteine transport	m5C writer–NSUN5	NSUN5 downregulation is correlated with reduced m^{5}C in FTH1/FTL, contributing to ferroptosis	Liu et al. (2022)
Human glioma cell line (U251)	Glutamine metabolism in the antioxidant system	A-to-I editing writer–ADAR	ATXN8OS was found to interact with ADAR and downstream interaction with ferroptosis-related targets is suspected to mediate ferroptosis. These targets include GLS2	Luo et al. (2022)

knowledge, we summarize some updates on ferroptosis and epitranscriptomic modifications in recent years and attempt to put a new perspective on the investigation of ferroptosis to facilitate the demystification of any connection between epitranscriptomics and ferroptosis.

Feed-forward interaction: how do epitranscriptomics shape the niche of ferroptotic homeostasis?

Ferroptosis and m^{6}A

Being the most characterized epitranscriptomic modification, m^{6}A has been widely investigated for its relationship with ferroptosis in different pathological phenomena, including cell cycle, drug resistance, biomarkers, or disease signatures. A couple of m^{6}A writers, readers, and erasers have been focused to study as a direct or indirect target to mediate ferroptosis, sorted out in Table 2. METTL14 upregulation resulted from doxorubicin treatment in AC16 cardiomyocytes and neonatal rat ventricle cardiomyocytes, and m^{6}A "writing" action was observed to be catalyzed on a sponge lncRNA KCNQ1OT1 for miR-7-5p, which cooperated with RNA-binding protein IGF2BP1 to inhibit miR-7-5p activity, leading to transferrin receptor upregulation and iron uptake increase. Such a phenomenon joins the ferroptotic signaling and increases the opportunity of having lipid peroxidation (Zhuang et al., 2021). Another research echoes

with the miR-7-5p and doxorubicin chemoresistance study carried out by Song et al. (2021) on exosomal miR-4443 and cisplatin resistance in non-small cell lung carcinoma. Tantamount to apoptosis, cisplatin simultaneously acts as a dual trigger of apoptosis and ferroptosis to kill cancer cells (Guo et al., 2018). On this groundwork, in tumoral and normal tissue-derived exosomes, their team discovered a distinctive expression level of miR-4443 between cisplatin-sensitive and cisplatin-resistant tissues and cell lines, and further functional and bioinformatics studies confirmed that m^6A writer METTL3 was negatively regulated by miR-4443 overexpression to lower the m^6A level on ferroptosis-suppressing protein 1 (FSP1), inhibiting its activity to suppress ferroptosis. Bioinformatics analyses on lncRNAs also revealed m^6A regulators, namely, FMR1, HNRNPC, METTL16, METTL3, and METTL5, were expressed in higher levels than those in ferroptosis low-risk groups (Jiang, W. et al., 2021a). The aforementioned studies provided evidence that epitranscriptomics are phenomenally involved in ferroptotic disease models, particularly in drug-resistant cancers that have the characteristic to overcome cell death events. As ferroptosis is a new type of PCD, the participation of miRNA, lncRNA, or other types of RNA with distinguished epitranscriptomic features is worth investigating to obtain a complete picture of its disease progress contribution, in order to potentiate clinical relevance for disease manipulation in the future. The theoretical basis on how epitranscriptomics shaped the ferroptosis signaling was also exemplified in pan-cancer *in vitro*, including in hepatocellular carcinoma (Fan et al., 2021), hepatic stellate cells (Shen et al., 2022) (Shen et al., 2021), lung adenocarcinoma (Xu et al., 2022), and glioblastoma (Sun et al., 2022).

Ferroptosis and other epitranscriptomic marks

A majority of the published articles were m^6A-based, and there is a huge lack of epitranscriptomic discoveries regarding other marks on ferroptosis. m^5C is second to m^6A in terms of the level being explored, and the investigation is still ongoing since we are only scratching the surface of the epitranscriptomic modifications aside from m^6A (Liu et al., 2022). In fact, one closely related work that is also one of the most recent discoveries bridging epitranscriptomics and ferroptosis was on m^5C and its exclusive writer NOP2/Sun RNA methyltransferase 5 (NSUN5). In bone marrow-derived mesenchymal stem cells (BMSCs), Liu's group reported a notable downregulation of NSUN5 in ferroptotic cells and unveiled the enhancement of Fe^{2+} ions in NSUN5 depletion *in vitro*. More importantly, NSUN5 overexpression, which was later confirmed as its methylating action on 5′UTR/3′UTR of ferritin heavy chain/light chain (FTH1/FTL), was correlated with TRAP1 recruitment on FTH1/FTL, a protein that governs the intracellular entry of iron ions, confirmed by LC-MS and co-immunoprecipitation (co-IP). Liu's group has impacted both the fields of ferroptosis and epitranscriptomics by expanding the discussion to other base modifications other than the predominant m^6A. Meanwhile, further studies on other disease or cell models, or more superior 3D culture and organoid models, necessitate to be carried out for proof-of-concept.

In addition to m^5C, in triple-negative breast cancer patients, investigating the tumor microenvironment (TME) guided the discovery of a rare epitranscriptomic feature that serves as a potential biomarker in microniches. Using spatial epitranscriptomic analyses on tumor microniches, Lee et al. (2022) sought to profile A-to-I editome and identified high A-to-I editing in GPX4 variants in IF-stained tissues full-length transcriptome. This result fitted their hypothesis that cancer stem cells (CSCs) contain high A-to-I editing characteristic for their niche shaping, and the future validation work can potentiate the druggability of such epitranscriptomic feature in this ferroptotic-signaling protein.

Feedback interaction one: how will lipid ROS accumulation potentially influence the nuanced epitranscriptomic features back?

Cellular signaling in biological systems evolved with harmonized crosstalk and attempting to inspect the entirety via a single chronological representation remains laborious to reach the finality. It becomes interesting whether the accumulating lipid ROS being non-eliminated construct a feedback influence on the epitranscriptomic marks. Oxygen atoms in –OH groups and phosphodiester backbone are the most vulnerable to be subjected to chemical damage or oxidation (Liu et al., 2022), and ROS onslaught has demonstrated evidently in mutations (Niedernhofer et al., 2003), cell arrest (Dixon & Stockwell, 2014), and epitranscriptomic induction (Kumar & Mohapatra, 2021). Particularly in cancer, m^6A induction has been studied and reviewed in response to the production of ROS, and a biphasic and conflicting effect on tumor growth, intriguingly, has been noticed (Chio & Tuveson, 2017) (Yang & Chen, 2021). The potential ROS effect in ferroptosis via epitranscriptomic mediation is hence plausible.

Since the concept of "global m^6A level can be ROS-induced" was revealed, one ROS-induced post-translational regulation on m^6A demethylase was discovered recently (Yu et al., 2021). In this study by Yu et al., human cell lines with high m^6A induced by ROS and determined by m^6A-seq, were employed to survey the intrinsic mechanism that contributed to the elevation, where SUMOylation in m^6A demethylase ALKBH5 was found to be associated using comet analysis, a single-cell gel electrophoresis assay that helps determine DNA damage and repair equilibrium at a single cell level. Particularly, SUMOylation-deficiency in ALKBH5 led to weakened DNA repair in H_2O_2-induced DNA damage, in other words, SUMOylation in ALKBH5 is essential in the increase of global m^6A level by limiting the activity of m^6A

erasers. As ROS also joins the ferroptotic signaling and can lead to ferroptotic cell death, how ROS can potentially construct a stressful environment and add on epitranscriptomic modifications of ferroptosis proteins remains to be extrapolated. Having a feedback loop discovered that thrusts in the cell death process offer a great potential to manipulate the pathways, and the prospects of targeting ferroptosis in therapeutic settings await.

Feedback interaction two: how does iron imbalance contribute to an epitranscriptomic mark level?

Dixon et al. (2012) extensively acknowledged the importance of iron in its mediation to the PCD event by coining the "ferro-" in the nomenclature of the iron-driven cell death, ferroptosis, assisted by the Nomenclature Committee of Cell Death (NCCD). Before then, prominent iron overload was observed among pathologies, such as hereditary hemochromatosis, along with the complications manifested, including organ damage, hypothyroidism, and hypogonadism. Managing iron homeostasis, thence, is necessitated from a medical standpoint, combined with the fact that ferroptosis is also dependent on intracellular iron status. In addition, *en route* to the research on how important iron to ferroptosis is, we also discovered some connections between iron and epitranscriptomic marks upon rummaging articles. We aimed to address the potential association of iron status and epitranscriptomics in ferroptosis and provided upcoming possible research directions to facilitate the elucidation of this mystery.

The fact that heme groups and Fe–S clusters are frequently under the attack of various kinds of ROS is well known (Imlay, 2006). This increases the intracellular level of Fe^{2+} apart from the LIP, though the LIP serves as the predominant source of Fe^{2+}. In fact, perturbations of epitranscriptomics that affect the iron level or iron metabolism have been shown via some direct studies. In a hypopharyngeal squamous cell carcinoma (HPSCC) study by Ye et al. (2020), transcriptomic analyses including m^{6}A-seq, RNA-seq, and RIP-seq identified m^{6}A reader YTHDF1's downstream target transferrin receptor (TFRC), simultaneously linking to poor prognosis in postoperative platinum-based chemoradiotherapy (CCT) or radiation patients in an m^{6}A-dependent manner. HPSCC patients with intratumorally elevated Fe^{2+} were also shown upregulated YTHDF1 expression, and knockdown YTHDF1 in HPSCC cells proved the suppression of cell proliferation and migration ability. Taken together, as YTHDF1 modifies TFRC mRNA in cytosol and modulates transcriptomic stability and fate, relationships between an RMP and an iron metabolism participant were speculated by this pioneering work. Additionally, a pancreatic ductal adenocarcinoma (PDAC) study by Huang et al. (2021) aimed at elucidating the connection of ALKBH5 and iron metabolism, concretely on mRNAs encoding ubiquitin ligase FBXL5 and iron importers SLC25A28 and SLC25A37. ALKBH5 was identified to be mechanistically associated to the RNA decay event for FBXL5, and the team has divulged its unique prognostic ability among multiple m^{6}A regulators analyzed in the study. Considering FBXL5-IRP2 serves as the cardinal part to iron metabolism (Wang et al., 2020), this study adds on the evidence of connecting epitranscriptomic-mediated iron metabolism since the bridge between FBXL5 and ALKBH5 can now be surmised through transcriptomic analyses, and further validation work awaits to confirm.

Prospect and unaddressed questions

Yet, tracing back to the fact that excess intracellular iron leads to disturbed redox imbalance, and hence impaired cellular metabolism, we shall also pay heed to the crosstalk between iron metabolism and epitranscriptomics. Despite limited direct studies on the biological functions, some RMPs are reported to be affected by iron levels. m^{6}A demethylase ALKBH5 was Fe^{2+}-dependent, proven in an optimization research study for downstream screening work by Li et al. (2016). Therefore, it leaves us with the following questions on 1) how much iron level deviation intracellularly can drive impaired ALKBH5 function; 2) how much Fe^{2+} perturbations can lead to redox imbalance, followed by the epitranscriptomic mark writing on RMPS that constitutes to a crosstalk signaling; and 3) what are the signaling paradigms required for iron-driven/ROS-induced epitranscriptomic mark writing and the potential involvement to ferroptosis. There are still many unsolved questions that build around the biological or biomedical conjectures on ferroptosis and epitranscriptomics that begin with iron imbalance and ROS induction. Addressing these outstanding questions shall help determine the direct involvement of distinct components in ferroptosis.

Concluding remarks

In retrospect, investigating a new topic in science has always been regarded as preposterous at the beginning, and the journey of vindication seems to be life-long and with collaborative efforts. Epitranscriptomics have indeed experienced a dejected period due to the lack of technological advancement, but the value *per se* is tantamount to epigenetic modifications owing to its importance in governing the ultimate phenotype of a gene. It is hard for us to ignore the participation of such element being pervasive on gene expression in ferroptosis, a new type of PCD discovered just in recent decades, and is still being explored for its potential clinical relevance. As the evidence regarding epitranscriptomics and ferroptosis began to pile up, with the associated indirect studies on the passengers of both, RMPs or lipid ROS, *videlicet*, we offered additional perspectives for readers

to define the pathways of ferroptosis with respect to epitranscriptomic modifications, and thus to provide foreseeable opportunities toward comprehensiveness of such topics.

Author contributions

JC conceived and wrote the manuscript. GD, YD, and NW commented and provided expertise in ferroptosis. SN secured funding. YD and SN supervised the study and revised the manuscript.

Funding

This project was supported by research funds from the Lim Peng Suan Charitable Trust Research Fund and National Natural Science Foundation of China (81871900). This project was supported in part by the Hong Kong Research Grants Council Area of Excellence Scheme (Ref. AoE/M-401/20) and Research Impact Fund (Ref. R4017-18).

Conflict of interest

The authors declare that the research was conducted in the absence of any commercial or financial relationships that could be construed as a potential conflict of interest.

Publisher's note

All claims expressed in this article are solely those of the authors and do not necessarily represent those of their affiliated organizations, or those of the publisher, the editors, and the reviewers. Any product that may be evaluated in this article, or claim that may be made by its manufacturer, is not guaranteed or endorsed by the publisher.

References

Aggarwal, V., Tuli, H. S., Varol, A., Thakral, F., Yerer, M. B., Sak, K., et al. (2019). Role of reactive oxygen species in cancer progression: Molecular mechanisms and recent advancements. *Biomolecules* 9 (11), E735. doi:10.3390/biom9110735

Bao, W. D., Pang, P., Zhou, X. T., Hu, F., Xiong, W., Chen, K., et al. (2021). Loss of ferroportin induces memory impairment by promoting ferroptosis in Alzheimer's disease. *Cell Death Differ.* 28 (5), 1548–1562. doi:10.1038/s41418-020-00685-9

Boccaletto, P., Machnicka, M. A., Purta, E., Piatkowski, P., Baginski, B., Wirecki, T. K., et al. (2018). Modomics: A database of RNA modification pathways. 2017 update. *Nucleic Acids Res.* 46 (D1), D303–D307. doi:10.1093/nar/gkx1030

Ceballos-Picot, I., Witko-Sarsat, V., Merad-Boudia, M., Nguyen, A. T., Thevenin, M., Jaudon, M. C., et al. (1996). Glutathione antioxidant system as a marker of oxidative stress in chronic renal failure. *Free Radic. Biol. Med.* 21 (6), 845–853. doi:10.1016/0891-5849(96)00233-x

Chio, I. I. C., and Tuveson, D. A. (2017). ROS in cancer: The burning question. *Trends Mol. Med.* 23 (5), 411–429. doi:10.1016/j.molmed.2017.03.004

Cozen, A. E., Quartley, E., Holmes, A. D., Hrabeta-Robinson, E., Phizicky, E. M., and Lowe, T. M. (2015). ARM-Seq: AlkB-facilitated RNA methylation sequencing reveals a complex landscape of modified tRNA fragments. *Nat. Methods* 12 (9), 879–884. doi:10.1038/nmeth.3508

Davis, F. F., and Allen, F. W. (1957). Ribonucleic acids from yeast which contain a fifth nucleotide. *J. Biol. Chem.* 227 (2), 907–915. doi:10.1016/s0021-9258(18)70770-9

Destefanis, E., Avsar, G., Groza, P., Romitelli, A., Torrini, S., Pir, P., et al. (2021). A mark of disease: How mRNA modifications shape genetic and acquired pathologies. *RNA* 27 (4), 367–389. doi:10.1261/rna.077271.120

Dias Amoedo, N., Dard, L., Sarlak, S., Mahfouf, W., Blanchard, W., Rousseau, B., et al. (2020). Targeting human lung adenocarcinoma with a suppressor of mitochondrial superoxide production. *Antioxid. Redox Signal.* 33 (13), 883–902. doi:10.1089/ars.2019.7892

Dixon, S. J., Lemberg, K. M., Lamprecht, M. R., Skouta, R., Zaitsev, E. M., Gleason, C. E., et al. (2012). Ferroptosis: An iron-dependent form of nonapoptotic cell death. *Cell* 149 (5), 1060–1072. doi:10.1016/j.cell.2012.03.042

Dixon, S. J., Patel, D. N., Welsch, M., Skouta, R., Lee, E. D., Hayano, M., et al. (2014). Pharmacological inhibition of cystine-glutamate exchange induces endoplasmic reticulum stress and ferroptosis. *Elife* 3, e02523. doi:10.7554/eLife.02523

Dixon, S. J., and Stockwell, B. R. (2014). The role of iron and reactive oxygen species in cell death. *Nat. Chem. Biol.* 10 (1), 9–17. doi:10.1038/nchembio.1416

Doll, S., Proneth, B., Tyurina, Y. Y., Panzilius, E., Kobayashi, S., Ingold, I., et al. (2017). ACSL4 dictates ferroptosis sensitivity by shaping cellular lipid composition. *Nat. Chem. Biol.* 13 (1), 91–98. doi:10.1038/nchembio.2239

Dolma, S., Lessnick, S. L., Hahn, W. C., and Stockwell, B. R. (2003). Identification of genotype-selective antitumor agents using synthetic lethal chemical screening in engineered human tumor cells. *Cancer Cell* 3 (3), 285–296. doi:10.1016/s1535-6108(03)00050-3

Dominissini, D., Moshitch-Moshkovitz, S., Amariglio, N., and Rechavi, G. (2015). Transcriptome-wide mapping of N^6-Methyladenosine by m^6A-seq. *Methods Enzymol.* 560, 131–147. doi:10.1016/bs.mie.2015.03.001

Du, Y., Han, M., Cao, K., Li, Q., Pang, J., Dou, L., et al. (2021). Gold nanorods exhibit intrinsic therapeutic activity via controlling N6-methyladenosine-based epitranscriptomics in acute myeloid leukemia. *ACS Nano* 15, 17689–17704. doi:10.1021/acsnano.1c05547

Dunin-Horkawicz, S., Czerwoniec, A., Gajda, M. J., Feder, M., Grosjean, H., and Bujnicki, J. M. (2006). Modomics: A database of RNA modification pathways. *Nucleic Acids Res.* 34, D145–D149. doi:10.1093/nar/gkj084

Eagle, H. (1955). Nutrition needs of mammalian cells in tissue culture. *Science* 122 (3168), 501–514. doi:10.1126/science.122.3168.501

Fan, Z., Yang, G., Zhang, W., Liu, Q., Liu, G., Liu, P., et al. (2021). Hypoxia blocks ferroptosis of hepatocellular carcinoma via suppression of METTL14 triggered YTHDF2-dependent silencing of SLC7A11. *J. Cell. Mol. Med.* 25 (21), 10197–10212. doi:10.1111/jcmm.16957

Forcina, G. C., and Dixon, S. J. (2019). GPX4 at the crossroads of lipid homeostasis and ferroptosis. *Proteomics* 19 (18), e1800311. doi:10.1002/pmic.201800311

Frye, M., Harada, B. T., Behm, M., and He, C. (2018). RNA modifications modulate gene expression during development. *Science* 361 (6409), 1346–1349. doi:10.1126/science.aau1646

Gaschler, M. M., Hu, F., Feng, H., Linkermann, A., Min, W., and Stockwell, B. R. (2018). Determination of the subcellular localization and mechanism of action of ferrostatins in suppressing ferroptosis. *ACS Chem. Biol.* 13 (4), 1013–1020. doi:10.1021/acschembio.8b00199

Gilbert, W. V., Bell, T. A., and Schaening, C. (2016). Messenger RNA modifications: Form, distribution, and function. *Science* 352 (6292), 1408–1412. doi:10.1126/science.aad8711

Gomez, M., Perez-Gallardo, R. V., Sanchez, L. A., Diaz-Perez, A. L., Cortes-Rojo, C., Meza Carmen, V., et al. (2014). Malfunctioning of the iron-sulfur cluster assembly machinery in Saccharomyces cerevisiae produces oxidative stress via

an iron-dependent mechanism, causing dysfunction in respiratory complexes. *PLoS One* 9 (10), e111585. doi:10.1371/journal.pone.0111585

Guo, J., Xu, B., Han, Q., Zhou, H., Xia, Y., Gong, C., et al. (2018). Ferroptosis: A novel anti-tumor action for cisplatin. *Cancer Res. Treat.* 50 (2), 445–460. doi:10.4143/crt.2016.572

Hawley, B. R., and Jaffrey, S. R. (2019). Transcriptome-wide mapping of m(6) A and m(6) Am at single-nucleotide resolution using miCLIP. *Curr. Protoc. Mol. Biol.* 126 (1), e88. doi:10.1002/cpmb.88

Heiss, M., Borland, K., Yoluc, Y., and Kellner, S. (2021). Quantification of modified nucleosides in the context of NAIL-MS. *Methods Mol. Biol.* 2298, 279–306. doi:10.1007/978-1-0716-1374-0_18

Helm, M., and Motorin, Y. (2017). Detecting RNA modifications in the epitranscriptome: Predict and validate. *Nat. Rev. Genet.* 18 (5), 275–291. doi:10.1038/nrg.2016.169

Hinson, J. A., Roberts, D. W., and James, L. P. (2010). Mechanisms of acetaminophen-induced liver necrosis. *Handb. Exp. Pharmacol.* 196, 369–405. doi:10.1007/978-3-642-00663-0_12

Huang, R., Yang, L., Zhang, Z., Liu, X., Fei, Y., Tong, W. M., et al. (2021). RNA m(6)A demethylase ALKBH5 protects against pancreatic ductal adenocarcinoma via targeting regulators of iron metabolism. *Front. Cell Dev. Biol.* 9, 724282. doi:10.3389/fcell.2021.724282

Imlay, J. A. (2006). Iron-sulphur clusters and the problem with oxygen. *Mol. Microbiol.* 59 (4), 1073–1082. doi:10.1111/j.1365-2958.2006.05028.x

Jiang, W., Song, Y., Zhong, Z., Gao, J., and Meng, X. (2021a). Ferroptosis-related long non-coding RNA signature contributes to the prediction of prognosis outcomes in head and neck squamous cell carcinomas. *Front. Genet.* 12, 785839. doi:10.3389/fgene.2021.785839

Jiang, X., Stockwell, B. R., and Conrad, M. (2021b). Ferroptosis: Mechanisms, biology and role in disease. *Nat. Rev. Mol. Cell Biol.* 22 (4), 266–282. doi:10.1038/s41580-020-00324-8

Kaludercic, N., and Di Lisa, F. (2020). Mitochondrial ROS formation in the pathogenesis of diabetic cardiomyopathy. *Front. Cardiovasc. Med.* 7, 12. doi:10.3389/fcvm.2020.00012

Ke, S., Alemu, E. A., Mertens, C., Gantman, E. C., Fak, J. J., Mele, A., et al. (2015). A majority of m6A residues are in the last exons, allowing the potential for 3' UTR regulation. *Genes Dev.* 29 (19), 2037–2053. doi:10.1101/gad.269415.115

Khoddami, V., and Cairns, B. R. (2013). Identification of direct targets and modified bases of RNA cytosine methyltransferases. *Nat. Biotechnol.* 31 (5), 458–464. doi:10.1038/nbt.2566

Konno, M., Koseki, J., Asai, A., Yamagata, A., Shimamura, T., Motooka, D., et al. (2019). Distinct methylation levels of mature microRNAs in gastrointestinal cancers. *Nat. Commun.* 10 (1), 3888. doi:10.1038/s41467-019-11826-1

Kumar, S., and Mohapatra, T. (2021). Deciphering epitranscriptome: Modification of mRNA bases provides a new perspective for post-transcriptional regulation of gene expression. *Front. Cell Dev. Biol.* 9, 628415. doi:10.3389/fcell.2021.628415

Lachaier, E., Louandre, C., Godin, C., Saidak, Z., Baert, M., Diouf, M., et al. (2014). Sorafenib induces ferroptosis in human cancer cell lines originating from different solid tumors. *Anticancer Res.* 34 (11), 6417–6422.

Lee, A. C., Lee, Y., Choi, A., Lee, H. B., Shin, K., Lee, H., et al. (2022). Spatial epitranscriptomics reveals A-to-I editome specific to cancer stem cell microniches. *Nat. Commun.* 13 (1), 2540. doi:10.1038/s41467-022-30299-3

Li, F., Kennedy, S., Hajian, T., Gibson, E., Seitova, A., Xu, C., et al. (2016). A radioactivity-based assay for screening human m6A-RNA methyltransferase, METTL3-METTL14 complex, and demethylase ALKBH5. *J. Biomol. Screen.* 21 (3), 290–297. doi:10.1177/1087057115623264

Li, F., Yi, Y., Miao, Y., Long, W., Long, T., Chen, S., et al. (2019a). N(6)-Methyladenosine modulates nonsense-mediated mRNA decay in human glioblastoma. *Cancer Res.* 79 (22), 5785–5798. doi:10.1158/0008-5472.CAN-18-2868

Li, J., Cao, F., Yin, H. L., Huang, Z. J., Lin, Z. T., Mao, N., et al. (2020). Ferroptosis: Past, present and future. *Cell Death Dis.* 11 (2), 88. doi:10.1038/s41419-020-2298-2

Li, T., Hu, P. S., Zuo, Z., Lin, J. F., Li, X., Wu, Q. N., et al. (2019b). METTL3 facilitates tumor progression via an m(6)A-IGF2BP2-dependent mechanism in colorectal carcinoma. *Mol. Cancer* 18 (1), 112. doi:10.1186/s12943-019-1038-7

Linkermann, A., Skouta, R., Himmerkus, N., Mulay, S. R., Dewitz, C., De Zen, F., et al. (2014). Synchronized renal tubular cell death involves ferroptosis. *Proc. Natl. Acad. Sci. U. S. A.* 111 (47), 16836–16841. doi:10.1073/pnas.1415518111

Liu, J., Ren, Z., Yang, L., Zhu, L., Li, Y., Bie, C., et al. (2022). The NSUN5-FTH1/FTL pathway mediates ferroptosis in bone marrow-derived mesenchymal stem cells. *Cell Death Discov.* 8 (1), 99. doi:10.1038/s41420-022-00902-z

Liu, L., Wang, M., Gong, N., Tian, P., and Deng, H. (2021). Se improves GPX4 expression and SOD activity to alleviate heat-stress-induced ferroptosis-like death in goat mammary epithelial cells. *Anim. Cells Syst.* 25 (5), 283–295. doi:10.1080/19768354.2021.1988704

Liu, N., Dai, Q., Zheng, G., He, C., Parisien, M., and Pan, T. (2015). N(6)-methyladenosine-dependent RNA structural switches regulate RNA-protein interactions. *Nature* 518 (7540), 560–564. doi:10.1038/nature14234

Liu, Z., Wang, Q., Wang, X., Xu, Z., Wei, X., and Li, J. (2020). Circular RNA cIARS regulates ferroptosis in HCC cells through interacting with RNA binding protein ALKBH5. *Cell Death Discov.* 6, 72. doi:10.1038/s41420-020-00306-x

Louandre, C., Ezzoukhry, Z., Godin, C., Barbare, J. C., Maziere, J. C., Chauffert, B., et al. (2013). Iron-dependent cell death of hepatocellular carcinoma cells exposed to sorafenib. *Int. J. Cancer* 133 (7), 1732–1742. doi:10.1002/ijc.28159

Luo, J., Bai, R., Liu, Y., Bi, H., Shi, X., and Qu, C. (2022). Long non-coding RNA ATXN8OS promotes ferroptosis and inhibits the temozolomide-resistance of gliomas through the ADAR/GLS2 pathway. *Brain Res. Bull.* 186, 27–37. doi:10.1016/j.brainresbull.2022.04.005

Machnicka, M. A., Milanowska, K., Osman Oglou, O., Purta, E., Kurkowska, M., Olchowik, A., et al. (2013). Modomics: A database of RNA modification pathways--2013 update. *Nucleic Acids Res.* 41, D262–D267. doi:10.1093/nar/gks1007

Manoharan, S., Guillemin, G. J., Abiramasundari, R. S., Essa, M. M., Akbar, M., and Akbar, M. D. (2016). The role of reactive oxygen species in the pathogenesis of alzheimer's disease, Parkinson's disease, and huntington's disease: A mini review. *Oxid. Med. Cell. Longev.* 2016, 8590578. doi:10.1155/2016/8590578

Nie, F., Feng, P., Song, X., Wu, M., Tang, Q., and Chen, W. (2020). Rnawre: A resource of writers, readers and erasers of RNA modifications. *Database* 2020, baaa049. doi:10.1093/database/baaa049

Niedernhofer, L. J., Daniels, J. S., Rouzer, C. A., Greene, R. E., and Marnett, L. J. (2003). Malondialdehyde, a product of lipid peroxidation, is mutagenic in human cells. *J. Biol. Chem.* 278 (33), 31426–31433. doi:10.1074/jbc.M212549200

Pereira, M., Francisco, S., Varanda, A. S., Santos, M., Santos, M. A. S., and Soares, A. R. (2018). Impact of tRNA modifications and tRNA-modifying enzymes on proteostasis and human disease. *Int. J. Mol. Sci.* 19 (12), E3738. doi:10.3390/ijms19123738

Perry, R. P., and Kelley, D. E. (1974). Existence of methylated messenger RNA in mouse L cells. *Cell* 1, 37–42. doi:10.1016/0092-8674(74)90153-6

Rana, A. K., and Ankri, S. (2016). Reviving the RNA world: An insight into the appearance of RNA methyltransferases. *Front. Genet.* 7, 99. doi:10.3389/fgene.2016.00099

Ranjan, N., and Leidel, S. A. (2019). The epitranscriptome in translation regulation: mRNA and tRNA modifications as the two sides of the same coin? *FEBS Lett.* 593 (13), 1483–1493. doi:10.1002/1873-3468.13491

Ruan, F., Zeng, J., Yin, H., Jiang, S., Cao, X., Zheng, N., et al. (2021). RNA m6A modification alteration by black phosphorus quantum dots regulates cell ferroptosis: Implications for nanotoxicological assessment. *Small Methods* 5 (3), e2001045. doi:10.1002/smtd.202001045

Sarkar, A., Gasperi, W., Begley, U., Nevins, S., Huber, S. M., Dedon, P. C., et al. (2021). Detecting the epitranscriptome. *Wiley Interdiscip. Rev. RNA* 12 (6), e1663. doi:10.1002/wrna.1663

Shen, M., Guo, M., Li, Y., Wang, Y., Qiu, Y., Shao, J., et al. (2022). m(6)A methylation is required for dihydroartemisinin to alleviate liver fibrosis by inducing ferroptosis in hepatic stellate cells. *Free Radic. Biol. Med.* 182, 246–259. doi:10.1016/j.freeradbiomed.2022.02.028

Shen, M., Li, Y., Wang, Y., Shao, J., Zhang, F., Yin, G., et al. (2021). N(6)-methyladenosine modification regulates ferroptosis through autophagy signaling pathway in hepatic stellate cells. *Redox Biol.* 47, 102151. doi:10.1016/j.redox.2021.102151

Shi, H., Wei, J., and He, C. (2019). Where, when, and how: Context-dependent functions of RNA methylation writers, readers, and erasers. *Mol. Cell* 74 (4), 640–650. doi:10.1016/j.molcel.2019.04.025

Song, H., Liu, D., Dong, S., Zeng, L., Wu, Z., Zhao, P., et al. (2020). Epitranscriptomics and epiproteomics in cancer drug resistance: Therapeutic implications. *Signal Transduct. Target. Ther.* 5 (1), 193. doi:10.1038/s41392-020-00300-w

Song, Z., Jia, G., Ma, P., and Cang, S. (2021). Exosomal miR-4443 promotes cisplatin resistance in non-small cell lung carcinoma by regulating FSP1 m6A modification-mediated ferroptosis. *Life Sci.* 276, 119399. doi:10.1016/j.lfs.2021.119399

Sun, S., Gao, T., Pang, B., Su, X., Guo, C., Zhang, R., et al. (2022). RNA binding protein NKAP protects glioblastoma cells from ferroptosis by promoting SLC7A11 mRNA splicing in an m(6)A-dependent manner. *Cell Death Dis.* 13 (1), 73. doi:10.1038/s41419-022-04524-2

Suzuki, T. (2021). The expanding world of tRNA modifications and their disease relevance. *Nat. Rev. Mol. Cell Biol.* 22 (6), 375–392. doi:10.1038/s41580-021-00342-0

Terajima, H., Yoshitane, H., Ozaki, H., Suzuki, Y., Shimba, S., Kuroda, S., et al. (2017). ADARB1 catalyzes circadian A-to-I editing and regulates RNA rhythm. *Nat. Genet.* 49 (1), 146–151. doi:10.1038/ng.3731

Tien Kuo, M., and Savaraj, N. (2006). Roles of reactive oxygen species in hepatocarcinogenesis and drug resistance gene expression in liver cancers. *Mol. Carcinog.* 45 (9), 701–709. doi:10.1002/mc.20240

Ursini, F., and Maiorino, M. (2020). Lipid peroxidation and ferroptosis: The role of GSH and GPx4. *Free Radic. Biol. Med.* 152, 175–185. doi:10.1016/j.freeradbiomed.2020.02.027

Visvanathan, A., Patil, V., Arora, A., Hegde, A. S., Arivazhagan, A., Santosh, V., et al. (2018). Essential role of METTL3-mediated m(6)A modification in glioma stem-like cells maintenance and radioresistance. *Oncogene* 37 (4), 522–533. doi:10.1038/onc.2017.351

Wagner, B. A., Buettner, G. R., and Burns, C. P. (1994). Free radical-mediated lipid peroxidation in cells: Oxidizability is a function of cell lipid bis-allylic hydrogen content. *Biochemistry* 33 (15), 4449–4453. doi:10.1021/bi00181a003

Wang, H., Shi, H., Rajan, M., Canarie, E. R., Hong, S., Simoneschi, D., et al. (2020). FBXL5 regulates IRP2 stability in iron homeostasis via an oxygen-responsive [2Fe2S] cluster. *Mol. Cell* 78 (1), 31–41. doi:10.1016/j.molcel.2020.02.011

Wei, J., and He, C. (2021). Chromatin and transcriptional regulation by reversible RNA methylation. *Curr. Opin. Cell Biol.* 70, 109–115. doi:10.1016/j.ceb.2020.11.005

Wein, S., Andrews, B., Sachsenberg, T., Santos-Rosa, H., Kohlbacher, O., Kouzarides, T., et al. (2020). A computational platform for high-throughput analysis of RNA sequences and modifications by mass spectrometry. *Nat. Commun.* 11 (1), 926. doi:10.1038/s41467-020-14665-7

Xu, Y., Lv, D., Yan, C., Su, H., Zhang, X., Shi, Y., et al. (2022). METTL3 promotes lung adenocarcinoma tumor growth and inhibits ferroptosis by stabilizing SLC7A11 m(6)A modification. *Cancer Cell Int.* 22 (1), 11. doi:10.1186/s12935-021-02433-6

Xue, C., Zhao, Y., Li, G., and Li, L. (2021). Multi-omic analyses of the m(5)C regulator ALYREF reveal its essential roles in hepatocellular carcinoma. *Front. Oncol.* 11, 633415. doi:10.3389/fonc.2021.633415

Yagoda, N., von Rechenberg, M., Zaganjor, E., Bauer, A. J., Yang, W. S., Fridman, D. J., et al. (2007). RAS-RAF-MEK-dependent oxidative cell death involving voltage-dependent anion channels. *Nature* 447 (7146), 864–868. doi:10.1038/nature05859

Yan, H. F., Zou, T., Tuo, Q. Z., Xu, S., Li, H., Belaidi, A. A., et al. (2021). Ferroptosis: Mechanisms and links with diseases. *Signal Transduct. Target. Ther.* 6 (1), 49. doi:10.1038/s41392-020-00428-9

Yang, B., and Chen, Q. (2021). Cross-talk between oxidative stress and m(6)A RNA methylation in cancer. *Oxid. Med. Cell. Longev.* 2021, 6545728. doi:10.1155/2021/6545728

Yang, W. S., SriRamaratnam, R., Welsch, M. E., Shimada, K., Skouta, R., Viswanathan, V. S., et al. (2014). Regulation of ferroptotic cancer cell death by GPX4. *Cell* 156 (1-2), 317–331. doi:10.1016/j.cell.2013.12.010

Yang, W. S., and Stockwell, B. R. (2008). Synthetic lethal screening identifies compounds activating iron-dependent, nonapoptotic cell death in oncogenic-RAS-harboring cancer cells. *Chem. Biol.* 15 (3), 234–245. doi:10.1016/j.chembiol.2008.02.010

Yang, X., Hu, X., Liu, J., Wang, R., Zhang, C., Han, F., et al. (2020). N6-methyladenine modification in noncoding RNAs and its function in cancer. *Biomark. Res.* 8 (1), 61. doi:10.1186/s40364-020-00244-x

Yang, X., Li, Y., Li, Y., Ren, X., Zhang, X., Hu, D., et al. (2017). Oxidative stress-mediated atherosclerosis: Mechanisms and therapies. *Front. Physiol.* 8, 600. doi:10.3389/fphys.2017.00600

Ye, J., Wang, Z., Chen, X., Jiang, X., Dong, Z., Hu, S., et al. (2020). YTHDF1-enhanced iron metabolism depends on TFRC m(6)A methylation. *Theranostics* 10 (26), 12072–12089. doi:10.7150/thno.51231

Yin, L., Zhu, X., Novak, P., Zhou, L., Gao, L., Yang, M., et al. (2021). The epitranscriptome of long noncoding RNAs in metabolic diseases. *Clin. Chim. Acta.* 515, 80–89. doi:10.1016/j.cca.2021.01.001

Yu, F., Wei, J., Cui, X., Yu, C., Ni, W., Bungert, J., et al. (2021). Post-translational modification of RNA m6A demethylase ALKBH5 regulates ROS-induced DNA damage response. *Nucleic Acids Res.* 49 (10), 5779–5797. doi:10.1093/nar/gkab415

Yuan, B. F. (2017). Liquid chromatography-mass spectrometry for analysis of RNA adenosine methylation. *Methods Mol. Biol.* 1562, 33–42. doi:10.1007/978-1-4939-6807-7_3

Yuan, H., Li, X., Zhang, X., Kang, R., and Tang, D. (2016). Identification of ACSL4 as a biomarker and contributor of ferroptosis. *Biochem. Biophys. Res. Commun.* 478 (3), 1338–1343. doi:10.1016/j.bbrc.2016.08.124

Yuan, Y., Ni, S., Zhuge, A., Li, B., and Li, L. (2021). Iron regulates the Warburg effect and ferroptosis in colorectal cancer. *Front. Oncol.* 11, 614778. doi:10.3389/fonc.2021.614778

Zeng, J., Li, M., Xu, J. Y., Xiao, H., Yang, X., Fan, J. X., et al. (2021). Aberrant ROS mediate cell cycle and motility in colorectal cancer cells through an oncogenic CXCL14 signaling pathway. *Front. Pharmacol.* 12, 764015. doi:10.3389/fphar.2021.764015

Zhuang, S., Ma, Y., Zeng, Y., Lu, C., Yang, F., Jiang, N., et al. (2021). METTL14 promotes doxorubicin-induced cardiomyocyte ferroptosis by regulating the KCNQ1OT1-miR-7-5p-TFRC axis. *Cell Biol. Toxicol.* doi:10.1007/s10565-021-09660-7

frontiers | Frontiers in Cell and Developmental Biology

TYPE Review
PUBLISHED 16 September 2022
DOI 10.3389/fcell.2022.982549

OPEN ACCESS

EDITED BY
Dan Lindholm,
University of Helsinki, Finland

REVIEWED BY
Maija Liisa Castrén,
University of Helsinki, Finland
Lisa Marie Julian,
Simon Fraser University, Canada

*CORRESPONDENCE
Lau Benson Wui-Man,
benson.lau@polyu.edu.hk

SPECIALTY SECTION
This article was submitted to Stem Cell Research,
a section of the journal
Frontiers in Cell and Developmental Biology

RECEIVED 30 June 2022
ACCEPTED 01 September 2022
PUBLISHED 16 September 2022

CITATION
Chan JN-M, Sánchez-Vidaña DI, Anoopkumar-Dukie S, Li Y and Benson Wui-Man L (2022), RNA-binding protein signaling in adult neurogenesis. *Front. Cell Dev. Biol.* 10:982549. doi: 10.3389/fcell.2022.982549

RNA-binding protein signaling in adult neurogenesis

Jackie Ngai-Man Chan[1], Dalinda Isabel Sánchez-Vidaña[1,2], Shailendra Anoopkumar-Dukie[3], Yue Li[4] and Lau Benson Wui-Man[1,2]*

[1]Department of Rehabilitation Sciences, The Hong Kong Polytechnic University, Hong Kong, Hong Kong SAR, China, [2]Mental Health Research Centre, The Hong Kong Polytechnic University, Hong Kong, Hong Kong SAR, China, [3]School of Pharmacy and Medical Sciences, Griffith University, Gold Coast, QLD, Australia, [4]State Key Laboratory of Component-Based Chinese Medicine, Institute of Traditional Chinese Medicine, Tianjin University of Traditional Chinese Medicine, Tianjin, China

The process of neurogenesis in the brain, including cell proliferation, differentiation, survival, and maturation, results in the formation of new functional neurons. During embryonic development, neurogenesis is crucial to produce neurons to establish the nervous system, but the process persists in certain brain regions during adulthood. In adult neurogenesis, the production of new neurons in the hippocampus is accomplished via the division of neural stem cells. Neurogenesis is regulated by multiple factors, including gene expression at a temporal scale and post-transcriptional modifications. RNA-binding Proteins (RBPs) are known as proteins that bind to either double- or single-stranded RNA in cells and form ribonucleoprotein complexes. The involvement of RBPs in neurogenesis is crucial for modulating gene expression changes and posttranscriptional processes. Since neurogenesis affects learning and memory, RBPs are closely associated with cognitive functions and emotions. However, the pathways of each RBP in adult neurogenesis remain elusive and not clear. In this review, we specifically summarize the involvement of several RBPs in adult neurogenesis, including CPEB3, FXR2, FMRP, HuR, HuD, Lin28, Msi1, Sam68, Stau1, Smaug2, and SOX2. To understand the role of these RBPs in neurogenesis, including cell proliferation, differentiation, survival, and maturation as well as posttranscriptional gene expression, we discussed the protein family, structure, expression, functional domain, and region of action. Therefore, this narrative review aims to provide a comprehensive overview of the RBPs, their function, and their role in the process of adult neurogenesis as well as to identify possible research directions on RBPs and neurogenesis.

KEYWORDS

adult neurogenesis, neurogenesis regulation, miRNA, RNA-binding proteins, gene regulaiton

Introduction

Neurogenesis is the formation process of new neurons derived from neural progenitor cells (NPCs), occurring in several regions of the brain including the olfactory epithelium, hippocampus, and subventricular zone (SVZ) (Kempermann et al., 2004). It consists of four stages namely cell proliferation, migration, differentiation, and integration into the existing circuit (Ming and Song, 2011). In adulthood, neurogenesis takes place mainly in two regions of the brain, the SVZ and subgranular zone (SGZ) of the dentate gyrus in the hippocampus (Sanai et al., 2004; Curtis et al., 2007; Semple et al., 2013; Sánchez-Vidaña et al., 2019). Hippocampal neurogenesis is a pivotal physiological process involved in the regulation of cognitive and emotional behaviors such as the formation of spatial memory in learning, the response to stress, and mood (Yau et al., 2011; Chan et al., 2017; Fung et al., 2021). Various gene modulatory pathways participate in the neuronal growth process which consists of neuronal relocation, neuronal plasticity, synaptic formations, and dendritic and axonal outgrowth (Mills and Janitz, 2012; Qu et al., 2020). The dynamic modulation of alternative splicing (AS) in the nervous system is essential for the orchestrated regulation of protein-protein interactions, transcription systems, and neuronal growth (Qu et al., 2020).

More than 500 RNA-binding proteins (RBPs) have been identified in the human genome (Vogel and Richard, 2012). RBPs are in charge of complex RNA-protein and protein-protein interactions to regulate RNA metabolism (Vogel and Richard, 2012). Each RBP interacts with RNA with different affinities (Vogel and Richard, 2012). Gene expression is regulated by a variety of proteins, but RBPs represent a distinct subgroup within these proteins (Gerstberger et al., 2014). RBPs are responsible for regulating gene expression in various ways, including splicing, cleavage, polyadenylation, RNA stabilization, RNA localization, RNA editing, and translation. Several genetic processes, e.g., AS and the utilization of poly(A) sites mediated by the neuro-oncological ventral antigen (NOVA) protein, an RBPs first identified in autoimmune motor neuron diseases, involve RBPs (Licatalosi et al., 2008; Eom et al., 2013; Tang et al., 2020). Malfunctioning RBPs are associated with genetic and somatic disorders, for instance neurodegenerative, autoimmune, and cancer diseases (Lukong et al., 2008). As post-transcriptional steps are usually carried out in membrane- and phase-separated subcellular compartments, RBPs' regulatory functions are also impacted by their subcellular localization.

Apart from RBPs, micro RNAs (miRNAs) are another common type of gene expression mediators. The regulation of gene expression by RBPs and miRNAs can take place in an antagonistic fashion in which RBPs and miRNAs can act on the same targets or nearby regulatory elements (Velasco et al., 2019). For example, several miRNAs preferentially bind to Pumilio (PUM), a group of the PUF family of sequence-specific RNA-blinding proteins, and have binding motifs that complement the PUM recognition sites in reverse order (Shao et al., 2013). Upon binding, miRNA-binding efficiency increases due to PUM binding to transcripts, which in turn leads to an increase in shared target decay (Shao et al., 2013). Alternatively, they can inhibit the expression of a common target, a single transcript, which suggests that the interaction between RBPs and miRNAs takes place in a complex manner (Velasco et al., 2019). These regulators are involved in neurogenesis and brain development processes (Velasco et al., 2019). Therefore, changes at functional or gene expression levels caused by RBPs and miRNAs could contribute to neurological disorders and brain tumors (Velasco et al., 2019).

The translation of numerous mRNAs in the brain are controlled by their interaction with ribonucleoprotein (RNP) granules, which are made up of translational machinery, core RBPs, and miRNAs (Kiebler and Bassell, 2006). RBPs regulate the trafficking of certain mRNAs into dendrites, bundle them into RNP granules, and may control the timing and location of their translation in response to the synaptic activity (Kiebler and Bassell, 2006). Due to these characteristics, RBPs are in a special position to regulate developmental processes by coordinating the translation of a group of functionally linked mRNAs (Moore, 2005; Keene, 2007). Neurons have the ability to adjust neuronal output and consolidate alterations in synaptic connections thanks to local protein synthesis (Bramham and Wells, 2007; Licatalosi et al., 2008). The moderation of nervous system architecture is subjected to a variety of spatio-temporal gene regulatory mechanisms, including control of protein synthesis *via* RBPs (Conlon and Manley, 2017; Qu et al., 2020). A comprehensive analysis of RBPs involved in neurogenesis, their structure, function, and RNA targets is presented below. A summary of the function of RBPs at the different stages of neurogenesis as well as the RBPs' RNA targets and neurogenic regions are shown in Figure 1 and the expression of RBPs in neurogenic regions is illustrated in Figure 2.

RNA-binding proteins involved in adult neurogenesis

Cytoplasmic Polyadenylation Element binding proteins—3

The RNA-binding protein known as the Cytoplasmic Polyadenylation Element-Binding Protein (CPEB) family is essential for synaptic plasticity (Fernández-Miranda and Méndez, 2012). The CPEB family consists of four members (CPEB1, CPEB2, CPEB3, and CPEB4) that recognize the same Cytoplasmic Polyadenylation Element (CPE) found in the 3′untranslated region (3′UTR) of target mRNAs

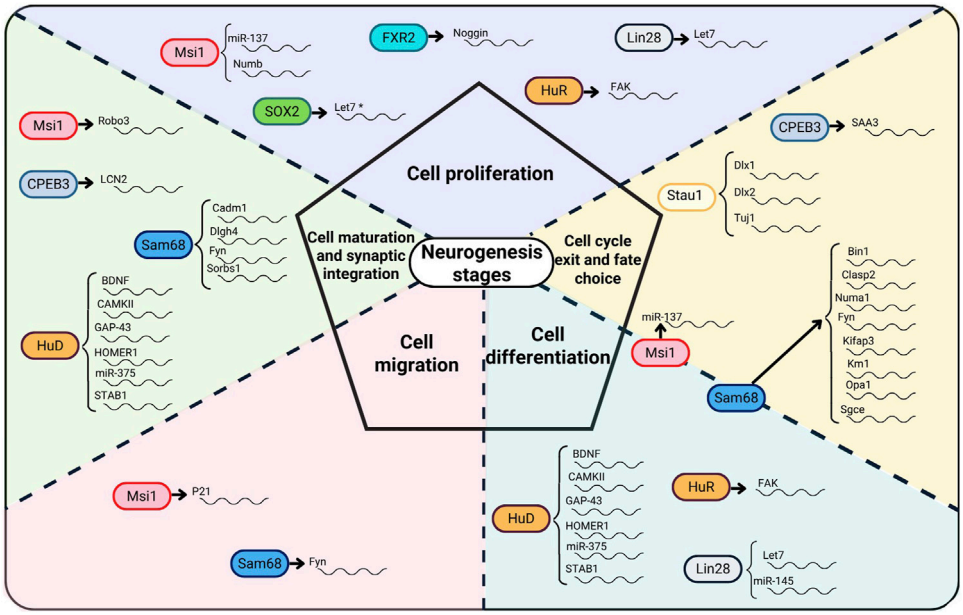

FIGURE 1
RBPs, their RNA targets, and the role of RBPs at different neurogenesis stages. RBPs acting on different stages of the neurogenesis process appear on the dotted lines of the neurogenesis stages that they regulate. In SOX2, * indicates an indirect interaction with let7 as SOX2 suppresses the expression of let7 expression by maintaining Lin28 expression.

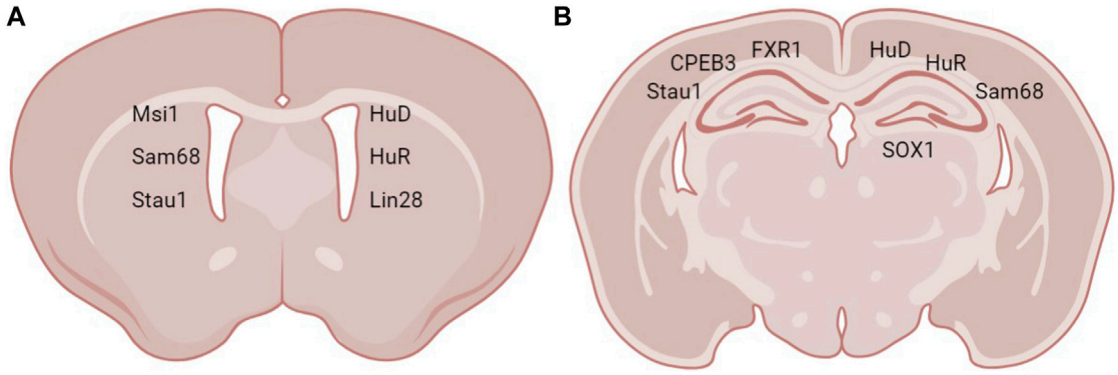

FIGURE 2
Expression sites of RBPs in neurogenic regions. RBPs expressed in **(A)** the SVZ and **(B)** the hippocampus.

(Fernández-Miranda and Méndez, 2012; Parisi et al., 2021). CPEBs 2–4 are highly related, while CPEB1 is the most distant member (Wang et al., 2010; Fernández-Miranda and Méndez, 2012). These proteins are expressed in the brain (Theis et al., 2003), and they share a similar structure (Huang et al., 2006) with the carboxy-terminal region consisting of two RNA recognition motifs (RRMs) and two zinc-fingers (Hake et al., 1998). CPEB proteins (CPEBs) are capable of repressing or activating the translation of target mRNAs by shortening or stretching the poly-A tail (Wakiyama et al., 2000).

A recent discovery of three later members in this family (CPEB2-4) revealed the additional regulatory potential and biological functions of cytoplasmic polyadenylation (Mendez and Richter, 2001; Wang et al., 2010). By controlling the translation of many plasticity-related proteins (PRPs) RNAs in

neurons, CPEBs limit the strength of glutamatergic synapses (Peng et al., 2010; Wang and Huang, 2012; Chao et al., 2013). CPEBs regulate the translation of mRNA that has been made inactive by closed-loop regulation. Translation is inhibited by a closed-loop structure between the 3′UTR and 5′UTR (Kang and Han, 2011).

In the process of establishing and maintaining neuronal development and synaptosomes, CPEB3 regulates translation by guiding necessary protein modifications (Qu et al., 2020). Therefore, CPEB3 serves as a mediator of translational activity in neurons of several identified mRNA targets (Ford et al., 2020). The function of CPEB3-related translation in neuronal development, migration, and synaptogenesis is modulated by several mechanisms (Peng et al., 2010; Hosoda et al., 2011). Genes related to transcription, neurodevelopment, and neurogenesis were enriched in CPEB3-bound genes. Several identified mRNA targets in neurons are translated by CPEB3. CPEB3 modulates the differential expression of genes associated with neurogenesis in HT22 cells, a mouse hippocampal cell line (Qu et al., 2020). CPEB3-regulated alternative splicing on control and CPEB3 overexpressing cells was examined using RNA-seq (Qu et al., 2020). By analyzing alternative splicing and differential gene expression, global CPEB3-RNA interaction has been elucidated using RNA-seq and iRIP-seq in neurons (Qu et al., 2020). In HT22 cells, CPEB3 had an insignificant impact on gene expression, involving 31 upregulated genes and 23 downregulated genes (Qu et al., 2020). Furthermore, overexpression of CPEB3 increased LCN2 mRNA levels in HT22 cells suggesting that CPEB3 modulates LCN2 pre-mRNA splicing (Qu et al., 2020). LCN2 is an alternative pathway for the delivery and uptake of physiological iron (Qu et al., 2020). The role of LCN2 in cell iron transport and homeostasis has recently been investigated (Devireddy et al., 2005; Bao et al., 2010). The LCN2 gene encodes an iron-binding protein that has been shown to regulate the density and morphology of hippocampal dendritic spines in the brain (Mucha et al., 2011). In addition, LCN2 plays a crucial role in neurogenesis, regulating NPCs maintenance, self-renewal, proliferation, differentiation as well as hippocampal plasticity (Mucha et al., 2011). Out of the four CPEBs, CPEB3 binds to LCN2 more efficiently (Qu et al., 2020). CPEB3 overexpression (CPEB3-OE) cell lines had an elevated level of SAA3, an acute-phase protein with cytokine-like properties. As a key modulator of neuronal survival and death, SAA3 is critical during inflammation (Huang et al., 2006). These findings contribute to the existing knowledge on the mechanisms that modulate neurogenesis and neuronal development mediated by CPEBs such as CPEB3 (Qu et al., 2020).

Fragile X-related proteins (Fragile X-related protein 1, FXR1)

The family Fragile X-Related Proteins (FXRs) includes the Fragile X Mental Retardation Protein (FMRP), involved in a condition known as fragile X syndrome, and FMPR's autosomal paralogs, the RBPs Fragile X-related protein 1 and 2 (Li and Zhao, 2014; Nishanth and Jha, 2022). FXRs are highly expressed in cortical neurons, cerebellar Purkinje neurons, and the brain stem (Patzlaff et al., 2018). FXRs are also expressed in dendrites, presynaptic spines, and axons in the thalamus, the CA3 region, and the olfactory bulb (Patzlaff et al., 2018). FXR2 is expressed in neuronal RNA granules containing FXRs and plays a critical role in the formation of such granules (Li and Zhao, 2014).

Structurally, FXR1 and FXR2 are very similar as they have two RNA-binding domains that are highly conserved, namely the polyribosome binding domain and the nuclear localization sequence (NLS) domain (Fernández et al., 2015; Patzlaff et al., 2017; Patzlaff et al., 2018). These proteins also contain an N-terminal protein-binding domain (NTD), which is responsible for the protein-protein interactions, two heterogeneous nuclear ribonucleoprotein (hnRNP) homology domains (KH), a nuclear export sequence (NES), and an arginine-glycine-glycine box (RGG) (Patzlaff et al., 2018). Although these proteins share some similar functional domains, they differ in the C termini region and the NLS domain (Li and Zhao, 2014). For instance, FXR2 contains an RG cluster in the C-terminal region which is not the case with FXR1 which contains an RGG box (Fernández et al., 2015). These structural differences explain their different RNA-binding properties (Fernández et al., 2015). The proteins of this family are homologous in their RNA-binding domains and can form hetero-multidimers. The heteromultimerization properties suggest that FXR1 and FXR2 have similar binding abilities to regulate protein translation (Patzlaff et al., 2018).

The members of this family can bind to RNA and associate with polyribosomes (Guo et al., 2011), and they can mediate RNA stability and translational efficiency (Patzlaff et al., 2018). One mechanism of action proposed for FXR2 is the recruitment of the translational machinery and therefore increase mRNA translation (Fernández et al., 2015). FXR2 regulates the circadian behavioral rhythms and plays a role in plasticity (Li and Zhao, 2014). FXR1 and FXR2 expression in the dentate gyrus is similar; however, from the functional point of view, these proteins play different roles (Patzlaff et al., 2017). FMRP, FX1, and FXR2 regulate adult neurogenesis having different functions (Guo et al., 2011; Li and Zhao, 2014; Patzlaff et al., 2017). For example, both FMRP and FXR2 suppress cell proliferation while FXR1 promotes it (Patzlaff et al., 2017). FXR2 is one of the several RBPs regarded as a critical regulator of neurogenesis (Nishanth and Jha, 2022).

FXR2 targets Noggin mRNA to regulate neurogenesis in the dentate gyrus of the adult brain (Nishanth and Jha, 2022). FXR2 inhibits Noggin protein expression by decreasing the stability of Noggin mRNA (Guo et al., 2011). Noggin's role is to maintain cell pluripotency in stem cells (Guo et al., 2011). It also acts as a bone morphogenetic protein (BMP) inhibitor to trigger cell proliferation and neuronal differentiation (Guo et al.,

2011). In the dentate gyrus NPCs lacking FXR2, the protein levels of Noggin increase, and the BMP pathway is blocked (Patzlaff et al., 2018).

In the dentate gyrus, the regulation of Noggin/BMP mediated signaling *via* FXR2 only takes place in this neurogenic region (Patzlaff et al., 2018) and FXR2 suppresses the expression levels of Noggin leading to an antagonistic effect on BMP signaling (Guo et al., 2011). On the contrary, this is not the case in the SVZ as FXR2 and Noggin are expressed in different cell types (Patzlaff et al., 2018). Consequently, the absence of FXR2 would not have any effect on the levels of the Noggin protein in the SVZ (Guo et al., 2011; Faigle and Song, 2013; Patzlaff et al., 2018). Considering that Noggin is found in the ependymal cells while FXR2 is expressed in neural progenitor cells, the regulation of Noggin expression by FXR2 is not direct (Guo et al., 2011). Noggin and FXR2 are colocalized in the dentate gyrus cells, and the lack of FXR2 in this type of cell results in increased cell proliferation of these cells (Guo et al., 2011). Furthermore, the lack of FXR2 results in decreased levels of PSD95 due to lower translational efficiency (Fernández et al., 2015). Low levels of FXR2 can affect stem cell proliferation and differentiation in the dentate gyrus of the hippocampus (Guo et al., 2011). However, this phenomenon is not observed in the SVZ (Guo et al., 2011; Faigle and Song, 2013).

Hu antigen D and Hu antigen R

Hu antigen R (HuR), also known as HuA or embryonic lethal, abnormal vision-like 1 (ELAVL1), is an RBP member of the protein family embryonic lethal abnormal vision, or ELAV/Hu (Yao et al., 1993). The ELAV family also includes HuB, HuC, and HuD, the latter also known as ELAVL4 (Yao et al., 1993; McMahon and Ruggero, 2018). HuD is one of the earliest markers of neuronal lineage and is abundantly expressed in the mature nervous system (Bronicki and Jasmin, 2013) while HuR is ubiquitously expressed and translocated between the cytoplasm and the nucleus through the hinge region (Han et al., 2022). HuD, as well as other members of the ELAV family, is predominantly expressed in differentiated neurons (Dell'Orco et al., 2020). Expression of HuD is mainly restricted to particular neuronal populations such as the large pyramidal-like neurons in the layer of the neocortex and the Purkinje cells in the cerebellar cortex, the CA1-4 of the hippocampus, dorsal root ganglia, motor neurons in the spinal cord, mitral cells in the olfactory bulb, ganglion and internal plexiform layers in the retina, and neurons in the enteric nervous system (Bronicki and Jasmin, 2013). HuD is found in the mitral cells of the olfactory bulb, which receive afferent fibers from different cell types in the olfactory system and are crucial for the analysis of signals at the olfactory bulb level (Tepper et al., 2021). HuR is ubiquitously expressed (Dell'Orco et al., 2020). Within the cell, HuR is abundantly found in the cytoplasm with low expression in the nucleus ((Bronicki and Jasmin, 2013; Wang et al., 2019). In adult NPCs, HuR is found in neurogenic regions (Wang et al., 2019).

The members of the ELAV family have three RNA binding domains which are known as RNA recognition motifs (RRMs) (Burd and Dreyfuss, 1994). The RRMs are highly conserved in these proteins, but the hinge region located between the second and third RRM is different among them (Good, 1995). HuD and HuR bind to adenosine/uridine (A/U)-rich elements (AREs) (Fernández et al., 2015). Both proteins are involved in the regulation of different functions such as splicing, translation, and stability of several mRNAs (Fernández et al., 2015). The RRMs in ELAV proteins are the recognition sites that bind to specific target RNAs (Bronicki and Jasmin, 2013). ELAV proteins can form homo- and multimers on target mRNAs which indicates that this property has been evolutionarily conserved (Bronicki and Jasmin, 2013). For instance, HuD interacts with other proteins, including homo- and hetero-mutimerization with other ELAV proteins, *via* the third RRM (Bronicki and Jasmin, 2013). HuD stabilizes target mRNAs by binding to the 3′UTR by the first and second MMRs and the poly (A) tails by the third MMR (Dell'Orco et al., 2020). For HuR to act, it translocates from the nucleus into the cytoplasm where it regulates transcription stability and translation (Ghosh et al., 2009).

In the adult brain, HuD is involved in the regulation of neuronal plasticity, nerve injury, learning and memory, and neuronal diseases (Bronicki and Jasmin, 2013; Dell'Orco et al., 2020; Tepper et al., 2021). HuD functions as a post-translational regulator of mRNAs associated with neuronal differentiation and synaptic plasticity, including STAB1, GAP-43, BDNF, CAMKII, and HOMER1 as well as mechanisms of learning and memory (Dell'Orco et al., 2020; Tepper et al., 2021). For instance, an increase in HuD levels in the hippocampus has been found during dissociative- and special-learning and memory paradigms (Dell'Orco et al., 2020). HuD is known to regulate about 131 non-coding RNAs such as Y3 RNA which is found to interact with HuD, but its function remains unknown (McMahon and Ruggero, 2018). HuD also plays a role in the regulation of cell fate (Tebaldi et al., 2018).

HuD participates in different stages of neuronal differentiation and maturation processes, including neurogenesis, axonal and dendritic outgrowth, and cell remodeling (Abdelmohsen et al., 2010; Dell'Orco et al., 2020). Recently, HuD has been shown to be a key role player in adult neurogenesis (Wang et al., 2015), particularly in NSC differentiation into neuronal lineage. Mechanistically, HuD enhances the stability of the pre-mRNA of special AT-rich DNA-binding protein 1 (SATB1) by binding to the 3′UTR (Wang et al., 2015). SATB1 is an essential component for neuronal differentiation, and HuD deficiency would trigger a decrease in SATB1, which would suppress NSC differentiation (Wang et al., 2015). HuD promotes mRNA stability, and it also mediates the localization and translation of transcripts in

neurites and the cytoplasm (Bronicki and Jasmin, 2013). For instance, GAP-43 and Tau are HuD target mRNAs that are involved in axonal outgrowth (Bronicki and Jasmin, 2013). HuD colocalizes GAP-43 and Tau during neuronal differentiation (Bronicki and Jasmin, 2013).

In the dentate gyrus of the hippocampus, HuD and its target mRNAs increase following neuro-toxin-induced injury (Bronicki and Jasmin, 2013). HuD has also been shown to localize to dendrite spines, and interact with mRNAs that encode synaptic proteins (Bronicki and Jasmin, 2013). These findings suggest that HuD is involved in neuronal plasticity mechanisms (Bronicki and Jasmin, 2013). In the hippocampus, higher binding of PSD95 mRNA and HuD takes place in the absence of FMRP (Fernández et al., 2015). FMRP, HuR, and HuD colocalize in different regions such as the neuronal cell bodies, dendritic processes in the CA3 region of the dentate gyrus, and primary neurons (Fernández et al., 2015). HuD acts by stabilizing PSD95 mRNA (Fernández et al., 2015). Both FMRP and HuD play an important role in the regulation of neuronal morphology, maturation, differentiation, and cytoskeletal organization (Fernández et al., 2015). Changes in the expression of HuD can affect mechanisms of special learning and memory processes in the hippocampus (Tepper et al., 2021).

HuD major effector is miR-375 which plays a role in neurite growth and dendritic maintenance (Abdelmohsen et al., 2010). Other HuD targets include those encoding for GAP-43, p21Waf1, and acetylcholinesterase, among others (Abdelmohsen et al., 2010). miR375 has an antagonistic effect on HuD as it suppresses its expression by destabilizing HuD mRNA which affects its translation (Abdelmohsen et al., 2010). Downregulation of HuD alters target genes involved in neuronal development, function, and neurite outgrowth (Abdelmohsen et al., 2010). This antagonistic regulatory effect of miR-375 on HuD affects translation processes that are essential for neurite growth, dendrite stability, and synapses as well as maintenance and plasticity of neuronal circuits (Abdelmohsen et al., 2010). For instance, the brain-derived neurotrophic factor (BDNF) is essential to maintaining neuronal mechanisms of plasticity, neuronal outgrowth, and neuronal differentiation (Abdelmohsen et al., 2010). Inhibition of BDNF mediated by miR-375 takes place as a result of the downregulation of HuD demonstrating that HuD can interact at posttranslational level with BDNF signaling to regulate neuronal function and morphology (Abdelmohsen et al., 2010).

HuR plays a role in adult neurogenesis (Wang et al., 2019) as it is known to translocate to the nucleolus where it functions as a regulator of alternative splicing processes (Nishanth and Jha, 2022). HuR also regulates the focal adhesion kinase (FAK) mRNA which is an essential key player in neurogenesis (Nishanth and Jha, 2022). HuR knockout in transgenic animals leads to a phenotype of neurogenesis and hippocampal-dependent learning in which defects can be observed (Wang et al., 2019). Lack of HuR results in a significant increase in the expression of the FAK isoform with shorter 5′ UTR regions. As a result, FAK function is stimulated which affects neurogenesis. On the other hand, FAK-mediated decreased neurogenesis can be reverted by blocking FAK activity (Bronicki and Jasmin, 2013).

Lin28

Lin28 is a highly conserved RNA-binding protein encoded by the Lin28 gene (Rehfeld et al., 2015). The Lin28 family includes the isoforms Lin28A and Lin28B, collectively known as Lin28 (Hennchen et al., 2015; Chen et al., 2019). Lin28 is often defined as a pluripotency factor that stimulates cell proliferation, but it also controls other mechanisms such as the timing of cell-time and lineage-specific decisions (Romer-Seibert et al., 2019). The lethal-7 (let7), a key pro-differentiation miRNA, orchestrates posttranslational silencing of mRNAs of neural stem cells (NSC) and acts as an interaction partner with Lin28 (Le Grand et al., 2015; Rehfeld et al., 2015). The members of the let7 family of miRNAs are abundantly expressed in adult tissues, including the brain (Rehfeld et al., 2015), and participate in cell differentiation processes (Hennchen et al., 2015). Lin28 is found in the cytoplasm and cytoplasmic bodies such as processing bodies and stress granules, and partially in the nucleus (Kawahara et al., 2012). While Lin28 is expressed in cell-renewing cells to promote cell proliferation, let7 is absent in stem cells (Rehfeld et al., 2015; Jang et al., 2019). Lin28B can be found in progenitor cells and the cerebral cortex whereas both Lin28A and Lin28B are expressed in neural progenitor cells expressing nestin and Pax6 in the ventricular and SVZ (Hennchen et al., 2015). The expression of Lin28A and Lin28B is not restricted to progenitor cells, but they can also be found in differentiated neuroblasts and expressed at low levels in postmitotic neurons (Hennchen et al., 2015). The expression pattern of Lin28 and let7 reflects the antagonistic interaction between these two players (Rehfeld et al., 2015). During neuron differentiation, let7 expression increases and this overexpression hinders proliferation and stem cell growth mechanisms (Hennchen et al., 2015). This mechanism is implicated in cell proliferation and differentiation of neural stem and precursor cells (Kawahara et al., 2012).

Lin28 contains a unique combination of two coupled and highly conserved functional domains, the N-terminal cold-shock-domain and two retroviral type CCHC-zinc knuckles (CCHCx2) (Rehfeld et al., 2015). Both domains participate in Lin28-mediated posttranscriptional regulation of gene expression as RNA binding takes place in these domains (Rehfeld et al., 2015). Lin28 interacts with the immature let7, also known as pre-let7, which contains the precursor element (PreE) (Rehfeld et al., 2015). The preE has a highly variable sequence structure constituting the loop of the precursor hairpin structure in pre-let7 (Rehfeld et al., 2015). The preE sequence in

pre-let7 shows higher sequence variability than the mature let7 form (Rehfeld et al., 2015). Pre-let7 also contains a conserved motif, the GGAG motif, which is highly enriched in let7 family members and is located 3' to the terminal loop (Rehfeld et al., 2015). The GGAG motif is crucial for the Lin28-mediated inhibition of the maturation of pre-let7 (Rehfeld et al., 2015).

Lin28 participates in several processes such as the generation of induced pluripotent cells from fibroblasts, glucose metabolism regulation, regeneration mechanisms in tissues, body size regulation, progression of cancer, and neurogenesis (Jang et al., 2019). Lin28 acts as one of the regulators participating in the reprogramming of adult cells and the modulatory translational mechanisms of mRNAs, enhancing or suppressing mRNA translation, by binding mRNAs (Parisi et al., 2021). At the early stages of neurogenesis, undifferentiated progenitor cells are present (Hennchen et al., 2015). These cells can be stimulated to proliferate by the action of several regulators. During neurogenesis, the expression of let7 continuously increases until the cell composition is resembling postmitotic neurons (Hennchen et al., 2015). Within the scope of the regulatory mechanisms of neurogenesis, the function of let7 is pivotal because it feeds itself onto the miRNA pathway to prepare the stage for other neurogenic miRNAs in charge of neuronal specifications and outgrowth (Rehfeld et al., 2015).

Lin28-mediated suppression activity of the let7 family promotes cell reprogramming to stimulate pluripotency (Kawahara et al., 2012). Furthermore, Lin28 has demonstrated regulatory effects of the neurite outgrowth process during cortical neurogenesis (Jang et al., 2019). Cell renewal, an event that involves dedifferentiation, is a useful mechanism in tissue regeneration to replace cells that were lost or damaged, and the ability of Lin28 in cell self-renewal could play an important role in this process (Rehfeld et al., 2015). The Lin28-let7 axis in neurogenesis regulates miRNA expression in terms of diversity and abundance during neural differentiation (Rehfeld et al., 2015). Lin28 plays an antagonistic role as it promotes the expression of gene expression patterns specific to stem cells by hindering let7 maturation (Cimadamore et al., 2013). Lin28 suppresses the downstream events regulated by let7 by interfering with the conversion of pre-let7 transcripts to mature let7, which in turn prevents the initiation of the pro-differentiation effect regulated by let7 (Rehfeld et al., 2015; Chen et al., 2019).

Lin28 selectively and strongly binds the conserved terminal loop site of pre-let7 through its specific RNA-binding activity (Kawahara et al., 2012). The interaction of Lin28 with pre-let7 triggers the recruitment of the uridylytransferases Tut4 or Tut7 (Parisi et al., 2021). These transferases catalyze the oligouridylylation of pre-let7 which leads to the degradation of pre-let7 mediated by the exonuclease Dis312 (Parisi et al., 2021). The interaction of Lin28 and let7 forms a self-amplifying system in which cell differentiation is triggered by the lower levels of Lin28 causing less repression of let7 processing and consequently higher levels of let7 and lower levels of Lin28 (Rehfeld et al., 2015; Morgado et al., 2016). Low expression of Lin28 decreases the expression of neuronal markers (Morgado et al., 2016). In the opposite scenario, self-renewal and pluripotency will take place as a result of high levels of Lin28 which cause a reduction in let7 processing resulting in lower levels of let7 and higher levels of Lin28 (Rehfeld et al., 2015; Morgado et al., 2016). The self-reinforcing mechanism of the interaction between Lin28 and let7, a double negative feedback loop, forms a bi-stable switch with two mutually exclusive states, that is, Lin28on-let7off and Lin28off-let7on (Kawahara et al., 2012; Rehfeld et al., 2015). The Lin28-let7 switch mechanism is one of the early events that take place at the onset of neurogenesis (Rehfeld et al., 2015). Lin28 expression significantly decreases during neural stem cell differentiation whereas higher expression of let7 takes place (Morgado et al., 2016). The factors driving the shift between the two interaction states have not been yet identified (Rehfeld et al., 2015).

A challenge in the understanding of the players involved in Lin28-let7 mediated mechanisms is the identification of mRNAs targeted by let7 (Rehfeld et al., 2015). During neurogenesis, let7 is upregulated and can act on important targets such as Lin28, Lin-41, c-Myc, Hmga2, and Tlx (Rehfeld et al., 2015). Some of those interactions participate in stem cell maintenance (Rehfeld et al., 2015) and neurogenesis functions such as cell proliferation (Lin28), axonal regeneration (Lin41), differentiation of Müller glial cells into retinal progenitors and pluripotency networks (c-Myc), stem cell plasticity in the SVZ (Hmga2), and cell cycle progression of NSC (Tlx) (Liu et al., 2014; Rehfeld et al., 2015). During neurogenesis, Lin28 expression is downregulated (Rehfeld et al., 2015).

Musashi1

Msi1 is a regulator that mediates the balance between self-renewal and cell differentiation (Velasco et al., 2019). Msi1 is expressed in neural stem/progenitor cells of the lateral ventricles, the olfactory subependymal region, and astrocytes in the adult brain (Toda et al., 2001; Takasawa et al., 2002). Low expression levels of Msi1 have been reported in the brain and the expression is limited to the SVZ (Kanemura et al., 2001; Toda et al., 2001), but it can also be found in the subgranular zone of the hippocampus (Ratti et al., 2006). The members of the Musashi family contain two highly conserved tandem RRMs (Toda et al., 2001). Msi1 functions by suppressing the translation of specific mRNA targets, regulating mRNA decay and polyadenylation by binding to transcripts with specific motifs containing ARE at the 3′UTR (Takasawa et al., 2002; Ratti et al., 2006). ARE can be recognized by numerous ARE-binding proteins including the neuronal-specific ELAV (nELAV)

RBPs, which are essential to induce neuronal differentiation (Ratti et al., 2006). mRNAs of genes with high turnover rates are known to contain ARE sequences which act as cis-acting regulatory motifs (Ratti et al., 2006). The relationship between Msi1 and nELAV proteins is shown by its co-expression and colocalization with Msi1 in the SVZ (Ratti et al., 2006). Both nELAV and Msi1 act as transcription regulators of Msi1 because of their specificity and ARE-binding activity for the Msi1 transcript (Ratti et al., 2006). nELAV, recognizes the Msi1 transcript in an ARE specific and dependent manner, it stabilizes Msi1 mRNA by decreasing its turnover rate, and this interaction controls proliferation and differentiation activities of neural stem/progenitor cells (Ratti et al., 2006). Therefore, the ARE sequence in the Msi1 gene is involved in mRNA stability and post-translational regulation of Msi1 (Ratti et al., 2006).

nELAV modulates actions of Msi1 at transcript and protein levels, which could alternate the cell cycle by shifting the stem/progenitor cells from cell proliferation to the cell differentiation phase in both neurogenic regions (i.e., SGZ and SVZ). (Ratti et al., 2006). The co-expression of these two proteins in the SVZ is limited to the sub-ependymal cell layer which suggests that they both may be involved in cell proliferation regulatory mechanisms in NSC (Ratti et al., 2006). The functions of Msi1 and nELAV are complementary and act differently on their target mRNAs. For instance, nELAV is responsible for the stabilization of the Msi1 transcript which in turn promotes its expression during the transition from cell proliferation to cell differentiation (Ratti et al., 2006). Overexpression of Msi1 is an indicator of the proliferation state (Ratti et al., 2006). Therefore, transcription and translational mechanisms regulating Msi1 expression will have an effect on Msi1 levels during the cell proliferation phases (Ratti et al., 2006). Msi1 is highly expressed during neurogenesis (Pötschke et al., 2020). nELAV RBPs are expressed in the SVZ and colocalize with Msi1 in neural stem/progenitor cells (Ratti et al., 2006). The inhibitory effect of Msi1 on cell differentiation is observed in neurogenesis. On the other hand, Msi1 is upregulated in NPCs, which supports its role in cell proliferation (Pötschke et al., 2020).

Msi1 expression during neurogenesis goes in the opposite direction to the expression levels of miR-137 (Velasco et al., 2019). In the SVZ, expression levels of Msi1 and miR-137 are inversely correlated (Velasco et al., 2019). miR-137 decreases self-renewal and cell proliferation while Mis1 increases cell proliferation (Velasco et al., 2019). Msi1 expression is higher in the SVZ where it promotes self-renewal and proliferation of stem cells while the expression of miR-137 is also high as it is required for lineage progression and cell differentiation (Velasco et al., 2019). miR-137 drives cell differentiation and inhibits Msi1 by suppressing the expression of shared targets (Velasco et al., 2019). miR-137 shares targets with miR-124 and miR-128, from which miR-128 is also known to regulate Msi1, and they all work in a synergistic fashion regulating neurogenesis (Velasco et al., 2019).

Msi1 acts on the Notch-mediated proliferation pathway in NSC where it binds and prevents the translation of Numb resulting in inhibition of Notch activation (Ratti et al., 2006; Pötschke et al., 2020). Msi1 participates in the downregulation of several regulators such as Numb, a negative regulator of Notch; p21, an inhibitor of cyclin-dependent kinases, and doublecortin, a microtubule-binding protein involved in cell migration (Glazer et al., 2012). Conversely, Mis1 promotes the upregulation of Rondabaout3 (Robo3), a receptor involved in axonal guidance (Glazer et al., 2012).

Another mediator of Msi1 activity is HuD which participates in the stabilization of Msi1 mRNA to promote Msi1-mediated cell proliferation of NPCs (Ratti et al., 2006; Pötschke et al., 2020). This mechanism allows the NPCs to keep dividing disregarding the transcriptional inactivation of Mis1 (Ratti et al., 2006). HuR positively regulates Msi1 expression (Velasco et al., 2019). Msi1 also interacts with Lin-7 by stimulating the inhibitory effect of Lin28 on let7 during cell differentiation (Lang and Shi, 2012).

Sam68

Sam68, the Src-associated substrate during mitosis of 68 kDa, also known as the human KH domain containing RNA binding signal transduction associated 1 (KHDRBS1), is a member of the Signal Transduction Activator of RNA (STAR) family of RBPs (Lim et al., 2006; Vogel and Richard, 2012; Danilenko et al., 2017). The proteins of the STAR family are highly conserved and participate in cell proliferation and cell differentiation processes (Bielli et al., 2011). Sam68 is mainly found in the nucleus, but it can also be expressed in the soma and dendrites of neurons in the hippocampus, cortex, and the SVZ (Lim et al., 2006; Chawla et al., 2009). Structurally, Sam68 has a 96-amino acid sequence at the N-terminus followed by a STAR domain, which contains a KH domain and flanking regions involved in protein-protein and protein-RNA interactions, an arginine-glycine rich domain, and a tyrosine-proline rich domain at the C-terminus (Huot et al., 2009; Danilenko et al., 2017). The arginine-glycine and tyrosine-proline domains are prone to posttranslational modifications (Danilenko et al., 2017). The highly conserved N- and C-terminal sequences are essential for RNA binding and homodimerization, and they are harbored by a single KH domain (Vogel and Richard, 2012).

Sam68 plays a role in RNA metabolism including polysomal recruitment of mRNAs and alternative splicing (Vogel and Richard, 2012). Sam68 regulates alternative splicing through the recognition of RNA sequences rich in adenine and uracil neighboring the included/excluded exons (Vogel and Richard, 2012). Sam68 can be subjected to post-translational modifications such as phosphorylation (serine/threonine and tyrosine), acetylation (lysine), methylation (arginine), and sumoylation (arginine) that regulate its subcellular

localization, interactions with signaling proteins, and affinity for target RNAs (Bielli et al., 2011; Vogel and Richard, 2012). For instance, the proline and tyrosine-rich regions make Sam68 a substrate of many kinases such as the Scr family kinases, phospholipase Cγ1, Grb2, Nck, and Csk (Huot et al., 2009). The tyrosine phosphorylation of Sam68 by Scr-related kinases greatly affects its ability to form homodimers and interact with target RNAs in the cell (Bielli et al., 2011). The arginine-rich region of Sam68 undergoes methylation by the methyltransferase PRMT1 (Bielli et al., 2011). The nuclear translocalization of newly formed Sam68 is affected by the arginine methyltransferase PRMT1 mediated methylation of Sam68, which hinders the interaction of Sam68 with SH domains (Bielli et al., 2011). Arginine methylation of Sam68 is a prerequisite for its successful nuclear localization (Côté et al., 2003).

Sam68 participates in the alternative splicing of mRNAs involved in neurogenesis (Huot et al., 2009). In neuronal cells, a set of 24 novel exons regulated by Sam68-mediated splicing had been identified and associated with neurogenesis (Chawla et al., 2009). Genes carrying Sam68 targets exons act in processes involved in neurogenesis such as cytoskeletal organization (Numa1, Clasp2, and Sgce), biogenesis, and transport of organelles (Bin1, Km1, Kifap3, and Opa1) and synaptogenesis (Cadm1, Dlgh4, and Sorbs1) (Chawla et al., 2009). Furthermore, Sam68 mediated the maintenance of splicing patterns needed after cell differentiation (Vogel and Richard, 2012). Sam68 is one of the 11 splicing factors highly expressed in the SVZ and the olfactory bulb core implicated in adult SVZ neurogenesis (Lim et al., 2006). Neuroblasts born in the SVZ can either integrate into the granule cell layer or migrate to the periglomerular layer in the olfactory bulb (Lim et al., 2006). Because alternative splicing allows the cells to regulate the same set of transcription factors that can affect the generation of different phenotypes of newborn neuroblasts in the SVZ, this mechanism may determine neuroblast migration or the cell fate choice (Lim et al., 2006). In the olfactory bulb core, Sam68 changes its subcellular localization, interaction with the spliceosome, and splice site selection upon phosphorylation by the kinase Fyn (Hartmann et al., 1999). Fyn overexpression in the olfactory bulb leads to changes in the Sam68-mediated mRNA splicing in type A cells resulting in cell cycle exit, radial migration, and integration of cells into local circuits (Lim et al., 2006). Furthermore, Sam68 associates the SVZ precursor RNA splicing machinery with the extracellular environment (Lim et al., 2006). For instance, the splicing activity of Sam68 in the SVZ is regulated by the extracellular signal-regulated kinase (ERK) (Lim et al., 2006).

Staufen 1

Stau1 and Stau2 are involved in RNA transport as well as mRNA stability and translation (Almasi and Jasmin, 2021). The Stau1 gene encodes the Stau1 protein (Bondy-Chorney et al., 2016). The five alternative splice variants produced by mature Stau1 mRNAs differ in their 5′UTR regions (Almasi and Jasmin, 2021). While Stau2 is abundant in the brain and only weakly expressed in other tissues, Stau1 is present in the majority of cell types, including neurons (Duchaîne et al., 2002). In mature hippocampus neurons, Stau1 is known to localize mRNA. The two proteins are mostly present in separate particles in the dendrites of hippocampal neurons, which may indicate that they have different roles (Duchaîne et al., 2002). Stau1 is also preset in the SVZ (Moon et al., 2018).There are two major kinds of Stau1 binding sites. Pairs of Alu elements in 3′ UTRs are included in the first class while non-Alu sequences are the second kind of Stau1-binding site (Almasi and Jasmin, 2021). Several target mRNAs have been found to include non-Alu 3′UTR binding sites (Almasi and Jasmin, 2021).

Stau1 and Stau2 are crucial for the transport and localization of certain mRNAs into the dendrites of adult hippocampal neurons and their knockdown in these cells impairs synaptic plasticity (Goetze et al., 2006; Vessey et al., 2008). Stau1 is involved in cell growth (Ghram et al., 2020), differentiation (Gautrey et al., 2005), migration, apoptosis (Gandelman et al., 2020), autophagy (Paul et al., 2021), and the stress response (Thomas et al., 2009; Bondy-Chorney et al., 2016; Paul et al., 2021). Stau1 is crucial for NPCs' development since over-expressing Stau1 in NPC cultures improves the detection of neuron-specific genes (Crawford Parks et al., 2017). In NPCs, Stau1 moves back and forth between the cytoplasm and nucleus (Kusek et al., 2012; Vessey et al., 2012). Stau1 can proceed *via* nuclear import and export in NPCs. Stau2 plays a critical role in the determination of cell fate during neurogenesis (Kusek et al., 2012; Vessey et al., 2012). Stau1 regulates neurogenesis by interacting with mRNA targets such as Dlx1, Dlx2, and Tuj1 (Moon et al., 2018). Stau1 acts by promoting the degradation of Dlx1, Dlx2, and Tuj1 mRNAs while knocking down Stau1 results in the inhibition of the degradation of target mRNAs suggesting that Stau1 is involved in the stability of those target mRNAs associated with neurogenesis (Moon et al., 2018).

SRY (sex-determining region)-box 2

The *Sry* (Sex-determining Region Y) gene was found as an initial member of the SOX gene family capable of determining the male phenotype (Gubbay et al., 1990). While members of the SOX family share similar DNA-binding properties, individual SOX proteins bind specific partner proteins to regulate their target genes (Kamachi et al., 2000; Tanaka et al., 2004). The SOX genes are divided into subgroups B1 (SOX1, SOX2, and SOX3) and B2 (SOX14 and SOX21) (Uchikawa et al., 1999). The SOX family of proteins contains a domain of 79 amino acids that allows them to bind specifically to the sequence (A/T A/T CAA A/T) (Harley et al., 1994) and two domains that function in transcriptional regulation (Pevny and Lovell-Badge, 1997). The

SOX proteins bind to the minor groove and, upon binding, induce strong bends in DNA (Michael, 1999).

Two types of NPCs express SOX2, the quiescent radial NPCs (type 1) and the amplifying progenitors (type 2a) (Ellis et al., 2004; Ferri et al., 2004; Garcia et al., 2004; Seri et al., 2004; Suh et al., 2007). Throughout life, SOX2 is expressed in the developing hippocampus, cortical hem (CH), and dentate neural epithelium (DNE), and then continues to be expressed in the dentate gyrus (Mercurio et al., 2022). Compared to surrounding tissues, SOX2 expression is significantly enriched in the CH (Ferri et al., 2004; Favaro et al., 2009; Mercurio et al., 2022), suggesting a critical role for SOX2 in this area. NPCs express SOX2 before turning it off in differentiated neurons (Hodge and Hevner, 2011). SOX2 expression decreases during differentiation when progenitor cells become postmitotic during their final cell cycle (Graham et al., 2003). A cell expressing SOX2 is capable of producing both identical cells and differentiated neural cells, two hallmarks of stem cells (Liu et al., 2019).

SOX2 is a well-known regulator of cell proliferation and neurogenesis, and it participates in the upstreaming events of the Lin28-let7 axis (Mukherjee et al., 2011; Rehfeld et al., 2015). In adult NSC in the subgranular zone of the hippocampus and the SVZ, Lin28 expression correlates with increased SOX2 activity (Rehfeld et al., 2015). SOX2 binds to the Lin28 promoter triggering the recruitment of histone deacetylase complexes which upregulates Lin28 expression (Rehfeld et al., 2015). The loss in neurogenesis caused by depletion of SOX2 can be partially compensated by overexpression of Lin28 by interfering with the functional maturation of let7 (Cimadamore et al., 2013; Rehfeld et al., 2015; Morgado et al., 2016). Another event demonstrating the cross-talk interaction of SOX2 and the Lin28-let7 axis in neurogenesis is that let7 downregulates the neurogenic basic-helix-loop-helix transcription factors Ascl1/Mash1 and neurogenin (Rehfeld et al., 2015). These series of events suggest that suppression of let7 expression by maintaining Lin28 expression is a requirement, at least in part, for SOX2 in neurogenesis (Rehfeld et al., 2015).

Discussion

In this review, RBPs involved in the different stages of the adult neurogenesis process were discussed. RBPs such as Sam68 and Msi1 are involved at all stages of neurogenesis (Figure 1). The regulatory specificity of Sam68 and Msi1 in neurogenesis may be driven by the interaction of these RBPs with different target mRNAs. The role of specific mRNA partnerships at each stage of neurogenesis suggests the possibility to manipulate a particular stage *via* a specific regulatory partnership. However, it can also be observed that the same RBP-mRNA partners (e.g., Msi1-miR137, Sam68-Fyn, HuR-Fak, Lin28-let7) also have the ability to act on different neurogenesis phases through the same mRNA targets. This phenomenon invites to ask whether other regulatory mechanisms are involved and whether there is a cross-talk among RBPs contributing to the regulation at each stage of the neurogenesis process. A clear case of an RBP-RBP cross-talk mechanism was shown in SOX2 in which this RBP interacts with the Lin28-let7 axis. Some RBPs such as HuD, Sam68, Msi1, and Stau1 act on multiple mRNA targets to regulate a specific stage of the neurogenesis process which raises the question whether there could be more target mRNAs that have not yet been identified for the other RBPs. At times, the process to activate or deactivate RBP mediated function has been clearly identified such as in Lin28 case, but often times the activation-deactivation process is not well understood. What is clear from the analysis presented in this review is that there is an intricate RBP-mediated regulatory network taking place in neurogenesis. Tracing the regulatory network mediated by RBPs in neurogenesis will potentially contribute to understanding the impact and clinical implications on cognition and mood. Therefore, efforts should be made to clarify the RBP-mediated regulatory mechanisms and to identify relevant mRNAs involved in neurogenesis.

Conclusion

Gene expression mechanisms, including the control of mRNA synthesis *via* RBPs, are backbone mechanisms that shape the architecture of the CNS. Several RBPs are involved in the intricate regulation of neurogenesis at all stages from, cell proliferation, migration, and differentiation, to integration into the existing circuit in both the SVZ and the dentate gyrus of the hippocampus (Ming and Song, 2011).

It is important to note that identifying potential therapeutic targets to modulate neurogenesis at a genetic level demands our understanding of RBPs considering 1) the bidirectional regulation of neurogenesis (e.g., agonistic and antagonistic regulatory effect on neurogenesis), 2) self-amplification effect (e.g., Lin28), 3) overlapping RBPs targets and effectors (e.g., Lin28 and Msi1, miR-145 mediating the downregulation of SOX2 and Lin28), and 4) complementary actions among RBPs (e.g., Msi1 and nELAV) as discussed in the review. Furthermore, the degree of understanding of the RBP mechanism, their molecular regulatory partners, and neurogenic region of action has been slowly emerging being HuD, HuR, FXR2, Lin28, Msi1, and Sam68 the most characterized RBPs to date. Despite the advances to understand the complex RBP-mediated regulation of neurogenesis, more research is needed to trace a clear map of the molecular regulatory mechanisms and the critical players to identify potential therapeutic neurogenic promoting targets.

Author contributions

All of the authors contributed to the conceptualization, manuscript writing, and revision. JC, DS, and BL designed the framework of the review and conducted the literature search. BL, YL, and SA revised and contributed to the structure and organization of the information in the manuscript. All authors contributed scientifically and approved the submission of the manuscript.

Funding

The study was supported by General Research Fund (Ref No: 15105621) by University Grant Council (Hong Kong) to BL and also supported by the National Natural Science Foundation of China (No. 82073832) to YL. Research Area Based Seed Fund (Project ID P0033824) by the department of rehabilitation Sciences (The Hong Kong Polytechnic University) to BL.

Conflict of interest

The authors declare that the research was conducted in the absence of any commercial or financial relationships that could be construed as a potential conflict of interest.

Publisher's note

References

Abdelmohsen, K., Hutchison, E. R., Lee, E. K., Kuwano, Y., Kim, M. M., Masuda, K., et al. (2010). miR-375 inhibits differentiation of neurites by lowering HuD levels. *Mol. Cell. Biol.* 30, 4197–4210. doi:10.1128/MCB.00316-10

Almasi, S., and Jasmin, B. J. (2021). The multifunctional RNA-binding protein Staufen1: an emerging regulator of oncogenesis through its various roles in key cellular events. *Cell. Mol. Life Sci.* 78, 7145–7160. doi:10.1007/s00018-021-03965-w

Bao, G., Clifton, M., Hoette, T. M., Mori, K., Deng, S.-X., Qiu, A., et al. (2010). Iron traffics in circulation bound to a siderocalin (Ngal)-catechol complex. *Nat. Chem. Biol.* 6, 602–609. doi:10.1038/nchembio.402

Bielli, P., Busà, R., Paronetto, M. P., and Sette, C. (2011). The RNA-binding protein Sam68 is a multifunctional player in human cancer. *Endocr. Relat. Cancer* 18, R91–R102. doi:10.1530/ERC-11-0041

Bondy-Chorney, E., Crawford Parks, T. E., Ravel-Chapuis, A., Jasmin, B. J., and Côté, J. (2016). Staufen1s role as a splicing factor and a disease modifier in Myotonic Dystrophy Type I. *Rare Dis.* 4, e1225644. doi:10.1080/21675511.2016.1225644

Bramham, C. R., and Wells, D. G. (2007). Dendritic mRNA: transport, translation and function. *Nat. Rev. Neurosci.* 8, 776–789. doi:10.1038/nrn2150

Bronicki, L. M., and Jasmin, B. J. (2013). Emerging complexity of the HuD/ELAVl4 gene; implications for neuronal development, function, and dysfunction. *RNA* 19, 1019–1037. doi:10.1261/rna.039164.113

Burd, C. G., and Dreyfuss, G. (1994). Conserved structures and diversity of functions of RNA-binding proteins. *Science* 265, 615–621. doi:10.1126/science.8036511

Chan, J. N.-M., Lee, J. C.-D., Lee, S. S. P., Hui, K. K. Y., Chan, A. H. L., Fung, T. K.-H., et al. (2017). Interaction effect of social isolation and high dose corticosteroid on neurogenesis and emotional behavior. *Front. Behav. Neurosci.* 11, 18. doi:10.3389/fnbeh.2017.00018

Chao, H.-W., Tsai, L.-Y., Lu, Y.-L., Lin, P.-Y., Huang, W.-H., Chou, H.-J., et al. (2013). Deletion of CPEB3 enhances hippocampus-dependent memory via increasing expressions of PSD95 and NMDA receptors. *J. Neurosci.* 33, 17008–17022. doi:10.1523/JNEUROSCI.3043-13.2013

Chawla, G., Lin, C.-H., Han, A., Shiue, L., Ares, M., and Black, D. L. (2009). Sam68 regulates a set of alternatively spliced exons during neurogenesis. *Mol. Cell. Biol.* 29, 201–213. doi:10.1128/MCB.01349-08

Chen, Y., Xie, C., Zheng, X., Nie, X., Wang, Z., Liu, H., et al. (2019). LIN28/let-7/PD-L1 pathway as a target for cancer immunotherapy. *Cancer Immunol. Res.* 7, 487–497. doi:10.1158/2326-6066.CIR-18-0331

Cimadamore, F., Amador-Arjona, A., Chen, C., Huang, C.-T., and Terskikh, A. V. (2013). SOX2-LIN28/let-7 pathway regulates proliferation and neurogenesis in neural precursors. *Proc. Natl. Acad. Sci. U. S. A.* 110, E3017–E3026. doi:10.1073/pnas.1220176110

Conlon, E. G., and Manley, J. L. (2017). RNA-binding proteins in neurodegeneration: mechanisms in aggregate. *Genes Dev.* 31, 1509–1528. doi:10.1101/gad.304055.117

Côté, J., Boisvert, F.-M., Boulanger, M.-C., Bedford, M. T., and Richard, S. (2003). Sam68 RNA binding protein is an *in vivo* substrate for protein arginine N-methyltransferase 1. *Mol. Biol. Cell* 14, 274–287. doi:10.1091/mbc.e02-08-0484

Crawford Parks, T. E., Marcellus, K. A., Langill, J., Ravel-Chapuis, A., Michaud, J., Cowan, K. N., et al. (2017). Novel roles for Staufen1 in embryonal and alveolar rhabdomyosarcoma via c-myc-dependent and -independent events. *Sci. Rep.* 7, 42342. doi:10.1038/srep42342

Curtis, M. A., Kam, M., Nannmark, U., Anderson, M. F., Axell, M. Z., Wikkelso, C., et al. (2007). Human neuroblasts migrate to the olfactory bulb via a lateral ventricular extension. *Science* 315, 1243–1249. doi:10.1126/science.1136281

Danilenko, M., Dalgliesh, C., Pagliarini, V., Naro, C., Ehrmann, I., Feracci, M., et al. (2017). Binding site density enables paralog-specific activity of SLM2 and Sam68 proteins in Neurexin2 AS4 splicing control. *Nucleic Acids Res.* 45, 4120–4130. doi:10.1093/nar/gkw1277

Dell'Orco, M., Oliver, R. J., and Perrone-Bizzozero, N. (2020). HuD binds to and regulates circular RNAs derived from neuronal development- and synaptic plasticity-associated genes. *Front. Genet.* 11, 790. doi:10.3389/fgene.2020.00790

Devireddy, L. R., Gazin, C., Zhu, X., and Green, M. R. (2005). A cell-surface receptor for lipocalin 24p3 selectively mediates apoptosis and iron uptake. *Cell* 123, 1293–1305. doi:10.1016/j.cell.2005.10.027

Duchaîne, T. F., Hemraj, I., Furic, L., Deitinghoff, A., Kiebler, M. A., and DesGroseillers, L. (2002). Staufen2 isoforms localize to the somatodendritic domain of neurons and interact with different organelles. *J. Cell Sci.* 115, 3285–3295. doi:10.1242/jcs.115.16.3285

Ellis, P., Fagan, B. M., Magness, S. T., Hutton, S., Taranova, O., Hayashi, S., et al. (2004). SOX2, a persistent marker for multipotential neural stem cells derived from embryonic stem cells, the embryo or the adult. *Dev. Neurosci.* 26, 148–165. doi:10.1159/000082134

Eom, T., Zhang, C., Wang, H., Lay, K., Fak, J., Noebels, J. L., et al. (2013). NOVA-dependent regulation of cryptic NMD exons controls synaptic protein levels after seizure. *eLife* 2, e00178. doi:10.7554/eLife.00178

Faigle, R., and Song, H. (2013). Signaling mechanisms regulating adult neural stem cells and neurogenesis. *Biochim. Biophys. Acta* 1830, 2435–2448. doi:10.1016/j.bbagen.2012.09.002

Favaro, R., Valotta, M., Ferri, A. L. M., Latorre, E., Mariani, J., Giachino, C., et al. (2009). Hippocampal development and neural stem cell maintenance require Sox2-dependent regulation of Shh. *Nat. Neurosci.* 12, 1248–1256. doi:10.1038/nn.2397

Fernández, E., Li, K. W., Rajan, N., De Rubeis, S., Fiers, M., Smit, A. B., et al. (2015). FXR2P exerts a positive translational control and is required for the activity-dependent increase of PSD95 expression. *J. Neurosci.* 35, 9402–9408. doi:10.1523/JNEUROSCI.4800-14.2015

Fernández-Miranda, G., and Méndez, R. (2012). The CPEB-family of proteins, translational control in senescence and cancer. *Ageing Res. Rev.* 11, 460–472. doi:10.1016/j.arr.2012.03.004

Ferri, A. L. M., Cavallaro, M., Braida, D., Di Cristofano, A., Canta, A., Vezzani, A., et al. (2004). Sox2 deficiency causes neurodegeneration and impaired neurogenesis in the adult mouse brain. *Development* 131, 3805–3819. doi:10.1242/dev.01204

Ford, L., Asok, A., Tripp, A. D., Parro, C., Fitzpatrick, M., Solis, C. A. de, et al. (2020). The low complexity motif of cytoplasmic polyadenylation element binding protein 3 (CPEB3) is critical for the trafficking of its targets in neurons. doi:10.1101/2020.05.16.100032

Fung, T. K. H., Lau, B. W. M., Ngai, S. P. C., and Tsang, H. W. H. (2021). Therapeutic effect and mechanisms of essential oils in mood disorders: Interaction between the nervous and respiratory systems. *Int. J. Mol. Sci.* 22, 4844. doi:10.3390/ijms22094844

Gandelman, M., Dansithong, W., Figueroa, K. P., Paul, S., Scoles, D. R., and Pulst, S. M. (2020). Staufen 1 amplifies proapoptotic activation of the unfolded protein response. *Cell Death Differ.* 27, 2942–2951. doi:10.1038/s41418-020-0553-9

Garcia, A. D. R., Doan, N. B., Imura, T., Bush, T. G., and Sofroniew, M. V. (2004). GFAP-expressing progenitors are the principal source of constitutive neurogenesis in adult mouse forebrain. *Nat. Neurosci.* 7, 1233–1241. doi:10.1038/nn1340

Gautrey, H., McConnell, J., Hall, J., and Hesketh, J. (2005). Polarised distribution of the RNA-binding protein Staufen in differentiated intestinal epithelial cells. *FEBS Lett.* 579, 2226–2230. doi:10.1016/j.febslet.2005.02.074

Gerstberger, S., Hafner, M., and Tuschl, T. (2014). A census of human RNA-binding proteins. *Nat. Rev. Genet.* 15, 829–845. doi:10.1038/nrg3813

Ghosh, M., Aguila, H. L., Michaud, J., Ai, Y., Wu, M.-T., Hemmes, A., et al. (2009). Essential role of the RNA-binding protein HuR in progenitor cell survival in mice. *J. Clin. Invest.* 119, 3530–3543. doi:10.1172/JCI38263

Ghram, M., Bonnet-Magnaval, F., Hotea, D. I., Doran, B., Ly, S., and DesGroseillers, L. (2020). Staufen1 is essential for cell-cycle transitions and cell proliferation via the control of E2F1 expression. *J. Mol. Biol.* 432, 3881–3897. doi:10.1016/j.jmb.2020.04.016

Glazer, R. I., Vo, D. T., and Penalva, L. O. F. (2012). Musashi1: an RBP with versatile functions in normal and cancer stem cells. *Front. Biosci.* 17, 54–64. doi:10.2741/3915

Goetze, B., Tuebing, F., Xie, Y., Dorostkar, M. M., Thomas, S., Pehl, U., et al. (2006). The brain-specific double-stranded RNA-binding protein Staufen2 is required for dendritic spine morphogenesis. *J. Cell Biol.* 172, 221–231. doi:10.1083/jcb.200509035

Good, P. J. (1995). A conserved family of elav-like genes in vertebrates. *Proc. Natl. Acad. Sci. U. S. A.* 92, 4557–4561. doi:10.1073/pnas.92.10.4557

Graham, V., Khudyakov, J., Ellis, P., and Pevny, L. (2003). SOX2 functions to maintain neural progenitor identity. *Neuron* 39, 749–765. doi:10.1016/s0896-6273(03)00497-5

Gubbay, J., Collignon, J., Koopman, P., Capel, B., Economou, A., Münsterberg, A., et al. (1990). A gene mapping to the sex-determining region of the mouse Y chromosome is a member of a novel family of embryonically expressed genes. *Nature* 346, 245–250. doi:10.1038/346245a0

Guo, W., Zhang, L., Christopher, D. M., Teng, Z.-Q., Fausett, S. R., Liu, C., et al. (2011). RNA-binding protein FXR2 regulates adult hippocampal neurogenesis by reducing Noggin expression. *Neuron* 70, 924–938. doi:10.1016/j.neuron.2011.03.027

Hake, L. E., Mendez, R., and Richter, J. D. (1998). Specificity of RNA binding by CPEB: requirement for RNA recognition motifs and a novel zinc finger. *Mol. Cell. Biol.* 18, 685–693. doi:10.1128/MCB.18.2.685

Han, X., Shen, X., Wang, M., Wang, X., Jian, Y., Yang, C., et al. (2022). Loss of RNA-binding protein HuR leads to defective ependymal cells and hydrocephalus. *J. Neurosci.* 42, 202–219. doi:10.1523/JNEUROSCI.1317-21.2021

Harley, V. R., Lovell-Badge, R., and Goodfellow, P. N. (1994). Definition of a consensus DNA binding site for SRY. *Nucleic Acids Res.* 22, 1500–1501. doi:10.1093/nar/22.8.1500

Hartmann, A. M., Nayler, O., Schwaiger, F. W., Obermeier, A., and Stamm, S. (1999). The interaction and colocalization of Sam68 with the splicing-associated factor YT521-B in nuclear dots is regulated by the Src family kinase p59(fyn). *Mol. Biol. Cell* 10, 3909–3926. doi:10.1091/mbc.10.11.3909

Hennchen, M., Stubbusch, J., Abarchan-El Makhfi, I., Kramer, M., Deller, T., Pierre-Eugene, C., et al. (2015). Lin28B and let-7 in the control of sympathetic neurogenesis and neuroblastoma development. *J. Neurosci.* 35, 16531–16544. doi:10.1523/JNEUROSCI.2560-15.2015

Hodge, R. D., and Hevner, R. F. (2011). Expression and actions of transcription factors in adult hippocampal neurogenesis. *Dev. Neurobiol.* 71, 680–689. doi:10.1002/dneu.20882

Hosoda, N., Funakoshi, Y., Hirasawa, M., Yamagishi, R., Asano, Y., Miyagawa, R., et al. (2011). Anti-proliferative protein Tob negatively regulates CPEB3 target by recruiting Caf1 deadenylase. *EMBO J.* 30, 1311–1323. doi:10.1038/emboj.2011.37

Huang, Y.-S., Kan, M.-C., Lin, C.-L., and Richter, J. D. (2006). CPEB3 and CPEB4 in neurons: analysis of RNA-binding specificity and translational control of AMPA receptor GluR2 mRNA. *EMBO J.* 25, 4865–4876. doi:10.1038/sj.emboj.7601322

Huot, M.-É., Vogel, G., and Richard, S. (2009). Identification of a Sam68 ribonucleoprotein complex regulated by epidermal growth factor. *J. Biol. Chem.* 284, 31903–31913. doi:10.1074/jbc.M109.018465

Jang, H.-J., Kim, J. Y., Kim, S. Y., and Cho, K.-O. (2019). Persistent Lin28 expression impairs neurite outgrowth and cognitive function in the developing mouse neocortex. *Mol. Neurobiol.* 56, 3780–3795. doi:10.1007/s12035-018-1297-0

Kamachi, Y., Uchikawa, M., and Kondoh, H. (2000). Pairing SOX off: with partners in the regulation of embryonic development. *Trends Genet.* 16, 182–187. doi:10.1016/s0168-9525(99)01955-1

Kanemura, Y., Mori, K., Sakakibara, S., Fujikawa, H., Hayashi, H., Nakano, A., et al. (2001). Musashi1, an evolutionarily conserved neural RNA-binding protein, is a versatile marker of human glioma cells in determining their cellular origin, malignancy, and proliferative activity. *Differentiation.* 68, 141–152. doi:10.1046/j.1432-0436.2001.680208.x

Kang, M. K., and Han, S. J. (2011). Post-transcriptional and post-translational regulation during mouse oocyte maturation. *BMB Rep.* 44, 147–157. doi:10.5483/BMBRep.2011.44.3.147

Kawahara, H., Imai, T., and Okano, H. (2012). MicroRNAs in neural stem cells and neurogenesis. *Front. Neurosci.* 6, 30. doi:10.3389/fnins.2012.00030

Keene, J. D. (2007). RNA regulons: coordination of post-transcriptional events. *Nat. Rev. Genet.* 8, 533–543. doi:10.1038/nrg2111

Kempermann, G., Wiskott, L., and Gage, F. H. (2004). Functional significance of adult neurogenesis. *Curr. Opin. Neurobiol.* 14, 186–191. doi:10.1016/j.conb.2004.03.001

Kiebler, M. A., and Bassell, G. J. (2006). Neuronal RNA granules: movers and makers. *Neuron* 51, 685–690. doi:10.1016/j.neuron.2006.08.021

Kusek, G., Campbell, M., Doyle, F., Tenenbaum, S. A., Kiebler, M., and Temple, S. (2012). Asymmetric segregation of the double-stranded RNA binding protein Staufen2 during mammalian neural stem cell divisions promotes lineage progression. *Cell Stem Cell* 11, 505–516. doi:10.1016/j.stem.2012.06.006

Lang, M.-F., and Shi, Y. (2012). Dynamic roles of microRNAs in neurogenesis. *Front. Neurosci.* 6, 71. doi:10.3389/fnins.2012.00071

Le Grand, J. N., Gonzalez-Cano, L., Pavlou, M. A., and Schwamborn, J. C. (2015). Neural stem cells in Parkinson's disease: a role for neurogenesis defects in onset and progression. *Cell. Mol. Life Sci.* 72, 773–797. doi:10.1007/s00018-014-1774-1

Li, Y., and Zhao, X. (2014). Concise review: Fragile X proteins in stem cell maintenance and differentiation. *Stem Cells* 32, 1724–1733. doi:10.1002/stem.1698

Licatalosi, D. D., Mele, A., Fak, J. J., Ule, J., Kayikci, M., Chi, S. W., et al. (2008). HITS-CLIP yields genome-wide insights into brain alternative RNA processing. *Nature* 456, 464–469. doi:10.1038/nature07488

Lim, D. A., Suárez-Fariñas, M., Naef, F., Hacker, C. R., Menn, B., Takebayashi, H., et al. (2006). *In vivo* transcriptional profile analysis reveals RNA splicing and chromatin remodeling as prominent processes for adult neurogenesis. *Mol. Cell. Neurosci.* 31, 131–148. doi:10.1016/j.mcn.2005.10.005

Liu, P., Verhaar, A. P., and Peppelenbosch, M. P. (2019). Signaling size: Ankyrin and SOCS box-containing ASB E3 ligases in action. *Trends biochem. Sci.* 44, 64–74. doi:10.1016/j.tibs.2018.10.003

Liu, Y., Zhou, J., and White, K. P. (2014). RNA-seq differential expression studies: more sequence or more replication? *Bioinformatics* 30, 301–304. doi:10.1093/bioinformatics/btt688

Lukong, K. E., Chang, K., Khandjian, E. W., and Richard, S. (2008). RNA-binding proteins in human genetic disease. *Trends Genet.* 24, 416–425. doi:10.1016/j.tig.2008.05.004

McMahon, M., and Ruggero, D. (2018). A translation tuning HuDdle for neurons. *Mol. Cell* 71, 195–196. doi:10.1016/j.molcel.2018.07.007

Mendez, R., and Richter, J. D. (2001). Translational control by CPEB: a means to the end. *Nat. Rev. Mol. Cell Biol.* 2, 521–529. doi:10.1038/35080081

Mercurio, S., Serra, L., Pagin, M., and Nicolis, S. K. (2022). Deconstructing Sox2 function in brain development and disease. *Cells* 11, 1604. doi:10.3390/cells11101604

Michael, W. (1999). From head to toes: the multiple facets of sox proteins. *Nucleic Acids Res.* 27, 1409–1420. doi:10.1093/nar/27.6.1409

Mills, J. D., and Janitz, M. (2012). Alternative splicing of mRNA in the molecular pathology of neurodegenerative diseases. *Neurobiol. Aging* 33, e11–e24. doi:10.1016/j.neurobiolaging.2011.10.030

Ming, G., and Song, H. (2011). Adult neurogenesis in the mammalian brain: Significant answers and significant questions. *Neuron* 70, 687–702. doi:10.1016/j.neuron.2011.05.001

Moon, B.-S., Bai, J., Cai, M., Liu, C., Shi, J., and Lu, W. (2018). Kruppel-like factor 4-dependent Staufen1-mediated mRNA decay regulates cortical neurogenesis. *Nat. Commun.* 9, 401. doi:10.1038/s41467-017-02720-9

Moore, M. J. (2005). From birth to death: the complex lives of eukaryotic mRNAs. *Science* 309, 1514–1518. doi:10.1126/science.1111443

Morgado, A. L., Rodrigues, C. M. P., and Solá, S. (2016). MicroRNA-145 regulates neural stem cell differentiation through the sox2-lin28/let-7 signaling pathway. *Stem Cells* 34, 1386–1395. doi:10.1002/stem.2309

Mucha, M., Skrzypiec, A. E., Schiavon, E., Attwood, B. K., Kucerova, E., and Pawlak, R. (2011). Lipocalin-2 controls neuronal excitability and anxiety by regulating dendritic spine formation and maturation. *Proc. Natl. Acad. Sci. U. S. A.* 108, 18436–18441. doi:10.1073/pnas.1107936108

Mukherjee, N., Corcoran, D. L., Nusbaum, J. D., Reid, D. W., Georgiev, S., Hafner, M., et al. (2011). Integrative regulatory mapping indicates that the RNA-binding protein HuR couples pre-mRNA processing and mRNA stability. *Mol. Cell* 43, 327–339. doi:10.1016/j.molcel.2011.06.007

Nishanth, M. J., and Jha, S. (2022). Global exploration of RNA-binding proteins in exercise-induced adult hippocampal neurogenesis: A transcriptome meta-analysis and computational study. *Biochem. Genet.* doi:10.1007/s10528-022-10230-7

Parisi, S., Castaldo, D., Piscitelli, S., D'Ambrosio, C., Divisato, G., Passaro, F., et al. (2021). Identification of RNA-binding proteins that partner with Lin28a to regulate Dnmt3a expression. *Sci. Rep.* 11, 2345. doi:10.1038/s41598-021-81429-8

Patzlaff, N. E., Nemec, K. M., Malone, S. G., Li, Y., and Zhao, X. (2017). Fragile X related protein 1 (FXR1P) regulates proliferation of adult neural stem cells. *Hum. Mol. Genet.* 26, 1340–1352. doi:10.1093/hmg/ddx034

Patzlaff, N. E., Shen, M., and Zhao, X. (2018). Regulation of adult neurogenesis by the fragile X family of RNA binding proteins. *Brain Plast.* 3, 205–223. doi:10.3233/BPL-170061

Paul, S., Dansithong, W., Figueroa, K. P., Gandelman, M., Scoles, D. R., and Pulst, S. M. (2021). Staufen1 in human neurodegeneration. *Ann. Neurol.* 89, 1114–1128. doi:10.1002/ana.26069

Peng, S.-C., Lai, Y.-T., Huang, H.-Y., Huang, H.-D., and Huang, Y.-S. (2010). A novel role of CPEB3 in regulating EGFR gene transcription via association with Stat5b in neurons. *Nucleic Acids Res.* 38, 7446–7457. doi:10.1093/nar/gkq634

Pevny, L. H., and Lovell-Badge, R. (1997). Sox genes find their feet. *Curr. Opin. Genet. Dev.* 7, 338–344. doi:10.1016/s0959-437x(97)80147-5

Pötschke, R., Haase, J., Glaß, M., Simmermacher, S., Misiak, C., Penalva, L. O. F., et al. (2020). MSI1 promotes the expression of the GBM stem cell marker CD44 by impairing miRNA-dependent degradation. *Cancers (Basel)* 12, E3654. doi:10.3390/cancers12123654

Qu, W., Jin, H., Chen, B.-P., Liu, J., Li, R., Guo, W., et al. (2020). CPEB3 regulates neuron-specific alternative splicing and involves neurogenesis gene expression. *Aging (Albany NY)* 13, 2330–2347. doi:10.18632/aging.202259

Ratti, A., Fallini, C., Cova, L., Fantozzi, R., Calzarossa, C., Zennaro, E., et al. (2006). A role for the ELAV RNA-binding proteins in neural stem cells: stabilization of Msi1 mRNA. *J. Cell Sci.* 119, 1442–1452. doi:10.1242/jcs.02852

Rehfeld, F., Rohde, A. M., Nguyen, D. T. T., and Wulczyn, F. G. (2015). Lin28 and let-7: ancient milestones on the road from pluripotency to neurogenesis. *Cell Tissue Res.* 359, 145–160. doi:10.1007/s00441-014-1872-2

Romer-Seibert, J. S., Hartman, N. W., and Moss, E. G. (2019). The RNA-binding protein LIN28 controls progenitor and neuronal cell fate during postnatal neurogenesis. *FASEB J.* 33, 3291–3303. doi:10.1096/fj.201801118R

Sanai, N., Tramontin, A. D., Quiñones-Hinojosa, A., Barbaro, N. M., Gupta, N., Kunwar, S., et al. (2004). Unique astrocyte ribbon in adult human brain contains neural stem cells but lacks chain migration. *Nature* 427, 740–744. doi:10.1038/nature02301

Sánchez-Vidaña, D. I., Po, K. K.-T., Fung, T. K.-H., Chow, J. K.-W., Lau, W. K.-W., So, P.-K., et al. (2019). Lavender essential oil ameliorates depression-like behavior and increases neurogenesis and dendritic complexity in rats. *Neurosci. Lett.* 701, 180–192. doi:10.1016/j.neulet.2019.02.042

Semple, B. D., Blomgren, K., Gimlin, K., Ferriero, D. M., and Noble-Haeusslein, L. J. (2013). Brain development in rodents and humans: Identifying benchmarks of maturation and vulnerability to injury across species. *Prog. Neurobiol.* 106 (107), 1–16. doi:10.1016/j.pneurobio.2013.04.001

Seri, B., García-Verdugo, J. M., Collado-Morente, L., McEwen, B. S., and Alvarez-Buylla, A. (2004). Cell types, lineage, and architecture of the germinal zone in the adult dentate gyrus. *J. Comp. Neurol.* 478, 359–378. doi:10.1002/cne.20288

Shao, J., Zhang, J., Zhang, Z., Jiang, H., Lou, X., Huang, B., et al. (2013). Alternative polyadenylation in glioblastoma multiforme and changes in predicted RNA binding protein profiles. *OMICS* 17, 136–149. doi:10.1089/omi.2012.0098

Suh, H., Consiglio, A., Ray, J., Sawai, T., D'Amour, K. A., and Gage, F. H. (2007). *In vivo* fate analysis reveals the multipotent and self-renewal capacities of Sox2+ neural stem cells in the adult hippocampus. *Cell Stem Cell* 1, 515–528. doi:10.1016/j.stem.2007.09.002

Takasawa, K., Kitagawa, K., Yagita, Y., Sasaki, T., Tanaka, S., Matsushita, K., et al. (2002). Increased proliferation of neural progenitor cells but reduced survival of newborn cells in the contralateral hippocampus after focal cerebral ischemia in rats. *J. Cereb. Blood Flow. Metab.* 22, 299–307. doi:10.1097/00004647-200203000-00007

Tanaka, S., Kamachi, Y., Tanouchi, A., Hamada, H., Jing, N., and Kondoh, H. (2004). Interplay of SOX and POU factors in regulation of the Nestin gene in neural primordial cells. *Mol. Cell. Biol.* 24, 8834–8846. doi:10.1128/MCB.24.20.8834-8846.2004

Tang, S., Zhao, Y., He, X., Zhu, J., Chen, S., Wen, J., et al. (2020). Identification of NOVA family proteins as novel β-catenin RNA-binding proteins that promote epithelial-mesenchymal transition. *RNA Biol.* 17, 881–891. doi:10.1080/15476286.2020.1734372

Tebaldi, T., Zuccotti, P., Peroni, D., Köhn, M., Gasperini, L., Potrich, V., et al. (2018). HuD is a neural translation enhancer acting on mTORC1-responsive genes and counteracted by the Y3 small non-coding RNA. *Mol. Cell* 71, 256–270. doi:10.1016/j.molcel.2018.06.032

Tepper, B., Koguc-Sobolewska, P., Jaslan, K., Turlejski, K., Bartkowska, K., and Djavadian, R. (2021). Impaired olfactory neurogenesis affects the performance of olfactory-guided behavior in aged female opossums. *Sci. Rep.* 11, 4418. doi:10.1038/s41598-021-83834-5

Theis, M., Si, K., and Kandel, E. R. (2003). Two previously undescribed members of the mouse CPEB family of genes and their inducible expression in the principal cell layers of the hippocampus. *Proc. Natl. Acad. Sci. U. S. A.* 100, 9602–9607. doi:10.1073/pnas.1133424100

Thomas, M. G., Martinez Tosar, L. J., Desbats, M. A., Leishman, C. C., and Boccaccio, G. L. (2009). Mammalian Staufen 1 is recruited to stress granules and impairs their assembly. *J. Cell Sci.* 122, 563–573. doi:10.1242/jcs.038208

Toda, M., Iizuka, Y., Yu, W., Imai, T., Ikeda, E., Yoshida, K., et al. (2001). Expression of the neural RNA-binding protein Musashi1 in human gliomas. *Glia* 34, 1–7. doi:10.1002/glia.1034

Uchikawa, M., Kamachi, Y., and Kondoh, H. (1999). Two distinct subgroups of group B sox genes for transcriptional activators and repressors: their expression during embryonic organogenesis of the chicken. *Mech. Dev.* 84, 103–120. doi:10.1016/s0925-4773(99)00083-0

Velasco, M. X., Kosti, A., Guardia, G. D. A., Santos, M. C., Tegge, A., Qiao, M., et al. (2019). Antagonism between the RNA-binding protein Musashi1 and miR-137 and its potential impact on neurogenesis and glioblastoma development. *RNA* 25, 768–782. doi:10.1261/rna.069211.118

Vessey, J. P., Amadei, G., Burns, S. E., Kiebler, M. A., Kaplan, D. R., and Miller, F. D. (2012). An asymmetrically localized Staufen2-dependent RNA complex regulates maintenance of mammalian neural stem cells. *Cell Stem Cell* 11, 517–528. doi:10.1016/j.stem.2012.06.010

Vessey, J. P., Macchi, P., Stein, J. M., Mikl, M., Hawker, K. N., Vogelsang, P., et al. (2008). A loss of function allele for murine Staufen1 leads to impairment of dendritic Staufen1-RNP delivery and dendritic spine morphogenesis. *Proc. Natl. Acad. Sci. U. S. A.* 105, 16374–16379. doi:10.1073/pnas.0804583105

Vogel, G., and Richard, S. (2012). Emerging roles for Sam68 in adipogenesis and neuronal development. *RNA Biol.* 9, 1129–1133. doi:10.4161/rna.21409

Wakiyama, M., Imataka, H., and Sonenberg, N. (2000). Interaction of eIF4G with poly(A)-binding protein stimulates translation and is critical for Xenopus oocyte maturation. *Curr. Biol.* 10, 1147–1150. doi:10.1016/s0960-9822(00)00701-6

Wang, C.-F., and Huang, Y.-S. (2012). Calpain 2 activated through N-methyl-D-aspartic acid receptor signaling cleaves CPEB3 and abrogates CPEB3-repressed translation in neurons. *Mol. Cell. Biol.* 32, 3321–3332. doi:10.1128/MCB.00296-12

Wang, T. J., Zhang, F., Richards, J. B., Kestenbaum, B., van Meurs, J. B., Berry, D., et al. (2010). Common genetic determinants of vitamin D insufficiency: a genome-wide association study. *Lancet* 376, 180–188. doi:10.1016/S0140-6736(10)60588-0

Wang, X., Han, Y., Zhang, A., and Sun, H. (2015). "Chapter 22 - metabolic profiling provides a system for the understanding of alzheimer's disease in rats post-treatment with kaixin san," in *Chinmedomics*. Editors X. Wang, A. Zhang, and H. Sun (Boston: Academic Press), 347–362. doi:10.1016/B978-0-12-803117-9.00022-6

Wang, Y., Guo, Y., Tang, C., Han, X., Xu, M., Sun, J., et al. (2019). Developmental cytoplasmic-to-nuclear translocation of RNA-binding protein HuR is required for adult neurogenesis. *Cell Rep.* 29, 3101–3117. doi:10.1016/j.celrep.2019.10.127

Yao, K. M., Samson, M. L., Reeves, R., and White, K. (1993). Gene elav of *Drosophila melanogaster*: a prototype for neuronal-specific RNA binding protein gene family that is conserved in flies and humans. *J. Neurobiol.* 24, 723–739. doi:10.1002/neu.480240604

Yau, S.-Y., Lau, B. W.-M., and So, K.-F. (2011). Adult hippocampal neurogenesis: a possible way how physical exercise counteracts stress. *Cell Transpl.* 20, 99–111. doi:10.3727/096368910X532846

frontiers | Frontiers in Cell and Developmental Biology

TYPE Review
PUBLISHED 21 March 2023
DOI 10.3389/fcell.2023.1164546

OPEN ACCESS

EDITED BY
Liang Zhou,
Southern Medical University, China

REVIEWED BY
Yang Yu,
Institute of Biophysics (CAS), China
Yangming Wang,
Peking University, China

*CORRESPONDENCE
Peng Tang,
tang_peng@gibh.ac.cn

SPECIALTY SECTION
This article was submitted to Signaling, a section of the journal Frontiers in Cell and Developmental Biology

RECEIVED 13 February 2023
ACCEPTED 03 March 2023
PUBLISHED 21 March 2023

CITATION
Deng M, Wang X, Xiong Z and Tang P (2023), Control of RNA degradation in cell fate decision.
Front. Cell Dev. Biol. 11:1164546.
doi: 10.3389/fcell.2023.1164546

Control of RNA degradation in cell fate decision

Mingqiang Deng[1,2], Xiwei Wang[3], Zhi Xiong[1,4] and Peng Tang[1]*

[1]Center for Cell Lineage and Development, Guangzhou Institutes of Biomedicine and Health, Chinese Academy of Sciences, Guangzhou, China, [2]Key Laboratory of Biological Targeting Diagnosis, Therapy and Rehabilitation of Guangdong Higher Education Institutes, The Fifth Affiliated Hospital of Guangzhou Medical University, Guangzhou, China, [3]Guangzhou Laboratory, Guangzhou, Guangdong, China, [4]Bioland Laboratory (Guangzhou Regenerative Medicine and Health GuangDong Laboratory), Guangzhou, China

Cell fate is shaped by a unique gene expression program, which reflects the concerted action of multilayered precise regulation. Substantial research attention has been paid to the contribution of RNA biogenesis to cell fate decisions. However, increasing evidence shows that RNA degradation, well known for its function in RNA processing and the surveillance of aberrant transcripts, is broadly engaged in cell fate decisions, such as maternal-to-zygotic transition (MZT), stem cell differentiation, or somatic cell reprogramming. In this review, we first look at the diverse RNA degradation pathways in the cytoplasm and nucleus. Then, we summarize how selective transcript clearance is regulated and integrated into the gene expression regulation network for the establishment, maintenance, and exit from a special cellular state.

KEYWORDS

RNA degradation, cell fate decision, stem cell, RNA alternative processing, post-transcriptional regulation

Introduction

Beginning with a fertilized egg, numerous identical or distinct cells are continually generated to ensure the proper organization and function of each tissue and organ during the lifespan of multicellular organisms (Tam and Behringer, 1997; Kojima et al., 2014). Deciphering the molecular mechanisms underlying the cell-type specific gene expression program, which ultimately shapes the cell fate and identity, is critically important not only in theory but also in the clinic. Improved knowledge of the regulatory mechanisms in cell fate decisions will deepen our understanding of normal or defective development and provide more detailed guidelines for regenerative medicine.

Pioneer works demonstrated that lineage conversion could be directed simply through the introduction of a specific transcription factor (Davis et al., 1987; Kulessa et al., 1995). In particular, somatic cells can be reprogramed into a pluripotent state *via* ectopic expression of a defined cocktail of transcription factors: Oct4, Klf4, Sox2, and Myc (Takahashi and Yamanaka, 2006). These and other additional lines of evidence convince us that transcription plays an instructive role in cell fate decisions. Consequently, regulation at the level of mRNA synthesis, in the context of transcription factors, epigenetics regulators, non-coding RNAs, and three-dimensional (3D) genome, is the primary research concern in cell fate decisions (Ng and Surani, 2011; Yadav et al., 2018; Stadhouders et al., 2019).

During the process of maternal-to-zygotic transition (MZT), the initial step of early embryo development in which fertilized egg is reprogrammed into a totipotent embryo, a subset of maternal RNAs must be cleared timely and efficiently apart from transcriptionally awakening the zygotic genome. Impediment in maternal RNA clearance by genetic

inactivation of the RNA degradation-associated genes *Btg4*, *Pabpn1l*, or *Cnot6l* leads to MZT failure and female infertility in mice (Liu et al., 2016; Yu et al., 2016; Sha et al., 2018; Zhao et al., 2020). A pairwise comparison of the RNA half-lives uncovered a significant discrepancy in the RNA decay rate for the genes uniformly expressed in both induced pluripotent stem (iPS) cells and the differentiated counterpart (Neff et al., 2012), implying a potential role of RNA degradation in pluripotency maintenance or somatic reprogramming. It has been reported that non-sense-mediated RNA decay or RNA N6-methyladenosine (m^6A) methylation could promote the degradation of specific pluripotency transcripts and facilitate mouse embryonic stem cell differentiation (Batista et al., 2014; Aguilo et al., 2015; Geula et al., 2015; Li et al., 2015), whereas RNA exosome complex restrains human embryonic stem cell differentiation by degrading differentiation-associated transcripts (Belair et al., 2019). In general, these compelling proofs indicate that RNA turnover should be an essential driving force in cell fate decisions.

Here, we briefly introduce the RNA degradation factors and describe how they orchestrate the highly regulated RNA degradation pathways. Furthermore, we outline how selective RNA turnover is regulated and becomes an integral part of the gene regulatory network in cell fate decisions.

RNA degradation machinery

For the majority of RNA polymerase II (Pol II) transcribed RNAs, a unique 7-methylguanosine (m^7G) cap will be installed at the 5′ end of nascent RNA (20–25 nucleotides in length), whereas a stretch of non-templated adenosines will be added to the 3′ end (poly(A) tail) (Shatkin and Manley, 2000; Rambout and Maquat, 2020; Passmore and Coller, 2022). m^7G cap and poly(A) tail act as versatile platforms to recruit diverse effector proteins and hence affect almost all aspects of RNA metabolism, such as RNA decay and translation efficiency (Furuichi et al., 1977; Shimotohno et al., 1977; Drummond et al., 1985; Bernstein et al., 1989; Caponigro and Parker, 1995; Rambout and Maquat, 2020; Passmore and Coller, 2022). Transcripts with unprotected ends will be swiftly removed by the RNA exonucleases. RNA exonucleases, together with many other core factors and co-factors of the RNA degradation machinery, orchestrate the RNA degradation pathways (Supplementary Table S1).

RNA exonucleases

During the whole life cycle, RNA is subject to surveillance by the RNA degradation machinery. RNA exonucleases clear the RNAs with exposed free ends in the 5′-to-3′ or 3′-to-5′ direction. In mammals, XRN1 and XRN2, located in the cytoplasm and nucleus, respectively, catalyze the 5′-to-3′ RNA hydrolysis processively (Nagarajan et al., 2013). Despite the difference in cellular localization, structure analysis reveals that XRN1 and XRN2 share an extensively conserved N-terminal domain, which is responsible for the exonucleolytic digestion of RNA with 5′-monophosphorylated ends, once activated by divalent cations (Jinek et al., 2011; Nagarajan et al., 2013; Overbeck et al., 2022).

Conversely, 3′-to-5′ RNA degradation is catalyzed by the multi-subunit complex, RNA exosome (Puno et al., 2019). The structure and composition of the RNA exosome are well conserved across species, wherein nine proteins form the barrel-shaped catalytically inactive core (EXO9), whereas the two catalytic subunits EXOSC10 and DIS3 (or DIS3L) are placed on the top and bottom of the EXO9 core, respectively (Zinder et al., 2016; Weick et al., 2018; Puno et al., 2019). EXOSC10 is a distributive 3′-to-5′ exonuclease, predominantly located in the nucleus, and trims RNAs with the 3′-hydroxyl terminus. By contrast, DIS3/DIS3L is a processive 3′-to-5′ exonuclease and digests RNAs with either 3′-hydroxyl or 3′-phosphate terminus. The majority of DIS3 resides in the nucleus, whereas DIS3L exclusively locates in the cytoplasm (Januszyk and Lima, 2014; Zinder et al., 2016; Puno et al., 2019). Acute protein depletion assays revealed that DIS3 principally contributes to the degradation of enhancer RNAs (eRNAs), promoter upstream transcripts (PROMPTs), and products of premature cleavage and polyadenylation (PCPA) in the nucleoplasm, whereas EXOSC10 primarily facilitates the trimming of short 3′ extended ribosomal and small nucleolar RNAs located in the nucleolus (Davidson et al., 2019).

Decapping and deadenylation complexes

As mentioned previously, RNA exonucleases can only attack RNA with exposed free 5′ or 3′ terminus. Thus, the cleavage of the 5′ cap structure (decapping) and/or removal of the 3′ poly(A) tail (deadenylation) is usually a prerequisite for RNA degradation.

Two factors, DCP1 and DCP2, act together as the decapping holoenzyme to cleave the m^7G cap and then release 5′ m^7GDP and 3′ fragment with monophosphate at the 5′ terminus. DCP2 specifically recognizes m^7G-cap or $m^{2,2,7}G$-cap and catalyzes their cleavage through its NUDIX domain, a motif shared in pyrophosphatases. However, DCP1 functions as a coactivator to enhance the decapping activity of DCP2 and bridges the interaction of the decapping complex with other co-factors (Ling et al., 2011; Vidya and Duchaine, 2022).

Compared with RNA decapping, RNA deadenylation seems more complicated that involves the PAN2–PAN3 and CCR4–NOT complexes, both functioning specifically on poly(A) sequences. A biphasic model is proposed for deadenylation: in the initial phase, poly(A)-binding protein PABPC1 facilitates the loading of the PAN2–PAN3 complex to remove the distal part of poly(A) tail through the distributive exonuclease PAN2. In the second, fast phase, the CCR4–NOT complex relays and digests the residual adenosines to a very few adenosines *via* the catalytic subunits CCR4 and CAF1 (Passmore and Coller, 2022).

RNA endonucleases

Although RNA exonucleases are required for complete RNA destruction, decapping and deadenylation are not essential. RNA exonucleolytic decay could be initiated at internal endonucleolytic sites within the RNA body (Coller and Parker, 2004; Tomecki and Dziembowski, 2010; Schoenberg, 2011). The RNA exonuclease DIS3, instead of its cytoplasmic paralog DIS3L, displays

endonucleolytic activity as well, which may cooperate with its exonuclease domain to clear RNAs more efficiently (Schaeffer et al., 2009; Schneider et al., 2009; Staals et al., 2010; Tomecki and Dziembowski, 2010; Tomecki et al., 2010). Cumulative evidence shows that RNA endonucleases have emerged as crucial modulators of gene expression (Tomecki and Dziembowski, 2010; Schoenberg, 2011).

Non-sense-mediated mRNA decay (NMD) and microRNAs (miRNAs)/small interfering RNA (siRNA)-mediated RNA interference (RNAi) in the cytoplasm may be the best-characterized cases involving the endonuclease activity. NMD is a quality control mechanism employed to eliminate transcripts harboring a premature termination codon (PTC) (Tomecki and Dziembowski, 2010; Schoenberg, 2011; Kurosaki et al., 2019). If a PTC locates ≥50–55 nucleotides (nt) upstream of an exon junction complex (EJC), the complex assembling ~24 nt upstream of the exon–exon junction following splicing, will induce ribosome stalling and sequentially activate the cascade of NMD to recruit the SMG5/SMG7 heterodimer or SMG6. SMG5 and SMG7 can recruit RNA decapping and deadenylation complex, whereas SMG6 can trigger endonucleolytic cleavage at the sites around the PTC (Kurosaki et al., 2019). These activities will be unified to initiate the clearance of faulty RNA substrates (Huntzinger et al., 2008; Eberle et al., 2009; Colombo et al., 2017; Boehm et al., 2021). Additionally, it was reported that transcripts with a 5′ upstream open reading frame (uORF) or an unusually long 3′ untranslated region (3′ UTR) could be NMD targets (Han et al., 2018; Kurosaki et al., 2019).

During RNAi, miRNA/siRNA associates with Argonaute (Ago) family protein and GW182 to form the functional RNA-induced silencing complex (RISC). Then, it silences its target expression by repressing translation or accelerating mRNA degradation, the latter of which is proved to be the major function of miRNAs in mammalian cells (Guo et al., 2010; Jonas and Izaurralde, 2015). Mechanistically, RISC could facilitate RNA deadenylation through the interaction of GW182 with the subunits of the deadenylation complexes, namely, PAN3, NOT1, and NOT9 (Jonas and Izaurralde, 2015). Alternatively, in the case of perfect base-pairing between miRNA/siRNA and its target, the endonucleolytic cleavage is favored *via* the slicing activity of the Ago2 protein (Valencia-Sanchez et al., 2006).

On the contrary, nuclear RNA endonucleases are under-reported. The Integrator complex is a metazoan-specific complex, originally identified in the biogenesis of non-coding RNA, such as small nuclear RNAs (snRNAs) and eRNAs (Lai et al., 2015). Recently, it was demonstrated that the Integrator would trigger premature transcription termination of many protein-coding genes through the endonucleolytic cleavage of the nascent transcripts (Elrod et al., 2019; Tatomer et al., 2019; Lykke-Andersen et al., 2021; Stein et al., 2022). In another scenario, Polycomb repressive complexes (PRCs) could recruit the Rixosome complex to the promoters of PRC target genes to silence their expression *via* endonucleolytic cleavage of the nascent RNAs, analogous to the Integrator complex (Zhou et al., 2022).

RNA degradation pathway

Most of our knowledge about RNA degradation pathways is from mRNA decay in the cytoplasm. In mammals, cytoplasmic mRNA degradation is usually initiated by deadenylation. Then, RNAs will be directly cleared through the 3′-to-5′ RNA decay pathway or will be decapped and followed by 5′-to-3′ degradation (Figure 1A). In terms of RNA endonucleases, such as SMG6 and Ago2, the transcripts are cleaved into the 5′ and 3′ fragments. The resulting intermediates will be subject to further clearance by cytoplasmic RNA exosome and XRN1, respectively (Figure 1B) (Coller and Parker, 2004).

By contrast, RNA degradation in the nucleus does not receive much attention. It has been demonstrated that the decapping complex is implicated in the degradation of U3 and U8 snoRNA in the nucleolus (Gaviraghi et al., 2018), Tsix RNA in the chromatin (Aeby et al., 2020), and nascent RNAs near the promoter-proximal pause sites (Brannan et al., 2012). However, decapping-dependent 5′-to-3′ RNA decay may not be a general nuclear RNA degradation way as RNA decapping usually requires the synergistic action of many auxiliary factors, most of which are concentrated in the cytoplasmic P body (Supplementary Table S1) (Coller and Parker, 2004; Ling et al., 2011; Vidya and Duchaine, 2022). Instead, the nuclear cap-binding complex (CBC) CBC20-CBC80 initially recognizes the 5′ m^7G cap, which in turn recruits the polyA tail exosome targeting (PAXT) or nuclear exosome targeting (NEXT) complex through the CBC-ARS2-ZC3H18 axis and serves to target the RNA substrates for degradation by nuclear RNA exosome (Figures 1C, D) (Garland and Jensen, 2020; Ogami and Suzuki, 2021). Alternatively, analogous to the described Integrator or Rixosome complex, RNA decay machinery may be co-transcriptionally recruited to the chromatin by the transcription machinery or histone modifiers for the degradation of target genes (Figure 1E) (Elrod et al., 2019; Tatomer et al., 2019; Lykke-Andersen et al., 2021; Garland et al., 2022; Stein et al., 2022; Zhou et al., 2022).

RNA degradation regulation in cell fate decision

As the general RNA decay machineries exhibit little substrate specificity, selective RNA degradation is determined largely by specific sequence features encoded in the RNA sequence and the cognate RNA-binding proteins (RBPs). Additionally, it is evidenced that RNA degradation is tightly interconnected with RNA processing (Tian and Manley, 2017; Kurosaki et al., 2019). In the following paragraphs, we will discuss how RNA degradation is regulated to specify cell fate.

Interplay between RNAs and RBPs dictates RNA decay in cell fate decision

RBP-mediated RNA decay regulation in cell fate decision

Approximately 1,900 and 1,400 proteins are cataloged as RBPs in *Homo sapiens* and *Mus musculus*, respectively, or more in other new datasets (Hentze et al., 2018). In principle, RBPs could bind to a specific sequence and/or structural motif in the RNA *via* their canonical or non-conventional RNA-binding domains (Hentze et al., 2018) and sequentially recruit different commitment

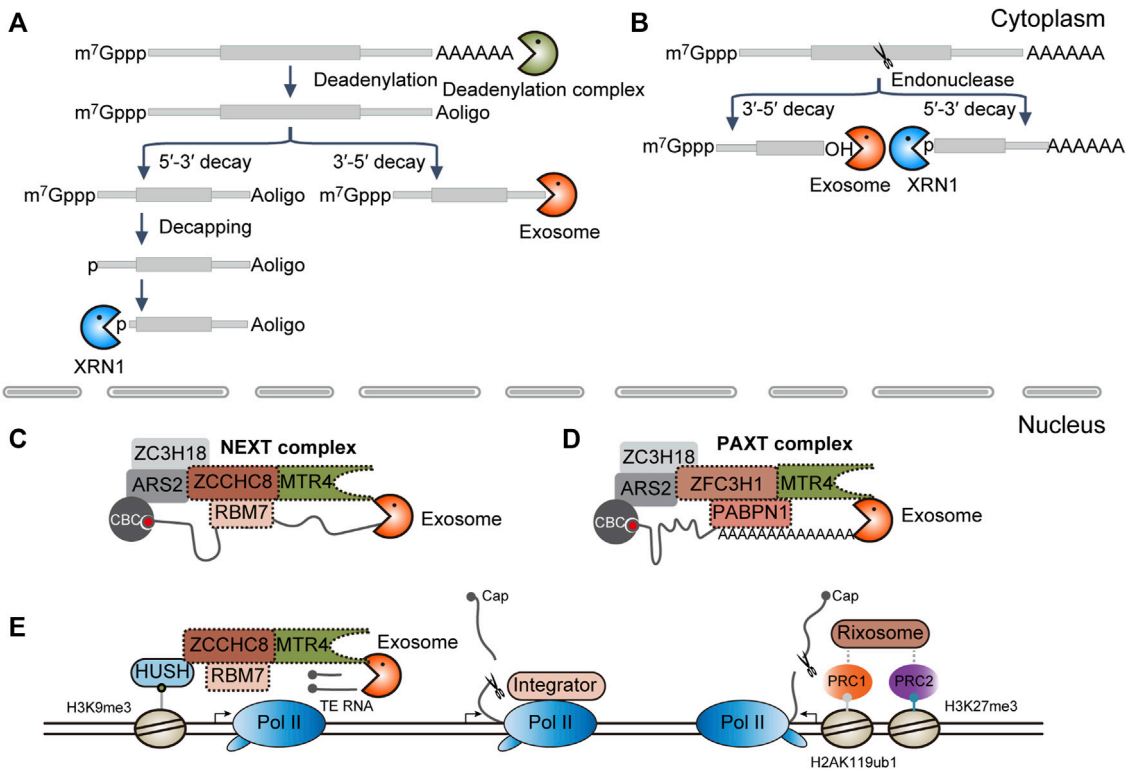

FIGURE 1
Diverse RNA decay pathways. **(A)** RNA exonucleolytic decay pathways in the cytoplasm. XRN1, 5′-to-3′ RNA exonuclease; exosome, 3′-to-5′ RNA exonuclease complex. **(B)** RNA endonucleolytic decay pathways in the cytoplasm. **(C)** NEXT complex-mediated RNA decay in the nucleus. CBC, cap-binding complex, composed of CBC20 and CBC80; NEXT, nuclear exosome targeting complex, composed of ZCCHC8, RBM7, and MTR4. **(D)** PAXT complex-mediated RNA decay in the nucleus. PAXT, PolyA tail exosome targeting complex, composed of ZFC3H1, PABPN1, and MTR4. **(E)** Co-transcriptional RNA decay pathways. Human silencing hub (HUSH) complex functions in the maintenance of the H3K9me3 modification. HUSH is composed of the chromodomain containing proteins MPP8, TASOR, and PPHLN1, in which MPP8 can interact directly with ZCCHC8, one subunit of the NEXT complex; Pol II, RNA polymerase II; Integrator is composed of 14 subunits, in which IntS11 along with IntS4 and 9 make up the endonucleolytic cleavage module. Integrator can directly bind to Pol II; PRC, Polycomb repressive complex; here, PRC1 and PRC2 can catalyze the mono-ubiquitination of histone H2A lysine 119 (H2AK119ub1) and tri-methylation of H3 lysine 27 (H3K27me3), respectively. Rixosome is composed of seven subunits, in which LAS1L is the endonucleolytic subunit, whereas the TEX10 subunit can interact with the PRC complex.

proteins or complex, such as RNA degradation machineries to regulate the fate of bound RNAs (He et al., 2022).

Upon oocyte meiotic resumption during mouse oocyte maturation, the MAPK signal pathway will be activated to extend the length of poly(A) tails of many maternal transcripts. Then, these transcripts will be activated translationally to produce more proteins, among which various RNA degradation factors are reported such as ZFP36L2, CNOT6L, CNOT7, BTG4, and PABPN1L (Liu et al., 2016; Yu et al., 2016; Sha et al., 2018; Zhao et al., 2020). At the early stage, increased ZFP36L2 recognizes AU-rich elements (AREs) containing transcripts and functions as an adapter to recruit the CCR4–NOT complex through interaction with the CNOT6L subunit (Sha et al., 2018). Later, PABPN1L specifically binds to the poly(A) tails and interacts with BTG4 to recruit the CCR4–NOT complex *via* the association with the CNOT7/8 subunit (Figure 2A) (Yu et al., 2016; Zhao et al., 2020). Together, they contribute to maternal transcripts clearance during oocyte maturation and MZT by accelerating deadenylation. Embryos with either BTG4 or PABPN1L depletion will be arrested at the 1~2-cell stage and characterized by female infertility (Liu et al., 2016; Yu et al., 2016; Zhao et al., 2020).

Murine primordial germ cells (PGCs) are first identified at the base of the incipient allantois around embryonic day (E) 7.25 (Saitou and Yamaji, 2012). *Dnd1* is transcriptionally activated during the stage E6.5–E6.75 in PGC precursors (Yabuta et al., 2006). DND1 could directly bind to transcripts with a UU(A/U) trinucleotide motif at the 3′ UTRs and then target substrates for degradation through recruiting the CCR4–NOT complex (Figure 2B). Especially, DND1 could preferentially suppress the expression of the regulators associated with apoptosis and inflammation, which is critical for the maintenance of the self-renewal of PGCs (Yamaji et al., 2017).

Small RNA-mediated RNA decay regulation in cell fate decision

Small RNAs of 20–30 nucleotides can be classified into three major classes—miRNAs, endogenous siRNAs (endo–siRNAs), and Piwi-interacting RNAs (piRNAs)—which differ in their biogenesis pathways and associated Argonaute-family proteins (Ghildiyal and Zamore, 2009; Kim et al., 2009). Generally, miRNAs/siRNAs could assemble with the Ago-subfamily proteins into the RISC complex and then target the base-paired targets for translation repression or

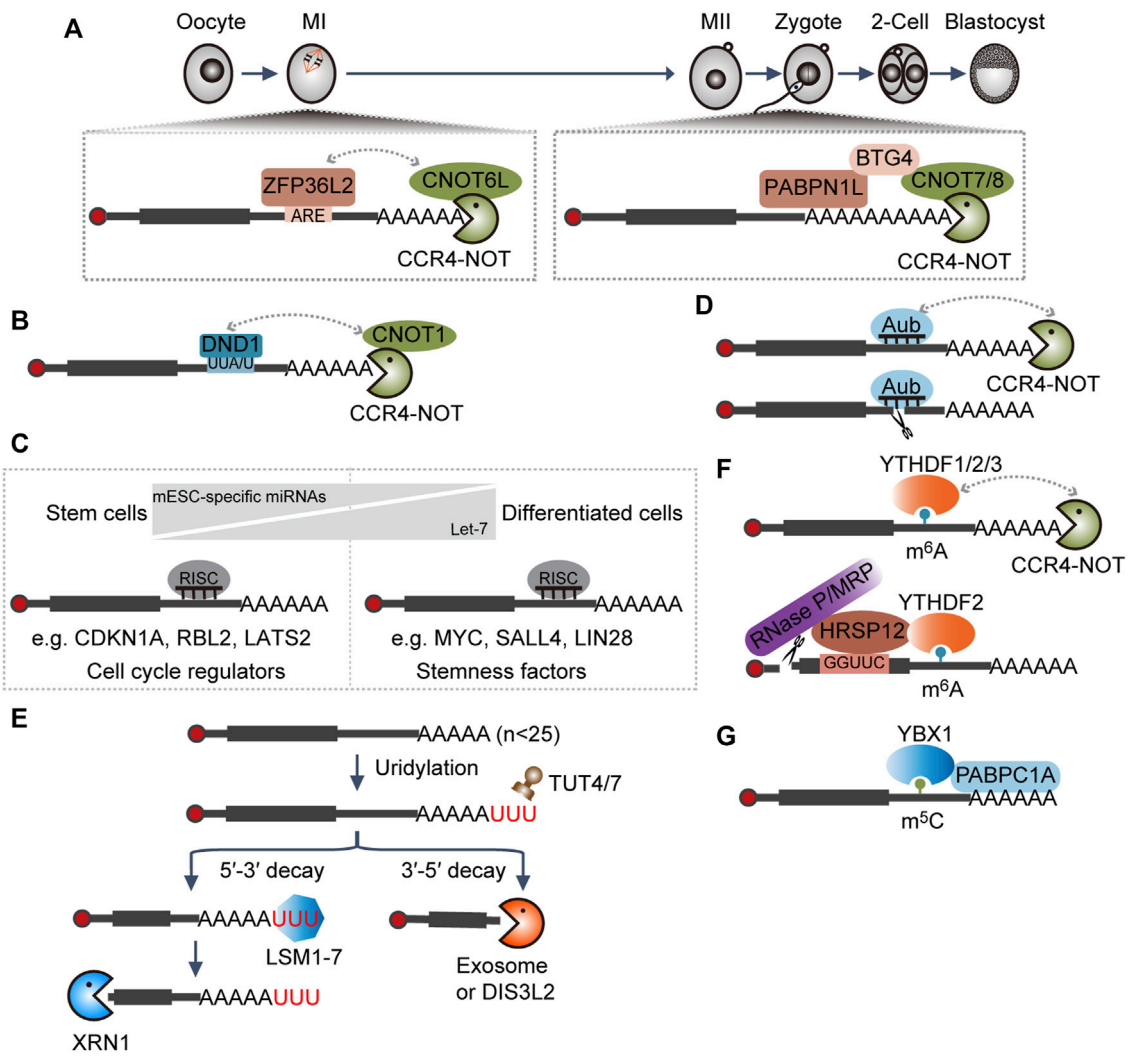

FIGURE 2
Interplay between RNAs and RNA-binding proteins (RBPs) dictates RNA decay. **(A,B)** RBP-mediated RNA degradation. ARE, AU-rich element; CCR4–NOT, RNA deadenylation complex. **(C)** miRNA-mediated RNA degradation. miRNA, microRNA; RISC, RNA-induced silencing complex; mESC-specific miRNAs, miRNAs specifically expressed in mouse embryonic stem cells: miR-291a-3p, miR-291b-3p, miR-294, miR-295, and miR-302. **(D)** piRNA-mediated RNA degradation. piRNA, Piwi-interacting RNA; Aubergine (Aub), the cytoplasmic Piwi proteins in *Drosophila*. **(E)** RNA uridylation-mediated RNA degradation. TUT4/7, RNA terminal uridylyltransferases; LSM1-7, a complex that especially recognizes the substrate with 3′ terminal oligoA tail and functions in facilitating RNA decapping; DIS3L2, RNA 3′-to-5′ exonuclease that especially functions in clearing RNAs with 3′ U- tail; XRN1, 5′-to-3′ RNA exonuclease; exosome, 3′-to-5′ RNA exonuclease complex. **(F)** m^6A-modification-mediated RNA degradation. m^6A, N6-methyladenosine; RNase P/MRP, a complex with endonucleolytic activity. **(G)** m^5C-modification-mediated RNA stabilization. m^5C, 5-methylcytosine.

RNA degradation, whereas piRNAs interact with Piwi-subfamily proteins and commonly function in transposon silencing (Ghildiyal and Zamore, 2009; Kim et al., 2009; Wang et al., 2022).

miRNAs can be further divided into canonical and non-canonical miRNAs; the former are initially transcribed as primary miRNAs and then processed into hairpin-shaped precursor (pre-miRNA) by the microprocessor, composed of DROSHA and DGCR8, in the nucleus. Subsequently, the resulting pre-miRNAs are exported into the cytoplasm, where they will be further cleaved by DICER into the miRNA duplex and assembled into the RISC complex (Ghildiyal and Zamore, 2009; Kim et al., 2009). Mouse embryonic stem cells (mESCs) with *Dgcr8* or *Dicer* knockout (KO) showed defects in proliferation and differentiation (Kanellopoulou et al., 2005; Murchison et al., 2005; Wang et al., 2007), indicating a dual role of miRNAs in pluripotency maintenance and differentiation. Mechanistically, mESC-specific miRNAs (miR-291a-3p, miR-291b-3p, miR-294, miR-295, and miR-302) shared similar seed regions and acted redundantly to reduce the level of *Cdkn1a*, *Rbl2*, and *Lats2*, negative regulators of G1-S cell cycle transition, thereby sustaining the high proliferation rate of mESCs (Wang Y. et al., 2008). Upon differentiation, mESC-specific miRNAs are downregulated, whereas mature let-7 are upregulated. Then, let-7 will bind to and facilitate the degradation of pluripotency-associated genes *Myc*, *Sall4*, and *Lin28*, thereby promoting mESC differentiation (Figure 2C) (Melton et al., 2010).

piRNAs are 23–31 nucleotides in length and are generated from single-stranded transcripts independent of DICER (Vagin et al.,

2006; Wang et al., 2022). In addition to the prominent role in transposon silencing, increasing evidence shows that the Piwi–piRNA complex is also implicated in the regulation of the stability or translation efficiency of protein-coding genes in germ cells (Wang et al., 2022). In early *Drosophila* embryos, piRNAs in complex with cytoplasmic Piwi protein Aubergine (Aub) or Argonaute 3 (Ago3) could target and direct the degradation of many maternal mRNAs involved in germ cell development by either direct endonucleolytic cleavage or recruitment of the CCR4–NOT deadenylation complex (Figure 2D) (Rouget et al., 2010; Barckmann et al., 2015).

endo-siRNAs are generated directly from long double-stranded RNAs by Dicer (Ghildiyal and Zamore, 2009; Kim et al., 2009). They co-exist with miRNAs and piRNAs in mouse oocytes (Tam et al., 2008; Watanabe et al., 2008). Mouse oocytes with Dicer but not Dgcr8 depletion showed meiotic arrest, accompanied by the dysregulation of many transcripts (Murchison et al., 2007; Tang et al., 2007; Suh et al., 2010), underscoring the essential role of endo-siRNAs in oogenesis. However, the exact transcripts for degradation remain unclear.

RNA modification-mediated RNA decay regulation in cell fate decision

Apart from the canonical 5′ m^7G cap and 3′ poly(A) tail modifications, RNAs are extensively decorated at the 3′ terminus or internal sites by other RNA modification enzymes, which have multifaceted roles in RNA metabolism, including RNA decay (Li and Mason, 2014; Yu and Kim, 2020).

TUT4 and TUT7 are terminal uridylyltransferases, which function redundantly in uridylating mRNAs with short poly(A) tails (shorter than ~25 nucleotides) (Lim et al., 2014). The LSM1–7 complex binds to short poly(A) tails with terminal uridylyl residues more efficiently and facilitates the assembly of the decapping complex (Chowdhury et al., 2007; Song and Kiledjian, 2007). Decapped mRNAs are then subject to degradation by XRN1, or alternatively, RNA exosome or DIS3L2 will digest the RNA from the 3′ end (Figure 2E) (Lim et al., 2014). Mice with *Tut4–Tut7* double-knockout failed to eliminate some maternal transcripts during oocyte maturation and cannot generate functional MII oocytes, thereby resulting in female infertility (Morgan et al., 2017; Chang et al., 2018).

m^6A, the most abundant internal modification in mRNAs, can be recognized by diverse readers to mediate different biological activities (Li and Mason, 2014). In the cytoplasm, YTHDF1/2/3 proteins redundantly bind to the same m^6A-modified mRNAs and directly recruit the CCR4–NOT deadenylase complex (Du et al., 2016; Zaccara and Jaffrey, 2020). In some instances, HRSP12 can bind to specific sequences upstream of the m^6A sites and facilitate the association between YTHDF2 and RNA endonuclease complex RNase P/MRP (Park et al., 2019). These activities, alone or together, contribute to accelerated RNA decay (Figure 2F) (Wang et al., 2014; Du et al., 2016; Park et al., 2019; Zaccara and Jaffrey, 2020). It was found that pluripotency factors, such as *Nanog*, *Sox2*, *Klf4*, and *c-Myc*, are modified by m^6A, ensuring their timely clearance and hence efficient exit from the self-renewal state during differentiation (Batista et al., 2014; Aguilo et al., 2015; Geula et al., 2015).

During MZT of zebrafish embryogenesis, Y-box-binding protein 1 (Ybx1) preferentially binds to a subset of maternal mRNAs with 5-methylcytosine (m^5C) modifications and protects them from degradation through the recruitment of the poly(A) tail-binding protein Pabpc1a (Figure 2G) (Yang et al., 2019), which ensures the production of sufficient associated proteins to support normal embryogenesis (Yang et al., 2019).

RNA alternative processing coupled RNA decay in cell fate decision

Alternative splicing coupled NMD in cell fate decision

As much as 95% of multiexon genes undergo alternative splicing in humans (Wang E. T. et al., 2008; Pan et al., 2008), greatly expanding the human proteome. Furthermore, transcriptome analysis revealed that ~30%–35% of the splicing events in human and mouse cells will introduce PTCs and thus can be NMD targets (Lewis et al., 2003; Pan et al., 2006; Weischenfeldt et al., 2012). Alternative splicing is dynamically regulated and coupled with NMD to regulate gene expression in diverse physiological activities (Kurosaki et al., 2019).

Mice with NMD factors KO typically suffered from embryonic lethality within the stage E5.5–E9.5, during which the three different germ layers' specialization initiates, implying that NMD may function in the progress from pluripotency toward differentiation (Medghalchi et al., 2001; Weischenfeldt et al., 2008; McIlwain et al., 2010; Li et al., 2015; Han et al., 2018). In line with this, it was expounded that the exit from naïve pluripotency was delayed if NMD-associated factors were depleted in the mESCs (Leeb et al., 2014; Li et al., 2015; Lackner et al., 2021; Huth et al., 2022).

Compared with the wide-type cells, *Smg6* KO mESCs displayed almost unaltered morphology and proliferation rate, suggesting SMG6 was dispensable for self-renewal maintenance. On the contrary, its differentiation potential was severely impaired, which could be recapitulated by the knockdown of other NMD factors (Li et al., 2015). Follow-up experiments revealed that NMD could target *c-Myc* for degradation through its 3′ UTR (Figure 3A). Hence, *c-Myc* is upregulated, which in turn blocks mESC differentiation upon *Smg6* KO (Cartwright et al., 2005; Li et al., 2015).

When *Smg5*, *Smg6*, and *Smg7* were knocked out independently in mESCs in another study, all these modified cell lines exhibited variable but pronounced impairment in differentiation (Huth et al., 2022), consistent with the previous study (Li et al., 2015). However, the authors did not observe an increased *c-Myc* level in NMD-deficient ESCs. Instead, they identified that *Eif4a2* was the NMD *bona fide* target responsible for differentiation delay (Huth et al., 2022). Mechanistically, *Eif4a2* could generate two isoforms through alternative splicing, one full-length isoform ($Eif4a2^{FL}$) and the other PTC-containing isoform ($Eif4a2^{PTC}$). NMD deficiency stabilized the $Eif4a2^{PTC}$ transcript to produce a truncated protein $Eif4a2^{PTC}$ (Figure 3B). $Eif4a2^{PTC}$ protein can specifically interact with the mTORC1 negative regulator TSC2 and dampen its activity. Thus, the mTORC1 activity increases and the translation rate is elevated in NMD-deficient ESCs, resulting in a delayed differentiation phenotype (Huth et al., 2022).

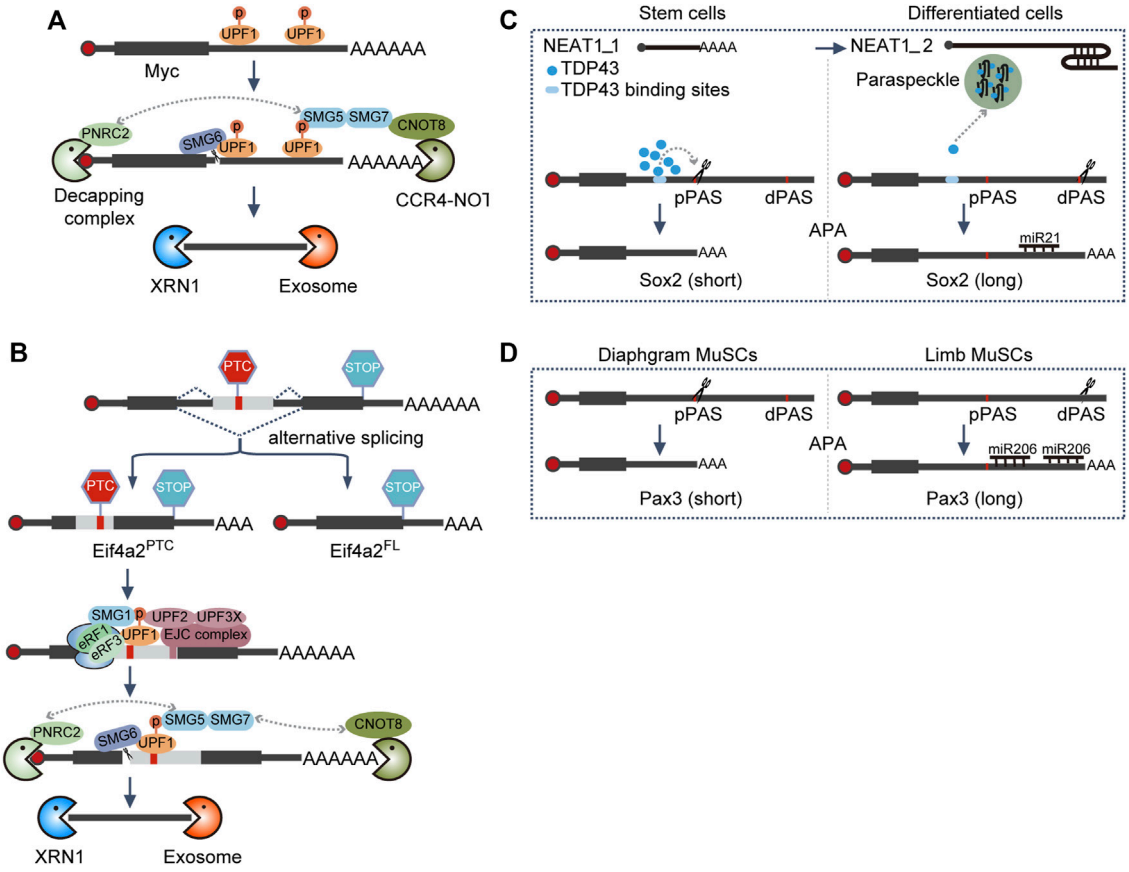

FIGURE 3
Alternative processing coupled RNA decay. **(A)** 3′ UTR-mediated NMD decay. Phosphorylation of UPF1, present on 3′ UTR, is a prerequisite for NMD activation, which in turn will recruit SMG5-SMG7 heterodimer and SMG6. NMD, non-sense-mediated RNA decay; SMG6, RNA endonuclease in the NMD pathway; CCR4-NOT, RNA deadenylation complex; PNRC2, a coactivator for RNA decapping, XRN1, 5′-to-3′ RNA exonuclease; exosome, 3′-to-5′ RNA exonuclease complex. **(B)** EJC-mediated NMD decay. PTC, located ≥50–55 nt upstream of an exon–exon junction, will trigger translation termination and activate the NMD pathway to phosphorylate UPF1, which in turn will recruit the SMG5-SMG7 heterodimer and SMG6. PTC, premature termination codon; STOP, normal stop codon; EJC, exon junction complex, which is assembled ~24 nt upstream of the exon–exon junction, following splicing. **(C)** APA-mediated RNA degradation regulation of Sox2. TDP43 binds to the element upstream of the pPAS of Sox2 and enhances pPAS processing. Upon differentiation, the transition from NEAT1_1 to NEAT1_2 will facilitate the formation of paraspeckles, ultimately leading to the sequestration of TDP43 and the utilization of dPAS of Sox2. NEAT1_1 and NEAT1_2 are short and long isoforms from gene *NEAT1*, respectively. pPAS, proximal polyA site; dPAS, distal polyA site; miR, microRNA; APA, alternative polyadenylation. **(D)** APA-mediated RNA degradation regulation of Pax3. MuSCs, muscle stem cells.

Alternative polyadenylation coupled RNA decay in cell fate decision

More than 70% of mammalian genes undergo alternative polyadenylation (APA), which could generate transcripts encoding different proteins or with different 3′ UTR lengths (Derti et al., 2012; Hoque et al., 2013). Longer 3′ UTR isoforms usually contain additional binding sites for RBPs or miRNAs and hence tend to exhibit differential stability, translation efficiency, or cellular localization compared with their shorter counterparts (Tian and Manley, 2017). Now, we know that APA is dynamically regulated and broadly engaged in cell fate transition, partially through the control of RNA decay (Sommerkamp et al., 2021).

By coinciding with the exit of pluripotency toward differentiation for both human ESCs (hESCs) and mESCs, the *NEAT1* gene switches from the short isoform NEAT1_1 in ESCs to express the long, full-length isoform NEAT1_2 (Modic et al., 2019), a scaffold RNA necessary for paraspeckle formation (Clemson et al., 2009; Sasaki et al., 2009; Sunwoo et al., 2009; Modic et al., 2019). TDP-43 will then be sequestered into the paraspeckles by NEAT1_2, resulting in the reduction of the available TDP-43. Thus, the ability of TDP43 to enhance proximal polyA site processing is lost, and the longer 3′ UTR transcripts of SOX2 would be favored in differentiated cells, which can be further targeted by miR-21 for degradation; thereby, the pluripotency factor SOX2 is suppressed, and the dissolution of pluripotency is promoted (Figure 3C) (Modic et al., 2019).

Likewise, although miR-206 exhibits similar expression levels in both limb and diaphragm muscle stem cells (MuSCs), it only downregulates the target gene *Pax3* expression in limb MuSCs. As *Pax3* preferentially chooses the proximal polyA site (pPAS) during APA in diaphragm MuSCs to circumvent the function of miR-206, thus a high PAX3 level is sustained to support the proliferation of diaphragm MuSCs (Figure 3D) (Boutet et al., 2012).

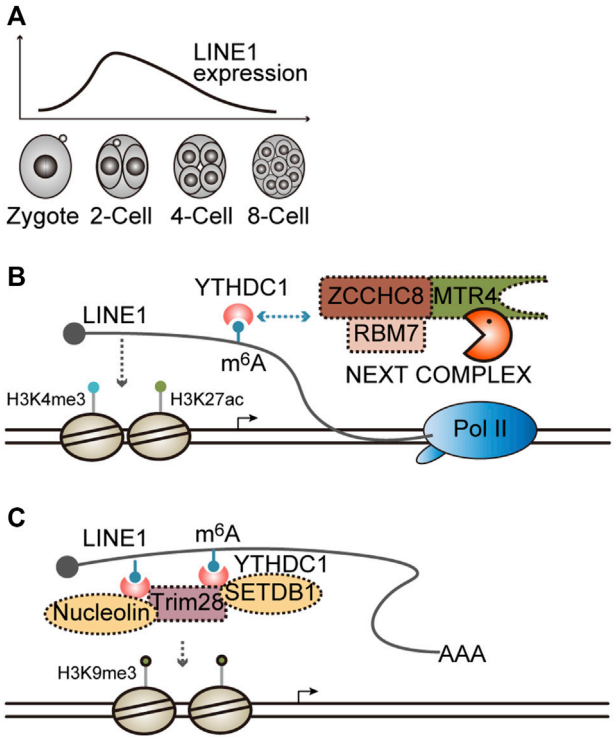

FIGURE 4
Functions and the degradation of LINE1 RNA. **(A)** Dynamic expression of LINE1 in mouse preimplantation embryos. LINE1, long interspersed nuclear element. **(B)** LINE1 RNA promotes an open chromatin state and is regulated by the NEXT complex. LINE1 can recruit histone modifiers that install activation marks H3K4me3/H3K27ac. LINE1 is modified by m^{6}A modification and can be recognized by the m^{6}A modification reader YTHDC1, which in turn recruits the NEXT complex to facilitate the decay of LINE1. m^{6}A, N6-methyladenosine; NEXT, nuclear exosome targeting complex, is an adapter for RNA exosome. **(C)** LINE1 RNA facilitates the formation of a close chromatin state. LINE1 is modified by m^{6}A modification and can be recognized by m^{6}A modification reader YTHDC1, which in turn recruits Trim28/nucleolin or the Trim28/SETDB1 complex to facilitate the disposition of repressive mark H3K9me3.

lncRNA decay coupled transcription regulation in cell fate decision

All the examples described previously focus on the roles of protein-coding gene decay in cell fate decisions. Given the crucial role of lncRNA in cell differentiation and development (Fatica and Bozzoni, 2014), despite being poorly characterized, the decay of lncRNA should also be involved in cell fate decisions.

The retrotransposon long interspersed nuclear element-1 (LINE1) is transcriptionally activated in mouse preimplantation development, especially at the two-cell (2C) stage (Figure 4A) (Jachowicz et al., 2017). When LINE1 expression is silenced through transcription repression immediately after fertilization, most of the embryos arrest at the 2C stage, which can be recapitulated through antisense oligo- (ASO)-mediated knockdown of LINE1 RNA, indicating the crucial role of LINE1 RNA in early embryogenesis (Jachowicz et al., 2017; Percharde et al., 2018). However, if LINE1 is enforced to express at a higher level beyond the 2C stage when LINE1 is naturally downregulated (Figure 4A), half of the embryos fail entry into the blastocyst stage (Jachowicz et al., 2017), suggesting LINE1 RNA should be maintained at a proper level to sustain mouse preimplantation embryogenesis.

Notably, LINE1 can be targeted for degradation by the NEXT complex in mouse ESCs and embryos. The depletion of Zcchc8, the scaffold subunit of the NEXT complex, will lead to LINE1 upregulation and developmental defects in mice (Wu et al., 2019). Furthermore, LINE1 is modified by m^{6}A methylation, which can be recognized by the nuclear m^{6}A reader YTHDC1 and then enhances the association between the NEXT complex and LINE1, thereby accelerating LINE1 degradation (Liu et al., 2020; Wei et al., 2022). When *Fto*, the m^{6}A demethylase, is knocked out, the LINE1 m^{6}A level is elevated, whereas its expression level is reduced accordingly. Moreover, Mice with *Fto* KO exhibit developmental defects analogous to *Zcchc8* KO (Wu et al., 2019; Wei et al., 2022). Mechanistically, it was demonstrated that LINE1 is essential for maintaining a global open chromatin state. An elevated LINE1 level results in greater chromatin accessibility, whereas a reduced LINE1 level causes chromatin condensation, which can be reflected by altered histone modifications (Figure 4B) (Jachowicz et al., 2017; Wu et al., 2019; Wei et al., 2022). Collectively, these results indicate that LINE1 is dynamically expressed during early development. Its degradation, at least partially, may contribute to the gradual chromatin compaction that occurs naturally in developmental progression, thereby ensures the ordered developmental program.

Interestingly, it was demonstrated in another two studies that the binding of YTHDC1 to LINE1 recruits Nucleolin/Trim28 or SETDB1/Trim28 complex to facilitate the deposition of H3K9me3 and then silences target gene expression, such as Dux, a master regulator of the 2C-specific transcriptome (Figure 4C) (Chen et al., 2021; Liu et al., 2021), implying that the function of LINE1 RNAs at different genomic loci may rely on the recruited effector proteins. However, how this difference is achieved remains elusive.

Conclusion and perspectives

RNA degradation machineries, composed of RNA exonucleases, endonucleases, and other co-factors, are involved in the processing and maturation of snoRNA, snRNA, and rRNA, among others, and clearing of aberrant mRNAs with PTCs or those without stop codons (Puno et al., 2019; Wolin and Maquat, 2019). Beyond these roles in RNA processing and quality control, RNA degradation is actively implicated in the control of RNA quantity and hence the regulation of gene expression in diverse physiological activities (Tomecki and Dziembowski, 2010; Schoenberg, 2011; Akira and Maeda, 2021).

RNA degradation is especially important in cell fate decisions because rapid shifts in the mRNA and protein constitution during the transition between different cell states require activating new gene expression programs, meanwhile silencing the old ones. RNA degradation can independently clear specific pre-existing RNAs associated with the previous cell type (Akira and Maeda, 2021), or it can synergize with transcriptional repression to consolidate the silencing effect (Yamaji et al., 2017; Garland et al., 2022; Zhou et al., 2022). The coordination of RNA synthesis and RNA decay determines cell identity and plasticity. It is evidenced that the

modulation of RNA decay by additional expression of certain miRNAs with transcription factors can significantly enhance the reprogramming efficiency (Judson et al., 2009; Liao et al., 2011), highlighting the important role and potential implication of RNA degradation control.

RNA deadenylation seems to be the initial and rate-limiting step in RNA degradation. RBPs (Yu et al., 2016; Yamaji et al., 2017; Sha et al., 2018; Zhao et al., 2020), small RNA (Wang Y. et al., 2008; Melton et al., 2010; Barckmann et al., 2015), RNA modification (Batista et al., 2014; Aguilo et al., 2015; Geula et al., 2015; Du et al., 2016), and NMD (Tomecki and Dziembowski, 2010; Schoenberg, 2011; Huth et al., 2022) can facilitate RNA degradation and alter the cell fate *via* the recruitment of the CCR4–NOT deadenylation complex. Although small RNA and NMD can trigger endonucleolytic cleavage of RNA (Valencia-Sanchez et al., 2006; Tomecki and Dziembowski, 2010; Schoenberg, 2011), no reported RNA endonuclease, analogous to the Regnase protein in the immunological system (Akira and Maeda, 2021), can function independently to regulate the cell fate. Maybe strategies developed to systematically map the endonucleolytic sites could enable us to identify such potential endonucleases (Karginov et al., 2010; Ibrahim and Mourelatos, 2019; Tang et al., 2022). Conversely, the RNA endonuclease complex can be co-transcriptionally loaded to cleave the nascent RNAs and trigger transcription termination (Elrod et al., 2019; Tatomer et al., 2019; Stein et al., 2022; Zhou et al., 2022); whether this or similar RNA degradation pathways are applied in regulate the cell fate awaits further investigation.

During the transition between different cellular states, the number of RBPs or miRNAs is dynamically regulated to control RNA degradation (Wang Y. et al., 2008; Melton et al., 2010; Liu et al., 2016; Yu et al., 2016; Yamaji et al., 2017; Sha et al., 2018; Zhao et al., 2020). As signal pathways are integrated to control the activity of transcription factors in pluripotency cells (Li and Belmonte, 2017), the connection between RNA degradation and signal pathways in other systems is also clear (Thapar and Denmon, 2013; Akira and Maeda, 2021). How signal pathways are linked with RNA degradation pathways to regulate cell fate is also of specific interest.

Author contributions

PT conceived the study. MD and PT wrote the manuscript. All authors discussed and approved the manuscript.

Acknowledgments

This work was supported by grants of the National Key Research and Development Program of China (no. 2021YFA1100401), the Natural Science Foundation of China (no. 32170745), GuangDong Basic and Applied Basic Research Foundation (no. 2020A1515110096), Science and Technology Planning Project of Guangzhou City (no. 202102020174), the China NSFC projects (no. 31800689).

Conflict of interest

The authors declare that the research was conducted in the absence of any commercial or financial relationships that could be construed as a potential conflict of interest.

Publisher's note

Supplementary material

The Supplementary Material for this article can be found online at: https://www.frontiersin.org/articles/10.3389/fcell.2023.1164546/full#supplementary-material

References

Aeby, E., Lee, H. G., Lee, Y. W., Kriz, A., Del Rosario, B. C., Oh, H. J., et al. (2020). Decapping enzyme 1A breaks X-chromosome symmetry by controlling Tsix elongation and RNA turnover. *Nat. Cell Biol.* 22 (9), 1116–1129. doi:10.1038/s41556-020-0558-0

Aguilo, F., Zhang, F., Sancho, A., Fidalgo, M., Di Cecilia, S., Vashisht, A., et al. (2015). Coordination of m(6)A mRNA methylation and gene transcription by ZFP217 regulates pluripotency and reprogramming. *Cell Stem Cell* 17 (6), 689–704. doi:10.1016/j.stem.2015.09.005

Akira, S., and Maeda, K. (2021). Control of RNA stability in immunity. *Annu Rev. Immunol.* 39, 481–509. doi:10.1146/annurev-immunol-101819-075147

Barckmann, B., Pierson, S., Dufourt, J., Papin, C., Armenise, C., Port, F., et al. (2015). Aubergine iCLIP reveals piRNA-dependent decay of mRNAs involved in germ cell development in the early embryo. *Cell Rep.* 12 (7), 1205–1216. doi:10.1016/j.celrep.2015.07.030

Batista, P. J., Molinie, B., Wang, J., Qu, K., Zhang, J., Li, L., et al. (2014). m(6)A RNA modification controls cell fate transition in mammalian embryonic stem cells. *Cell Stem Cell* 15 (6), 707–719. doi:10.1016/j.stem.2014.09.019

Belair, C., Sim, S., Kim, K. Y., Tanaka, Y., et al. (2019). The RNA exosome nuclease complex regulates human embryonic stem cell differentiation. *J. Cell Biol.* 218 (8), 2564–2582. doi:10.1083/jcb.201811148

Bernstein, P., Peltz, S. W., and Ross, J. (1989). The poly(A)-poly(A)-binding protein complex is a major determinant of mRNA stability *in vitro*. *Mol. Cell Biol.* 9 (2), 659–670. doi:10.1128/mcb.9.2.659

Boehm, V., Kueckelmann, S., Gerbracht, J. V., Kallabis, S., Britto-Borges, T., Altmuller, J., et al. (2021). SMG5-SMG7 authorize nonsense-mediated mRNA decay by enabling SMG6 endonucleolytic activity. *Nat. Commun.* 12 (1), 3965. doi:10.1038/s41467-021-24046-3

Boutet, S. C., Cheung, T. H., Quach, N. L., Liu, L., Prescott, S. L., Edalati, A., et al. (2012). Alternative polyadenylation mediates microRNA regulation of muscle stem cell function. *Cell Stem Cell* 10 (3), 327–336. doi:10.1016/j.stem.2012.01.017

Brannan, K., Kim, H., Erickson, B., Glover-Cutter, K., Kim, S., Fong, N., et al. (2012). mRNA decapping factors and the exonuclease Xrn2 function in widespread premature termination of RNA polymerase II transcription. *Mol. Cell* 46 (3), 311–324. doi:10.1016/j.molcel.2012.03.006

Caponigro, G., and Parker, R. (1995). Multiple functions for the poly(A)-binding protein in mRNA decapping and deadenylation in yeast. *Genes Dev.* 9 (19), 2421–2432. doi:10.1101/gad.9.19.2421

Cartwright, P., McLean, C., Sheppard, A., Rivett, D., Jones, K., and Dalton, S. (2005). LIF/STAT3 controls ES cell self-renewal and pluripotency by a Myc-dependent mechanism. *Development* 132 (5), 885–896. doi:10.1242/dev.01670

Chang, H., Yeo, J., Kim, J. G., Kim, H., Lim, J., Lee, M., et al. (2018). Terminal uridylyltransferases execute programmed clearance of maternal transcriptome in vertebrate embryos. *Mol. Cell* 70 (1), 72–82. doi:10.1016/j.molcel.2018.03.004

Chen, C., Liu, W., Guo, J., Liu, Y., Liu, X., Liu, J., et al. (2021). Nuclear m(6)A reader YTHDC1 regulates the scaffold function of LINE1 RNA in mouse ESCs and early embryos. *Protein Cell* 12 (6), 455–474. doi:10.1007/s13238-021-00837-8

Chowdhury, A., Mukhopadhyay, J., and Tharun, S. (2007). The decapping activator Lsm1p-7p-Pat1p complex has the intrinsic ability to distinguish between oligoadenylated and polyadenylated RNAs. *RNA* 13 (7), 998–1016. doi:10.1261/rna.502507

Clemson, C. M., Hutchinson, J. N., Sara, S. A., Ensminger, A. W., Fox, A. H., Chess, A., et al. (2009). An architectural role for a nuclear noncoding RNA: NEAT1 RNA is essential for the structure of paraspeckles. *Mol. Cell* 33 (6), 717–726. doi:10.1016/j.molcel.2009.01.026

Coller, J., and Parker, R. (2004). Eukaryotic mRNA decapping. *Annu Rev. Biochem* 73, 861–890. doi:10.1146/annurev.biochem.73.011303.074032

Colombo, M., Karousis, E. D., Bourquin, J., Bruggmann, R., and Muhlemann, O. (2017). Transcriptome-wide identification of NMD-targeted human mRNAs reveals extensive redundancy between SMG6-and SMG7-mediated degradation pathways. *RNA* 23 (2), 189–201. doi:10.1261/rna.059055.116

Davidson, L., Francis, L., Cordiner, R. A., Eaton, J. D., Estell, C., Macias, S., et al. (2019). Rapid depletion of DIS3, EXOSC10, or XRN2 reveals the immediate impact of exoribonucleolysis on nuclear RNA metabolism and transcriptional control. *Cell Rep.* 26 (10), 2779–2791. doi:10.1016/j.celrep.2019.02.012

Davis, R. L., Weintraub, H., and Lassar, A. B. (1987). Expression of a single transfected cDNA converts fibroblasts to myoblasts. *Cell* 51 (6), 987–1000. doi:10.1016/0092-8674(87)90585-x

Derti, A., Garrett-Engele, P., Macisaac, K. D., Stevens, R. C., Sriram, S., Chen, R., et al. (2012). A quantitative atlas of polyadenylation in five mammals. *Genome Res.* 22 (6), 1173–1183. doi:10.1101/gr.132563.111

Drummond, D. R., Armstrong, J., and Colman, A. (1985). The effect of capping and polyadenylation on the stability, movement and translation of synthetic messenger RNAs in Xenopus oocytes. *Nucleic Acids Res.* 13 (20), 7375–7394. doi:10.1093/nar/13.20.7375

Du, H., Zhao, Y., He, J., Zhang, Y., Xi, H., Liu, M., et al. (2016). YTHDF2 destabilizes m(6)A-containing RNA through direct recruitment of the CCR4-NOT deadenylase complex. *Nat. Commun.* 7, 12626. doi:10.1038/ncomms12626

Eberle, A. B., Lykke-Andersen, S., Muhlemann, O., and Jensen, T. H. (2009). SMG6 promotes endonucleolytic cleavage of nonsense mRNA in human cells. *Nat. Struct. Mol. Biol.* 16 (1), 49–55. doi:10.1038/nsmb.1530

Elrod, N. D., Henriques, T., Huang, K. L., Tatomer, D. C., Wilusz, J. E., Wagner, E. J., et al. (2019). The integrator complex attenuates promoter-proximal transcription at protein-coding genes. *Mol. Cell* 76 (5), 738–752. doi:10.1016/j.molcel.2019.10.034

Fatica, A., and Bozzoni, I. (2014). Long non-coding RNAs: New players in cell differentiation and development. *Nat. Rev. Genet.* 15 (1), 7–21. doi:10.1038/nrg3606

Furuichi, Y., LaFiandra, A., and Shatkin, A. J. (1977). 5'-Terminal structure and mRNA stability. *Nature* 266 (5599), 235–239. doi:10.1038/266235a0

Garland, W., and Jensen, T. H. (2020). Nuclear sorting of RNA. *Wiley Interdiscip. Rev. RNA* 11 (2), e1572. doi:10.1002/wrna.1572

Garland, W., Muller, I., Wu, M., Schmid, M., Imamura, K., Rib, L., et al. (2022). Chromatin modifier HUSH co-operates with RNA decay factor NEXT to restrict transposable element expression. *Mol. Cell* 82 (9), 1691–1707.e8. doi:10.1016/j.molcel.2022.03.004

Gaviraghi, M., Vivori, C., Pareja Sanchez, Y., Invernizzi, F., Cattaneo, A., Santoliquido, B. M., et al. (2018). Tumor suppressor PNRC1 blocks rRNA maturation by recruiting the decapping complex to the nucleolus. *EMBO J.* 37, e99179. doi:10.15252/embj.201899179

Geula, S., Moshitch-Moshkovitz, S., Dominissini, D., Mansour, A. A., Kol, N., Salmon-Divon, M., et al. (2015). Stem cells. m6A mRNA methylation facilitates resolution of naïve pluripotency toward differentiation. *Science* 347 (6225), 1002–1006. doi:10.1126/science.1261417

Ghildiyal, M., and Zamore, P. D. (2009). Small silencing RNAs: An expanding universe. *Nat. Rev. Genet.* 10 (2), 94–108. doi:10.1038/nrg2504

Guo, H., Ingolia, N. T., Weissman, J. S., and Bartel, D. P. (2010). Mammalian microRNAs predominantly act to decrease target mRNA levels. *Nature* 466 (7308), 835–840. doi:10.1038/nature09267

Han, X., Wei, Y., Wang, H., Wang, F., Ju, Z., and Li, T. (2018). Nonsense-mediated mRNA decay: A 'nonsense' pathway makes sense in stem cell biology. *Nucleic Acids Res.* 46 (3), 1038–1051. doi:10.1093/nar/gkx1272

He, S., Valkov, E., Cheloufi, S., and Murn, J. (2022). The nexus between RNA-binding proteins and their effectors. *Nat. Rev. Genet*. doi:10.1038/s41576-022-00550-0

Hentze, M. W., Castello, A., Schwarzl, T., and Preiss, T. (2018). A brave new world of RNA-binding proteins. *Nat. Rev. Mol. Cell Biol.* 19 (5), 327–341. doi:10.1038/nrm.2017.130

Hoque, M., Ji, Z., Zheng, D., Luo, W., Li, W., You, B., et al. (2013). Analysis of alternative cleavage and polyadenylation by 3' region extraction and deep sequencing. *Nat. Methods* 10 (2), 133–139. doi:10.1038/nmeth.2288

Huntzinger, E., Kashima, I., Fauser, M., Sauliere, J., and Izaurralde, E. (2008). SMG6 is the catalytic endonuclease that cleaves mRNAs containing nonsense codons in metazoan. *RNA* 14 (12), 2609–2617. doi:10.1261/rna.1386208

Huth, M., Santini, L., Galimberti, E., Ramesmayer, J., Titz-Teixeira, F., Sehlke, R., et al. (2022). NMD is required for timely cell fate transitions by fine-tuning gene expression and regulating translation. *Genes Dev.* 36 (5-6), 348–367. doi:10.1101/gad.347690.120

Ibrahim, F., and Mourelatos, Z. (2019). Capturing 5' and 3' native ends of mRNAs concurrently with Akron sequencing. *Nat. Protoc.* 14 (5), 1578–1602. doi:10.1038/s41596-019-0151-9

Jachowicz, J. W., Bing, X., Pontabry, J., Boskovic, A., Rando, O. J., and Torres-Padilla, M. E. (2017). LINE-1 activation after fertilization regulates global chromatin accessibility in the early mouse embryo. *Nat. Genet.* 49 (10), 1502–1510. doi:10.1038/ng.3945

Januszyk, K., and Lima, C. D. (2014). The eukaryotic RNA exosome. *Curr. Opin. Struct. Biol.* 24, 132–140. doi:10.1016/j.sbi.2014.01.011

Jinek, M., Coyle, S. M., and Doudna, J. A. (2011). Coupled 5' nucleotide recognition and processivity in Xrn1-mediated mRNA decay. *Mol. Cell* 41 (5), 600–608. doi:10.1016/j.molcel.2011.02.004

Jonas, S., and Izaurralde, E. (2015). Towards a molecular understanding of microRNA-mediated gene silencing. *Nat. Rev. Genet.* 16 (7), 421–433. doi:10.1038/nrg3965

Judson, R. L., Babiarz, J. E., Venere, M., and Blelloch, R. (2009). Embryonic stem cell-specific microRNAs promote induced pluripotency. *Nat. Biotechnol.* 27 (5), 459–461. doi:10.1038/nbt.1535

Kanellopoulou, C., Muljo, S. A., Kung, A. L., Ganesan, S., Drapkin, R., Jenuwein, T., et al. (2005). Dicer-deficient mouse embryonic stem cells are defective in differentiation and centromeric silencing. *Genes Dev.* 19 (4), 489–501. doi:10.1101/gad.1248505

Karginov, F. V., Cheloufi, S., Chong, M. M., Stark, A., Smith, A. D., and Hannon, G. J. (2010). Diverse endonucleolytic cleavage sites in the mammalian transcriptome depend upon microRNAs, Drosha, and additional nucleases. *Mol. Cell* 38 (6), 781–788. doi:10.1016/j.molcel.2010.06.001

Kim, V. N., Han, J., and Siomi, M. C. (2009). Biogenesis of small RNAs in animals. *Nat. Rev. Mol. Cell Biol.* 10 (2), 126–139. doi:10.1038/nrm2632

Kojima, Y., Tam, O. H., and Tam, P. P. (2014). Timing of developmental events in the early mouse embryo. *Semin. Cell Dev. Biol.* 34, 65–75. doi:10.1016/j.semcdb.2014.06.010

Kulessa, H., Frampton, J., and Graf, T. (1995). GATA-1 reprograms avian myelomonocytic cell lines into eosinophils, thromboblasts, and erythroblasts. *Genes Dev.* 9 (10), 1250–1262. doi:10.1101/gad.9.10.1250

Kurosaki, T., Popp, M. W., and Maquat, L. E. (2019). Quality and quantity control of gene expression by nonsense-mediated mRNA decay. *Nat. Rev. Mol. Cell Biol.* 20 (7), 406–420. doi:10.1038/s41580-019-0126-2

Lackner, A., Sehlke, R., Garmhausen, M., Giuseppe Stirparo, G., Huth, M., Titz-Teixeira, F., et al. (2021). Cooperative genetic networks drive embryonic stem cell transition from naive to formative pluripotency. *EMBO J.* 40 (8), e105776. doi:10.15252/embj.2020105776

Lai, F., Gardini, A., Zhang, A., and Shiekhattar, R. (2015). Integrator mediates the biogenesis of enhancer RNAs. *Nature* 525 (7569), 399–403. doi:10.1038/nature14906

Leeb, M., Dietmann, S., Paramor, M., Niwa, H., and Smith, A. (2014). Genetic exploration of the exit from self-renewal using haploid embryonic stem cells. *Cell Stem Cell* 14 (3), 385–393. doi:10.1016/j.stem.2013.12.008

Lewis, B. P., Green, R. E., and Brenner, S. E. (2003). Evidence for the widespread coupling of alternative splicing and nonsense-mediated mRNA decay in humans. *Proc. Natl. Acad. Sci. U S A* 100 (1), 189–192. doi:10.1073/pnas.0136770100

Li, M., and Belmonte, J. C. (2017). Ground rules of the pluripotency gene regulatory network. *Nat. Rev. Genet.* 18 (3), 180–191. doi:10.1038/nrg.2016.156

Li, S., and Mason, C. E. (2014). The pivotal regulatory landscape of RNA modifications. *Annu Rev. Genomics Hum. Genet.* 15, 127–150. doi:10.1146/annurev-genom-090413-025405

Li, T., Shi, Y., Wang, P., Guachalla, L. M., Sun, B., Joerss, T., et al. (2015). Smg6/Est1 licenses embryonic stem cell differentiation via nonsense-mediated mRNA decay. *EMBO J.* 34 (12), 1630–1647. doi:10.15252/embj.201489947

Liao, B., Bao, X., Liu, L., Feng, S., Zovoilis, A., Liu, W., et al. (2011). MicroRNA cluster 302-367 enhances somatic cell reprogramming by accelerating a mesenchymal-to-epithelial transition. *J. Biol. Chem.* 286 (19), 17359–17364. doi:10.1074/jbc.C111.235960

Lim, J., Ha, M., Chang, H., Kwon, S. C., Simanshu, D. K., Patel, D. J., et al. (2014). Uridylation by TUT4 and TUT7 marks mRNA for degradation. *Cell* 159 (6), 1365–1376. doi:10.1016/j.cell.2014.10.055

Ling, S. H., Qamra, R., and Song, H. (2011). Structural and functional insights into eukaryotic mRNA decapping. *Wiley Interdiscip. Rev. RNA* 2 (2), 193–208. doi:10.1002/wrna.44

Liu, J., Dou, X., Chen, C., Chen, C., Liu, C., Xu, M. M., et al. (2020). N (6)-methyladenosine of chromosome-associated regulatory RNA regulates chromatin state and transcription. *Science* 367 (6477), 580–586. doi:10.1126/science.aay6018

Liu, J., Gao, M., He, J., Wu, K., Lin, S., Jin, L., et al. (2021). The RNA m(6)A reader YTHDC1 silences retrotransposons and guards ES cell identity. *Nature* 591 (7849), 322–326. doi:10.1038/s41586-021-03313-9

Liu, Y., Lu, X., Shi, J., Yu, X., Zhang, X., Zhu, K., et al. (2016). BTG4 is a key regulator for maternal mRNA clearance during mouse early embryogenesis. *J. Mol. Cell Biol.* 8 (4), 366–368. doi:10.1093/jmcb/mjw023

Lykke-Andersen, S., Zumer, K., Molska, E. S., Rouviere, J. O., Wu, G., Demel, C., et al. (2021). Integrator is a genome-wide attenuator of non-productive transcription. *Mol. Cell* 81 (3), 514–529.e6. doi:10.1016/j.molcel.2020.12.014

McIlwain, D. R., Pan, Q., Reilly, P. T., Elia, A. J., McCracken, S., Wakeham, A. C., et al. (2010). Smg1 is required for embryogenesis and regulates diverse genes via alternative splicing coupled to nonsense-mediated mRNA decay. *Proc. Natl. Acad. Sci. U S A* 107 (27), 12186–12191. doi:10.1073/pnas.1007336107

Medghalchi, S. M., Frischmeyer, P. A., Mendell, J. T., Kelly, A. G., Lawler, A. M., and Dietz, H. C. (2001). Rent1, a trans-effector of nonsense-mediated mRNA decay, is essential for mammalian embryonic viability. *Hum. Mol. Genet.* 10 (2), 99–105. doi:10.1093/hmg/10.2.99

Melton, C., Judson, R. L., and Blelloch, R. (2010). Opposing microRNA families regulate self-renewal in mouse embryonic stem cells. *Nature* 463 (7281), 621–626. doi:10.1038/nature08725

Modic, M., Grosch, M., Rot, G., Schirge, S., Lepko, T., Yamazaki, T., et al. (2019). Cross-regulation between TDP-43 and paraspeckles promotes pluripotency-differentiation transition. *Mol. Cell* 74 (5), 951–965. doi:10.1016/j.molcel.2019.03.041

Morgan, M., Much, C., DiGiacomo, M., Azzi, C., Ivanova, I., Vitsios, D. M., et al. (2017). mRNA 3' uridylation and poly(A) tail length sculpt the mammalian maternal transcriptome. *Nature* 548 (7667), 347–351. doi:10.1038/nature23318

Murchison, E. P., Partridge, J. F., Tam, O. H., Cheloufi, S., and Hannon, G. J. (2005). Characterization of Dicer-deficient murine embryonic stem cells. *Proc. Natl. Acad. Sci. U S A* 102 (34), 12135–12140. doi:10.1073/pnas.0505479102

Murchison, E. P., Stein, P., Xuan, Z., Pan, H., Zhang, M. Q., Schultz, R. M., et al. (2007). Critical roles for Dicer in the female germline. *Genes Dev.* 21 (6), 682–693. doi:10.1101/gad.1521307

Nagarajan, V. K., Jones, C. I., Newbury, S. F., and Green, P. J. (2013). XRN 5'-->3' exoribonucleases: Structure, mechanisms and functions. *Biochim. Biophys. Acta* 1829 (6-7), 590–603. doi:10.1016/j.bbagrm.2013.03.005

Neff, A. T., Lee, J. Y., Wilusz, J., Tian, B., and Wilusz, C. J. (2012). Global analysis reveals multiple pathways for unique regulation of mRNA decay in induced pluripotent stem cells. *Genome Res.* 22 (8), 1457–1467. doi:10.1101/gr.134312.111

Ng, H. H., and Surani, M. A. (2011). The transcriptional and signalling networks of pluripotency. *Nat. Cell Biol.* 13 (5), 490–496. doi:10.1038/ncb0511-490

Ogami, K., and Suzuki, H. I. (2021). Nuclear RNA exosome and pervasive transcription: Dual sculptors of genome function. *Int. J. Mol. Sci.* 22, 13401. doi:10.3390/ijms222413401

Overbeck, J. H., Stelzig, D., Fuchs, A. L., Wurm, J. P., and Sprangers, R. (2022). Observation of conformational changes that underlie the catalytic cycle of Xrn2. *Nat. Chem. Biol.* 18, 1152–1160. doi:10.1038/s41589-022-01111-6

Pan, Q., Saltzman, A. L., Kim, Y. K., Misquitta, C., Shai, O., Maquat, L. E., et al. (2006). Quantitative microarray profiling provides evidence against widespread coupling of alternative splicing with nonsense-mediated mRNA decay to control gene expression. *Genes Dev.* 20 (2), 153–158. doi:10.1101/gad.1382806

Pan, Q., Shai, O., Lee, L. J., Frey, B. J., and Blencowe, B. J. (2008). Deep surveying of alternative splicing complexity in the human transcriptome by high-throughput sequencing. *Nat. Genet.* 40 (12), 1413–1415. doi:10.1038/ng.259

Park, O. H., Ha, H., Lee, Y., Boo, S. H., Kwon, D. H., Song, H. K., et al. (2019). Endoribonucleolytic cleavage of m(6)a-containing RNAs by RNase P/MRP complex. *Mol. Cell* 74 (3), 494–507. doi:10.1016/j.molcel.2019.02.034

Passmore, L. A., and Coller, J. (2022). Roles of mRNA poly(A) tails in regulation of eukaryotic gene expression. *Nat. Rev. Mol. Cell Biol.* 23 (2), 93–106. doi:10.1038/s41580-021-00417-y

Percharde, M., Lin, C. J., Yin, Y., Guan, J., Peixoto, G. A., Bulut-Karslioglu, A., et al. (2018). A LINE1-nucleolin partnership regulates early development and ESC identity. *Cell* 174 (2), 391–405. doi:10.1016/j.cell.2018.05.043

Puno, M. R., Weick, E. M., Das, M., and Lima, C. D. (2019). SnapShot: The RNA exosome. *Cell* 179 (1), 282. doi:10.1016/j.cell.2019.09.005

Rambout, X., and Maquat, L. E. (2020). The nuclear cap-binding complex as choreographer of gene transcription and pre-mRNA processing. *Genes Dev.* 34 (17-18), 1113–1127. doi:10.1101/gad.339986.120

Rouget, C., Papin, C., Boureux, A., Meunier, A. C., Franco, B., Robine, N., et al. (2010). Maternal mRNA deadenylation and decay by the piRNA pathway in the early Drosophila embryo. *Nature* 467 (7319), 1128–1132. doi:10.1038/nature09465

Saitou, M., and Yamaji, M. (2012). Primordial germ cells in mice. *Cold Spring Harb. Perspect. Biol.* 4, a008375. doi:10.1101/cshperspect.a008375

Sasaki, Y. T., Ideue, T., Sano, M., Mituyama, T., and Hirose, T. (2009). MENepsilon/beta noncoding RNAs are essential for structural integrity of nuclear paraspeckles. *Proc. Natl. Acad. Sci. U S A* 106 (8), 2525–2530. doi:10.1073/pnas.0807899106

Schaeffer, D., Tsanova, B., Barbas, A., Reis, F. P., Dastidar, E. G., Sanchez-Rotunno, M., et al. (2009). The exosome contains domains with specific endoribonuclease, exoribonuclease and cytoplasmic mRNA decay activities. *Nat. Struct. Mol. Biol.* 16 (1), 56–62. doi:10.1038/nsmb.1528

Schneider, C., Leung, E., Brown, J., and Tollervey, D. (2009). The N-terminal PIN domain of the exosome subunit Rrp44 harbors endonuclease activity and tethers Rrp44 to the yeast core exosome. *Nucleic Acids Res.* 37 (4), 1127–1140. doi:10.1093/nar/gkn1020

Schoenberg, D. R. (2011). Mechanisms of endonuclease-mediated mRNA decay. *Wiley Interdiscip. Rev. RNA* 2 (4), 582–600. doi:10.1002/wrna.78

Sha, Q. Q., Yu, J. L., Guo, J. X., Dai, X. X., Jiang, J. C., Zhang, Y. L., et al. (2018). CNOT6L couples the selective degradation of maternal transcripts to meiotic cell cycle progression in mouse oocyte. *EMBO J.* 37, e99333. doi:10.15252/embj.201899333

Shatkin, A. J., and Manley, J. L. (2000). The ends of the affair: Capping and polyadenylation. *Nat. Struct. Biol.* 7 (10), 838–842. doi:10.1038/79583

Shimotohno, K., Kodama, Y., Hashimoto, J., and Miura, K. I. (1977). Importance of 5'-terminal blocking structure to stabilize mRNA in eukaryotic protein synthesis. *Proc. Natl. Acad. Sci. U S A* 74 (7), 2734–2738. doi:10.1073/pnas.74.7.2734

Sommerkamp, P., Cabezas-Wallscheid, N., and Trumpp, A. (2021). Alternative polyadenylation in stem cell self-renewal and differentiation. *Trends Mol. Med.* 27 (7), 660–672. doi:10.1016/j.molmed.2021.04.006

Song, M. G., and Kiledjian, M. (2007). 3' Terminal oligo U-tract-mediated stimulation of decapping. *RNA* 13 (12), 2356–2365. doi:10.1261/rna.765807

Staals, R. H., Bronkhorst, A. W., Schilders, G., Slomovic, S., Schuster, G., Heck, A. J., et al. (2010). Dis3-like 1: A novel exoribonuclease associated with the human exosome. *EMBO J.* 29 (14), 2358–2367. doi:10.1038/emboj.2010.122

Stadhouders, R., Filion, G. J., and Graf, T. (2019). Transcription factors and 3D genome conformation in cell-fate decisions. *Nature* 569 (7756), 345–354. doi:10.1038/s41586-019-1182-7

Stein, C. B., Field, A. R., Mimoso, C. A., Zhao, C., Huang, K. L., Wagner, E. J., et al. (2022). Integrator endonuclease drives promoter-proximal termination at all RNA polymerase II-transcribed loci. *Mol. Cell* 82 (22), 4232–4245.e11. doi:10.1016/j.molcel.2022.10.004

Suh, N., Baehner, L., Moltzahn, F., Melton, C., Shenoy, A., Chen, J., et al. (2010). MicroRNA function is globally suppressed in mouse oocytes and early embryos. *Curr. Biol.* 20 (3), 271–277. doi:10.1016/j.cub.2009.12.044

Sunwoo, H., Dinger, M. E., Wilusz, J. E., Amaral, P. P., Mattick, J. S., and Spector, D. L. (2009). MEN epsilon/beta nuclear-retained non-coding RNAs are up-regulated upon muscle differentiation and are essential components of paraspeckles. *Genome Res.* 19 (3), 347–359. doi:10.1101/gr.087775.108

Takahashi, K., and Yamanaka, S. (2006). Induction of pluripotent stem cells from mouse embryonic and adult fibroblast cultures by defined factors. *Cell* 126 (4), 663–676. doi:10.1016/j.cell.2006.07.024

Tam, O. H., Aravin, A. A., Stein, P., Girard, A., Murchison, E. P., Cheloufi, S., et al. (2008). Pseudogene-derived small interfering RNAs regulate gene expression in mouse oocytes. *Nature* 453 (7194), 534–538. doi:10.1038/nature06904

Tam, P. P., and Behringer, R. R. (1997). Mouse gastrulation: the formation of a mammalian body plan. *Mech. Dev.* 68 (1-2), 3–25. doi:10.1016/s0925-4773(97)00123-8

Tang, F., Kaneda, M., O'Carroll, D., Hajkova, P., Barton, S. C., Sun, Y. A., et al. (2007). Maternal microRNAs are essential for mouse zygotic development. *Genes Dev.* 21 (6), 644–648. doi:10.1101/gad.418707

Tang, P., Yang, Y., Li, G., Huang, L., Wen, M., Ruan, W., et al. (2022). Alternative polyadenylation by sequential activation of distal and proximal PolyA sites. *Nat. Struct. Mol. Biol.* 29 (1), 21–31. doi:10.1038/s41594-021-00709-z

Tatomer, D. C., Elrod, N. D., Liang, D., Xiao, M. S., Jiang, J. Z., Jonathan, M., et al. (2019). The Integrator complex cleaves nascent mRNAs to attenuate transcription. *Genes Dev.* 33 (21-22), 1525–1538. doi:10.1101/gad.330167.119

Thapar, R., and Denmon, A. P. (2013). Signaling pathways that control mRNA turnover. *Cell Signal* 25 (8), 1699–1710. doi:10.1016/j.cellsig.2013.03.026

Tian, B., and Manley, J. L. (2017). Alternative polyadenylation of mRNA precursors. *Nat. Rev. Mol. Cell Biol.* 18 (1), 18–30. doi:10.1038/nrm.2016.116

Tomecki, R., and Dziembowski, A. (2010). Novel endoribonucleases as central players in various pathways of eukaryotic RNA metabolism. *RNA* 16 (9), 1692–1724. doi:10.1261/rna.2237610

Tomecki, R., Kristiansen, M. S., Lykke-Andersen, S., Chlebowski, A., Larsen, K. M., Szczesny, R. J., et al. (2010). The human core exosome interacts with differentially localized processive RNases: hDIS3 and hDIS3L. *EMBO J.* 29 (14), 2342–2357. doi:10.1038/emboj.2010.121

Vagin, V. V., Sigova, A., Li, C., Seitz, H., Gvozdev, V., and Zamore, P. D. (2006). A distinct small RNA pathway silences selfish genetic elements in the germline. *Science* 313 (5785), 320–324. doi:10.1126/science.1129333

Valencia-Sanchez, M. A., Liu, J., Hannon, G. J., and Parker, R. (2006). Control of translation and mRNA degradation by miRNAs and siRNAs. *Genes Dev.* 20 (5), 515–524. doi:10.1101/gad.1399806

Vidya, E., and Duchaine, T. F. (2022). Eukaryotic mRNA decapping activation. *Front. Genet.* 13, 832547. doi:10.3389/fgene.2022.832547

Wang, E. T., Sandberg, R., Luo, S., Khrebtukova, I., Zhang, L., Mayr, C., et al. (2008). Alternative isoform regulation in human tissue transcriptomes. *Nature* 456 (7221), 470–476. doi:10.1038/nature07509

Wang, X., Lu, Z., Gomez, A., Hon, G. C., Yue, Y., Han, D., et al. (2014). N6-methyladenosine-dependent regulation of messenger RNA stability. *Nature* 505 (7481), 117–120. doi:10.1038/nature12730

Wang, X., Ramat, A., Simonelig, M., and Liu, M. F. (2022). Emerging roles and functional mechanisms of PIWI-interacting RNAs. *Nat. Rev. Mol. Cell Biol.* 24, 123–141. doi:10.1038/s41580-022-00528-0

Wang, Y., Baskerville, S., Shenoy, A., Babiarz, J. E., Baehner, L., and Blelloch, R. (2008). Embryonic stem cell-specific microRNAs regulate the G1-S transition and promote rapid proliferation. *Nat. Genet.* 40 (12), 1478–1483. doi:10.1038/ng.250

Wang, Y., Medvid, R., Melton, C., Jaenisch, R., and Blelloch, R. (2007). DGCR8 is essential for microRNA biogenesis and silencing of embryonic stem cell self-renewal. *Nat. Genet.* 39 (3), 380–385. doi:10.1038/ng1969

Watanabe, T., Totoki, Y., Toyoda, A., Kaneda, M., Kuramochi-Miyagawa, S., Obata, Y., et al. (2008). Endogenous siRNAs from naturally formed dsRNAs regulate transcripts in mouse oocytes. *Nature* 453 (7194), 539–543. doi:10.1038/nature06908

Wei, J., Yu, X., Yang, L., Liu, X., Gao, B., Huang, B., et al. (2022). FTO mediates LINE1 m(6)A demethylation and chromatin regulation in mESCs and mouse development. *Science* 376 (6596), 968–973. doi:10.1126/science.abe9582

Weick, E. M., Puno, M. R., Januszyk, K., Zinder, J. C., DiMattia, M. A., and Lima, C. D. (2018). Helicase-dependent RNA decay illuminated by a cryo-EM structure of a human nuclear RNA exosome-MTR4 complex. *Cell* 173 (7), 1663–1677. doi:10.1016/j.cell.2018.05.041

Weischenfeldt, J., Damgaard, I., Bryder, D., Theilgaard-Monch, K., Thoren, L. A., Nielsen, F. C., et al. (2008). NMD is essential for hematopoietic stem and progenitor cells and for eliminating by-products of programmed DNA rearrangements. *Genes Dev.* 22 (10), 1381–1396. doi:10.1101/gad.468808

Weischenfeldt, J., Waage, J., Tian, G., Zhao, J., Damgaard, I., Jakobsen, J. S., et al. (2012). Mammalian tissues defective in nonsense-mediated mRNA decay display highly aberrant splicing patterns. *Genome Biol.* 13 (5), R35. doi:10.1186/gb-2012-13-5-r35

Wolin, S. L., and Maquat, L. E. (2019). Cellular RNA surveillance in health and disease. *Science* 366 (6467), 822–827. doi:10.1126/science.aax2957

Wu, Y., Liu, W., Chen, J., Liu, S., Wang, M., Yang, L., et al. (2019). Nuclear exosome targeting complex core factor Zcchc8 regulates the degradation of LINE1 RNA in early embryos and embryonic stem cells. *Cell Rep.* 29 (8), 2461–2472. doi:10.1016/j.celrep.2019.10.055

Yabuta, Y., Kurimoto, K., Ohinata, Y., Seki, Y., and Saitou, M. (2006). Gene expression dynamics during germline specification in mice identified by quantitative single-cell gene expression profiling. *Biol. Reprod.* 75 (5), 705–716. doi:10.1095/biolreprod.106.053686

Yadav, T., Quivy, J. P., and Almouzni, G. (2018). Chromatin plasticity: A versatile landscape that underlies cell fate and identity. *Science* 361 (6409), 1332–1336. doi:10.1126/science.aat8950

Yamaji, M., Jishage, M., Meyer, C., Suryawanshi, H., Der, E., Yamaji, M., et al. (2017). DND1 maintains germline stem cells via recruitment of the CCR4-NOT complex to target mRNAs. *Nature* 543 (7646), 568–572. doi:10.1038/nature21690

Yang, Y., Wang, L., Han, X., Yang, W. L., Zhang, M., Ma, H. L., et al. (2019). RNA 5-methylcytosine facilitates the maternal-to-zygotic transition by preventing maternal mRNA decay. *Mol. Cell* 75 (6), 1188–1202. doi:10.1016/j.molcel.2019.06.033

Yu, C., Ji, S. Y., Sha, Q. Q., Dang, Y., Zhou, J. J., Zhang, Y. L., et al. (2016). BTG4 is a meiotic cell cycle-coupled maternal-zygotic-transition licensing factor in oocytes. *Nat. Struct. Mol. Biol.* 23 (5), 387–394. doi:10.1038/nsmb.3204

Yu, S., and Kim, V. N. (2020). A tale of non-canonical tails: Gene regulation by post-transcriptional RNA tailing. *Nat. Rev. Mol. Cell Biol.* 21 (9), 542–556. doi:10.1038/s41580-020-0246-8

Zaccara, S., and Jaffrey, S. R. (2020). A unified model for the function of YTHDF proteins in regulating m(6)a-modified mRNA. *Cell* 181 (7), 1582–1595. doi:10.1016/j.cell.2020.05.012

Zhao, L. W., Zhu, Y. Z., Chen, H., Wu, Y. W., Pi, S. B., Chen, L., et al. (2020). PABPN1L mediates cytoplasmic mRNA decay as a placeholder during the maternal-to-zygotic transition. *EMBO Rep.* 21 (8), e49956. doi:10.15252/embr.201949956

Zhou, H., Stein, C. B., Shafiq, T. A., Shipkovenska, G., Kalocsay, M., Paulo, J. A., et al. (2022). Rixosomal RNA degradation contributes to silencing of Polycomb target genes. *Nature* 604 (7904), 167–174. doi:10.1038/s41586-022-04598-0

Zinder, J. C., Wasmuth, E. V., and Lima, C. D. (2016). Nuclear RNA exosome at 3.1 A reveals substrate specificities, RNA paths, and allosteric inhibition of rrp44/dis3. *Mol. Cell* 64 (4), 734–745. doi:10.1016/j.molcel.2016.09.038

frontiers | Frontiers in Cell and Developmental Biology

TYPE Mini Review
PUBLISHED 17 May 2023
DOI 10.3389/fcell.2023.1205540

OPEN ACCESS

EDITED BY
Liang Zhou,
Southern Medical University, China

REVIEWED BY
Krishna Shrinivas,
Harvard University, United States

*CORRESPONDENCE
Yu Zhao,
zhaoyu25@mail.sysu.edu.cn

RECEIVED 14 April 2023
ACCEPTED 09 May 2023
PUBLISHED 17 May 2023

CITATION
Chen Q, Zeng Y, Kang J, Hu M, Li N, Sun K and Zhao Y (2023), Enhancer RNAs in transcriptional regulation: recent insights. *Front. Cell Dev. Biol.* 11:1205540. doi: 10.3389/fcell.2023.1205540

Enhancer RNAs in transcriptional regulation: recent insights

Qi Chen[1], Yaxin Zeng[2], Jinjin Kang[2], Minghui Hu[2], Nianle Li[2], Kun Sun[3] and Yu Zhao[2]*

[1]The Eighth Affiliated Hospital, Sun Yat-sen University, Shenzhen, China, [2]Molecular Cancer Research Center, School of Medicine, Shenzhen Campus of Sun Yat-sen University, Sun Yat-sen University, Shenzhen, China, [3]Institute of Cancer Research, Shenzhen Bay Laboratory, Shenzhen, China

Enhancers are a class of *cis*-regulatory elements in the genome that instruct the spatiotemporal transcriptional program. Last decade has witnessed an exploration of non-coding transcripts pervasively transcribed from active enhancers in diverse contexts, referred to as enhancer RNAs (eRNAs). Emerging evidence unequivocally suggests eRNAs are an important layer in transcriptional regulation. In this mini-review, we summarize the well-established regulatory models for eRNA actions and highlight the recent insights into the structure and chemical modifications of eRNAs underlying their functions. We also explore the potential roles of eRNAs in transcriptional condensates.

KEYWORDS

eRNA, transcriptional regulation, chromatin looping, phase separation, epitranscriptome

Introduction

Enhancers are distal *cis*-regulatory elements in the genome that direct spatiotemporal transcription programs in response to diverse cues (Andersson et al., 2014; Long et al., 2016). An estimate of over 400,000 putative enhancers in human genome, plus the identification of disease-associated traits within enhancers, underscores the essence of exploring the regulatory grammar encrypted within these elements (Consortium, 2012; Long et al., 2016; Sur and Taipale, 2016; Furlong and Levine, 2018; Schoenfelder and Fraser, 2019).

The advent of state-of-art genomic approaches unveils that the human genome is pervasively transcribed, yielding a plethora of non-coding RNA (ncRNA) species (Hangauer et al., 2013). Among them, RNA transcripts emanating from enhancers, dubbed enhancer RNA (eRNAs), have attracted a particular interest considering their potential roles in enhancer regulation (De Santa et al., 2010; Kim et al., 2010; Lam et al., 2014; Li et al., 2016; Sartorelli and Lauberth, 2020; Harrison and Bose, 2022). It is noteworthy that distinct terms, e.g., eRNAs and enhancer-associated lncRNAs (elncRNAs), appear in the literature to represent transcripts from enhancer regions (Orom et al., 2010; Marques et al., 2013; Andersson et al., 2014; Li et al., 2016; Hon et al., 2017; Statello et al., 2021; Mattick et al., 2023). Strictly, eRNAs are short, bidirectional ones, which are generally non-polyadenylated and unstable, whereas elncRNAs are usually polyadenylated and have higher stability (Li et al., 2016; Statello et al., 2021; Mattick et al., 2023). However, concerning gene-activating mechanisms, elncRNAs and eRNAs share some common themes (Orom et al., 2010; Wang et al., 2011; Lai et al., 2013; Grossi et al., 2020) and we do not distinguish these different terms in this mini-review. As an integral component of active enhancers, eRNA transcription generally correlates with enhancer activation and can serve as an independent marker of active enhancers (Carullo et al., 2020). Although there isn't yet a consensus regarding whether the functions come from the transcription process or eRNA transcripts *per se*,

accumulating evidence has shown a subset of eRNAs are pivotal for the transcription of cognate targets and coined several well-appreciated themes for eRNA actions.

In this mini-review, we outline current models for eRNA actions in transcriptional regulation. In addition, we highlight recent findings concerning eRNAs secondary structure and post-transcriptional modifications in bestowing diverse functional features of eRNAs. Finally, we discuss an emerging paradigm of transcriptional condensates wherein eRNAs partaken and contribute.

The interplay between eRNAs and protein partners in transcriptional regulation

The well-appreciated model for enhancer action is that chromatin loops form between enhancers and cognate promoters bringing these two elements into physically close proximity, which involves the participation of cohesin complex, and transcriptional coactivator Mediator complex (Kagey et al., 2010). Li et al. provided the first piece of evidence that estrogen-induced eRNAs bind with SMC3 and RAD21, components of cohesin complex. Depletion of eRNAs abrogates cohesin increment to enhancers, thus abolishing enhancer-promoter interactions and target genes activation (Li et al., 2013). Similarly, Lai et al. (2013) revealed that ncRNA-a interacts with Mediator subunits and is involved in chromatin looping between ncRNA-a loci and their regulated promoters. Since then, further studies identify the direct interactions between eRNAs and chromatin looping factors [e.g., hnRNPU (Jiao et al., 2018), CTCF (Xiang et al., 2014), MED1 (Hsieh et al., 2014), MED12 (Tan et al., 2019)], suggesting modulating chromatin looping is one common theme underlying eRNA functions (Figure 1A).

In addition to regulating chromatin looping, eRNAs can directly intervene with transcription machinery (Figure 1B). Lines of evidence suggest eRNAs can modulate RNA polymerase II (Pol II) pause release (Schaukowitch et al., 2014; Zhao et al., 2016; Shi et al., 2018). Schaukowitch et al. found eRNAs bind to NELF-E, and decoy this negative elongation factor (NELF) complex away from immediate early genes, thus promoting Pol II pause release into the productive elongation stage (Schaukowitch et al., 2014). In another study, Zhao et al. uncovered that *PSA* eRNA stimulates transcription through forming a complex with the positive elongation factor (P-TEFb) (Zhao et al., 2016). Congruent with these works, the following studies added more examples demonstrating interactions between eRNAs and NELF or P-TEFb (Shi et al., 2018). Besides these direct interactions, our group identified eRNAs interact with hnRNPL via a CAAA tract and modulate the appropriate loading of hnRNPL to the target locus (Zhao et al., 2019). hnRNPL has been shown to interact with KMT3A to regulate H3K36me3 enrichment (Yuan et al., 2009) and impinge on

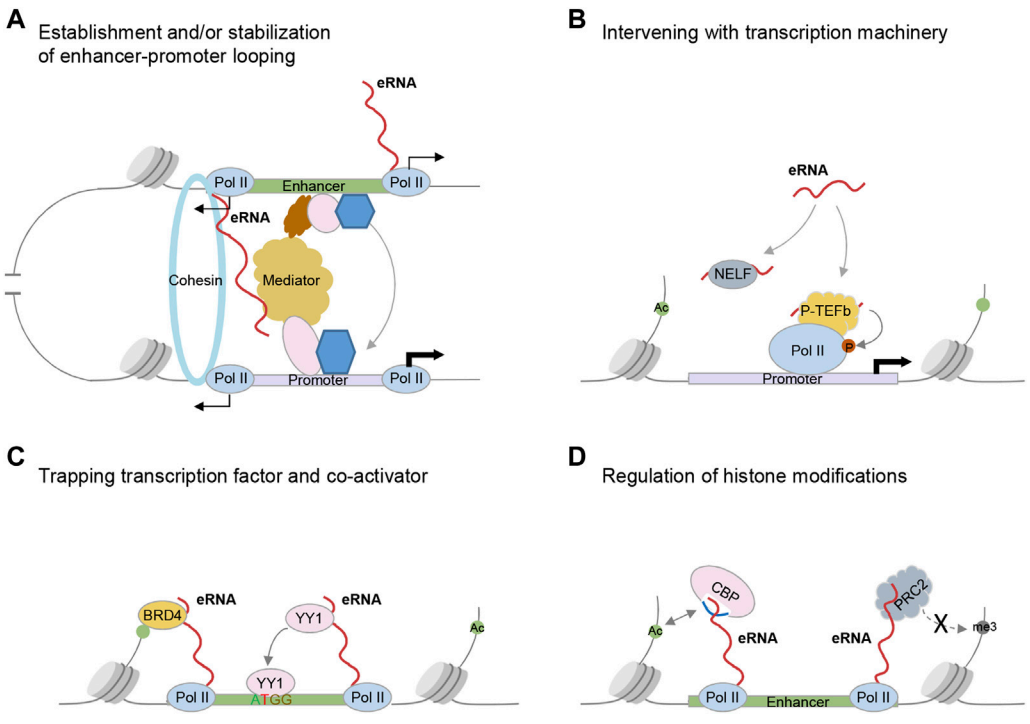

FIGURE 1
Established mechanisms underlying eRNA functions in transcriptional regulation. **(A)** Regulating chromatin looping. eRNAs interact with Cohesin complex or Mediator to establish and/or stabilize enhancer-promoter looping. **(B)** Intervening with the transcription machinery. eRNAs promote RNAP II pause release into productive elongation stage via acting as decoy for NELF and interacting with the P-TEFb. eRNAs also stimulate transcription through the intermediate hnRNPL. **(C)** Trapping transcription factors or transcription coactivators. eRNAs enhance the enhancer binding of TF YY1 and transcription coactivator BRD4 through direct interaction with them. **(D)** Modulating enhancer chromatin environment. eRNAs interact with CBP, stimulate its catalytic activity, and increase the deposition of histone acetylation on enhancers. eRNAs also inhibit the catalytic activity of PRC2 by binding the EZH2 subunit and inhibit repressive H3K27me3 deposition.

transcription elongation via interacting with P-TEFb components, CDK9 and CCNT1 (Giraud et al., 2014). In this scenario, hnRNPL acts as an intermediate to bridge the interaction between eRNAs and transcription machinery.

Another important paradigm of eRNA functions is that eRNAs can trap transcription factors and transcription co-activators, and enhance their binding to local chromatin (Figure 1C). Sigova et al. showed nascent RNAs transcribed from enhancers and promoters, through interactions with transcription factor (TF) YY1, increase YY1 binding to these regulatory elements (Sigova et al., 2015). One recent study reinforces this idea, showing a broad scope of TFs bind to RNA through arginine-rich motif (ARM)-like domains and such interactions contribute to TF association with chromatin (Oksuz et al., 2022). Deletion of ARM-like domains skews TF nuclear dynamics: it reduces the immobile and subdiffusive fractions of TFs while enhancing the diffusing molecules. A positive-feedback loop is thus proposed that nascent RNA produced from enhancer (eRNA) or promoter regions can trap dissociating TFs through RNA-mediated weak interactions, which facilitates TFs rebind to these regulatory elements and augments the transcription outputs. Similarly, eRNAs interact directly with BRD4 via its bromodomains and promote BRD4 binding to acetylated histones, which in turn maintains enhancers in an active state (Rahnamoun et al., 2018).

Lastly, eRNAs can modulate chromatin state. Depletion of eRNAs has been shown to decrease chromatin accessibility at enhancers and cognate promoters (Mousavi et al., 2013; Tsai et al., 2018). Besides these, eRNAs can directly interact with chromatin modifiers that deposit histone acetylation or methylation marks (Figure 1D). Specifically, Bose et al. demonstrated eRNAs interact with histone acetyltransferase CBP via its RNA binding region within the activation loop of HAT domain (Bose et al., 2017). Such interaction displaces the activation loop from the catalytic site and enhances CBP binding to its histone substrate. Similarly, eRNAs can also stimulate p300 catalytic activity and increase H3K27 acetylation at enhancers (Hou and Kraus, 2022). In addition to promoting histone acetylation, eRNAs also repel the PRC2-mediated deposition of the repressive histone modification H3K27me3 (Ounzain et al., 2015). Consistently, PRC2 binds to nascent RNA promiscuously at nearly all active genes, which antagonizes its binding to chromatin and thus alleviates the deposition of the repressive H3K27me3 mark (Beltran et al., 2016; Wang et al., 2017).

As mentioned above, caution needs to be taken to discern whether eRNAs function in a transcript-dependent or -independent manner. Engreitz et al. (2016) provided compelling evidence to show regulatory roles of many lncRNA loci stem from DNA elements or transcription processes, instead of their specific transcripts. Similar findings have been reported in other works (Kaikkonen et al., 2013; Anderson et al., 2016; Paralkar et al., 2016; Winkler et al., 2022). Thus, more rigorous methodologies are warranted in future studies to distinguish this point (Engreitz et al., 2016; Joung et al., 2017).

eRNA structures instruct their regulatory roles

Despite the substantial advances concerning eRNA functions and mechanisms, their regulatory roles instructed by eRNA structures are poorly studied. As mentioned above, eRNA can interact with and activate P-TEFb. Such interaction requires a TAR RNA-like (TAR-L) motif, whose secondary structure is akin to the 3′ end of the small nuclear RNA *7SK*. *AR-eRNA*, through competitive binding with P-TEFb, can help release P-TEFb from the inhibitory complex (7SK snRNP) and promotes effective transcription elongation (Zhao et al., 2016). On the contrary, interactions between eRNAs and NELF may not depend on structural motifs. Instead, adequate length (>200 nt) and the presence of unpaired guanosines are indispensable, which enables simultaneous and allosteric interactions between eRNAs and NELF subunits -A and -E (Gorbovytska et al., 2022).

The ^{DRR}*eRNA* (also known as *MUNC*) is a well-studied pro-myogenic eRNA, which is transcribed from an enhancer region of the myogenic master TF, MyoD (Mousavi et al., 2013; Mueller et al., 2015). ^{DRR}*eRNA* functions *in trans* to activate *Myogenin* transcription through directing cohesin loading at *Myogenin* locus (Cichewicz et al., 2018; Tsai et al., 2018). A recent study employed SHAPE-MaP (2′-hydroxyl acylation analyzed by primer extension coupled with mutational profiling) chemical probing approach to decode the secondary structure of ^{DRR}*eRNA* and unraveled multiple structural domains that confer distinct features of ^{DRR}*eRNA* for cohesion binding, genomic interaction, and gene expression regulation (Przanowska et al., 2022).

In addition to structured features embedded in eRNAs themselves, accumulating evidence underpins the regulatory code underlying intermolecular interactions. A prominent example comes from *MALAT1*, which interacts with many pre-mRNAs at active gene loci indirectly through RNA binding protein (RBP) intermediates (Engreitz et al., 2014; West et al., 2014). Recently, Cai et al. (2020) developed a novel approach termed RIC-seq (RNA *in situ* conformation sequencing), which can map RNA-RNA interactions *in situ* in an unbiased manner, and discovered *MALAT1* interaction with highly transcribed nascent RNAs. Similarly, in this study, researchers also revealed extensive interactions between eRNAs and promoter upstream antisense RNAs (uaRNAs), which can be leveraged to infer enhancer-promoter connections. Intriguingly, modulating such interaction between eRNAs and uaRNAs influences chromatin looping (Figure 2A). Specifically, depletion of the super-enhancer-derived lncRNA *CCAT1-5L* markedly attenuates the chromatin looping between its parental *CCAT1* locus and *MYC* locus, and weakens Pol II deposition at *MYC* promoter. In this specific scenario, the interaction relies on the RBP hnRNPK, which can physically interact with Pol II and form a homodimer. Thus, hnRNPK-mediated interaction between eRNA-uaRNA pairs may serve as modulator for enhancer-promoter chromatin interactions and Pol II delivery from enhancer regions to target promoter regions.

Besides the RNA structures through RNA-RNA interactions, eRNAs can form DNA/RNA hybrid structure co-transcriptionally, termed R-loops. Competing evidence about R-loop functions comes from individual studies. Watts et al. (2022) found the enhancer RNA *AANCR* transcription leads to R-loops formation and in the R-loops eRNA is enzymatically modified to bear abasic sites, which helps stabilize R-loops, thus resulting in RNA Pol II pausing. Upon hypertonic stress, the R-loops are resolved and eRNA is fully transcribed to activate the target *APOE* activation. On the contrary, Tan-Wong et al. (2019) demonstrate that R-loops, often

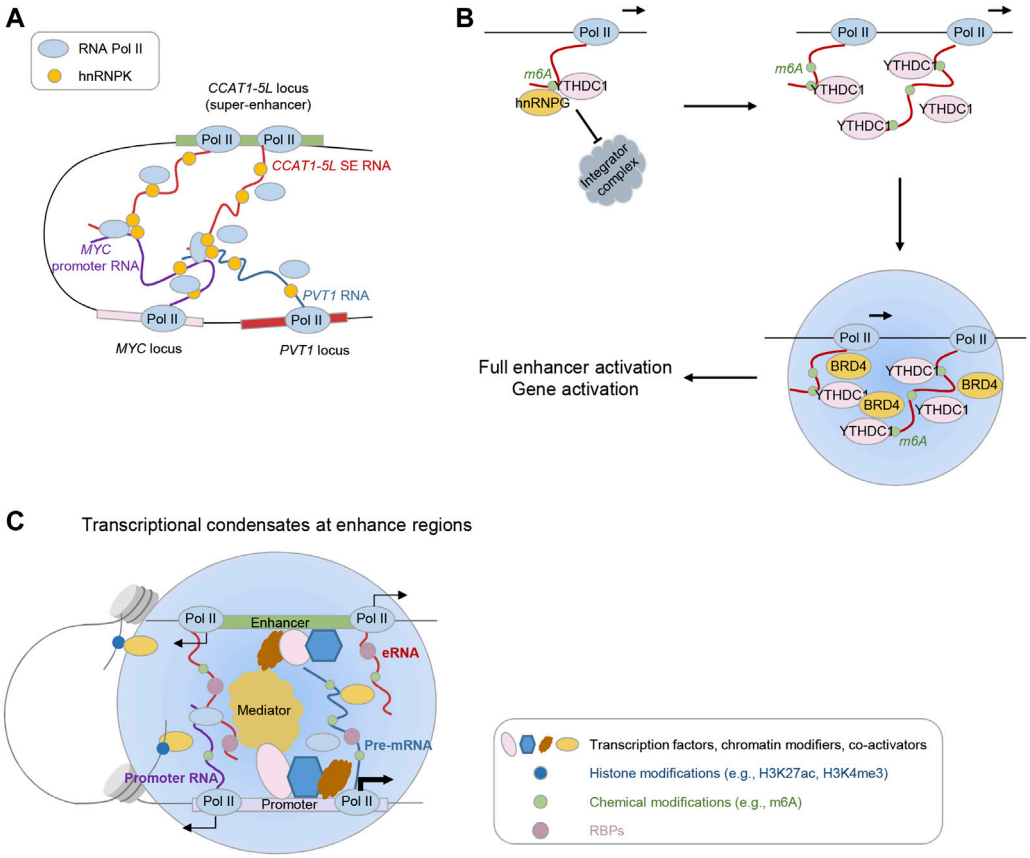

FIGURE 2
Expanding themes contributing to eRNA function. **(A)** Inter-molecular eRNA-uaRNA pair modulates enhancer-promoter chromatin interactions. **(B)** m6A modifications on eRNAs feed back on transcription. **(C)** eRNA-mediated regulation in transcriptional condensate formation.

found at promoters, enhancers, and terminators, promote antisense transcription in these regions. More recently, local R-loops formation between an antisense eRNA *PEARL* and HS5-1 enhancer region facilitates chromatin looping between distal enhancers and target promoters (Zhou et al., 2021).

Chemical modifications on eRNAs feed back on transcription

N6-methyladenosine (m6A) methylation, the most abundant RNA internal modification, has been shown to deposit on chromatin associated RNAs, including eRNAs (Louloupi et al., 2018; Xiao S. et al., 2019; Liu et al., 2020; Xu et al., 2021). Notably, the distribution of m6A methylation on these transcripts is not restricted to the 3′ end and is proven to regulate chromatin state and transcription directly (Louloupi et al., 2018; Xiao S. et al., 2019; Liu et al., 2020; Liu et al., 2021; Xu et al., 2021). Liu et al. found m6A-marked eRNAs, recognized by the nuclear reader YTHDC1, are subject to subsequent nuclear degradation by the nuclear exosome targeting (NEXT) complex. Knockout of the m6A writer *Mettl3* increases carRNAs abundance and promotes downstream transcription in mouse embryonic stem cells (mESCs). Mechanistically, m6A erasure upon *Mettl3* knockout stabilizes the carRNAs, rendering the following recruitment of active TFs (e.g., YY1 and CBP/EP300) and repelling of repressive factors (e.g., PRC2), thus tunes the nearby active chromatin state and stimulates downstream transcription.

The effects of m6A methylation on nuclear nascent transcripts and the transcription process could vary depending on different cell contexts. The recent two findings, on the contrary, show that m6A modification protects eRNAs from nuclear degradation, enhances the recruitment of m6A machinery components on enhancers and promoters, and stimulates effective transcription progress (Figure 2B) (Lee et al., 2021; Xu et al., 2022). In one study, Xu et al. (2022) revealed the chromatin binding of m6A methyltransferase complex (MTC) components METTL3/METTL14/WTAP locates at active enhancers and in turn decorates m6A modification on the 5′ end of nascent RNAs, neighboring to MTC chromatin binding sites. METTL3 depletion results in a loss of nascent RNAs emanating from enhancers at the TSS (transcription start site) proximal regions. Mechanistically, m6A modification recruits m6A reader/binder proteins such as hnRNPG and YTHDC1 to the nascent RNAs (including eRNAs), which protects these transcripts from cleavage by the Integrator complex. Loss of MTC would otherwise promote the recruitment of INS11 (the endonuclease subunit of the Integrator complex), leading

to premature transcription termination. Of note, MTC recruitment to the promoter is augmented by active transcription elongation (Akhtar et al., 2021). Thus, m6A modification along with m6A reader proteins shields nascent eRNAs from premature termination, and the productive elongation in turn fosters MTC recruitment, establishing a positive feedback control over the transcription process.

In the other study, Lee et al. (2021) employed a high-sensitive method dubbed methylation-inscribed nascent transcripts sequencing (MINT-seq) to capture m6A methylome directly on nascent RNAs. They uncovered m6A is pervasively decorated with enrichment in the middle of eRNA transcripts and m6A modification positively correlates with eRNA length and abundance. In agreement with the canonical "RRACH" motif identified on mRNAs, "GGACT" motif sequences are identified with eRNA m6A peaks. Functionally, m6A-modified eRNAs can stimulate enhancer activation through reader protein YTHDC1 recruitment. Targeted m6A erasure, genetic and chemical perturbation of m6A writer and reader impair the enhancer activation, eRNA transcription, and subsequent target gene activation. Mechanistically, YTHDC1 can phase-separate into liquid-like condensates and co-assemble into BRD4 transcriptional condensates, while m6A-eRNAs presence augments the size of condensates. Concordantly, either perturbation of YTHDC1 levels or its condensate formation ability attenuates BRD4 recruitment to enhancers and BRD4 condensate formation.

In addition to m6A modification, enrichment of 5-methylcytosine (m5C) marked eRNAs were found at a set of enhancers upon metabolic stress (Aguilo et al., 2016). Under this circumstance, the interaction between PGC-1a and the NOP2/Sun RNA methyltransferase 7 (NSUN7) is essential in instructing m5C deposition on eRNAs.

eRNAs and transcriptional condensates

Recent studies have shown liquid-liquid phase separation (LLPS) occurs at super-enhancers, which compartmentalizes crowded transcription regulators (e.g., TFs, transcriptional co-activators, RNA Pol II, and RNA) and promotes the formation of transcriptional condensates (Hnisz et al., 2017; Boija et al., 2018; Cho et al., 2018; Sabari et al., 2018; Shrinivas et al., 2019). Considering the established multivalent interactions between eRNAs with a myriad of factors (e.g., TFs, chromatin modifiers, DNA, RNA), eRNAs could potentially play a broad role in the formation of transcriptional condensates at enhancers (Roden and Gladfelter, 2021). Nair et al. (2019) recently reported an indispensable role of eRNA in controlling the assembly of MegaTrans complex at the ligand-activated enhancers, which exhibit properties of phase-separated components. Intriguingly, the complex components include several transcription factors (e.g., GATA3, ERα, RARA, FOXA1, AP2γ), which harbor intrinsically disordered regions (IDRs). The authors demonstrated two of them, GATA3 and ERα, are capable of liquid phase condensation at enhancers. Depletion of eRNA affects the diffusion properties of MegaTrans components, thus abolishing the full assembly of MegaTrans at the cognate enhancer. Notably, chronic enhancer activation alters the physicochemical properties of this enhancer RNA-dependent ribonucleoprotein (eRNP) complex to a more gel-like state. This study provides compelling evidence showing eRNAs directly contribute to the formation of phase-separated condensates and enhancer activation.

Based on current findings, we can extrapolate eRNAs play a broad role in controlling the formation, dissociation, and dynamics of transcriptional condensates at enhancers and/or cognate promoters via scaffolding multivalent interactions between condensate components (Maharana et al., 2018; Henninger et al., 2021; Quinodoz et al., 2021; Roden and Gladfelter, 2021). First, eRNAs may have a role in contributing to the formation of transcriptional condensates. Many eRNAs-interacting protein partners, as mentioned above, harbor IDRs that are essential in the induction of phase separation. For example, eRNAs interact with MED1 and BRD4, the IDRs of which have been demonstrated to foster super-enhancer formation through phase separation (Cho et al., 2018; Sabari et al., 2018). eRNAs also interact with P-TEFb and the recent finding supports the promoting role of CCNT1, a component of P-TEFb, in phase separation via its histidine-rich domain, which subsequently compartmentalizes RNA Pol II C-terminal domain (CTD) into CCNT1 droplets to ensure CTD hyperphosphorylation and transcription elongation (Lu et al., 2018). In addition to TFs and co-activators, increasing evidence has shown RBPs pervasively bind to regulatory elements and mediate the phase separation (Xiao et al., 2019a; Shao et al., 2022). Shao et al. discovered one RBP PSPC1 exhibits liquid-like properties and the presence of RNA augments the PSPC1-mediated transcriptional condensates that compartmentalize the CTD for enhanced phosphorylation. The low-complexity sequences (LCS) and RNA recognition motifs (RRMs) of PSPC1 are the prerequisites for the synergistic interplay between PSPC1 and RNA, the resultant PSPC1 chromatin binding and phase separation. Remarkably, the discovery that chrRBPs tend to co-occupy at regulatory regions, such as super-enhancers and promoters, provides a chance that diverse RBPs act collaboratively, in synergy with RNAs from these regulatory elements, in promoting the formation of transcriptional condensates. Second, eRNAs may not only engage in the formation but also regulate the dissociation and composition of transcriptional condensates. Maharana et al. proposed that RNA concentration determines distinct phase separation behaviors: higher RNA concentration impedes phase separation of RBPs in the nucleus, while lower RNA concentration facilitates aggregation (Maharana et al., 2018). Consistently, Henninger et al. (2021) recently reported low levels of RNA generated due to transcription initiation at regulatory elements, including eRNAs, promote condensate formation, whereas high production of RNAs during transcription elongation results in condensate dissolution. Considering the majority of eRNAs are short, unstable, and lowly expressed, eRNAs more likely partaken in the formation of transcriptional condensates. Interestingly, a recent work revealed nascent RNAs primarily impede the association of diverse categories of proteins with chromatin, including transcriptional regulators and chromatin modifiers (Skalska et al., 2021). RNA directly binds to these factors, and in turn blocks their binding to nucleosomes, suggesting an antagonistic relationship between their RNA- and chromosome-binding. Whether these proteins contribute to the formation of phase-separated condensates awaits further

investigation. In addition, the phosphorylation status of RNAPII CTD affects the compartmentalization of RNAPII into distinct condensates (Guo et al., 2019). As eRNAs are proven to interact with protein components from different condensates (e.g., Mediator complex and RBPs involved in RNA processing and splicing), they are likely to influence the dynamic exchange of RNAPII between different condensates.

Conclusion

Despite the substantial progress of eRNA studies, much more efforts are warranted in delineating their functions and underlying mechanisms, considering the heterogenous nature in terms of their expression, length, secondary structures, and post-transcriptional modifications. For instance, our understanding of eRNA structures is poorly explored. To tackle this situation, more structural studies (e.g., SHAPE-MaP) are anticipated to uncover intramolecular secondary structures crucial for distinct properties of eRNAs. Equally important is the cataloging a more comprehensive list of eRNA binding partners (e.g., RBPs). Analyses of such data can provide insights into how eRNAs interact, and whether common sequence motifs or structural features of eRNAs exist conferring the interaction specificity. It will be also important to further explore the recently identified intermolecular RNA-RNA interactions and RNA-chromatin interactions, which present an intriguing possibility that eRNAs potentially participate in nuclear compartmentalization (Cai et al., 2020; Quinodoz et al., 2021). Besides, the existence and functions of epitranscriptomic modifications on eRNAs, such as m6A, m5C, hydroxymethyl cytosine (5hmC), and methyl-1-adenosine (m1A), need to be further explored. One trending direction is to demystify the regulatory feedback from these chemical modifications on nascent RNAs (including eRNAs) to chromatin and transcription. As mentioned above, pieces of evidence point to the involvement of eRNAs in phase-separated transcriptional condensates. Multivalent interactions mediated by eRNAs, e.g., RNA-RNA, RNA-protein, RNA-DNA interactions, render them great potential in mediating phase separation (Figure 2C). Several important questions need to be addressed in the future. How do eRNAs contribute to the formation of transcriptional condensates and what features are important (e.g., length, motifs, secondary structures, intermolecular RNA-RNA interactions, and post-transcriptional modifications)? Do eRNAs regulate the transition from transcription initiation into elongation condensates? In addition, the linkage is largely unclear between eRNA-involved transcriptional condensate formation and higher-order 3D genome organization. Finally, functional investigations are required to delineate the roles of eRNAs in disease entities (Zhang et al., 2019; Chen and Liang, 2020) and to dissect how the altered eRNA features favor disease development. Answers to these questions will provide deeper insights not only into eRNA functions and regulatory mechanisms but also into eRNA-centric therapeutic strategies.

Author contributions

YZ and QC conceived the project; QC, YZ, JK, MH, NL, KS, and YZ performed the investigation; QC and YZ wrote the paper. YZ created figures. All authors listed have made a substantial, direct, and intellectual contribution to the work and approved it for publication.

Funding

This work was supported by the Natural Science Foundation of Guangdong Province, China (2021A1515012058 to YZ); National Natural Science Foundation of China (NSFC) (Grant No: 32270587, 32100673 to YZ).

Conflict of interest

The authors declare that the research was conducted in the absence of any commercial or financial relationships that could be construed as a potential conflict of interest.

Publisher's note

All claims expressed in this article are solely those of the authors and do not necessarily represent those of their affiliated organizations, or those of the publisher, the editors and the reviewers. Any product that may be evaluated in this article, or claim that may be made by its manufacturer, is not guaranteed or endorsed by the publisher.

References

Aguilo, F., Li, S., Balasubramaniyan, N., Sancho, A., Benko, S., Zhang, F., et al. (2016). Deposition of 5-methylcytosine on enhancer RNAs enables the coactivator function of PGC-1α. *Cell. Rep.* 14, 479–492. doi:10.1016/j.celrep.2015.12.043

Akhtar, J., Renaud, Y., Albrecht, S., Ghavi-Helm, Y., Roignant, J. Y., Silies, M., et al. (2021). m(6)A RNA methylation regulates promoter-proximal pausing of RNA polymerase II. *Mol. Cell.* 81, 3356–3367.e6. doi:10.1016/j.molcel.2021.06.023

Anderson, K. M., Anderson, D. M., Mcanally, J. R., Shelton, J. M., Bassel-Duby, R., and Olson, E. N. (2016). Transcription of the non-coding RNA upperhand controls Hand2 expression and heart development. *Nature* 539, 433–436. doi:10.1038/nature20128

Andersson, R., Gebhard, C., Miguel-Escalada, I., Hoof, I., Bornholdt, J., Boyd, M., et al. (2014). An atlas of active enhancers across human cell types and tissues. *Nature* 507, 455–461. doi:10.1038/nature12787

Beltran, M., Yates, C. M., Skalska, L., Dawson, M., Reis, F. P., Viiri, K., et al. (2016). The interaction of PRC2 with RNA or chromatin is mutually antagonistic. *Genome Res.* 26, 896–907. doi:10.1101/gr.197632.115

Boija, A., Klein, I. A., Sabari, B. R., Dall'agnese, A., Coffey, E. L., Zamudio, A. V., et al. (2018). Transcription factors activate genes through the phase-separation capacity of their activation domains. *Cell.* 175, 1842–1855. doi:10.1016/j.cell.2018.10.042

Bose, D. A., Donahue, G., Reinberg, D., Shiekhattar, R., Bonasio, R., and Berger, S. L. (2017). RNA binding to CBP stimulates histone acetylation and transcription. *Cell.* 168, 135–149. doi:10.1016/j.cell.2016.12.020

Cai, Z., Cao, C., Ji, L., Ye, R., Wang, D., Xia, C., et al. (2020). RIC-seq for global *in situ* profiling of RNA-RNA spatial interactions. *Nature* 582, 432–437. doi:10.1038/s41586-020-2249-1

Carullo, N. V. N., Phillips, R. A., Iii, Simon, R. C., Soto, S. a. R., Hinds, J. E., Salisbury, A. J., et al. (2020). Enhancer RNAs predict enhancer-gene regulatory links and are critical for enhancer function in neuronal systems. *Nucleic Acids Res.* 48, 9550–9570. doi:10.1093/nar/gkaa671

Chen, H., and Liang, H. (2020). A high-resolution map of human enhancer RNA loci characterizes super-enhancer activities in cancer. *Cancer Cell.* 38, 701–715. doi:10.1016/j.ccell.2020.08.020

Cho, W. K., Spille, J. H., Hecht, M., Lee, C., Li, C., Grube, V., et al. (2018). Mediator and RNA polymerase II clusters associate in transcription-dependent condensates. *Science* 361, 412–415. doi:10.1126/science.aar4199

Cichewicz, M. A., Kiran, M., Przanowska, R. K., Sobierajska, E., Shibata, Y., and Dutta, A. (2018). MUNC, an enhancer RNA upstream from the MYOD gene, induces a subgroup of myogenic transcripts in trans independently of MyoD. *Mol. Cell. Biol.* 38, e00655-17. doi:10.1128/MCB.00655-17

Consortium, E. P. (2012). An integrated encyclopedia of DNA elements in the human genome. *Nature* 489, 57–74. doi:10.1038/nature11247

De Santa, F., Barozzi, I., Mietton, F., Ghisletti, S., Polletti, S., Tusi, B. K., et al. (2010). A large fraction of extragenic RNA pol II transcription sites overlap enhancers. *PLoS Biol.* 8, e1000384. doi:10.1371/journal.pbio.1000384

Engreitz, J. M., Sirokman, K., Mcdonel, P., Shishkin, A. A., Surka, C., Russell, P., et al. (2014). RNA-RNA interactions enable specific targeting of noncoding RNAs to nascent Pre-mRNAs and chromatin sites. *Cell.* 159, 188–199. doi:10.1016/j.cell.2014.08.018

Engreitz, J. M., Haines, J. E., Perez, E. M., Munson, G., Chen, J., Kane, M., et al. (2016). Local regulation of gene expression by lncRNA promoters, transcription and splicing. *Nature* 539, 452–455. doi:10.1038/nature20149

Furlong, E. E. M., and Levine, M. (2018). Developmental enhancers and chromosome topology. *Science* 361, 1341–1345. doi:10.1126/science.aau0320

Giraud, M., Jmari, N., Du, L., Carallis, F., Nieland, T. J., Perez-Campo, F. M., et al. (2014). An RNAi screen for Aire cofactors reveals a role for Hnrnpl in polymerase release and Aire-activated ectopic transcription. *Proc. Natl. Acad. Sci. U. S. A.* 111, 1491–1496. doi:10.1073/pnas.1323535111

Gorbovytska, V., Kim, S. K., Kuybu, F., Gotze, M., Um, D., Kang, K., et al. (2022). Enhancer RNAs stimulate Pol II pause release by harnessing multivalent interactions to NELF. *Nat. Commun.* 13, 2429. doi:10.1038/s41467-022-29934-w

Grossi, E., Raimondi, I., Goni, E., Gonzalez, J., Marchese, F. P., Chapaprieta, V., et al. (2020). A lncRNA-SWI/SNF complex crosstalk controls transcriptional activation at specific promoter regions. *Nat. Commun.* 11, 936. doi:10.1038/s41467-020-14623-3

Guo, Y. E., Manteiga, J. C., Henninger, J. E., Sabari, B. R., Dall'agnese, A., Hannett, N. M., et al. (2019). Pol II phosphorylation regulates a switch between transcriptional and splicing condensates. *Nature* 572, 543–548. doi:10.1038/s41586-019-1464-0

Hangauer, M. J., Vaughn, I. W., and Mcmanus, M. T. (2013). Pervasive transcription of the human genome produces thousands of previously unidentified long intergenic noncoding RNAs. *PLoS Genet.* 9, e1003569. doi:10.1371/journal.pgen.1003569

Harrison, L. J., and Bose, D. (2022). Enhancer RNAs step forward: New insights into enhancer function. *Development* 149, dev200398. doi:10.1242/dev.200398

Henninger, J. E., Oksuz, O., Shrinivas, K., Sagi, I., Leroy, G., Zheng, M. M., et al. (2021). RNA-mediated feedback control of transcriptional condensates. *Cell.* 184, 207–225.e24. doi:10.1016/j.cell.2020.11.030

Hnisz, D., Shrinivas, K., Young, R. A., Chakraborty, A. K., and Sharp, P. A. (2017). A phase separation model for transcriptional control. *Cell.* 169, 13–23. doi:10.1016/j.cell.2017.02.007

Hon, C. C., Ramilowski, J. A., Harshbarger, J., Bertin, N., Rackham, O. J., Gough, J., et al. (2017). An atlas of human long non-coding RNAs with accurate 5' ends. *Nature* 543, 199–204. doi:10.1038/nature21374

Hou, T. Y., and Kraus, W. L. (2022). Analysis of estrogen-regulated enhancer RNAs identifies a functional motif required for enhancer assembly and gene expression. *Cell. Rep.* 39, 110944. doi:10.1016/j.celrep.2022.110944

Hsieh, C. L., Fei, T., Chen, Y., Li, T., Gao, Y., Wang, X., et al. (2014). Enhancer RNAs participate in androgen receptor-driven looping that selectively enhances gene activation. *Proc. Natl. Acad. Sci. U. S. A.* 111, 7319–7324. doi:10.1073/pnas.1324151111

Jiao, W., Chen, Y., Song, H., Li, D., Mei, H., Yang, F., et al. (2018). HPSE enhancer RNA promotes cancer progression through driving chromatin looping and regulating hnRNPU/p300/EGR1/HPSE axis. *Oncogene* 37, 2728–2745. doi:10.1038/s41388-018-0128-0

Joung, J., Engreitz, J. M., Konermann, S., Abudayyeh, O. O., Verdine, V. K., Aguet, F., et al. (2017). Genome-scale activation screen identifies a lncRNA locus regulating a gene neighbourhood. *Nature* 548, 343–346. doi:10.1038/nature23451

Kagey, M. H., Newman, J. J., Bilodeau, S., Zhan, Y., Orlando, D. A., Van Berkum, N. L., et al. (2010). Mediator and cohesin connect gene expression and chromatin architecture. *Nature* 467, 430–435. doi:10.1038/nature09380

Kaikkonen, M. U., Spann, N. J., Heinz, S., Romanoski, C. E., Allison, K. A., Stender, J. D., et al. (2013). Remodeling of the enhancer landscape during macrophage activation is coupled to enhancer transcription. *Mol. Cell.* 51, 310–325. doi:10.1016/j.molcel.2013.07.010

Kim, T. K., Hemberg, M., Gray, J. M., Costa, A. M., Bear, D. M., Wu, J., et al. (2010). Widespread transcription at neuronal activity-regulated enhancers. *Nature* 465, 182–187. doi:10.1038/nature09033

Lai, F., Orom, U. A., Cesaroni, M., Beringer, M., Taatjes, D. J., Blobel, G. A., et al. (2013). Activating RNAs associate with Mediator to enhance chromatin architecture and transcription. *Nature* 494, 497–501. doi:10.1038/nature11884

Lam, M. T., Li, W., Rosenfeld, M. G., and Glass, C. K. (2014). Enhancer RNAs and regulated transcriptional programs. *Trends Biochem. Sci.* 39, 170–182. doi:10.1016/j.tibs.2014.02.007

Lee, J. H., Wang, R., Xiong, F., Krakowiak, J., Liao, Z., Nguyen, P. T., et al. (2021). Enhancer RNA m6A methylation facilitates transcriptional condensate formation and gene activation. *Mol. Cell.* 81, 3368–3385.e9. doi:10.1016/j.molcel.2021.07.024

Li, W., Notani, D., Ma, Q., Tanasa, B., Nunez, E., Chen, A. Y., et al. (2013). Functional roles of enhancer RNAs for oestrogen-dependent transcriptional activation. *Nature* 498, 516–520. doi:10.1038/nature12210

Li, W., Notani, D., and Rosenfeld, M. G. (2016). Enhancers as non-coding RNA transcription units: Recent insights and future perspectives. *Nat. Rev. Genet.* 17, 207–223. doi:10.1038/nrg.2016.4

Liu, J., Dou, X., Chen, C., Chen, C., Liu, C., Xu, M. M., et al. (2020). N (6)-methyladenosine of chromosome-associated regulatory RNA regulates chromatin state and transcription. *Science* 367, 580–586. doi:10.1126/science.aay6018

Liu, J., Gao, M., He, J., Wu, K., Lin, S., Jin, L., et al. (2021). The RNA m(6)A reader YTHDC1 silences retrotransposons and guards ES cell identity. *Nature* 591, 322–326. doi:10.1038/s41586-021-03313-9

Long, H. K., Prescott, S. L., and Wysocka, J. (2016). Ever-changing landscapes: Transcriptional enhancers in development and evolution. *Cell.* 167, 1170–1187. doi:10.1016/j.cell.2016.09.018

Louloupi, A., Ntini, E., Conrad, T., and Orom, U. a. V. (2018). Transient N-6-Methyladenosine transcriptome sequencing reveals a regulatory role of m6A in splicing efficiency. *Cell. Rep.* 23, 3429–3437. doi:10.1016/j.celrep.2018.05.077

Lu, H., Yu, D., Hansen, A. S., Ganguly, S., Liu, R., Heckert, A., et al. (2018). Phase-separation mechanism for C-terminal hyperphosphorylation of RNA polymerase II. *Nature* 558, 318–323. doi:10.1038/s41586-018-0174-3

Maharana, S., Wang, J., Papadopoulos, D. K., Richter, D., Pozniakovsky, A., Poser, I., et al. (2018). RNA buffers the phase separation behavior of prion-like RNA binding proteins. *Science* 360, 918–921. doi:10.1126/science.aar7366

Marques, A. C., Hughes, J., Graham, B., Kowalczyk, M. S., Higgs, D. R., and Ponting, C. P. (2013). Chromatin signatures at transcriptional start sites separate two equally populated yet distinct classes of intergenic long noncoding RNAs. *Genome Biol.* 14, R131. doi:10.1186/gb-2013-14-11-r131

Mattick, J. S., Amaral, P. P., Carninci, P., Carpenter, S., Chang, H. Y., Chen, L. L., et al. (2023). Long non-coding RNAs: Definitions, functions, challenges and recommendations. *Nat. Rev. Mol. Cell. Biol.* Online ahead of print. doi:10.1038/s41580-022-00566-8

Mousavi, K., Zare, H., Dell'orso, S., Grontved, L., Gutierrez-Cruz, G., Derfoul, A., et al. (2013). eRNAs promote transcription by establishing chromatin accessibility at defined genomic loci. *Mol. Cell.* 51, 606–617. doi:10.1016/j.molcel.2013.07.022

Mueller, A. C., Cichewicz, M. A., Dey, B. K., Layer, R., Reon, B. J., Gagan, J. R., et al. (2015). MUNC, a long noncoding RNA that facilitates the function of MyoD in skeletal myogenesis. *Mol. Cell. Biol.* 35, 498–513. doi:10.1128/MCB.01079-14

Nair, S. J., Yang, L., Meluzzi, D., Oh, S., Yang, F., Friedman, M. J., et al. (2019). Phase separation of ligand-activated enhancers licenses cooperative chromosomal enhancer assembly. *Nat. Struct. Mol. Biol.* 26, 193–203. doi:10.1038/s41594-019-0190-5

Oksuz, O., Henninger, J. E., Warneford-Thomson, R., Zheng, M. M., Erb, H., Overholt, K. J., et al. (2022). *Transcription factors interact with RNA to regulate genes*. bioRxiv. New York, NY: Cold Spring Harbor Laboratory. doi:10.1101/2022.09.27.509776

Orom, U. A., Derrien, T., Beringer, M., Gumireddy, K., Gardini, A., Bussotti, G., et al. (2010). Long noncoding RNAs with enhancer-like function in human cells. *Cell.* 143, 46–58. doi:10.1016/j.cell.2010.09.001

Ounzain, S., Micheletti, R., Arnan, C., Plaisance, I., Cecchi, D., Schroen, B., et al. (2015). CARMEN, a human super enhancer-associated long noncoding RNA controlling cardiac specification, differentiation and homeostasis. *J. Mol. Cell. Cardiol.* 89, 98–112. doi:10.1016/j.yjmcc.2015.09.016

Paralkar, V. R., Taborda, C. C., Huang, P., Yao, Y., Kossenkov, A. V., Prasad, R., et al. (2016). Unlinking an lncRNA from its associated cis element. *Mol. Cell.* 62, 104–110. doi:10.1016/j.molcel.2016.02.029

Przanowska, R. K., Weidmann, C. A., Saha, S., Cichewicz, M. A., Jensen, K. N., Przanowski, P., et al. (2022). Distinct MUNC lncRNA structural domains regulate transcription of different promyogenic factors. *Cell. Rep.* 38, 110361. doi:10.1016/j.celrep.2022.110361

Quinodoz, S. A., Jachowicz, J. W., Bhat, P., Ollikainen, N., Banerjee, A. K., Goronzy, I. N., et al. (2021). RNA promotes the formation of spatial compartments in the nucleus. *Cell.* 184, 5775–5790.e30. doi:10.1016/j.cell.2021.10.014

Rahnamoun, H., Lee, J., Sun, Z., Lu, H., Ramsey, K. M., Komives, E. A., et al. (2018). RNAs interact with BRD4 to promote enhanced chromatin engagement and transcription activation. *Nat. Struct. Mol. Biol.* 25, 687–697. doi:10.1038/s41594-018-0102-0

Roden, C., and Gladfelter, A. S. (2021). RNA contributions to the form and function of biomolecular condensates. *Nat. Rev. Mol. Cell. Biol.* 22, 183–195. doi:10.1038/s41580-020-0264-6

Sabari, B. R., Dall'agnese, A., Boija, A., Klein, I. A., Coffey, E. L., Shrinivas, K., et al. (2018). Coactivator condensation at super-enhancers links phase separation and gene control. *Science* 361, eaar3958. doi:10.1126/science.aar3958

Sartorelli, V., and Lauberth, S. M. (2020). Enhancer RNAs are an important regulatory layer of the epigenome. *Nat. Struct. Mol. Biol.* 27, 521–528. doi:10.1038/s41594-020-0446-0

Schaukowitch, K., Joo, J. Y., Liu, X., Watts, J. K., Martinez, C., and Kim, T. K. (2014). Enhancer RNA facilitates NELF release from immediate early genes. *Mol. Cell.* 56, 29–42. doi:10.1016/j.molcel.2014.08.023

Schoenfelder, S., and Fraser, P. (2019). Long-range enhancer-promoter contacts in gene expression control. *Nat. Rev. Genet.* 20, 437–455. doi:10.1038/s41576-019-0128-0

Shao, W., Bi, X., Pan, Y., Gao, B., Wu, J., Yin, Y., et al. (2022). Phase separation of RNA-binding protein promotes polymerase binding and transcription. *Nat. Chem. Biol.* 18, 70–80. doi:10.1038/s41589-021-00904-5

Shi, L., Li, S., Maurer, K., Zhang, Z., Petri, M., and Sullivan, K. E. (2018). Enhancer RNA and NFκB-dependent P300 regulation of ADAMDEC1. *Mol. Immunol.* 103, 312–321. doi:10.1016/j.molimm.2018.09.019

Shrinivas, K., Sabari, B. R., Coffey, E. L., Klein, I. A., Boija, A., Zamudio, A. V., et al. (2019). Enhancer features that drive formation of transcriptional condensates. *Mol. Cell.* 75, 549–561. doi:10.1016/j.molcel.2019.07.009

Sigova, A. A., Abraham, B. J., Ji, X., Molinie, B., Hannett, N. M., Guo, Y. E., et al. (2015). Transcription factor trapping by RNA in gene regulatory elements. *Science* 350, 978–981. doi:10.1126/science.aad3346

Skalska, L., Begley, V., Beltran, M., Lukauskas, S., Khandelwal, G., Faull, P., et al. (2021). Nascent RNA antagonizes the interaction of a set of regulatory proteins with chromatin. *Mol. Cell.* 81, 2944–2959.e10. doi:10.1016/j.molcel.2021.05.026

Statello, L., Guo, C. J., Chen, L. L., and Huarte, M. (2021). Gene regulation by long non-coding RNAs and its biological functions. *Nat. Rev. Mol. Cell. Biol.* 22, 96–118. doi:10.1038/s41580-020-00315-9

Sur, I., and Taipale, J. (2016). The role of enhancers in cancer. *Nat. Rev. Cancer* 16, 483–493. doi:10.1038/nrc.2016.62

Tan, S. H., Leong, W. Z., Ngoc, P. C. T., Tan, T. K., Bertulfo, F. C., Lim, M. C., et al. (2019). The enhancer RNA ARIEL activates the oncogenic transcriptional program in T-cell acute lymphoblastic leukemia. *Blood* 134, 239–251. doi:10.1182/blood.2018874503

Tan-Wong, S. M., Dhir, S., and Proudfoot, N. J. (2019). R-loops promote antisense transcription across the mammalian genome. *Mol. Cell.* 76, 600–616. doi:10.1016/j.molcel.2019.10.002

Tsai, P. F., Dell'orso, S., Rodriguez, J., Vivanco, K. O., Ko, K. D., Jiang, K., et al. (2018). A muscle-specific enhancer RNA mediates cohesin recruitment and regulates transcription in trans. *Mol. Cell.* 71, 129–141. doi:10.1016/j.molcel.2018.06.008

Wang, K. C., Yang, Y. W., Liu, B., Sanyal, A., Corces-Zimmerman, R., Chen, Y., et al. (2011). A long noncoding RNA maintains active chromatin to coordinate homeotic gene expression. *Nature* 472, 120–124. doi:10.1038/nature09819

Wang, X., Paucek, R. D., Gooding, A. R., Brown, Z. Z., Ge, E. J., Muir, T. W., et al. (2017). Molecular analysis of PRC2 recruitment to DNA in chromatin and its inhibition by RNA. *Nat. Struct. Mol. Biol.* 24, 1028–1038. doi:10.1038/nsmb.3487

Watts, J. A., Grunseich, C., Rodriguez, Y., Liu, Y., Li, D., Burdick, J. T., et al. (2022). A common transcriptional mechanism involving R-loop and RNA abasic site regulates an enhancer RNA of APOE. *Nucleic Acids Res.* 50, 12497–12514. doi:10.1093/nar/gkac1107

West, J. A., Davis, C. P., Sunwoo, H., Simon, M. D., Sadreyev, R. I., Wang, P. I., et al. (2014). The long noncoding RNAs NEAT1 and MALAT1 bind active chromatin sites. *Mol. Cell.* 55, 791–802. doi:10.1016/j.molcel.2014.07.012

Winkler, L., Jimenez, M., Zimmer, J. T., Williams, A., Simon, M. D., and Dimitrova, N. (2022). Functional elements of the cis-regulatory lincRNA-p21. *Cell. Rep.* 39, 110687. doi:10.1016/j.celrep.2022.110687

Xiang, J. F., Yin, Q. F., Chen, T., Zhang, Y., Zhang, X. O., Wu, Z., et al. (2014). Human colorectal cancer-specific CCAT1-L lncRNA regulates long-range chromatin interactions at the MYC locus. *Cell. Res.* 24, 513–531. doi:10.1038/cr.2014.35

Xiao, R., Chen, J. Y., Liang, Z., Luo, D., Chen, G., Lu, Z. J., et al. (2019a). Pervasive chromatin-RNA binding protein interactions enable RNA-based regulation of transcription. *Cell.* 178, 107–121. doi:10.1016/j.cell.2019.06.001

Xiao, S., Cao, S., Huang, Q., Xia, L., Deng, M., Yang, M., et al. (2019b). The RNA N(6)-methyladenosine modification landscape of human fetal tissues. *Nat. Cell. Biol.* 21, 651–661. doi:10.1038/s41556-019-0315-4

Xu, W., Li, J., He, C., Wen, J., Ma, H., Rong, B., et al. (2021). METTL3 regulates heterochromatin in mouse embryonic stem cells. *Nature* 591, 317–321. doi:10.1038/s41586-021-03210-1

Xu, W., He, C., Kaye, E. G., Li, J., Mu, M., Nelson, G. M., et al. (2022). Dynamic control of chromatin-associated m(6)A methylation regulates nascent RNA synthesis. *Mol. Cell.* 82, 1156–1168.e7. doi:10.1016/j.molcel.2022.02.006

Yuan, W., Xie, J., Long, C., Erdjument-Bromage, H., Ding, X., Zheng, Y., et al. (2009). Heterogeneous nuclear ribonucleoprotein L Is a subunit of human KMT3a/Set2 complex required for H3 Lys-36 trimethylation activity *in vivo*. *J. Biol. Chem.* 284, 15701–15707. doi:10.1074/jbc.M808431200

Zhang, Z., Lee, J. H., Ruan, H., Ye, Y., Krakowiak, J., Hu, Q., et al. (2019). Transcriptional landscape and clinical utility of enhancer RNAs for eRNA-targeted therapy in cancer. *Nat. Commun.* 10, 4562. doi:10.1038/s41467-019-12543-5

Zhao, Y., Wang, L., Ren, S., Wang, L., Blackburn, P. R., Mcnulty, M. S., et al. (2016). Activation of P-TEFb by androgen receptor-regulated enhancer RNAs in castration-resistant prostate cancer. *Cell. Rep.* 15, 599–610. doi:10.1016/j.celrep.2016.03.038

Zhao, Y., Zhou, J., He, L., Li, Y., Yuan, J., Sun, K., et al. (2019). MyoD induced enhancer RNA interacts with hnRNPL to activate target gene transcription during myogenic differentiation. *Nat. Commun.* 10, 5787. doi:10.1038/s41467-019-13598-0

Zhou, Y., Xu, S., Zhang, M., and Wu, Q. (2021). Systematic functional characterization of antisense eRNA of protocadherin α composite enhancer. *Genes. Dev.* 35, 1383–1394. doi:10.1101/gad.348621.121

Frontiers in
Cell and Developmental Biology

Explores the fundamental biological processes of life, covering intracellular and extracellular dynamics.

The world's most cited developmental biology journal, advancing our understanding of the fundamental processes of life. It explores a wide spectrum of cell and developmental biology, covering intracellular and extracellular dynamics.

Discover the latest Research Topics

See more →

Frontiers

Avenue du Tribunal-Fédéral 34
1005 Lausanne, Switzerland
frontiersin.org

Contact us

+41 (0)21 510 17 00
frontiersin.org/about/contact